WEATHERING OF AUSTRALIAN GRANITIC ROCKS: A STUDY OF VARIATIONS IN TRACE ELEMENTS AND ISOTOPIC RATIOS

by

J.M. Worden, B.Sc. (Hons)

THESIS SUBMITTED AS A REQUIREMENT FOR
ADMISSION TO THE DEGREE OF DOCTOR OF PHILOSOPHY,
AUSTRALIAN NATIONAL UNIVERSITY, 1970.

The work and results presented in this thesis are my own except where due reference is made in the text.

J.M. Worden

J.M. WORDEN

ACKNOWLEDGEMENTS

I am grateful to my supervisors, Professor K.S. Heier during the early part of this study and later Dr S.R. Taylor, for assistance and advice.

Instruction to all aspects of Rb-Sr geochemistry by Dr W. Compston and Mr M.J. Vernon is gratefully acknowledged. Dr H.H. Veeh analysed samples from the Snowy Mountains for U-Th disequilibrium and instructed the author in analytical procedures.

Determination of U and Th by X.R.F. was carried out in the Department of Geology and I thank Dr B.W. Chappell for advice and Professor D.A. Brown for use of the facilities in his department.

Mr E. Kiss kindly analysed some rock samples for total H_2O and ferrous iron. His advice and help with analytical chemistry is gratefully acknowledged.

Messrs. E. Pedersen and A. Powell prepared thin sections of rock samples and Messrs. H. Berry and M. Cowan prepared rock powders of West Australian samples.

Dr R. Brewer of C.S.I.R.O., Division of Soils had thin sections made and his guidance in their interpretation, is acknowledged.

Mrs T.R. Martin operated the X.R.F. equipment during analysis of West Australian materials.

Helpful discussions have been held with many staff members and students in the Department of Geophysics and Geochemistry, Australian National University.

I also wish to thank Mr J.B. Gill for constructive criticism of the manuscript and helpful discussion.

I am extremely grateful to my wife for typing the various drafts of this thesis and for considerable help with drafting of the figures. The final manuscript was typed by Mrs J. Barton.

Drill Holes DH 2401, DH 2511 and DH 2660 were obtained through the courtesy of the Snowy Mountains Authority. The active cooperation of the Snowy Mountains Authority and permission to use their reports are gratefully acknowledged.

Diamond Drill Hole MD 1 was kindly made available by Western Mining Corporation.

This research has been conducted during the tenure of a Commonwealth Postgraduate Award and an Australian National University Research Scholarship.

WEATHERING OF AUSTRALIAN GRANITIC ROCKS: A STUDY OF VARIATIONS IN TRACE ELEMENTS AND ISOTOPIC RATIOS

TABLE OF CONTENTS

Page

CHAPTER 1

INTRODUCTION

1.1 AIMS OF THESIS

The results of geochemical and isotopic investigations of weathering on granitic rocks are presented in this thesis.

The aims of this study were as follows:

i) to establish changes in element compositions during breakdown of high temperature magmatic assemblages to low temperature hydrated mineralogies;

ii) to define the migration of elements from mineral lattices into solution and their subsequent chemical behaviour;

iii) to establish initial fresh rock variation, rock heterogeneity and the presence or absence of late-stage hydrothermal alteration;

iv) to investigate the effect of weathering upon the age recorded by the total rock and its possible relevance to the interpretation of both sediment and shale ages;

v) to study the behaviour of U and Th isotopes during weathering;

vi) to define at which stage of weathering the "rock" begins to differ significantly from the fresh parent rock, both with regard to trace element geochemistry and for geochronological purposes;

vii) to elucidate the dominant controls of weathering processes (i.e. climate, parent rock mineralogy etc.) and to test the validity of the mineral stability series proposed by Goldich (1938).

1.2 DISCUSSION OF AIMS

The selection of rock types was governed by considerations of average crustal compositions (Taylor and White, 1966; Taylor, 1968 and references cited therein). An andesitic composition has been proposed for the crust and partial melting of this could produce a granodioritic upper and a residual anorthositic lower crust. Most if not all of the upper crust has passed through the weathering cycle at least once (Barth, 1961). Weathering is potentially an "effective separator" of elements and Welby (1958) for example concluded that much of the geochemical separation of alkali metals in the external cycle occurs during the weathering process.

A granodioritic crustal composition has been proposed and is based on the average of exposed rocks at the earths surface (Taylor, op cit). Investigation of granodiorite and diorite weathering would be relevant to both models. A limiting example would be provided by analysis of weathering on a granite (sensuo stricto).

Aims (iii) and (vi) ideally require long drill cores permitting the analysis of fresh rock variation and if present, hydrothermal alteration. Hydrothermal alteration may be difficult or impossible to distinguish from weathering as both represent adjustments of high temperature magmatic mineralogies to lower temperature hydrated assemblages (Harriss and Adams, 1966). Fresh rock variation constitutes a "background noise or inherent data scatter" and must be evaluated. To be significant, any process must produce variations which exceed this "background noise level".

The requirements of specific compositions and satisfactory drill core footage were best met within the Snowy Mountains Region of New South Wales. A quartz diorite (see Chapter 3) was selected as a close approximation to an andesitic composition while the Khancoban granite (see Chapter 5) is similar to an average granodioritic composition. The Scamels granite is a leucocratic granite (Kolbe and Taylor, 1966) and provides an example of siliceous magmatic compositions.

The first and second aims involved analysing major and trace elements for either representative samples (major elements) or for all samples (trace elements). Emphasis has been placed on the determination of trace elements, Rb, Sr, Ba, Pb, Y, Zr, U and Th. The behaviour of elemental ratios during weathering has been used extensively as they are independent of volume changes and have gained wide acceptance within igneous, sedimentary and metamorphic geochemistry (Taylor, 1966; Hart, 1969 and many others). Only chemically coherent elements (i.e. K and Rb, Ca and Sr and K and Na) have been used for ratio studies, and the effect of weathering on their coherence has been examined.

Because the Palaeozoic rocks of the Snowy Mountains Region have low Rb/Sr ratios (see Chapter 6), rocks with higher Rb/Sr and enriched Sr^{87}/Sr^{86} ratios were necessary to study the effects of surficial alteration on whole rock ages by Rb-Sr isotopic techniques. The Yilgarn block of the West Australian Shield is both ancient and has been subjected to prolonged and intensive weathering as a relatively flat, tectonically stable unit. Areas are covered by lateritic profiles considered to have formed during the Miocene (Woolnough, 1927). Samples were collected from three widely spaced localities on the shield (see Chapter 7) representing both lateritic and present-day, iron-staining weathering. Two additional localities were sampled but were considered unsuitable for Rb-Sr studies of weathering effects because of complex intrusive and thermal histories (Compston and Arriens, 1968).

Both Th and U are important in crustal model considerations and heat flow investigations. Pliler and Adams (1962) and Rogers, et al., (1965) have demonstrated appreciable migration of these elements at considerable depths as a consequence of leaching. The purpose of U and Th studies was not confined to abundances alone but incorporated disequilibrium investigations (Chapter 11). The laterite profiles may have formed under different climatic conditions during the Miocene (Woolnough, op cit). The U-decay series will be in equilibrium if there has been no subsequent alteration post-dating the Miocene. The presence of significant disequilibrium would indicate continuing equilibration to the present climate.

The last aim (vii) involved contrasting weathering in the Snowy Mountains and West Australia. Cold temperatures prevail in the Snowy Mountains whereas localities in Western Australia range from warm Mediterranean to arid desert type climates. The influence of climate, a multivariate factor, is very difficult to assess quantitatively. Vegetation is directly related to climate, however in eucalyptus country there is little leaf litter and scant production of organic decay products. As eucalyptus flora cover most climatic belts of Australia, the relative importance of organic material during soil formation is reduced. Grim (1953) states that all factors are interdependent and their relative importance is not always the same.

Goldich (1938) proposed a mineral stability series, effectively the reverse of the Bowen reaction series. Harriss and Adams (op cit) maintain that the order of relative mineral stability is consistently observed regardless of climate or local physiochemical variations. Deep weathering in Australia for at least the Tertiary may have a different stability sequence.

The rationale of the whole study was to assess these aspects and, if possible by means of trace element and isotopic analysis, to delineate the factors controlling weathering.

CHAPTER 2

SNOWY MOUNTAINS REGION

2.1 GEOLOGICAL SETTING AND FIELD RELATIONSHIPS

The Tasman Geosyncline of Eastern Australia has been divided into a southern Lachlan Geosyncline and a younger New England Geosyncline to the northeast, by Packham (1960), (Fig. 1). In the Snowy Mountains region of southeastern New South Wales, Late Ordovician sediments are extensively intruded by large granodioritic and granitic batholiths (Fig. 2). Ordovician sediments which trend north-northeast, are dominantly interbedded shales, siltstones and fine grained sandstones. Although metamorphic intensity varies, it is usually of low regional grade with tight folding and fold axes striking north-northwest.

Two extensive north-south trending metamorphic belts have been defined by Moye et al., (1963). The Western belt is relatively narrow at the Victorian-New South Wales border and in the Snowy Mountains Region, but it widens to the north. An eastern belt is reduced in extent and has been intruded to the north by granites comprising the Murrumbidgee Batholith.

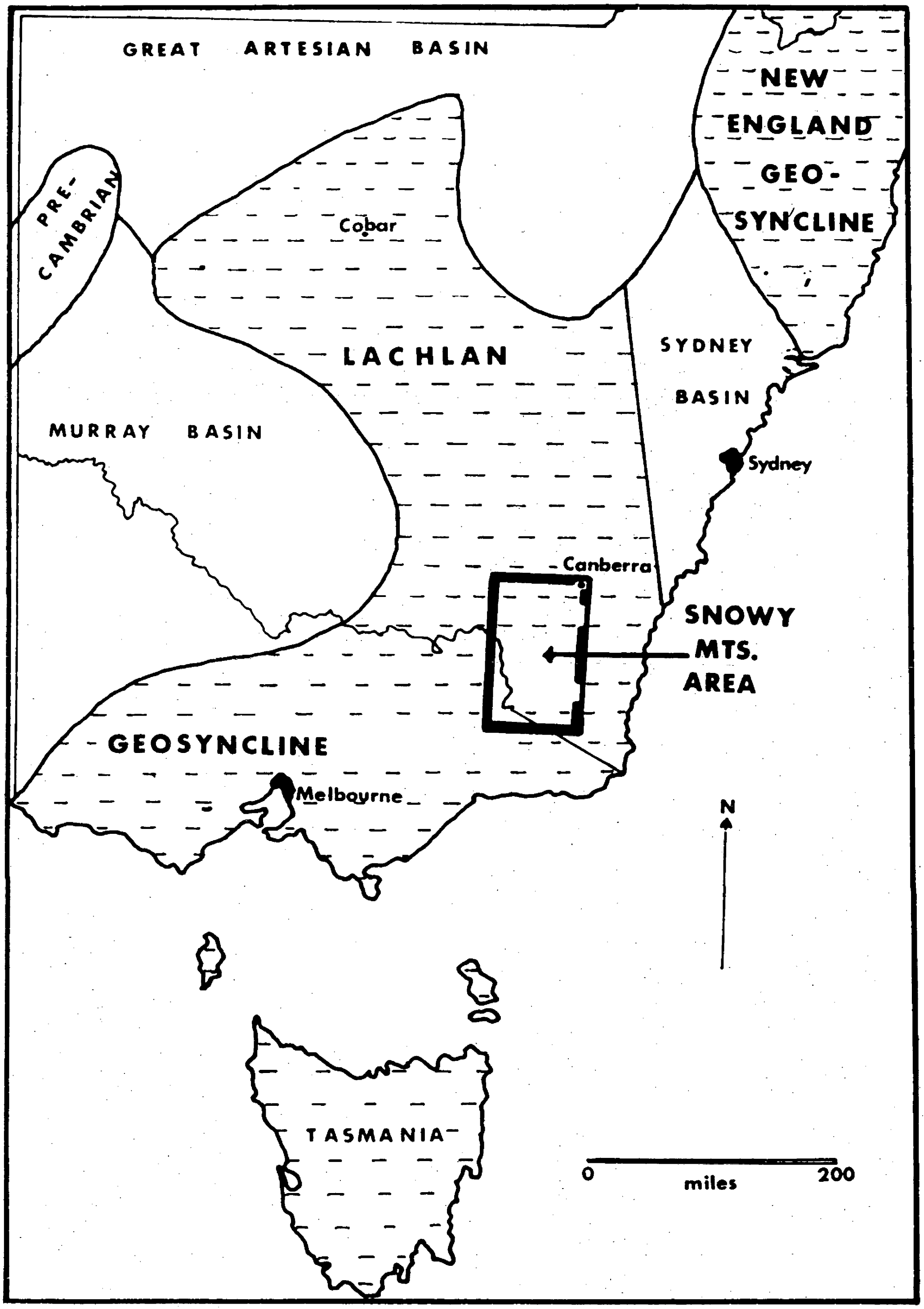

Fig. 1 Regional setting of the Snowy Mountains area, New South Wales, Australia.

A greater part of the Snowy Mountains area is granite with four major granitic batholiths generally elongated and concordant with the north-south trending Ordovician sediments. The Kosciusko Batholith extends from south of the Victorian border to north of Kiandra (105 km) and includes the highest area of the Australian continent. To the west and northwest it is separated from the Maragle Batholith (Vallance 1953, 1960; Moye et al., 1963) by a narrow belt of Silurian sediments and the Western metamorphic belt (Grey Mare Metamorphics). The eastern margin is marked by Upper Ordovician sediments and faulting. To the east, the Berridale Batholith (Joplin, 1942; Lambert, 1963; Lambert and White, 1965) intrudes Upper Ordovician sediments forming a contact aureole of quartzite, hornfels and chiastolite slate. Further to the northeast lies the Murrumbidgee Batholith (Snelling, 1960).

Evernden and Richards (1962) demonstrated, by K-Ar dating that there was a sequence of intrusions from Middle Silurian to Carboniferous. The locii of intrusions tended to move to the northeast with time. Most granites were intruded during early l.c./ Devonian times but the possibility of Argon loss giving younger ages, cannot be ignored. Pidgeon and

Compston (1965) using Rb-Sr isotopic techniques, determined the age of the Cooma granite and units of the surrounding metamorphic envelope. They conclude that K-Ar ages determined by Evernden and Richards (1962), for the Cooma granite are low owing to Ar-loss. The exact amount of Ar-leakage cannot be resolved because of possible systematic errors in decay constants.

The Snowy Mountains region is noted for deep weathering. Large scale operations of the Snowy Mountains Hydro Electric Authority provided an opportunity to examine weathering processes in conjunction with initial fresh rock variation. The Snowy Mountains Authority while constructing the Island Bend-Murray I-Murray II hydro electric scheme carried out extensive diamond drilling, tunnelling and dam construction across the Kosciusko Batholith, through the intervening sediments and western metamorphic belt into the Maragle Batholith (Fig. 3).

During construction of the Geehi Dam and associated works, a belt of intermediate to basic rocks, similar to those of the Jagungal-Kiandra area (Joplin, 1958), were mapped. Diamond drill core DH 2401 was drilled in quartz diorite (Windy Creek Diorite) adjacent to the Geehi Outlet-Inlet structure.

The Murray I pressure tunnel (11.6 km) passes through the narrow belt of Silurian sediments and the western belt of metamorphics (Grey Mare Metamorphics). Approximately 7.2 km from the Geehi Dam, the Bogong Creek Intake works are located in the Scamels Granite. Drilling of this typical leucocratic granite was undertaken at Bogong Creek (DH 2511).

Below Murray I Power Station, the Murray II pressure tunnel passes under Clews Ridge passing at first through Bogong Creek Beds (Upper Ordovician) and later into the Khancoban granite. At the western end of the pressure tunnel and slightly to the north, drill hole DH 2660 was drilled as an exploratory probe for siting an underground power station.

2.2 INTRUSIVE RELATIONSHIPS

The Windy Creek Diorite (DH 2401) may be a marginal phase of the Kosciusko Batholith, however this diorite is probably older than the batholith on field evidence. The outcrop area is elongated, trending north-northeast and may form part of a narrow, discontinuous belt of basic rocks extending through Mount Jagungal.

The diorite body is a dyke-like mass, approximately 1.2 km wide and dipping to the east at between 30° and

50°. It has been mapped over an outcrop length of 4 kilometres by Snowy Mountains Authority geologists but continues for an unknown distance to the north and apparently thins out to the south. To the east the Windy Creek Diorite is bounded by the Leaning Rock Gneiss although the contact is not exposed. To the west, a sharp contact with the Twins Creek Gneiss can be seen. Sharp contacts (within 5 cms) are typical although locally gradational contacts up to 7 metres are observed, (Moye and Sharp, 1961). In DH 2403, a narrow contact zone (<1 metre) is gradational although very fine grained. The Twins Creek Gneiss is grey at the contact but a pinkish-grey colour is dominant away from the contact zone.

Vallance in Packham (1969) notes that basic bodies usually predate granites of the Murrumbidgee type and Joplin (1958) regards the pyroxenite to monzonite suite of Mt Jagungal-Kiandra as older than granites of the Kosciusko Batholith. The Windy Creek Diorite may be a metamorphosed dyke or a concordant quartz diorite intrusion.

The Scamels granite forms massive outcrops at Granite Knob and bouldery outcrops along the western bank of Bogong Creek. It is an elongated intrusion, approximately 1.7 km wide and 4.2 km long and intrusive into the Bogong Creek Beds (Moye and Sharp, 1961). Contact aureoles of spotted hornfels have formed and local silicified zones are not uncommon. Contacts dip gently to the east along the eastern margin and to the west at the western margin suggesting that the current erosion level has not uncovered the bulk of the granitic mass.

The Khancoban granite also intrudes the Bogong Creek Beds producing a contact aureole of spotted hornfels and quartzite along a zone varying from a hundred metres at steeply dipping contacts to thousands of metres where contacts are flat lying, Moye et al in Packham (1969); Guy (1969). The Khancoban granite is concordant, elongated (approximately 8.5 km wide and 18.7 km long) and forms Clews Ridge. The eastern contact dips steeply while the western contact with the Swampy Plain Metamorphics is obscured by the Khancoban-Yellow Bog fault and alluvials of the Swampy Plain River. Xenoliths are uncommon in all three rock types.

2.3 STRUCTURE

All rock masses studied trend north-northeast, parallel to the regional trend of Ordovician sediments. The elongation of both Khancoban and Scamels granites is parallel to this trend although both have intrusive relationships with the Bogong Creek Beds. Foliation is lacking although broad jointing is evident. The Windy Creek Diorite is massive with joint spacings ranging from 2 cms to 6 metres but averaging 10 cms to 20 cms. Many joints are discontinuous but every metre there are major joints which persist for approximately 6 metres. The Scamels granite is broadly jointed with joint spacings up to 6 metres or more. In some areas, minor faulting, or shear zones are common and jointing is closer, especially in the vicinity of minor lineaments (Bogong Creek Fault). The Khancoban granite joint spacing closely resembles that of the Scamels granite, however the proximity of the Khancoban-Yellow Bog fault zone, on the western side, has produced a very closely jointed granite.

Geological logs of the three drill holes (DH 2401, DH 2511, and DH 2660) are included in Appendix A.

2.4 TOPOGRAPHY

The Snowy Mountains are part of a high plateau mostly more than 1370 metres above sea level, reaching a maximum elevation of 2230 metres at Mount Kosciusko. The mountains are parallel to the geological trend and are flanked to the east by lower tablelands. To the west the mountains fall rapidly to hilly low lands, mostly at elevations of 350 to 700 metres along broad valleys of the Murray River and its tributaries (Fig. 3). All country above 2100 metres is referred to as the Kosciusko Plateau. The eastern side of the Kosciusko Plateau is drained by the Snowy River and its tributaries while the western side is drained by the Murray River and its tributaries, Geehi River (which in its lower reaches becomes Swampy Plain River), Bogong Creek and Khancoban Creek. Drainage patterns reflect the dominant control of jointing and strike directions of the underlying rock types.

Windy Creek drains to the north-northwest into Geehi River along broad valleys separated by very rocky ridges. The ridge tops are fairly level but fall sharply to the valley floors. The floors of many valleys are rather swampy and reflect Pleistocene glaciation. The valleys were shaped by glaciation and the deposits along valley floors are either glacial or fluvioglacial residuals.

The Geehi River flows southwesterly in a deep, youthful, rugged gorge through the western margin of the Kosciusko Plateau. Stream incision is asymmetrical with the high Kosciusko Plateau to the east and the lower Grey Mare Range to the west.

The Bogong Creek Valley is remarkably straight, slightly west of the Bogong Creek fault and trending south-southwest. The valley cut by Bogong Creek is youthful with the stream entrenched almost 700 metres below Grey Mare and Dargals Ranges. Outcrops of Scamels Granite form Granite Knob a high point of the Dargals Range.

Khancoban Creek and its tributaries have deeply dissected the Dargals Range and are entrenched in youthful valleys. A dendritic drainage pattern locally controlled by faults drains into the Swampy Plain River.

During the Tertiary, uplift and block faulting elevated an old peneplain forming an elevated plateau. Streams were rejuvenated and cut deeply entrenched valleys often forming deeply incised gorges. The Kosciusko Plateau is terminated by Geehi Valley to the west, beyond which a series of descending ridges (Grey Mare Range, Bogong Creek Valley, Dargals Range, Khancoban Back Creek, Clews Ridge and Swampy Plain valley) and intermediate valleys fall away to a lower elevation. Block faulting is now obscured by weathered rocks and soil with little evidence of faulting readily seen. The exceptions to this are the Bogong Creek and Khancoban-Yellow Bog fault zones.

The latter is a very large fault zone and in the lowermost section of DH 2660 a splinter fault from this zone has severely affected the granite.

2.5 WEATHERING

The extent of weathering is variable and has been shown on geological logs in Appendix A. Weathering normally commences at the joint planes, penetrating from here into adjacent rock. Frequently zones of completely weathered material occur along joints or fractures separated by relatively fresher rock. Weathering usually is more intense at or near the surface, decreasing gradually with increasing depth. Upper Valley slopes and plateau outcrops are usually extensively and deeply weathered, however, youthful stream valleys may expose relatively fresh rock in creek beds.

Initial weathering is represented by outlining of the groundmass by "limonite" or iron rich alteration products. Kaolinization of feldspars preceded by decomposition of biotite occurs with increased weathering. Weathering rates are largely controlled by joint spacings. If joints are closely spaced, granitic rocks are rapidly altered but if joints are less frequent, spheroidal weathering normally results.

All rock types exposed along the Snowy-Geehi and Murray I Pressure Tunnels have very low porosity and are practically impervious to water if the rock is unweathered. A summary of weathering terms used, in Table 1, is that of Snowy Mountains Authority geologists and this system has been followed.

TABLE 1

DESCRIPTION OF WEATHERING PRODUCTS OF GRANITIC ROCKS

MATERIAL (abbreviations on drawings and core logs)	DESCRIPTION
Slopewash and soil	Clayey, silty or sandy soil with no recognizable rock texture. It is derived from weathered granitic rocks, the surface layer often containing humus and plant roots.
Completely weathered granite (C W)	Granite completely decomposed in situ by weathering, but still possessing a recognizable granite fabric; the original feldspars are completely decomposed to clay minerals which remain as grains of clay; biotite may be decomposed to varying degrees. Completely weathered granite disintegrates into clay, silt and sand when immersed in water.
Highly weathered granite (H W)	Intensely weathered granite, weakened to the extent that pieces the size of NX drill core (2.1/8 inch diameter) can be broken and crumbled by hand. Does not disintegrate when immersed in water.
Moderately weathered granite (M W)	Granite considerably weathered throughout, but possessing strength such that pieces of NX core cannot be broken by hand.
Slightly weathered granite (S W)	Granite distinctly weathered throughout the fabric of the rock, as shown by slight limonite staining and some slight kaolinization of the feldspars, but its strength approaches that of fresh granite.
Fresh granite with limonite stained joints (Fr St)	Joint faces coated or stained with limonite, but the granite block between joints is unweathered.
Fresh granite (Fr)	Unweathered granite. Possible joint coatings include chlorite, calcite, pyrites and clay.

NOTE: These definitions and properties refer to granitic rocks which are not crushed or sheared. The degree of weathering of other rock types has been described in a similar way, although their engineering properties are frequently determined more by the weathering along joint planes with the resulting loss of strength, than by weathering of the rock mass as a whole.

CHAPTER 3

PETROGRAPHY AND CHEMISTRY OF THE WINDY CREEK DIORITE

Moye and Sharp (1961) have noted that

> ... natural exposures of the diorite are few and practically restricted to about 50 feet above the Geehi River and the bed of Windy Creek. As a consequence detailed information on structures and field relationships with other rocks is scant, except where explored by trenching or drilling..., (see Fig. 4)

The diorite is typically dark greenish-grey, rather speckled and fine to medium grained (1-3 mm) in hand specimen. It is massive, although considerable variation in grain size and composition exists throughout. Moye and Sharp (1961) state that

> ... in places, medium to coarse grained bands from 1 inch to 30 feet wide apparently intrude the finer-grained rock, perhaps as a pegmatitic phase ....

Considerable compositional variation is evident if modes of analysed samples (Table 2) are compared with the average composition determined from a number of thin sections by Moye and Sharp (1961). Diorite in DH 2401 is distinctly quartz rich in comparison, however, these authors have also noted, upstream in Windy Creek, a more quartz-rich diorite than normal.

Basic dykes ranging from less than 2 cms to 4.5 metres intrude the diorite and are either altered lamprophyres

Fig. 4 The location of DH 2401 and geology of the adjacent area.

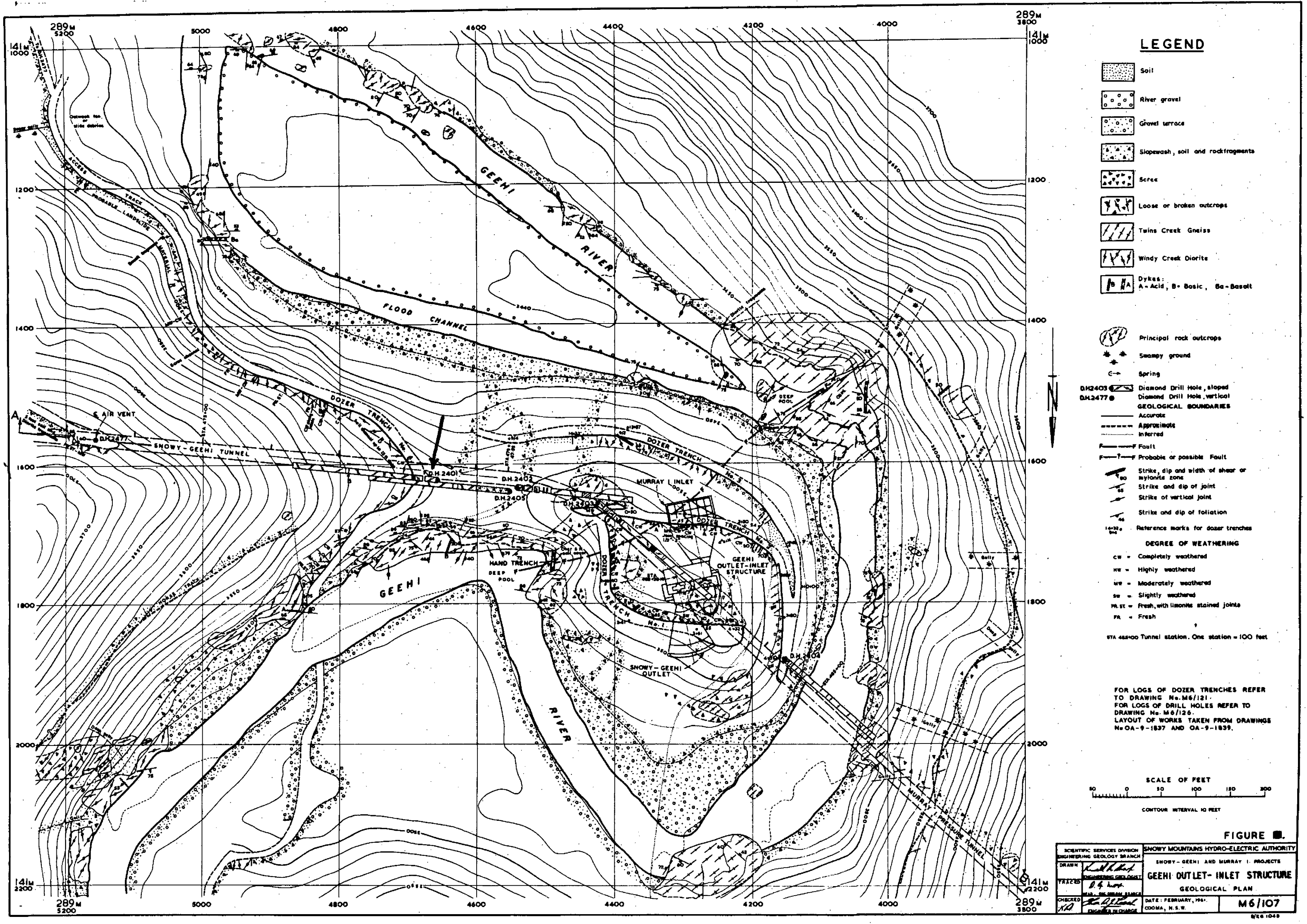

or monchiquites (analcite basalts). In DH 2401, a 15 cm fine-grained, greenish-black dyke intrudes the diorite striking north-south and dipping 70° west. In thin section this dyke is an altered lamprophyre.

3.1 FRESH ROCK VARIATION

3.1.1 Petrography

Fresh diorite displays variations in grain size and colour index. The lower section of DH 2401 is dark grey, mostly fine to medium-grained and massive (see Appendix A). Joint surfaces commonly have thin calcite coatings. Below 185 feet, the diorite is fresh (sample series 6048-6065 and 6151-6169), "speckled" in appearance and almost uniform. All changes in grain size or ferromagnesian content are gradational. In thin section, the diorite consists dominantly of plagioclase, hornblende and quartz with lesser biotite and accessory opaques, apatite, zircon and occasional garnet. Evidence of late-stage alteration is provided by chlorite interleaves in biotite flakes and the presence of sericite with carbonate as alteration on plagioclase.

Plagioclase is the most abundant mineral phase occupying from 48% to 58% of the rock. Crystals are subhedral, often lath-like and complexly twinned. A range of grain size and occasionally a mild phenocrystic tendency exist. Zoning is ubiquitous with patchy, normal, reverse and oscillatory zoning types. The cores of large crystals are more heavily sericitized than the rims, the alteration being related to shattered, slightly brown, calcic cores. Although cores are shattered and broken they have been healed by later more sodic plagioclase. Heaviest alteration is localised along cracks, fractures or cleavage traces.

Hornblende forms poikilitic crystals generally, although subhedral single crystals dominate in finer-grained phases. Two distinct types with differing pleochroism (one type has pale brown-green to deep green, whilst the other is green to deep blue-green) are present. The latter type appears to be secondary or later, often forming margins at crystals of the former. Hornblende frequently forms ragged crystals which are occasionally twinned. Very numerous inclusions of quartz, opaques and apatite occur in hornblende and occasional chlorite crystals are associated with hornblende aggregates.

Quartz commonly ranges from 13% to 21% and usually forms aggregates or quartz mosaics in intergranular areas. Small veins or fractures are filled with small interlocking quartz grains and contribute to the range of quartz content. Patches of quartz crystals are frequently associated with biotite and may have fine biotite crystals dispersed in the quartz aggregate. Biotite usually forms separate clumps of crystals but may be intergrown with hornblende in large aggregates. Pleochroism is typically pale straw-yellow to olive-green. Small inclusions of iron oxides may be present and pleochroic halos are relatively few. Apatite and large opaque grains are associated with biotite and interlayers of chlorite replacing biotite are occasionally seen. Chloritic replacement of biotite is highly variable from sample to sample but is notable in sample 6044.

Accessory minerals include magnetite, apatite, odd zircon, epidote and garnet crystals. Chlorite, calcite and sericite occur as alteration products.

3.1.2 Modal analyses

Modal analyses for seven diorite samples which display the widest dispersion of colour index are listed in Table 2. Variable hornblende to biotite ratios appear to control the colour index and on a quartz-hornblende-biotite plot these minerals vary considerably (Fig. 5). Lower hornblende contents are accompanied by increases in biotite and to a lesser extent, quartz. A quartz-feldspar-mafics diagram

Table 2

Micrometric Analyses of the Windy Creek Diorite

Sample	Plag.	Hbl.	Biot.	Qtz.	Acc.	Colour Index
6065	47.9	24.3	7.8	17.4	3.1	35.2
6059	58.3	23.1	4.6	13.7	0.3	28.0
6055	51.6	24.6	5.7	17.1	1.0	31.2
6054	49.4	19.9	11.9	16.7	2.1	33.9
6050	49.4	22.6	10.3	14.9	2.8	35.7
6049	53.6	11.2	14.5	20.4	0.3	26.0
6038	61.7	7.9	13.8	16.2	0.3	22.1
Av. Composition Moye and Sharp (1961)	36	57		4		

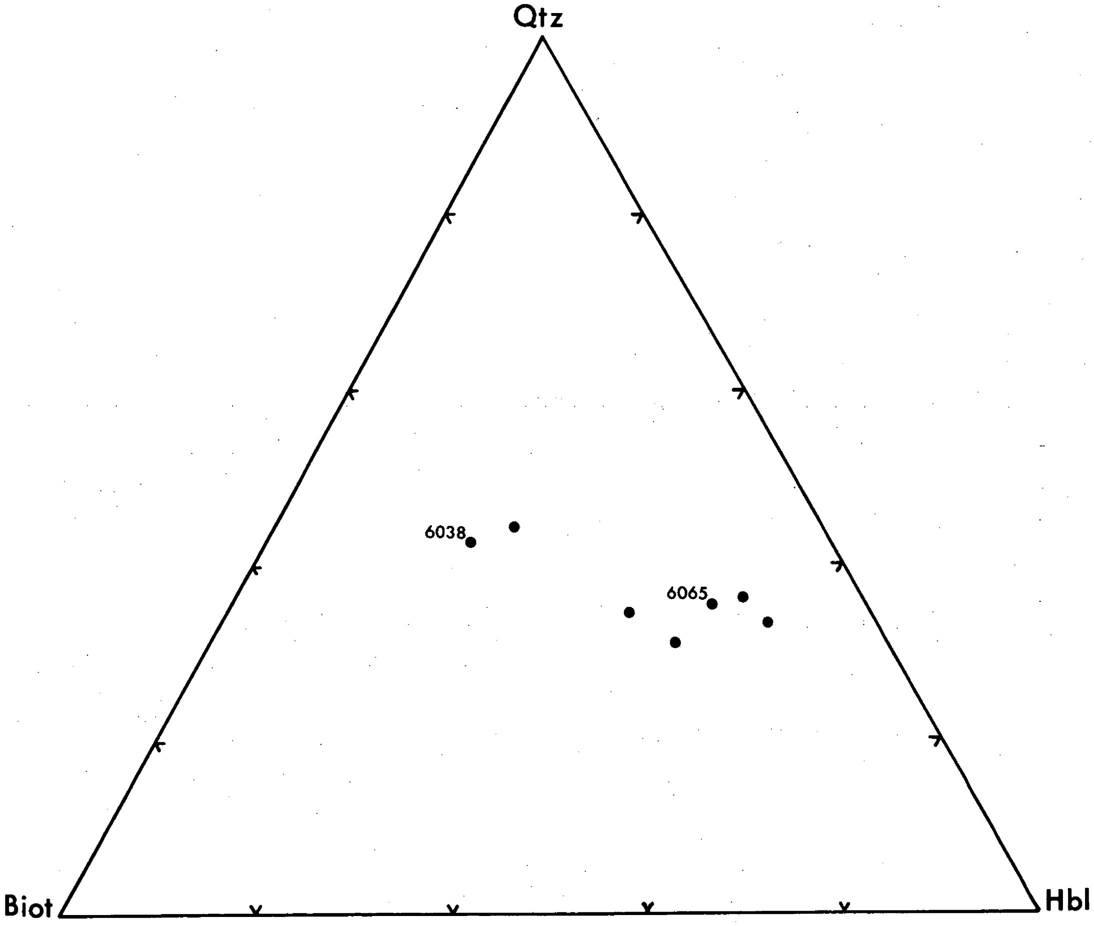

Fig. 5 Quartz-Biotite-Hornblende relationships in the Windy Creek Diorite.

confirms minor quartz variation and significant changes in the feldspar/mafics ratio (Fig. 6).

3.1.3 Chemistry

Major element chemistry for the Windy Creek Diorite is listed in Table B-1, Appendix B, and a composite diagram (Fig. 7) illustrates variations in individual oxides. Considerable fluctuation within the fresh diorite is due to varying hornblende/biotite and feldspar/mafics ratios. Silica contents are restricted, ranging from 58.7% to 61.9%, although typically about 59.9%. The higher silica content of sample 6049 (Table B-1) corresponds to high quartz in the mode (Table 2). Two peaks in the Al_2O_3 variation diagram (samples 6059 and 6049) correspond with higher Na_2O contents, lower FeO and MgO contents and increased amounts of modal feldspar.

Sample 6049 has minimal MgO, TiO_2, CaO and P_2O_5 contents but has the highest Fe_2O_3. The level of K_2O may be used as an index of biotite content. A majority of oxides occur as major constituents of more than one mineral phase (i.e. CaO in plagioclase and hornblende) and consequently elemental ratios will not be sensitive indicators of mineral variation. A lower CaO content may reflect either lower feldspar or hornblende and ratios involving calcium will not vary in a straightforward manner.

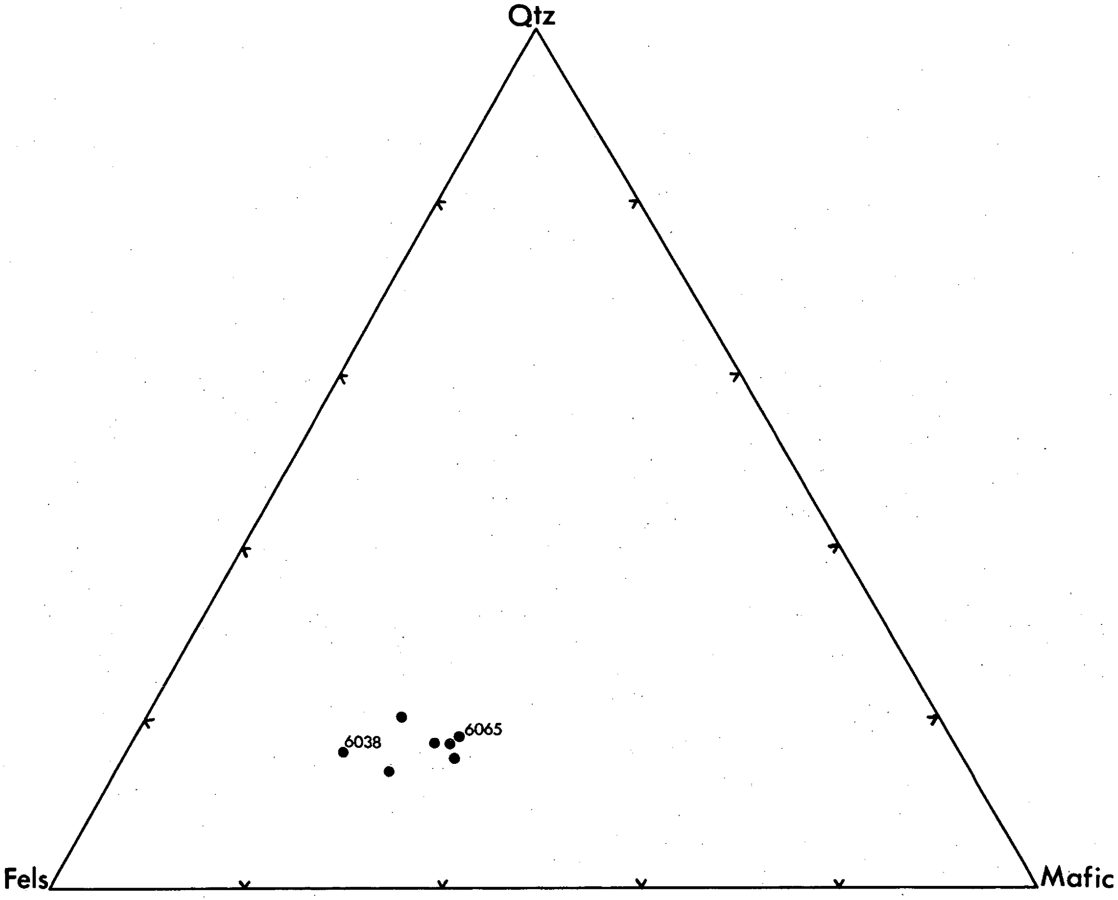

Fig. 6 Quartz-Feldspar-Mafics relationships in the Windy Creek Diorite.

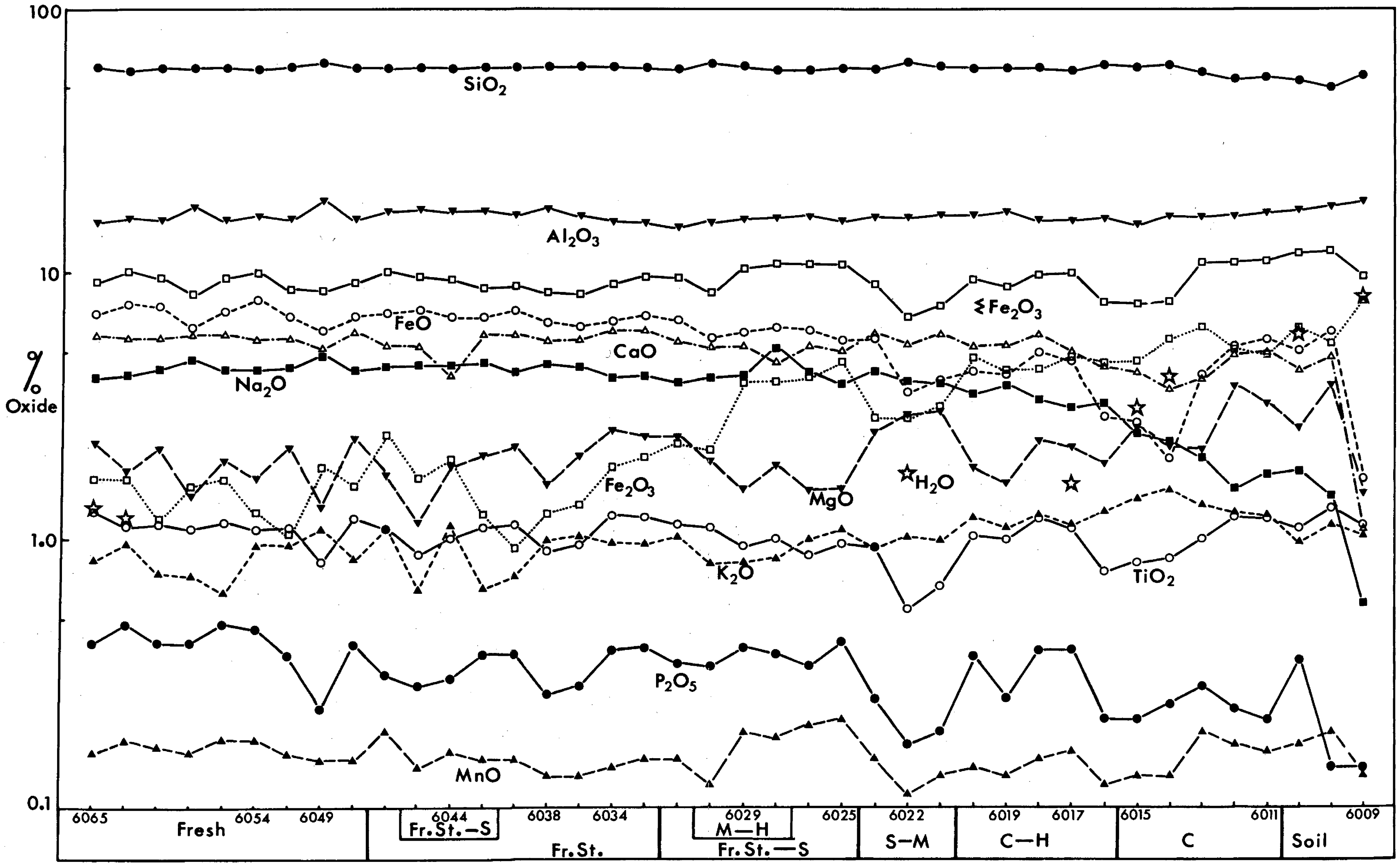

Fig. 7 Oxide variation diagram for fresh and weathered Windy Creek Diorite.

Table B-1 includes Fe^{++}/Fe^{+++}, Na/K, Na/Ca, Ca/Mg and Fe/Mg ratios. The Fe^{++}/Fe^{+++} ratio will indicate the degree of oxidation or weathering while the remaining ratios may be useful for tracing the susceptibility of different minerals to weathering.

3.2 WEATHERING VARIATION

3.2.1 Fresh-stained joints (FR.ST)

Weathering of the quartz diorite is not uniform and generally coarse-grained rock weathers preferentially. The contact zone with the Twins Creek gneiss is frequently deeply weathered but localised faulting or shearing noticeably enhances weathering processes.

Samples from the interval 118 feet to 190 feet have minor limonite stains on a majority of joints although some are sealed with calcite. Initial weathering is typified by coated joints with fresh rock in between. Joints may provide channel-ways for percolating groundwater. Below 134 feet (sample 6036), quartz diorite has retained its character with only a grain size change (a majority is medium to coarse-grained - Appendix A). Fine grained diorite predominates in the interval (118-134 feet) and a light grey colour is normal. Variable sericitic alteration of plagioclase and chloritisation of biotite are the only gross mineralogical changes seen in this zone. The drill log (Appendix A) notes a small basic dyke between 172 feet and 173 feet with a slightly altered zone extending from 170 feet to 180 feet (sample 6043-6045). Samples 6045 to 6043 display variable degrees of retrogressive alteration as shown by biotite (6044) which is nearly totally replaced with chlorite and heavy sericitisation of feldspar.

Major element changes are predictably minor and continue to reflect varying felsics/mafics and hornblende/biotite ratios. Altered joint material will constitute a small fraction of the bulk sample while the majority will be essentially fresh rock. Consequently SiO_2, Al_2O_3, FeO, Na_2O, TiO_2, K_2O and P_2O_5 values lie within the range of fresh rock variation. Remaining oxides however do show larger variations either as a consequence of dyke intrusion (samples 6043-6045) or incipient weathering. The CaO content of sample 6044 is noticeably lower and may be attributed to chloritisation of hornblende and alteration of plagioclase. A larger dispersion of Fe_2O_3 reflects the nature of sampling procedure and variable weathering processes.

The finer grain-sized phase of the diorite appears to be more hornblendic, a conclusion supported by higher

MgO contents for samples 6035 to 6033. Lower MnO contents are also related to varying feldspar/mafics and hornblende/biotite ratios.

3.2.2 Fresh-stained to slight weathering (FR.ST.-S)

Below 70 feet, the diorite has been slightly weathered but the interval 94 feet to 111 feet is moderately to highly altered. Core loss occurred between 101 feet and 104 feet and it is probable that this zone is completely to highly altered. Samples 6028 to 6031 are from the altered zone but petrographically do not reveal a marked change in mineralogy.

The remaining samples 6032 and 6027 to 6025 have altered biotites set in a groundmass outlined by alteration products. Sample 6032 marks the change from a olive-green biotite to those with a rusty orange colour. This colour change is associated with considerable liberation of limonite or iron oxides which stain the groundmass. Disaggregation is enhanced by swelling biotite as it exfoliates. Duller colours develop for some cleavage fragments and many of the cleavage traces or edges develop a "fine crinkled edge". Sericitic cover on plagioclase is highly variable and reaches a maximum for sample 6029.

Unfortunately the diorite varies considerably in this interval (Appendix A).

Initial variation due to parent rock heterogeneity still controls the nature of chemical changes.

3.2.3 Slight-moderate alteration (S-M)

Petrographically little change is visible within this zone and weathering is generally marked by a loss of cohesion, greater iron staining and incipient disaggregation. Plagioclase crystals do not display sharp grain boundaries, but sericitic alteration is only slight.

Variations in chemistry can again be related to dominant mineralogical control and sample 6022 is clearly quartz-rich. A considerable decrease in total iron, TiO_2, MnO and P_2O_5 is associated with appreciable increases in MgO. The Fe^{++}/Fe^{+++} ratio has decreased and weathering is progressively oxidising the FeO in the "diorite" (Fig. 7).

3.2.4 Completely-highly altered diorite (C-H)

In addition to exfoliated and altered biotites, plagioclase crystals show signs of breaking up and are extensively fractured. Sericitic cover on feldspars increases and may obliterate twinning and zoning for the more calcic cores. Hornblende appears to be unaffected by weathering processes, with only minor iron staining of cleavage traces and a possible rim of slightly bleached hornblende.

Above 40 feet, dry drilling was carried out with an NXC bit resulting in a good recovery of loose material above the water table but the core is intensely disturbed. Samples below 44 feet were thin-sectioned with normal techniques, but from the surface to this depth soil sections were made by Dr R. Brewer, CSIRO, Division of Soils. Textural studies have little relevance owing to the type of core material, but the extent of alteration of mineral phases originating from the parent diorite can be assessed.

Although parent rock induced variation is still present, weathering processes assert a dominating influence on the chemistry.

Destruction of plagioclase is reflected in loss of Na_2O and CaO towards the top of this zone. Ferrous/ferric ratios decrease and are generally less than unity. All elements associated with hornblende and biotite, i.e. FeO, MnO, MgO and TiO_2 continue to reflect the relative amounts of hornblende and biotite in the pre-existing parent rock. The dispersion of all oxides excluding Na_2O, CaO and K_2O lies within that shown by the fresh diorite.

Both K_2O and ΣH_2O increase, although water probably increases in sample 6016 only. The relative retention of K is related to secondary mica formation and clays which preferentially adsorb potassium. Both Na_2O and CaO are lost in solution.

3.2.5 Completely altered diorite (C)

Weathering processes remove plagioclase, and leave hornblende with quartz as relict phases. Practically all the biotite has been altered to a brown micaceous-like clay mineral. Samples 6015 and 6014 are similar chemically to the completely to highly altered zone. Progressive oxidation continues to sample 6014 but above this a reversal occurs. Total iron (ΣFe as Fe_2O_3) increases with a corresponding increase in FeO. Other oxides paralleling this effect are MgO, CaO and TiO_2 suggesting a relative enrichment of hornblende. Soil thin sections near this depth have increased amounts of hornblende which appears greenish-grey instead of slightly brown. Decreases in Na_2O and K_2O correlate with progressive removal of plagioclase and the decreasing importance of biotite or mica-like clays. Silica (SiO_2) commences to fall with sample 6013 departing from the restricted range of initial rock variation for the first time. Slight increase in Al_2O_3 and a notable rise in total water (ΣH_2O) is evident in Fig. 7. Minor oxides P_2O_5 and MnO roughly conform with the behaviour of oxides involved in hornblende residual enrichment.

Weathering continues normally to sample 6014 above which the residual enrichment of hornblende controls the major element chemistry.

3.2.6 Soil

The relative abundance and retention of hornblende exerts a dominant influence on the mineralogy and chemistry of material below 2.5 feet and above 10 feet. The uppermost surficial zone is impoverished in hornblende (sample 6009) and the green colour of the lower part of this zone is replaced by a strong brown. Soil thin sections do not demonstrate a definite reason for the sudden reduction in hornblende content between 1 and 2 feet (below 6009 and above 6127). The majority of hornblende crystals are fresh but many larger ones are surrounded by heavy iron oxide rims and all cleavage traces are heavily coated with a similar film. Hornblende may be removed by preferential settling through the soil matrix to a greater depth or, strong alteration in the uppermost soil horizons. The increase in slightly deeper parts of the core (upper completely altered zone) may support the former, although chemical attack cannot be denied.

Samples 6010 and 6127 are very similar to samples from the upper section of the completely altered zone but loss of hornblende for sample 6009 alters many oxides. Only SiO_2, Al_2O_3, Fe_2O_3 and total H_2O increase, while the remaining oxides sharply decrease.

Advanced weathering involving destruction of plagioclase and possibly hornblende (?) is only shown by sample 6009. Below this sample major element chemistry is either controlled by a relict mineral phase or by the total mineralogy of the parent rock.

3.3 ELEMENTAL RATIOS

A majority of elemental ratios fail to define distinct trends during the earlier stages of weathering, because many elements occur in more than one mineral phase. Variations in hornblende and biotite are difficult to monitor since CaO, FeO, MnO, TiO_2 and MgO are also essential components of either plagioclase or biotite. Modal analyses of fresh rocks demonstrate that high modal hornblende is accompanied by low modal biotite and vice versa (Fig. 5). Felsic to mafic ratios also vary with quartz remaining relatively constant.

Table B-1, includes the following ratios; Fe^{++}/Fe^{+++}, Na/K, Na/Ca, Ca/Mg and Fe/Mg. Little change is evident for Fe/Mg, Ca/Mg and Na/Ca until the completely to highly weathered zone is reached. Beyond this all ratios tend to decrease. The remaining ratios, Fe^{++}/Fe^{+++} and Na/K are sensitive to progressive alteration. The

Na/K ratio is effectively a measure of the plagioclase/biotite ratio, and the Fe^{++}/Fe^{+++} ratio a measure of weathering intensity. Fig. 8 a plot of iron oxidation state versus Na/K reveals a progressive decrease in both ratios as plagioclase weathers and iron is progressively oxidised. Other ratios are affected by the preferential retention of hornblende in all but the top sample, but they also show a similar decrease for very weathered material.

3.4 X-RAY DIFFRACTION STUDIES

The changing mineralogy has been studied by petrographic rock thin sections, soil thin sections and X-ray diffraction. Fresh rock variation can be determined by modal analysis and confirmed by the relative intensities of diffraction peaks characteristic of quartz, hornblende, plagioclase and biotite.

Alteration displayed by samples 6043-6045 as a result of dyke intrusion is confirmed by X-ray diffraction. Biotite lines disappear and are replaced by sharp reflections of chlorite. Both quartz and feldspar seem relatively unaffected but hornblende lines are reduced in intensity, corresponding with lower hornblende contents. Chlorite development is most marked in sample 6044, while sample 6045 has only minor

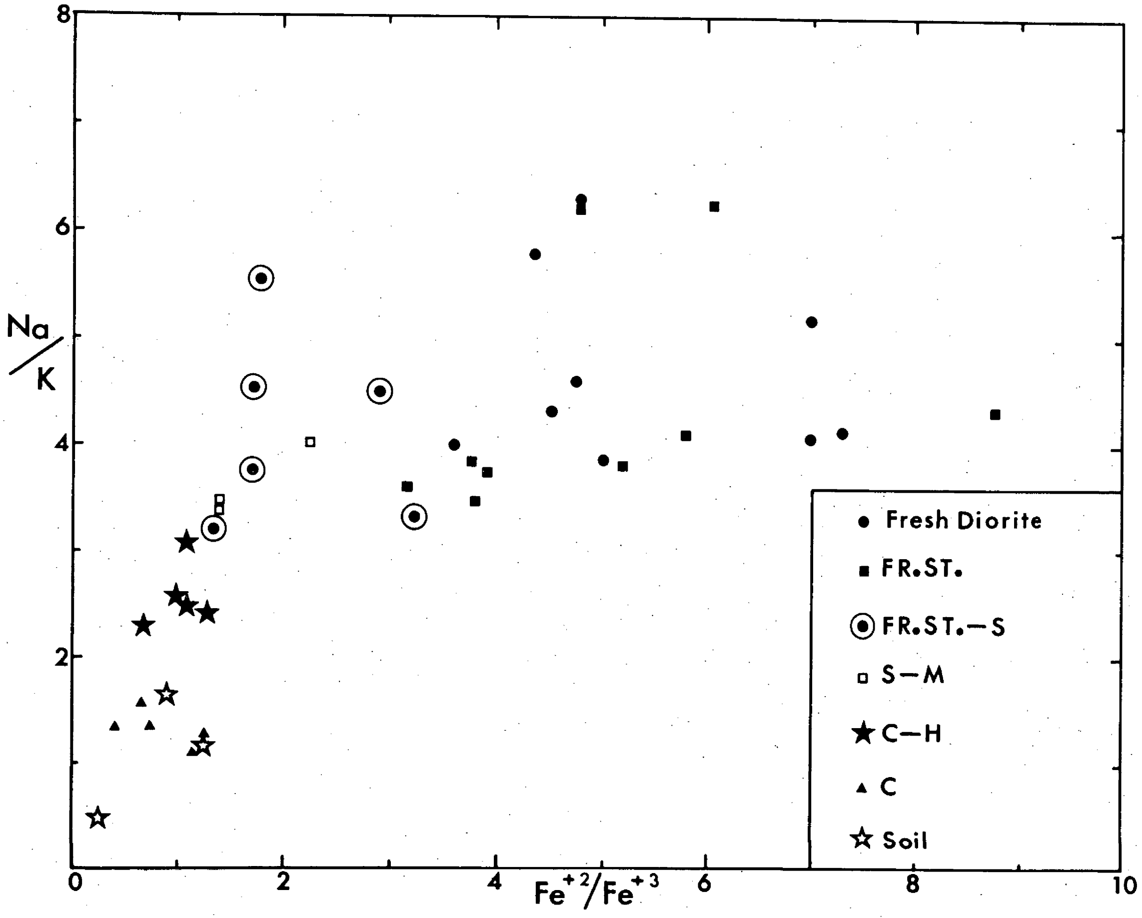

Fig. 8 Na/K and Fe^{+2}/Fe^{+3} behaviour during weathering of quartz diorite.

chlorite associated with reduced plagioclase, quartz and hornblende peaks.

Whole "rock" powders only reveal a significant chlorite-vermiculite component above sample 6020, excluding alteration of samples 6045-6043. Below this depth, all changes shown by diffraction patterns are due to the variability of the parent rock. Above 6020 the chlorite-vermiculite component gradually increases with the biotite percentage. A noticeable broadening of biotite 10Å peaks occurs with decreasing depth. This trend continues up to sample 6011 (depth 10 feet) above which 10Å peaks disappear. Samples 6010, 6127 and 6009 consist largely of relict quartz and hornblende with clay minerals. Weak feldspar (plagioclase) reflections are still present in sample 6009 but plagioclase increases markedly with increasing depth. Hornblende, although present in sample 6009, is much more abundant in samples 6127 and 6010, confirming the residual enrichment seen in soil thin sections. Sharp reflections for hornblende in these samples also suggest that little alteration of residual crystals has occurred. The absence of biotite reflections in samples 6009, and 6127 supports petrographic observation of lack of biotite, although fine size fractions ($< 2\mu$-5μ) were not examined.

In the absence of combined sedimentation and size fraction studies, definite clay mineral identification cannot be obtained. A detailed study of clay types or polymorphs was not the aim of this work, but X-ray diffraction patterns suggest the formation of complex inter-layered or inter-stratified vermiculite-chlorite with illite and possibly minor kaolinite. This type of clay mineral assemblage requires a combination of methods including DTA, infra-red and X-ray techniques for precise identification.

CHAPTER 4

PETROGRAPHY AND CHEMISTRY OF THE SCAMELS GRANITE

The Scamels Granite forms massive outcrops at Granite Knob and bouldery outcrops on the west bank of Bogong Creek. Adjacent to DH 2511, there are few outcrops of granite except for broadly jointed exposures, in deeply entrenched sections of Bogong Creek (Fig. 9).

The granite is pale pink to grey, medium to coarse-grained and has a small percentage of biotite. Muscovite is locally abundant. Guy (1969) has mapped both the Dargals Granite to the north and Scamels granite as the one mass. The main mass of Dargals granite includes the Welumba granite (Ja-1 of Kolbe and Taylor, 1966).

4.1 FRESH ROCK VARIATION

4.1.1 Petrography

The potash feldspar to plagioclase and biotite to muscovite ratios vary as a result of late-stage hydrothermal alteration. Joints in the fresh granite are frequently slickensided with calcite veneers and clay fillings suggesting movement along joint planes. Dark grey fine-grained zones, (geological log, Appendix

Fig. 9 The location of DH 2511 and geology of the adjacent area.

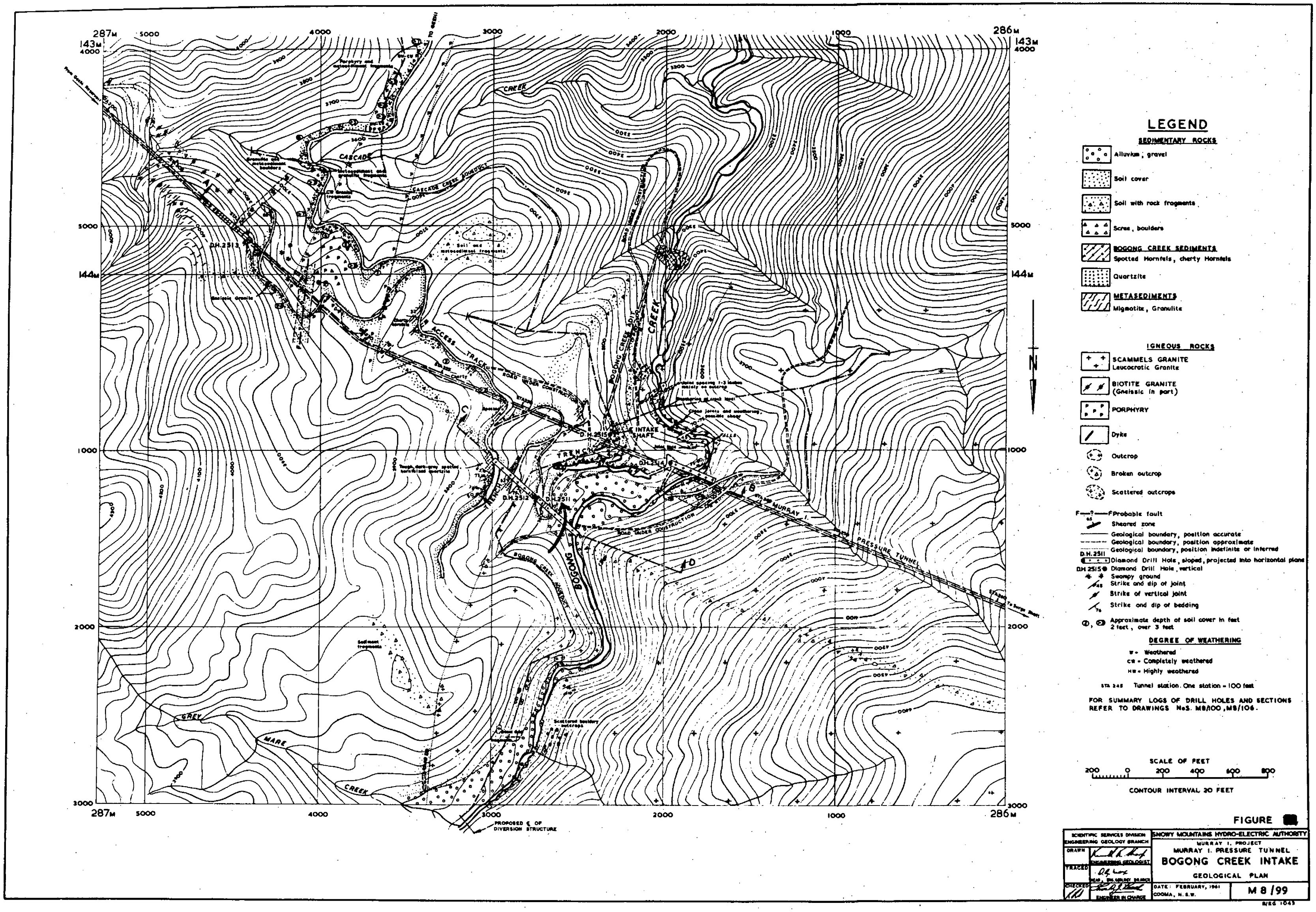

A) were avoided during sampling, although fine bands occurring at regular sampling intervals were included. Fresh granite was intersected below 243 feet in DH 2511 (sample sequence 6101-6066).

Quartz, potassium feldspar, plagioclase and biotite are essential minerals with accessory opaques, muscovite, fluorite and zircon. Incomplete and partial alteration of biotite to chlorite or masses of iron oxides are frequently noted within the area of one thin section. The intensity of secondary sericitization is directly related to the extent of biotite alteration and the presence of fractures.

Quartz is variable in amount and frequently displays undulose extinction. Large crystals with rare inclusions of muscovite are present in the major phase of the granite. Porphyritic phases, however, have bipyramidal quartz with embayments or invaginations of fine groundmass and signs of resorption. Quartz veins are rare but highly altered variants (dark grey zones) have higher quartz contents (sample 6079).

Potassium feldspar commonly ranges from 30% to 40% and displays Carlsbad twinning. Patch, stringer and vein perthites are well developed with occasional discontinuous rims of exsolved soda feldspar. Complete alteration of potassium feldspar in dark grey zones has occurred and its absence has been confirmed by staining.

Plagioclase varies from 20% to 36% of the granite often forming large subhedral laths in addition to smaller grains. Large crystals (An_{10}) are mildly zoned, twinned and rarely broken by fracturing. Occasional minor patches of myrmekite are developed. Alteration products normally are dominated by sericite but minor epidote and carbonate also are present. Cores of zoned crystals are more altered than the rims with sericite obscuring the feldspar.

Biotite is usually ragged, frequently altered and often has many pleochroic halos around small inclusions. A complete range from fresh flakes to completely altered patches commonly occurs within the area of one thin section. Alteration to chlorite is less common than to an iron oxide patch with occasional interleaves of biotite or chlorite. Fresh biotite is pleochroic, dark green-olive to a pale straw-yellow, but occasionally dark red-brown to pale straw. Both calcite (carbonate) interlayers and muscovite replacement have been noted petrographically.

Muscovite in unaltered granite is usually a rare accessory but in altered samples it may increase to 17% of the granite. Muscovite development is related to fractures and fissures in the granite. Blades of muscovite appear to grow away from fractures into feldspars initially but may eventually replace all feldspars with a mass of muscovite.

Carbonate is a secondary mineral phase strongly related to fracture zones and alteration processes. Small microcrystalline grains are present on altering feldspars only when large fractures have carbonate fillings. A direct relationship between carbonate and muscovite content is lacking although both phases are related to the development of shear or fracture zones.

Accessory minerals include opaques (magnetite and less commonly haematite), zircon, fluorite, chlorite as alteration of biotite, and epidote as alteration of plagioclase and biotite adjacent to rare quartz veins.

4.1.2 Modal analyses

Table 3 lists modal analyses for three granite samples (6067, 6082 and 6089) and one altered sample (6079). Two modal analyses from Kolbe and Taylor (1966) and Guy (1969) have been included in Table 3. The plagioclase to potash feldspar ratio is variable.

4.1.3 Chemistry

Analyses of DH 2511, Scamels granite are given in Table B-2, Appendix B, and displayed in Fig. 10. Table 4 compares the average unaltered composition of fresh granite from DH 2511 with analyses of Scamels Granite

Table 3

Micrometric Analysis of Scamels Granite

Sample	Quartz	Potash Feldsp.	Plag.	Biot.	Access.[*]
6067	31.1	37.1	28.8	2.9	0.1
6082	36.0	30.3	29.2	3.3	1.1
6089	30.5	30.2	35.7	3.5	0.1
6079	50.8	6.2	20.8	-	22.3[+]
SC-1[1]	40-45	40	20	2-3	-
Ja-1[2]	45	15	35-40	2	1
21821[3]	39.2	30.4	27.7	2.4	0.2
21827[4]	36.0	40.2	19.7	4.0	0.1

[*] May include Muscovite

[+] Includes 16.5 Muscovite
1.6 Carbonate
4.2 Access.

[1] Kolbe and Taylor (1966). Sample SC-1, leucogranite

[2] Kolbe and Taylor (1966). Sample Ja-1, leucogranite

[3] Guy (1969). Spec. 21821, Adamellite, Dargals Granite

[4] Guy (1969) Spec. 21827, Granite, Dargals Granite

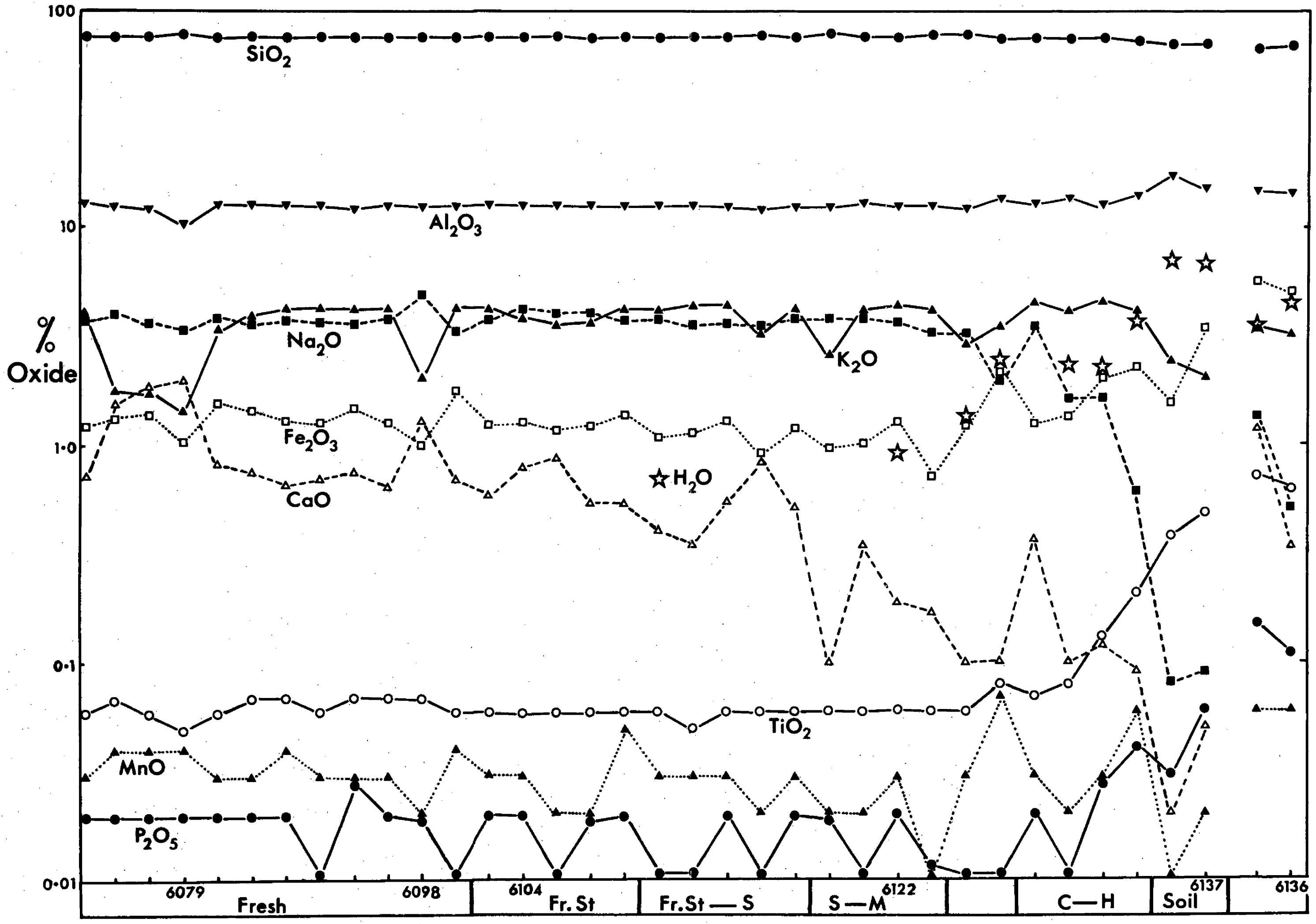

Fig. 10 Oxide variation diagram for fresh and weathered Scamels Granite.

Table 4

Chemical Analyses of Scamels and Dargals Granites

Oxide	1	2	3	4	5
SiO_2	76.48	75.10	75.37	77.02	76.74
TiO_2	0.07	0.10	0.06	0.10	0.01
Al_2O_3	12.88	13.85	13.8	12.02	12.53
Fe_2O_3	1.44	1.29	0.87	0.61	0.33
FeO				0.61	0.92
MnO	0.03	0.03	0.06	0.06	0.07
MgO	0.02	0.16	0.086	0.23	0.18
CaO	0.71	0,78	0.50	0.65	0.65
Na_2O	3.72	3.72	3.65	3.63	3.35
K_2O	4.13	4.46	4.71	4.79	4.79
P_2O_5	0.02	-	-	0.01	0.03
H_2O^+	-	-	-	0.41	0.48
H_2O^-	0.16	-	-	0.09	0.10
CO_2	-	-	-	-	-
	99.66	99.46	99.05	100.23	100.18

1. Average of eight analyses of fresh, unaltered Scamels granite from DH 2511
2. Spec. SC-1, leucogranite, Kolbe and Taylor (1966)
3. Spec. Ja-1, leucogranite, Kolbe and Taylor (1966)
4. Spec. 21821, Adamellite, Guy (1969)
5. Spec. 21827, Granite, Guy (1969)

(SC-1, Kolbe and Taylor, 1966) and Dargals Granite (Ja-1, Kolbe and Taylor, 1966; 21821 and 21827, Guy, 1969).

Fresh granite from DH 2511 is characterized by high SiO_2 (76% to 77%), and low total iron, MgO and CaO. In Fig. 10, variations in Na_2O, K_2O and CaO are related to secondary muscovite and carbonate formation with breakdown of potash feldspar in sample 6079 (Table 3). The total alkali content is high, but samples 6070, 6074, 6079 and 6098 have low K_2O, higher CaO and variable Na_2O contents relative to fresh unaltered granite. Total alteration has only approached completion for sample 6079 in which higher SiO_2, lower Al_2O_3, TiO_2 and total iron contents are significantly different from fresh granite.

High CaO and CO_2 contents can be petrographically related to the presence of secondary carbonate for samples 6079 and 6098.

All remaining fresh granite analyses are remarkably uniform for a granite with considerable variation in grain size and porphyritic character.

Elemental ratios are sensitive to alteration processes but many elements occur in more than one mineral lattice as essential components. K/Na, Na/Ca and Fe^{++}/Fe^{+++} ratios are decreased by alteration processes but Ca/Mg ratios are variable.

In Table 4, an average of eight fresh unaltered Scamels granite samples are compared with analyses from Kolbe and Taylor (1966) and Guy (1969). Guy (1969) has mapped all granites as members of the one granitic mass and the major element chemistry is very uniform. Minor variations in Na_2O and K_2O are the only differences and a Na_2O-CaO-K_2O plot (Fig. 11) supports the leucocratic character of all granites analyses from this mass.

4.2 WEATHERING VARIATION

4.2.1 Fresh-stained joints (FR.ST.)

Scamels granite is mildly porphyritic within this interval with phenocrystic quartz and feldspar. Petrographic evidence for iron staining (limonite) is visible in sample 6106, but the geological log (Appendix A) places the base of limonite staining at 243 feet, (between samples 6101 and 6102). Biotite alteration is highly variable and ranges from chlorite to iron-rich residual grains. Samples 6104 to 6106 have carbonate veins and occasional grains of carbonate as alteration products on feldspar. The development of secondary muscovite is limited, however, sample 6107 has pronounced secondary muscovite alteration modified by limonite staining. Samples 6108 to 6110 lack evidence of

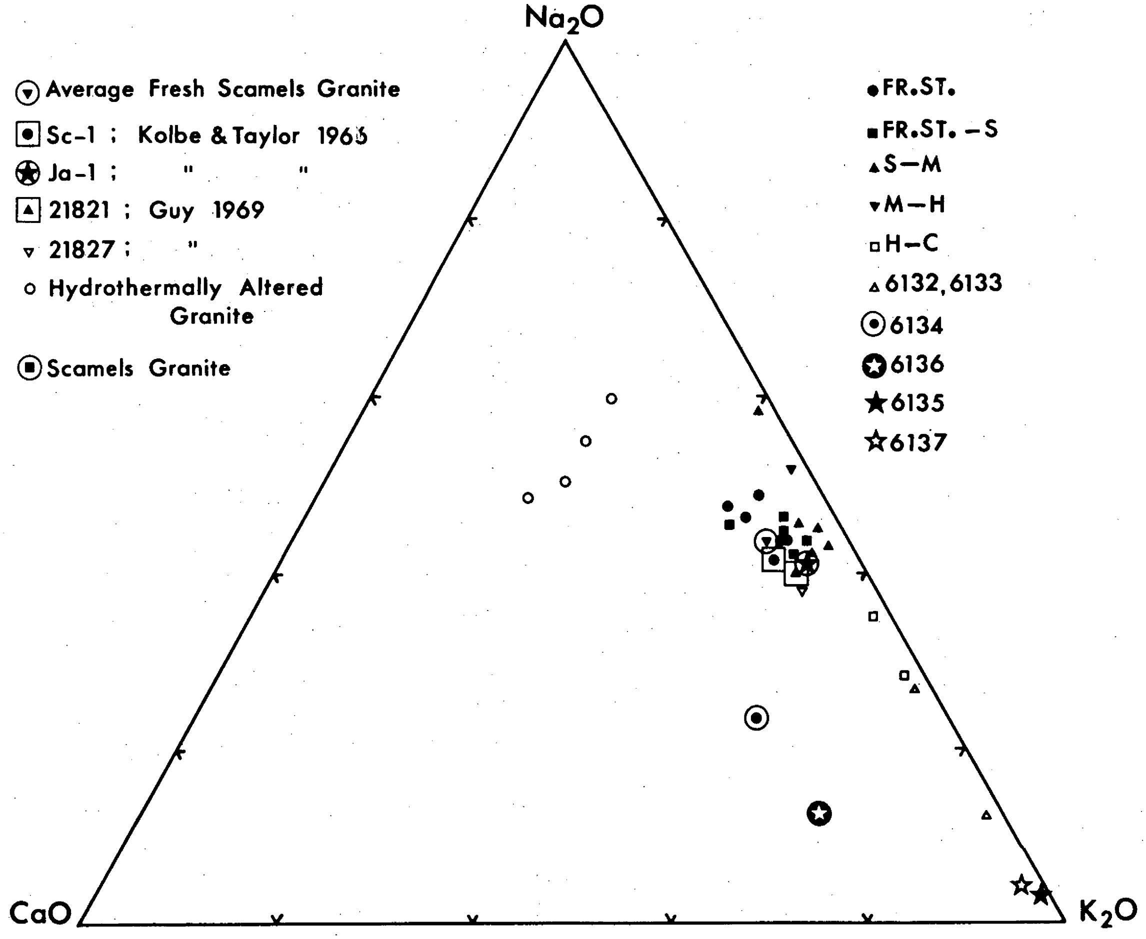

Fig. 11 Na_2O-CaO-K_2O diagram of data from the Scamels Granite.

iron-staining and may be unaffected by weathering processes. Wider joint spacings (Appendix A) reduce the percentage of joint alteration in samples.

Table B-2 and Fig. 10 confirm the lack of significant change for a majority of elements. Higher carbonate contents of samples 6104 and 6105 are supported by higher CaO contents. Muscovite alteration noted for sample 6107 has not altered the major element chemistry significantly although K_2O and CaO contents are lower. K/Na and Ca/Mg ratios do not change appreciably but Na/Ca ratios increase marginally.

4.2.2 Fresh-stained to slight weathering (FR.ST.-S)

The interval from 158 feet to 200 feet (samples 6111 to 6118) has stained joints and is slightly weathered granite. A pronounced porphyritic variant of the granite is represented by samples 6111 to 6116 (Appendix A), and although sample 6118 has a reduced phenocryst content it is similar chemically to the former granite. An altered zone within this interval is represented by sample 6117. This sample has relict quartz phenocrysts distributed in a muscovite and fine quartz groundmass. Extensive shearing with secondary infilled carbonate has considerably altered this sample.

Little change in chemistry is apparent in Fig. 10. With the exception of sample 6117, all oxides lie within the range of fresh rock contents. The alteration of samples 6079, 6098 and 6117 is similar and they share common differences from the fresh granite. Higher SiO_2 and CaO with lower Al_2O_3, K_2O, Na_2O, total iron and MnO are a result of potash feldspar breakdown to form muscovite. Fractures and shears have aided this alteration and were later filled with carbonate. Weathering proceeds down fissures and shears at a faster rate than laterally into the granite.

K/Na and Ca/Mg ratios are insensitive to these weathering processes but the Na/Ca ratio increases with weathering.

4.2.3 Slight to moderate weathering (S-M)

This zone is marked by samples which are relatively unweathered (6120, 6122) and highly fractured samples adjacent to joint planes (samples 6119, 6121 and 6123). Iron staining or limonite films are absent in samples 6120 and 6122 but sample 6119 is extensively altered. Sample 6124 is more weathered than samples 6120 and 6122. Muscovite development without carbonate is well pronounced in sample 6119, however feldspar is still present. Plagioclase crystals are sericitized and alteration products obscure the central sections of many crystals.

With the exception of sample 6119 major element oxides are relatively uniform. Preferential weathering of plagioclase is suggested by slightly lower Na_2O and CaO contents and a low total iron content of sample 6124 may support leaching. Samples 6079 and 6119 are similar and hydrothermal alteration produces a consistent chemical change. The loss of CaO may be related to active leaching along fractures and joints by weathering solutions.

Although K/Na ratios remain constant, Na/Ca ratios increase markedly while Ca/Mg ratios decrease. Progressive oxidation is suggested by a lower Fe^{++}/Fe^{+++} ratio and increasing hydration by a higher total water content.

Sample 6128 (110 feet) is also slightly to moderately weathered and may represent the core of a buried weathered boulder. Although TiO_2 is marginally higher, this sample is similar to samples 6120, 6122 and 6124.

4.2.4 Moderate to high weathering (M-H)

Only one sample (6125) represents a narrow zone (121 feet to 130 feet) with this degree of weathering. Thin sections reveal limonite staining and complete alteration of biotite to iron oxides. The presence of minor muscovite may indicate slight hydrothermal alteration with a heavier development of sericite on feldspars.

Al_2O_3, Na_2O, K_2O and CaO decrease and remaining oxides increase slightly. These changes are small but the increase in total water indicates advancing hydration and low Fe^{++}/Fe^{+++}, high Na/Ca and lower Ca/Mg ratios also support a greater degree of weathering alteration.

4.2.5 High to complete weathering (H-C)

This zone surrounds the fresher sample 6128 and is represented by samples 6126 and 6130. Both samples are heavily iron stained along grain boundaries and in fracture zones. Disaggregation is increasing with a loss of cohesion between individual grains.

Increased Al_2O_3, slightly higher total iron and TiO_2 are associated with lower Na_2O, K_2O and CaO contents. Increased weathering intensity is supported by high Na/Ca, low Ca/Mg and low Fe^{++}/Fe^{+++} ratios.

4.2.6 Complete to highly weathered granite (C-H)

Although three samples were taken from the interval 80 feet to 90 feet, discontinuous core recovery and disturbed samples made sample identification difficult. Sample 6132 is weathered Scamels granite but sample 6134 is a highly weathered biotite granite of different mineralogy than the Scamels granite. Sample 6133 may be a composite sample, with a minor amount of weathered biotite granite. Weathering of Scamels granite as shown by sample 6132 is represented by increasing loss of cohesion and limonite staining. Sericitic alteration of feldspars is no heavier than for sample 6125 but feldspars may be altering to clay.

Increasing P_2O_5, MnO, TiO_2, total iron, total water and Al_2O_3 with decreasing CaO, Na_2O, K_2O and SiO_2 suggest progressive weathering of feldspars with formation of clays.

4.2.7 Soil

Although samples 6135 and 6137 are covered by a considerable thickness of slopewash (Appendix A) they probably represent a residual soil developed from Scamels granite. Petrographically both samples consist largely of quartz, altered feldspar, minor muscovite and odd grains of biotite in a silasepic groundmass, Brewer (1964). Extreme disturbance during drilling does not permit fabric analysis.

Large chemical changes are confined to Na_2O, CaO and K_2O, which decrease markedly, and TiO_2 and H_2O which sharply increase. Subdued changes are shown by MnO, Al_2O_3 and SiO_2 which decrease slightly while total iron increases marginally. The Fe^{++}/Fe^{+++} ratio is very low while the K/Na ratios are high. In the upper section of the weathering profile Ca/Mg ratios fall along with Na/Ca ratios as a consequence of feldspar alteration.

The weathered biotite granite boulder (samples 6134 and 6136) conforms to the weathering trend displayed by the Scamels granite. The Fe^{++}/Fe^{+++} ratio decreases along with Ca/Mg ratios however K/Na and Na/Ca ratios increase. Although both granites are unrelated, Figs. 12 and 13 include data for samples 6134 and 6136.

4.3 ELEMENTAL RATIOS

A plot of Fe^{++}/Fe^{+++} ratio versus Na/Ca ratio (Fig. 12) reveals an early marked decrease in Fe^{++}/Fe^{+++} ratio. This initial drop is a consequence of low primary iron content and limonite staining. Further weathering is not readily monitored by Fe^{++}/Fe^{+++} ratios as early oxidation masks later changes. Hydrothermal alteration of the granite to a muscovite-quartz-carbonate assemblage also reduces the Fe^{++}/Fe^{+++} ratio and decreases the Na/Ca ratio.

As alteration intensity increases the Na/Ca ratio increases with removal of carbonate and selective weathering of the more calcic cores of plagioclase crystals. Total alteration of plagioclase however reverses the trend of Na/Ca ratios.

Weathering of both biotite and Scamels granites results in a convergence towards a common end product in Figs. 12 and 13.

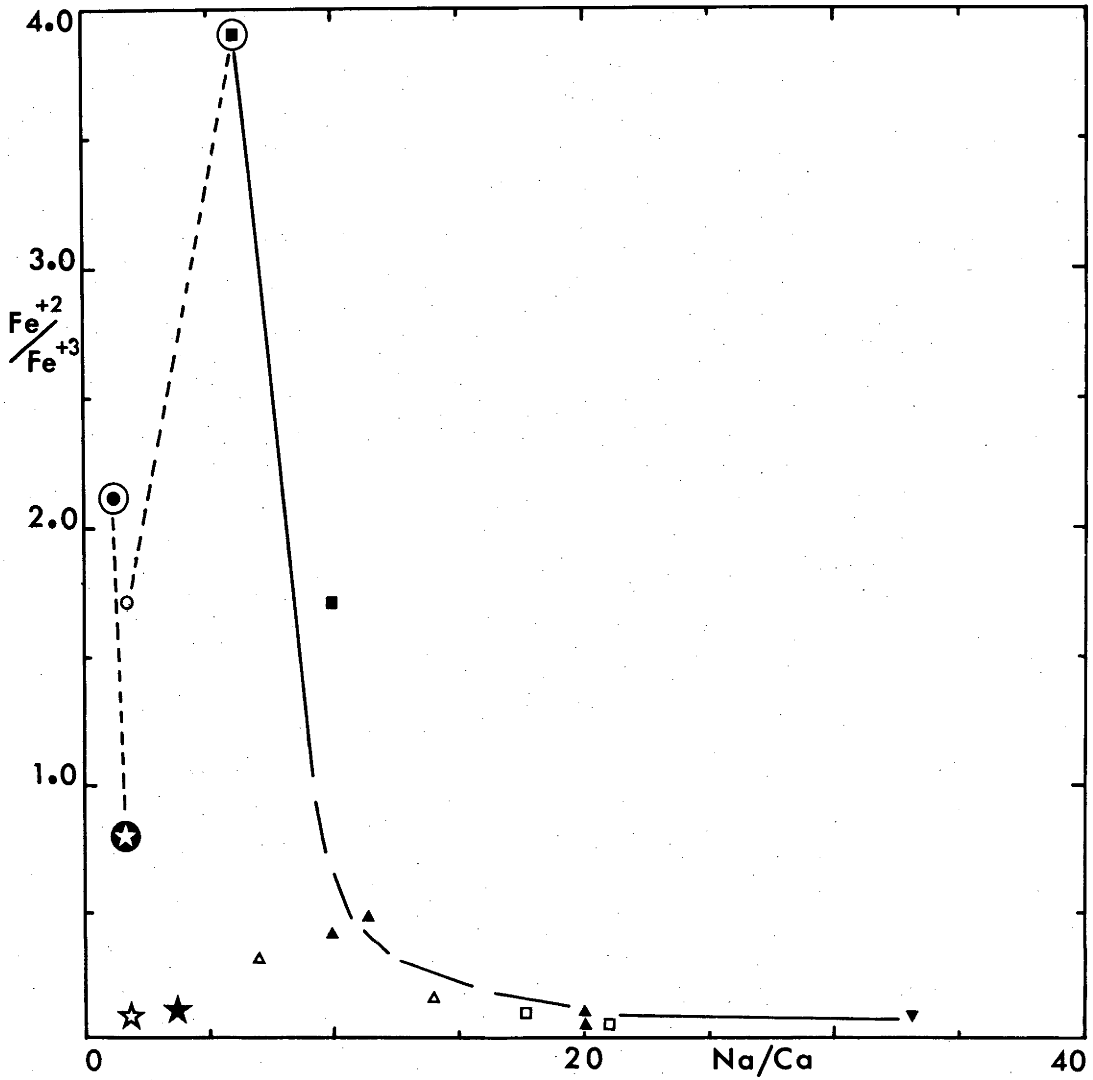

Fig. 12 Fe^{+2}/Fe^{+3} and Na/Ca behaviour during weathering of Scamels Granite. (Symbols as in Fig. 11).

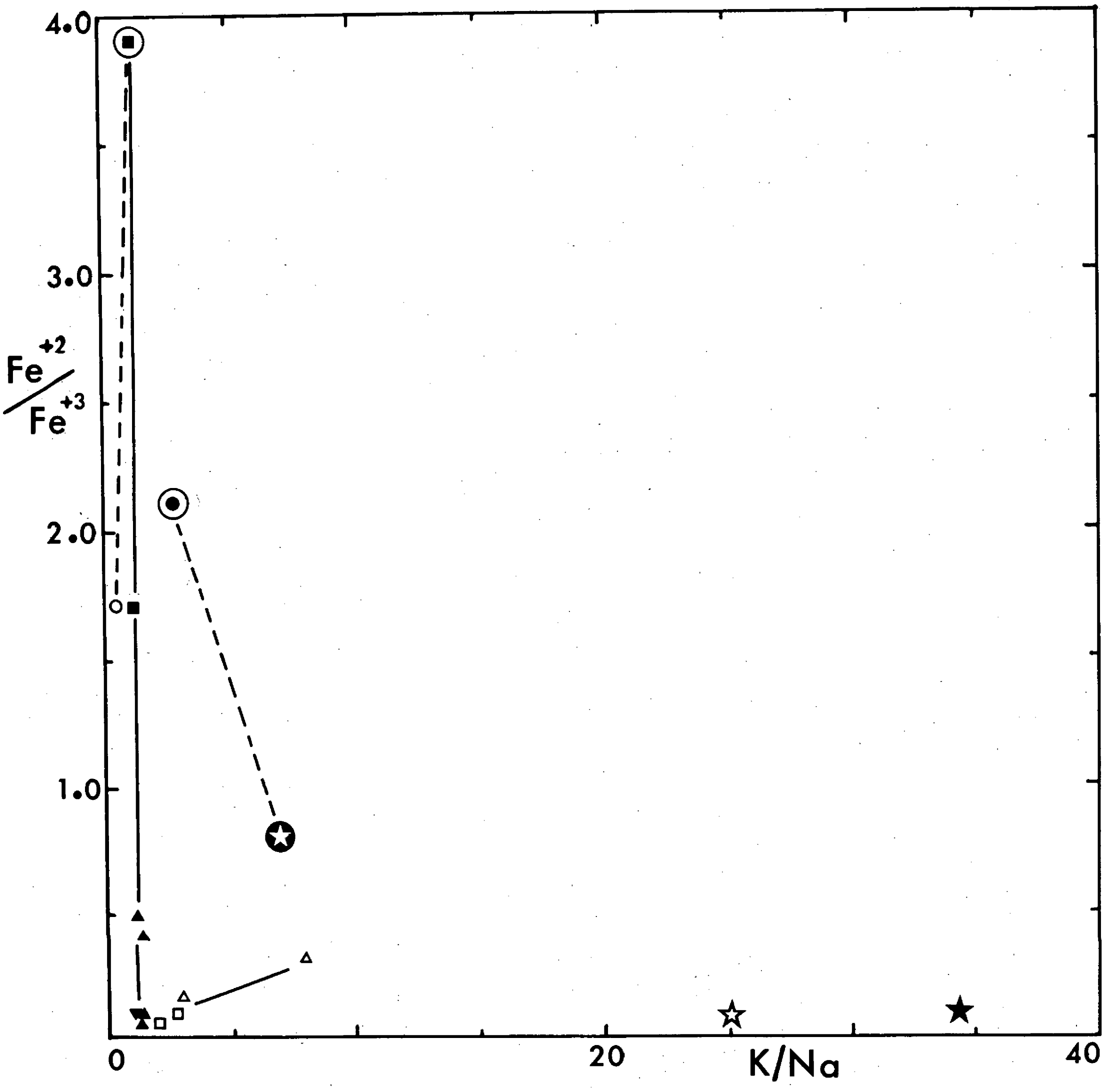

Fig. 13 Fe^{+2}/Fe^{+3} and K/Na behaviour during weathering of leucogranite. (Symbols as in Fig. 11).

Fig. 13, also suggests the possibility of contamination of sample 6133 with weathered biotite granite. Soil samples may have dual parentage and this possibility cannot be excluded on the basis of major element data.

4.4 X-RAY DIFFRACTION STUDIES

Diffractometer traces confirm varying proportions of plagioclase and potash feldspar with variable muscovite contents. With weathering minor iron oxide lines appear and plagioclase lines decrease in intensity. A 7Å phase forms and the area under the 10Å muscovite peak broadens. These changes suggest the formation of kaolinite and illite from feldspar weathering. In the progression 6130-6132-6135-6137 kaolinite increases along with quartz and illite. Gibbsite appears in samples 6135 and 6137 and hydrated iron oxide peaks disappear. Feldspars decrease, with plagioclase altering more rapidly than potash feldspar. Minor traces of potash feldspar are still present in sample 6137. The percentage of muscovite does not appear to increase noticeably.

Samples 6134 and 6136 consist largely of quartz, plagioclase and biotite with lesser amounts of potash feldspar. Although sample 6134 is highly weathered, complete weathering (6136) involves further loss of plagioclase and potash feldspar. Biotite peaks are many times more intense than weak muscovite reflections shown by Scamels granite samples, but decreasing biotite is shown by sample 6136. Kaolinite and illite increase also.

Sample 6133 has a 10Å reflection intermediate between samples 6132 and 6134 suggesting the possibility of appreciable addition of weathered biotite granite to weathered Scamels granite.

The absence of appreciable vermiculite-chlorite or biotite reflections in samples 6135 and 6137 supports derivation from weathered Scamels granite. Sample 6133 however may have an appreciable weathered biotite granite component.

CHAPTER 5

PETROGRAPHY AND CHEMISTRY OF THE KHANCOBAN GRANITE

Khancoban granite exposures consist largely of boulders and broadly jointed outcrops except along the western side of Clews Ridge. In the vicinity of the Khancoban-Yellow Bog Fault there are practically no outcrops, all exposures being highly to completely weathered (Fig. 14).

The granite is pale pink to grey, medium to coarse-grained and generally massive. The mineralogy is variable but is "usually within" the following limits: quartz 28% to 35%, potash feldspar 18% to 20%, plagioclase 39% to 45%, biotite 6% to 8% and traces of muscovite (Sharp and Boucaut, 1963). Local phases are quartz rich and contain up to 8% muscovite with very little biotite. Guy (1969) has noted that most granitic phases are strictly granodiorites with biotite contents as high as 12%.

Minor aplite dykes intrude the granite locally and vary from inches to 20 feet in width. In DH 2660 two types of "dykes" were intersected and both have been described in the geological log (Appendix A) as "aplites" by SMA geologists. One aplite is a true potash aplite, however the other may be an altered phase of the granite rather than an unusual "soda aplite".

5.1 FRESH ROCK VARIATION

5.1.1 Petrography

The lower section of DH 2660 (samples 6228-6243) displays extensive evidence of shearing, fracturing and late-stage hydrothermal alteration. Unaltered granite is pale grey, medium to coarse-grained and massive (see Appendix A). Hydrothermal alteration is indicated by development of pink feldspars and chloritization of biotite. Occasional narrow altered zones are deep pink, crystalline and rather soft.

Many joints are polished and/or chlorite coated with a few slickensided and containing clay. Between 314 feet and 340 feet an "aplite" (geological log, Appendix A) was intersected by the drill hole, however it may be altered granite rather than aplite.

Quartz, plagioclase, potash feldspar, biotite and variable muscovite comprise the granite with additional minor chlorite and epidote. Accessory minerals include zircon, apatite, opaques and rarely tourmaline.

Plagioclase dominates the mineralogy (35% to > 40%) and is accumulophyric. Patchy zoning and twinning is often quite marked but may be obscured by sericitic alteration. Adjacent to fractures the cores of plagioclase crystals have patches of fine muscovite blades and epidote surrounded by heavy sericitic alteration. Details of the plagioclase crystals are frequently hidden and can be described only from less altered samples. Compositions range from approximately An_{20} to An_{40}.

Quartz is heavily stressed and grain boundaries appear to be sutured. The development of undulose extinction and kink bands is related to slip along planes within individual crystals.

Potash Feldspar is distinctly poikilitic enclosing plagioclase and biotite crystals. Fine perthite lamellae are visible and are rarely altered. Anomalous extinction and signs of stress and/or deformation are not uncommon. Fine myrmekite is developed epitaxially on plagioclase crystals enclosed in or abutting potash feldspar.

Biotite varies considerably from less than 5% to approximately 10% of the granite and is the only significant ferromagnesian mineral. Pleochroism is from dark olive-brown to straw-yellow, although a deep brown colour is shown by a few crystals. Pleochroic halos are common and alteration to epidote and chlorite is variable. Carbonate bands may separate chlorite layers in almost completely altered biotite (i.e. sample 6239).

Muscovite commonly crosscuts earlier formed minerals and is highly variable in amount. Large blades may be primary while smaller crystals on plagioclase laths represent alteration of the feldspar. Rarely muscovite-chlorite pseudomorphs occur after biotite.

Alteration minerals include chlorite, epidote, sericite and less commonly carbonate. Accessory minerals normally consist of zircon, apatite, opaque minerals, alteration products and rarely large grains of tourmaline near quartz veins.

5.1.2 Modal analyses

Heavy sericitic alteration and medium to coarse grain-size reduce the significance of micrometric analyses unless many thin sections are measured. Guy (1969) and Sharp and Boucaut (1963) have both stressed the variability of the granite which varies from granodiorite to adamellite locally. In thin section the relative amounts of plagioclase and potash feldspar vary but biotite contents are related to the intensity of hydrothermal alteration. Ranges of approximate modal analyses are given in Table 5.

5.1.3 Chemistry

Chemical analyses of the Khancoban granite are given in Appendix B, Table B-3 and displayed in oxide variation diagrams (Figs. 15 and 16). Table 5 lists

Table 5

Chemical analyses and modes of rocks from the Khancoban Granite

Oxide	1	2	3
SiO_2	70.90	70.20	73.26
TiO_2	0.28	0.26	0.24
Al_2O_3	14.12	15.83	12.79
Fe_2O_3	3.19	3.04	0.47
FeO			1.90
MnO	0.06	0.08	0.08
MgO	0.93	0.75	0.62
CaO	2.37	2.87	2.28
Na_2O	2.27	2.97	3.77
K_2O	3.21	3.57	4.23
P_2O_5	0.11	-	0.03
H_2O^+	(1.27)	-	0.46
H_2O^-		-	0.06
Total	98.71	99.57	100.19
Quartz	35-40	35-40	36.0
K-feldspar	20-25	30-35	21.0
Plagioclase	30-35	20	34.7
Biotite	5-10	7	8.3
Muscovite	1-5	2	-
Chlorite	<1-3	-	-
Epidote	1	1	-

1. Average of thirteen samples of fresh unweathered Khancoban granite
2. Spec. Kh-1, adamellite, Kolbe and Taylor (1966)
3. Spec. 21817, granodiorite, Guy (1969)

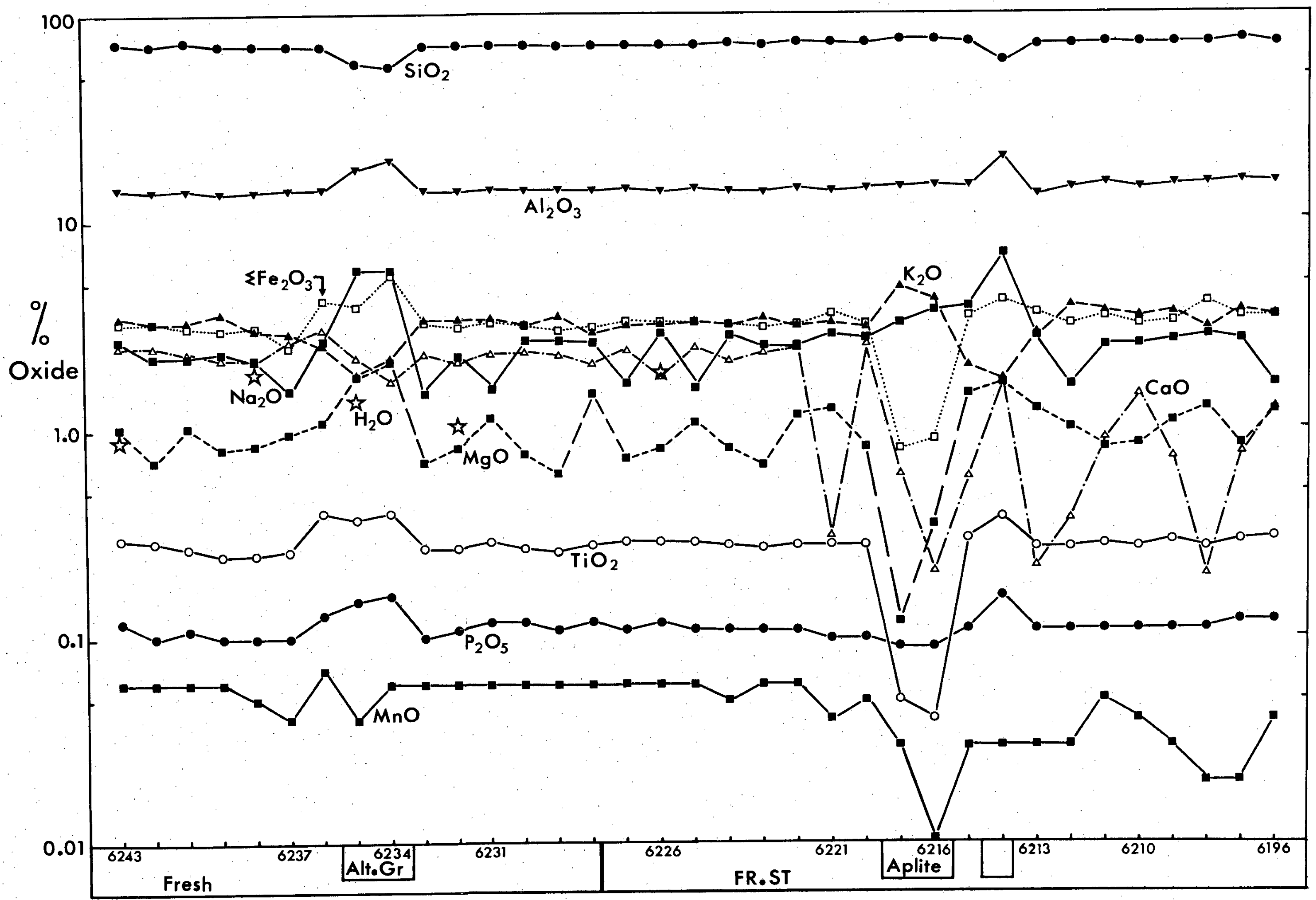

Fig. 15 Oxide variation diagram for fresh and weathered Khancoban Granite.

analyses from Kolbe and Taylor (1966) and Guy (1969) with the average of all fresh granite analyses from DH 2660. Kolbe and Taylor (1966) analysed a sample from 262 feet in DH 2660 (Column 2, Table 5). A comparison of analyses from these three sources reveals general similarity although CaO, K_2O and Na_2O vary considerably. The low total (Column 1, Table 5) and lower CaO, K_2O and Na_2O contents for my analyses suggests underestimation of the former oxides and/or the presence of appreciable hydrothermal alteration. Although Kolbe and Taylor (1966) do not give a water content, the value determined by Guy (1969) is significantly lower than the "average ΣH_2O" listed in column 1, Table 5.

In the absence of ΣH_2O determinations for all samples, this question cannot be resolved.

With the exception of samples 6236 and 6237, the granite is relatively uniform in composition (Fig. 15). Increases in total iron, MgO and TiO_2 are due to increased chlorite content while higher P_2O_5 contents reflect additional apatite. Variable potash feldspar/plagioclase ratios and sericitic alteration control all significant fluctuations in Na_2O, K_2O and CaO shown by the granite. The exceptions, samples 6236 and 6237 display heavy sericitization of feldspars and addition of carbonate which is probably related to the processes which severely affected samples 6234 and 6235. The chemistry of samples 6234 and 6235 does not correspond with that of a soda-aplite but resembles an albite porphyry (Joplin, 1964). Alternatively the granite has been altered by fluids rich in Na_2O and carbonate resulting in desilicification and partial albitization. The latter process is considered more likely; explaining the alteration shown by adjacent samples 6237 and 6236.

With the exception of samples 6234 and 6235, K/Na ratios vary in response to sericitization of plagioclase and to a lesser degree, chloritization of biotite. Na/Ca, Ca/Mg and Fe/Mg ratios reflect both these processes and the extent of carbonate addition. Samples 6234 and 6235 have distinctly lower K/Na and Ca/Mg and higher Na/Ca ratios.

5.2 WEATHERING VARIATION

5.2.1 Fresh-stained joints (FR.-ST.)

From just below 110 feet to 260 feet an extensive zone of limonite stained-joints constitutes a large part of the weathered granite profile. Thin sections reveal limonite staining above sample 6198 (140 feet) and below this the granite appears fresh. This emphasizes the difficulty of sampling initial weathering where it is confined to joint and fracture zones.

Numerous small bands of pink alteration (zeolitization) and development of pink feldspars (heavy sericitization) occur within this zone (geological log, Appendix A). A vein of pink alteration and patches of needle-like crystals were included in sample 6226, however, little or no change in oxides is observed (Fig. 15). Between samples 6220 (190 feet) and 6213 (165 feet) an altered phase of the granite and two aplites were intersected. The altered granite (sample 6214) is similar to samples 6234 and 6235, if the numerous vugs of sample 6214 are considered to represent leached carbonate grains.

Aplite samples (6217 and 6216) are noticeably poor in ferromagnesian minerals with only odd grains of chlorite, increased potash feldspar and large raggy flakes of muscovite.

With the exception of the aplite-altered granite zone, all changes can be attributed to variable sericitization, addition of carbonate and chloritization of biotite. The low CaO contents of samples 6221, 6213 and 6198 (Fig. 15) correlate with very heavy sericitization of plagioclase and concom~~m~~itant chloritization of biotite.

The mineralogical similarity of sample 6214 to samples 6234 and 6235 is additionally supported by similar chemistries (Fig. 15). Aplite samples 6217 and 6216 have higher SiO_2, K_2O and Na_2O accompanied by lower total iron, CaO, MgO, TiO_2, MnO and P_2O_5 than the Khancoban granite.

All elemental ratios are insensitive to weathering intensity displayed by this zone. The higher Na/Ca and lower Ca/Mg ratios of samples 6198, 6221 and 6213 are a consequence of heavier alteration than in other granite samples. Different rock types and relative alteration intensities control the values of all ratios.

5.2.2 Fresh-stained to slight weathering (FR.ST.-S)

This zone extends from 90 to 110 feet (samples 6192 to 6188) and is marked by limonite staining of the groundmass. There is little alteration of mineral phases which can be attributed to weathering but evidence of late-stage hydrothermal alteration is shown by all samples. Sample 6188 is clearly the most weathered with biotite liberating limonite and iron oxides which stain the groundmass and surrounding sericitic patches. Other samples are less weathered and do not show biotite alteration.

Chemical changes (Fig. 16) are relatively minimal and element variation is considerably reduced in comparison with deeper unweathered zones of the granite. The low MgO content of sample 6188 may

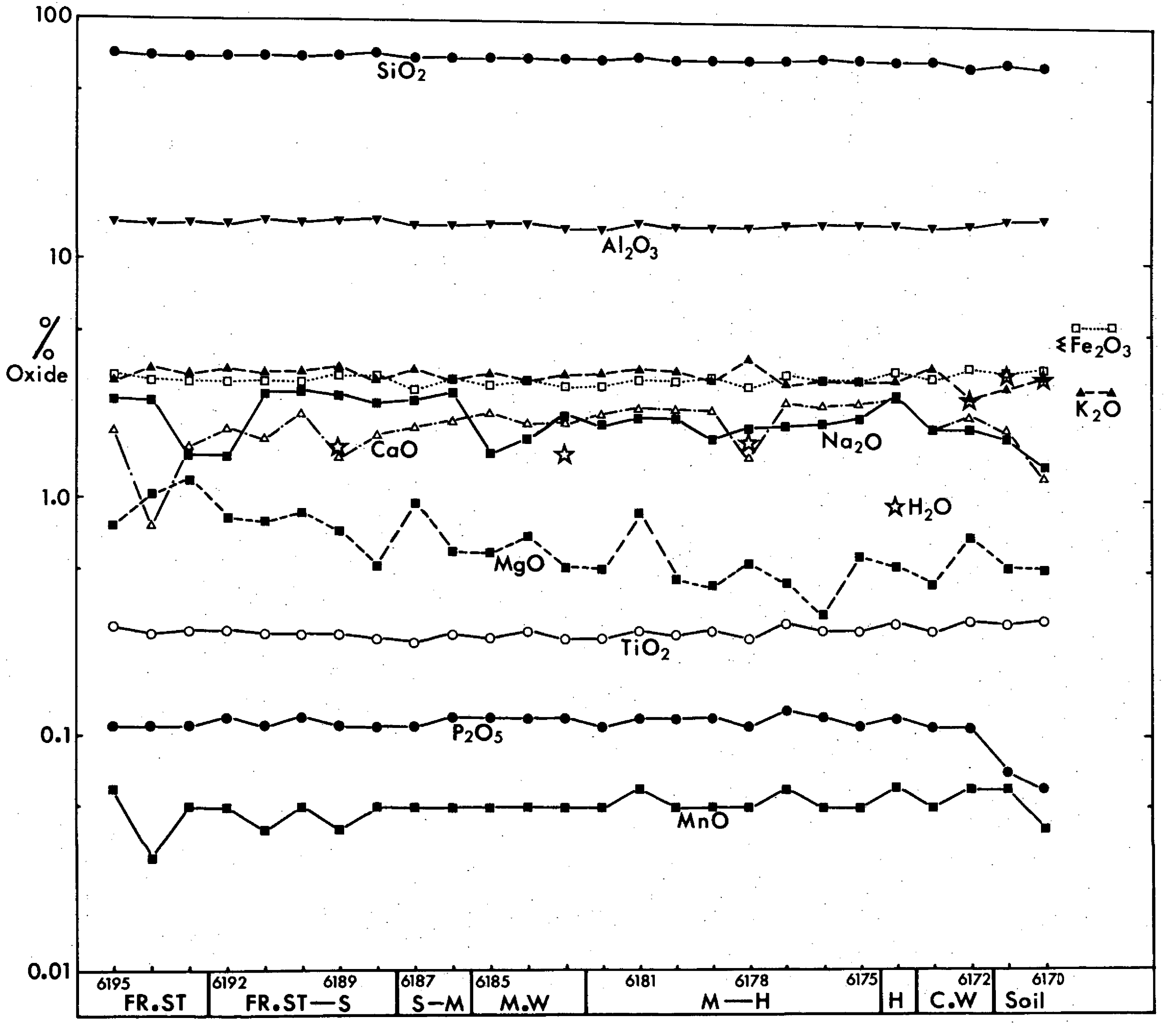

Fig. 16 Oxide variation diagram for weathered Khancoban Granite.

reflect weathering of biotite while the low Na_2O content of sample 6192 is due to heavier sericitization of the plagioclase. Apart from sample 6188 (MgO content) all element variations and ratios lie within the range of fresh rock values.

5.2.3 Slight to moderate weathering (S-M)

Biotite and plagioclase show greater weathering alteration: biotite swells and exfoliates while liberating limonite and iron oxides, and plagioclase fragments and appears to "fade". Considerable migration of iron alteration products stains the groundmass around "biotite" crystals and leaves a green biotite residual. Quartz appears to be unaltered, but potash feldspar is incipiently altered along fine fractures, cracks and cleavage traces to a fine brown sericite. Epidote, an alteration mineral of biotite in the fresh granite, is stained red but its resistance to weathering is not apparent. Initial fresh rock variation remains the dominant control of the mineralogy.

Major element chemistry is remarkably constant throughout this zone. Fluctuations in oxide contents and ratios are readily explained by processes which affect the fresh granite. A slight overall decrease in MgO may reflect progressive alteration of biotite.

5.2.4 Moderately to highly weathered granite (M-H)

Mineralogical changes are restricted to biotite exfoliation and outlining of the groundmass. Increasing lack of cohesion and fragmentation of major mineral phases is apparently due to a cause other than weathering (i.e. faulting). Within this zone, limonite staining is highly variable and some samples (6181, 6179, 6177 and 6176) are only slightly weathered. The degree of weathering alteration is closely related to rock coherency, a factor controlled by the adjacent Khancoban-Yellow Bog Fault zone.

Changes in major element chemistry are again limited and confined essentially to one sample (6178) (Fig. 16). This sample is extensively limonite stained and biotites are considerably altered relative to other samples from the same zone. The lack of sensitivity to weathering shown by CaO and Na_2O is notable, and substantiates a low weathering intensity.

Elemental ratios again lie within the range of fresh granite values with the exception of Fe/Mg ratios. Weathering of biotite is shown by an increased Fe/Mg, however all remaining ratios reflect earlier hydrothermal alteration.

5.2.5 Completely weathered granite (C)

The upper section of DH 2660 was drilled with a NXC bit and consequently the core recovered is highly disturbed. Soil thin sections reveal all mineral phases of the granite although biotite flakes have been shredded and constitute the sample matrix. Fragments of rock occur in a partly crushed and shredded matrix and it is difficult to accurately assess either relative mineral proportions or the degree of alteration.

With the exception of increased total H_2O and lower SiO_2 there is little chemical change (Table B-3; Fig. 16). Fe/Mg ratios are higher, reaching a maximum value in sample 6173. Other ratios are insensitive to the degree of weathering alteration.

5.2.6 Soil

The uppermost samples (6170 and 6171) may not be "in situ" with regard to the underlying weathered granite. For this reason the upper four feet of DH 2660 have been termed slopewash (geological log, Appendix A). All minerals which occur in the granite are visible in soil thin sections, however the plagioclase content may be lower.

Higher ΣH_2O contents are associated with a slight increase in Al_2O_3 and decreases in SiO_2, Na_2O, CaO and P_2O_5.

5.3 ELEMENTAL RATIOS

The virtual absence of pronounced weathering is reflected in relatively constant ratios, however the

Fe/Mg ratio does change as biotite alters. Significant changes in all ratios occur with either different rock type (i.e. aplite) or considerable hydrothermal alteration (Appendix B, Table B-3). A plot of Na/Ca versus Fe/Mg ratios (Fig. 17) illustrates the wide range of Na/Ca values for hydrothermally altered samples (i.e. 6198, 6221, 6215 and 6212) and different rock types (sample 6216, 6217, 6234 and 6235). This ratio is insensitive to weathering. Conversely the Fe/Mg ratio varies with the degree of biotite alteration. The lack of Fe^{++} determinations is unfortunate as the progress of slight weathering is best followed with Fe^{++}/Fe^{+++} ratios (see Chapter 4).

5.4 X-RAY DIFFRACTION STUDIES

Altered granite phases and aplites were also analysed by X-ray diffraction and the relative proportions of minerals examined. The lowermost "soda-aplite" samples 6234 and 6235 are very similar and differ only in relative quartz, epidote and an unidentified mineral phase (2.78Å) proportions. The major minerals of both samples are plagioclase (oligoclase-albite) and muscovite. Sample 6214, which is similar chemically, differs mineralogically with higher chlorite and carbonate, lower muscovite and

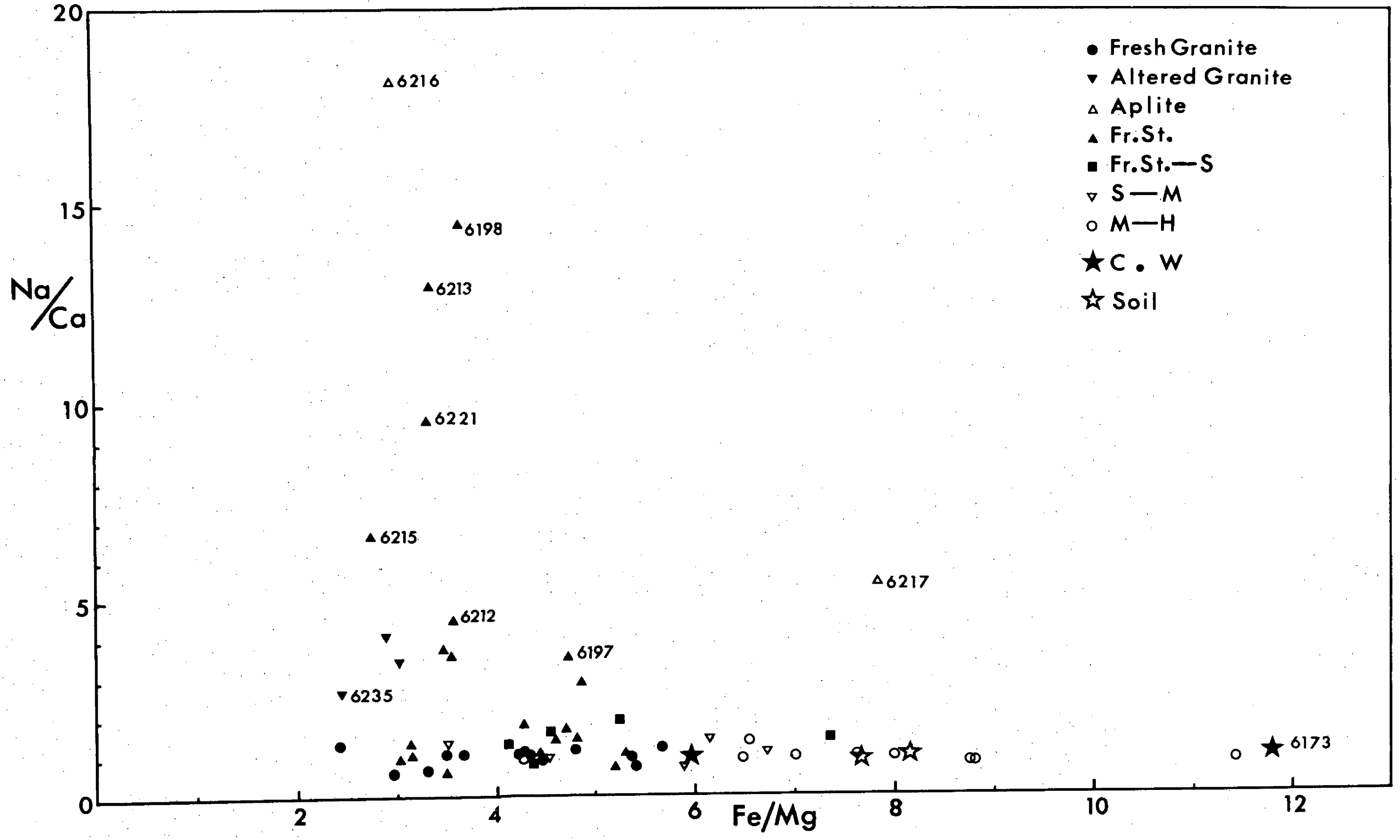

Fig. 17 Na/Ca and Fe/Mg behaviour during weathering of the Khancoban Granite.

absence of the 2.78Å reflection.

Aplites (6216, 6217) differ from each other only in the relative proportions of plagioclase, potash feldspar and muscovite. The paucity of ferromagnesian minerals justifies use of the term aplite.

Hydrothermal alteration as shown by samples 6198 and 6237 has increased chlorite and muscovite at the expense of biotite and for sample 6237, potash feldspar.

Weathering has had little effect on the granite (sample 6188, 6176, 6173) and secondary clay minerals are absent from weathered granite zones. The two soil samples (slopewash) may have kaolinite and chlorite-vermiculite phases, however these have not been examined further (see Chapter 3). The total feldspar, biotite and muscovite contents appear to be lower while quartz is relatively more abundant.

CHAPTER 6

TRACE ELEMENT CHEMISTRY

All samples have been analysed for the following trace elements:

Rb, Sr, Ba, Pb, Y and Zr - by X-ray
fluorescence spectrometry (X.R.F.)
using the techniques of Norrish and
Chappell (1967).

U and Th - by gamma ray spectrometry.

The determination of Rb and Sr by isotope dilution (I.D.) is discussed separately (Appendix C) and a comparison of values obtained by each method given in Appendix D. Selected samples were analysed for U and Th by X.R.F. and I.D. (Appendix C) with a comparison of determinations by three methods outlined in Appendix E.

The analysis of many trace element data and direct comparisons necessitate the use of statistical parameters. The following terms have been used:

1. Arithmetic mean ($\bar{x}$)
2. Standard Deviation (s) where s = $((x-\bar{x})^2/n-1)^{\frac{1}{2}}$. This implies that 68 percent of values lie within ± one standard deviation and that 95.5 percent lie within ± two standard deviations.

3. Coefficient of Variation (C_v) where $C_v = s.100/\bar{x}$. The standard deviation is expressed as a percentage of the mean.
4. Correlation Coefficient (R). The degree of linear association between two independent variables (elements) may be tested using a correlation coefficient which has values ranging from 0 (no statistical correlation) to -1 and +1. A positive correlation corresponds to a correlation greater than zero while a negative correlation is suggested by values between zero and -1. A probability level of 0.01% has been chosen to assess the significance of correlations.

In general, only elements and/or ratios which are significantly correlated, have been given in Tables. However as correlations change from fresh samples to weathered samples, tables include correlations which may not be significant for one group of data. Direct comparisons of correlation coefficients for a particular pair of elements or ratios may enable an understanding of their behaviour during weathering processes.

6.1 WINDY CREEK DIORITE

6.1.1 Fresh Rock Variation

Trace element and element ratios are listed in Appendix F, Tables F-1 and F-2. The variation of trace elements with depth is displayed in Figs. 18 and 19.

Inspection of Fig. 18 indicates the following relationships:

1. Strong positive correlations exist between K and Rb and U and Th.
2. Strontium and yttrium are strongly correlated but the correlation is negative.

Table 6 demonstrates that significant correlations exist for a number of elements and ratios, however, the data are from one rock type covering a limited range of element concentrations. The variability of all elements except Pb and U greatly exceeds the analytical precision. The precision of Pb analyses at this concentration level is lower than the indicated standard deviation for Pb, however U is slightly more variable than the determined precision (Appendix C).

The lowest coefficients of variation are shown by Ba and Sr followed by Th/U, Ba/Sr and K/Rb ratios. Larger coefficients of variation are displayed by Rb, Th/K ratios and Zr which has an exceptionally high

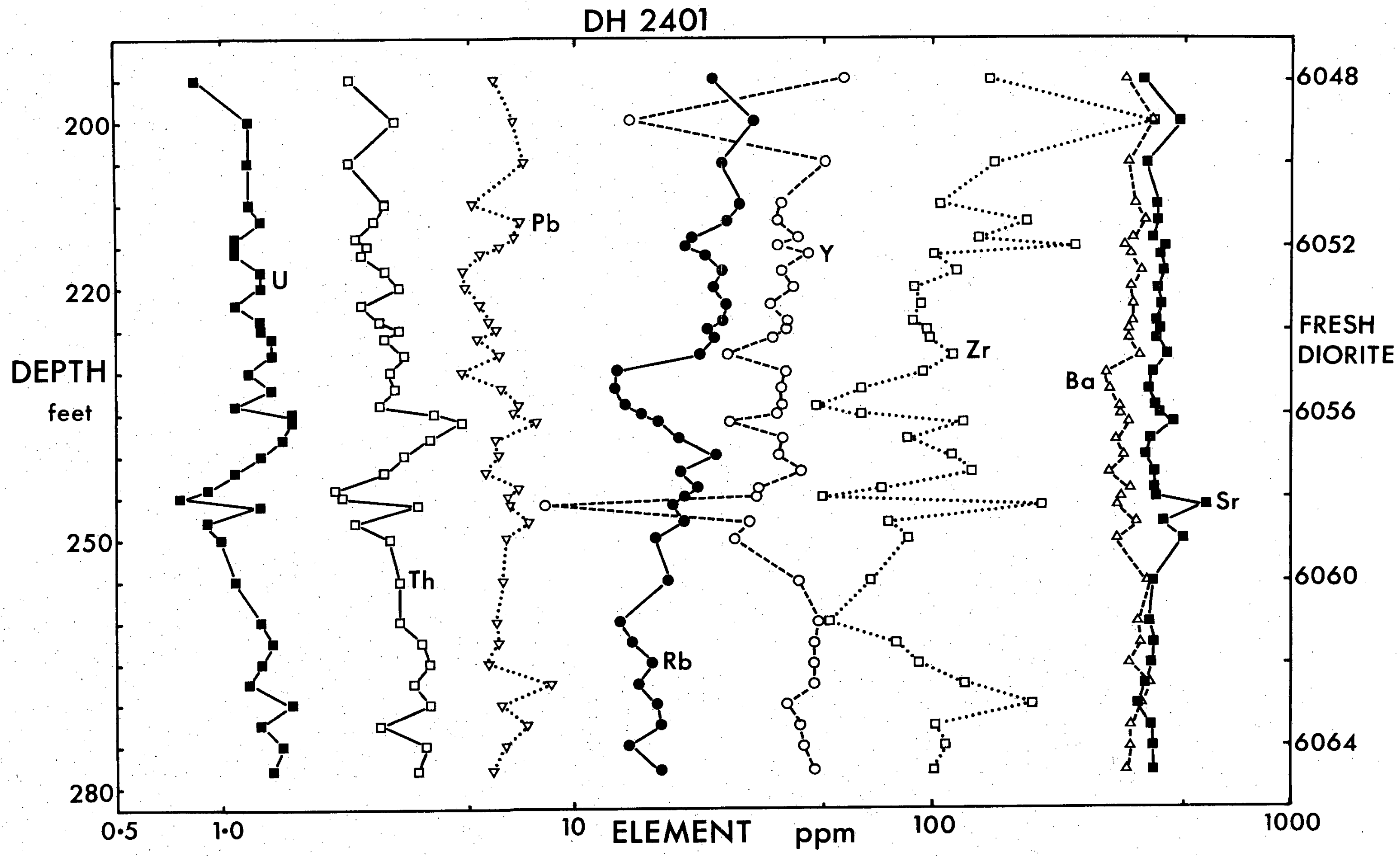

Fig. 18 Trace element variation with depth in DH 2401.

Table 6

Correlations between trace elements and elemental ratios for fresh and weathered Windy Creek Diorite

X	Y	Fresh Diorite[1] R	Weathered Diorite[2] R
K	Rb	0.937	0.890
K	Ba	0.402	0.588
K	Rb/Sr	0.952	0.466
K	Ba/Rb	-0.846	-0.788
Rb	Sr	0.165	-0.697
Rb	Th	-0.418	0.563
Rb	K/Ba	0.816	0.781
Rb	Ba/Sr	0.100	0.676
Rb	U/K	-0.734	-0.554
Rb	Th/K	-0.768	-0.131
Sr	Y	-0.832	-0.221
Sr	Th	0.087	-0.629
Sr	K/Rb	-0.405	0.642
Sr	K/Ba	0.001	-0.636
Sr	Ba/Rb	-0.238	0.675
Sr	Th/U	0.247	-0.582
U	Th	0.832	0.626
U	Th/K	0.669	0.486
Th	Ba/Sr	-0.033	0.701
Th	Rb/Sr	-0.448	0.753
Th	U/K	0.763	0.110

[1] Number of samples, n = 36; minimum value of R for significance = 0.60.

[2] Number of samples, n = 41; minimum value of R for significance = 0.56.

value (Table 7). Highly variable zircon content is a feature of the diorite and samples with low colour indices have higher Zr contents (i.e. sample 6049).

The feldspar/mafic, hornblende/biotite, and plagioclase/biotite ratios vary within the sampled diorite and large coefficients of variation for many trace elements reflect these relationships. Yttrium normally occurs in both hornblende and apatite, while Sr is located dominantly in plagioclase and apatite. Lack of correlation between P_2O_5 and Y or P_2O_5 and Sr suggests that little Y and Sr are located in apatite. Lower plagioclase/hornblende ratios favour lower Sr and higher Y contents. The existence of different plagioclase/hornblende ratios has already been shown (Chapter 3) and these explain the inverse correlation between Y and Sr.

Both K and Rb are located largely in biotite with very small concentrations in plagioclase and hornblende (Gulson, 1968). The high correlation coefficient for these two elements reflects their coherence, however the lack of Ba correlation with either K or Rb is unexpected. Barium would normally be expected to substitute for K in biotite and to therefore reflect the biotite content. The lowest coefficient of variation is shown by Ba suggesting that it is either

Table 7

Statistical analyses of chemical data and elemental ratios for the Windy Creek Diorite

Variable	Mean[1] $\bar{x}$	Standard Deviation s	Coefficient of Variation C_v
K[2]	0.71	0.108	15.286
Rb	20.5	5.024	24.522
Sr	426	36.584	8.582
Ba	354	26.344	7.433
Y	37.7	8.795	23.317
Zr	116	67.116	57.896
Pb	6.26	0.864	13.787
U	1.24	0.193	15.480
Th	3.10	0.593	19.099
K/Rb	353	40.635	11.520
K/Ba	19.9	2.794	14.024
Rb/Sr	0.048	0.012	24.104
Ba/Sr	0.84	0.090	10.704
Ba/Rb	18.3	4.342	23.798
U/K	1.81	0.443	24.426
Th/K	4.55	1.308	28.761
Th/U	2.50	0.265	10.607

[1] Number of samples, n = 36

[2] Potassium concentration in percent; trace elements in ppm.

located in a relatively constant major mineral phase or in at least two mineral phases which mutually vary maintaining a relatively constant Ba content. Jakeš (1970) has found that the Ba content of andesites is not simply a function of the biotite content but is dependent on modal hornblende and biotite contents. Barium is distributed between biotite and hornblende in a ratio of approximately 6:1 but if biotite is not present, practically all Ba is located in the hornblende. The distribution of Ba is therefore related to both biotite and hornblende and its failure to correlate with K and Rb explained.

Lead does not correlate with any other trace element and is probably present as a sulphide in submicroscopic grains or in accessory opaque minerals. Lack of correlation with P_2O_5 confirms that Pb does not substitute for Ca in apatite.

The existence of a strong correlation between U and Th for the diorite is significant. If the diorite had been affected by late-stage alteration or was a product of hybridisation, the correlation between these elements would be poor. A low coefficient of variation and a low value for the Th/U ratio suggests that these elements may be located either in an accessory mineral with a relatively low Th/U ratio of 2.5, or distributed amongst the major mineral phases.

The mean value, standard deviation and coefficient of variation for trace elements and elemental ratios are given in Table 7. An arbitary limit of two standard deviations (2s) has been taken beyond which values for weathered samples will be regarded as significantly different.

6.1.2 Weathered Rock Variation

Trace element contents of weathered diorite (the upper 195 feet of DH 2401) are shown in Fig. 19 and correlation coefficients given in Table 6. The mean, standard deviation and coefficient of variation for individual trace elements and ratios are listed in Table 8.

A majority of trace elements show little change until the uppermost five feet of drill core. The exceptions are Sr, Rb and K. Above 55 feet (sample 6020), a consistent decrease in Sr and an increase in Rb are apparent with minor zones reflecting changes at greater depths. The 2s (± 2 standard deviations) limits for each element in the fresh rock are indicated immediately below sample 6048 (195 feet) in Fig. 19. Potassium contents increase in a similar manner until the soil horizon is reached. Retention of hornblende

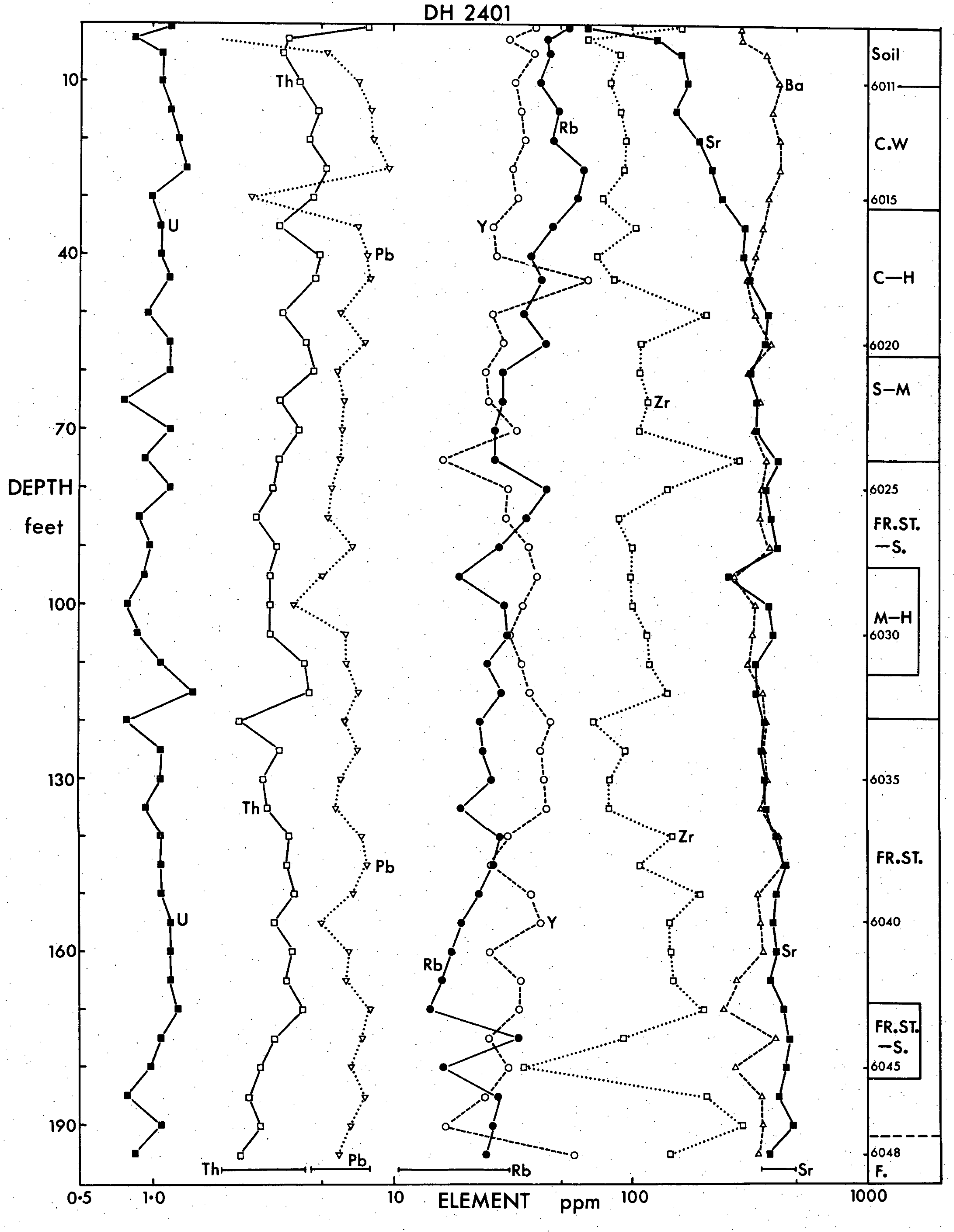

Fig. 19 Trace element variation during weathering of Windy Creek Diorite.

Table 8

Statistical analyses of chemical data and elemental ratios for weathered Windy Creek Diorite

Variable	Mean[1] $\bar{x}$	Standard Deviation s	Coefficient of Variation C_v
K[2]	0.84	0.172	20.469
Rb	32.3	12.242	37.901
Sr	341	100.774	29.593
Ba	353	45.672	12.930
Y	33.7	9.346	27.698
Zr	124	55.603	44.935
Pb	6.30	1.790	28.407
U	1.07	0.171	15.954
Th	3.75	1.004	26.800
K/Rb	278	54.973	19.775
K/Ba	23.8	3.981	16.745
Rb/Sr	0.129	0.141	109.646
Ba/Sr	1.23	0.737	60.103
Ba/Rb	12.2	3.873	31.639
U/K	1.33	0.358	26.982
Th/K	4.62	1.281	27.749
Th/U	3.55	0.746	21.031

[1] Number of samples, n = 41.

[2] Potassium concentration in percent; trace elements in ppm.

and its subsoil residual enrichment control both Ba and Y concentrations.

Resistant accessory minerals accumulate in the soil horizon but all major mineral phases are altered to low temperature-pressure and hydrated assemblages.

Statistical analysis will tend to subdue the character of weathering trends as a majority of samples are only slightly weathered. However the coefficient of variation will change significantly from that shown by elements or ratios in fresh diorite. With the exception of Zr and Th/K ratios, all elements and ratios have larger coefficients of variation (Tables 7 and 8). This effect is very marked for Sr, Rb/Sr ratio and the Ba/Sr ratio all of which show a three fold increase. A comparison of correlation coefficients for selected elements and ratios in both fresh and weathered diorite is summarized in Table 6. All ten significant correlations between selected variables in the fresh diorite have lower correlation coefficients in the weathered diorite. Of the ten correlations, only four remain significant at the 0.01% level. There are fifteen significantly correlated variables in the weathered diorite, eleven of which were not significant in the fresh diorite. A very slight positive correlation may change to a significant negative correlation with weathering. Notable examples are the Rb and Sr and Sr and Th correlations.

The changing pattern of correlation coefficients reflects the selective destruction of plagioclase and biotite forming low temperature hydrated silicates. The behaviour of an element in a magma at elevated temperatures and pressures will differ from that at the surface in a low temperature hydrous system. If the element is present as an ion, it will have a hydration envelope which will strongly influence cation exchange and adsorption phenomena. A reduction of the correlation between K and Rb and the larger increase in Rb concentrations during weathering is a consequence of different hydration energies. Rubidium, with a lower hydration energy, is preferentially retained in comparison with K. The absence of significant U loss is in contrast to the frequently cited ease of U migration during leaching (Rogers _et al_, 1965; Clark _et al_, 1966). The actual location of U and Th in the diorite is unknown, however the apparent retention of both elements during weathering suggests that they are present in crystal lattice sites. Low concentrations for both elements may be accommodated in major minerals, however, the lowered significance of the U-Th correlation in weathered diorite may support preferential weathering of a mineral phase with a differing Th/U ratio. The behaviour of these elements during weathering will be considered in Chapter 11.

The extent of plagioclase destruction can be monitored by the Sr content and related to the degree of residual accumulation of Th and retention of Rb. Hence correlations between Rb and Sr, Sr and Th and Sr with various ratios are a consequence of varying stages of weathering. The fresh rock correlation between Sr and Y is lost during weathering as plagioclase is removed. This type of alteration is not analogous to a change of plagioclase/hornblende ratio and Y and Sr cease to be significantly correlated.

6.2 SCAMELS GRANITE

6.2.1 Fresh Granite Variation

Trace element and elemental ratios are detailed in Appendix F, Tables F-3 and F-4.

Trace elements have been plotted against depth in Fig. 20 and strong positive correlations between the elements K and Rb, K and Ba, K and Pb, Rb and Ba, Rb and Pb and Ba and Pb are readily discernable. Statistical analysis (Table 9) confirms the strong positive correlations between K, Rb, Ba and Pb. These

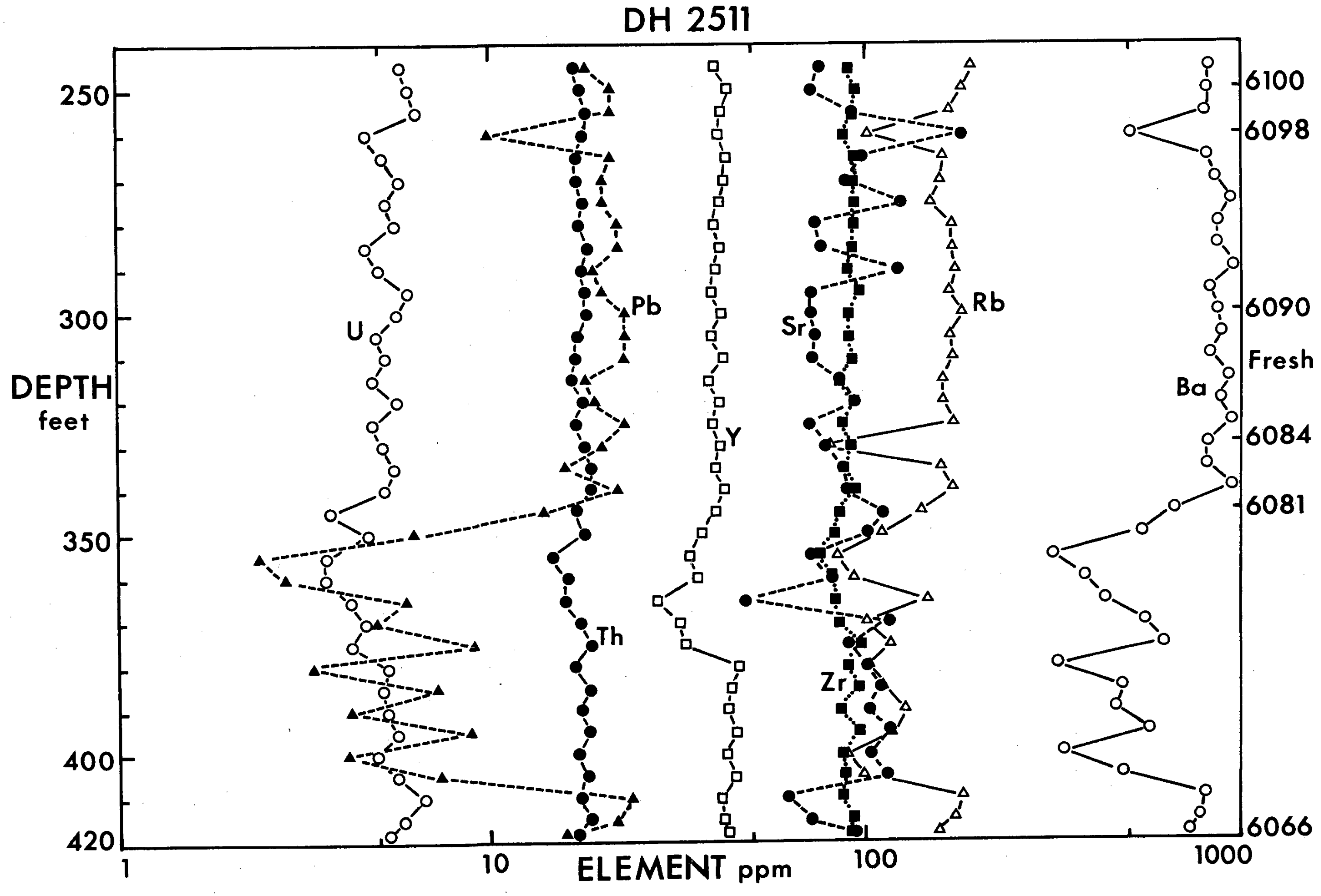

Fig. 20 Trace element variation with depth in DH 2511.

Table 9

Correlations between trace elements and ratios for fresh and weathered Scamels leucogranite

X	Y	Fresh Granite R[1]	Weathered Granite R[2]
K	Rb	0.880	0.766
K	Ba	0.949	0.697
K	Pb	0.967	0.187
K	Rb/Sr	0.691	-0.087
K	Ba/Sr	0.897	0.064
Rb	Ba	0.797	0.523
Rb	Pb	0.822	0.237
Rb	Ba/Sr	0.817	0.326
Rb	U/K	-0.776	-0.325
Rb	Th/K	-0.870	-0.689
Ba	Pb	0.938	0.046
Ba	U/K	-0.901	-0.312
Ba	Th/K	-0.937	-0.722
Zr	Th	0.689	0.335
Zr	K/Rb	0.319	-0.763
Zr	Th/K	-0.463	0.693
Pb	Rb/Sr	0.644	0.064
Pb	Ba/Sr	0.880	0.029
Pb	U/K	-0.864	0.009
Pb	Th/K	-0.937	-0.125
Y	Th/U	-0.548	-0.652

[1] Number of analyses, n = 36; minimum value of R for significance = 0.60

[2] Number of analyses, n = 33; minimum value of R for significance = 0.62.

elements are located in potash feldspar and to a lesser extent biotite, two phases which are susceptible to late-stage hydrothermal alteration. In Chapter 4, the alteration of feldspars, and in particular potash feldspar, to muscovite has been discussed and shown to be associated with complete alteration of biotite. The effect of hydrothermal alteration has been to lower the Ba, Rb, Pb and K contents while Sr and CaO increase. Remaining trace elements, U, Th, Y and Zr are largely unaffected by alteration processes although U and Y are slightly lower in samples with a pronounced development of muscovite.

The variability shown by all elements greatly exceeds the error due to analytical precision. Both Zr and Th are significantly correlated (Table 9) but the correlation coefficient for Y and U (R = 0.599) is just below the level taken for significant R values. The correlation of Zr and Th may indicate that a bulk of the Th is located in zircon or that the process controlling the concentrations of both elements are related. Additional correlations between trace elements and ratios are given in Table 9.

The extent of hydrothermal alteration within the granite is unknown and it is therefore impossible to reject altered samples during statistical treatment of the data. The inclusion of these analyses strongly influences the coefficients of variation for many elements (Table 10). Coefficients of variation for Th, Zr and Y are unusually small for elements which are located in accessory mineral phases. A majority of elemental ratios have coefficients of variation in excess of 20% with the exception of K/Ba and Th/U ratios. The insensitivity of the Th/U ratio to hydrothermal alteration is remarkable and indicates that a majority of the U and Th is not located in mobile sites (i.e. grain boundaries, fractures or alteration minerals along grain boundaries). Mild depletion of U in hydrothermal zones may represent leaching of weakly held U present at grain boundaries.

The Rb/Sr ratio is the most sensitive indicator of alteration and consequently has the highest coefficient of variation.

The limits of ± 2s (standard deviations) are wide especially for elements which are susceptible to hydrothermal alteration.

6.2.2 Weathered Granite Variation

Trace element contents for the upper section of DH 2511 have been plotted against depth in Fig. 21 and statistical analysis of weathered samples listed in Table 11.

Table 10

Statistical analyses of chemical data for the Scamels leucogranite

Variable	Mean[1] $\bar{x}$	Standard Deviation s	Coefficient of Variation C_v
K*	2.77	0.807	29.169
Rb	143	33.692	23.541
Sr	91.2	23.738	26.042
Ba	704	203.515	28.907
Y	40.1	3.752	9.353
Zr	89.4	4.918	5.502
Pb	15.1	7.443	49.435
U	5.12	0.706	13.808
Th	17.5	0.862	4.925
K/Rb	193	42.737	22.140
K/Ba	39.5	3.830	9.699
Rb/Sr	1.70	0.668	39.251
Ba/Sr	8.30	3.149	37.950
Ba/Rb	4.94	1.223	24.741
U/K	2.01	0.615	30.652
Th/K	7.01	2.461	35.099
Th/U	3.48	0.456	13.095

*Potassium concentration in percent; trace elements in ppm.

[1] Number of samples, n = 36.

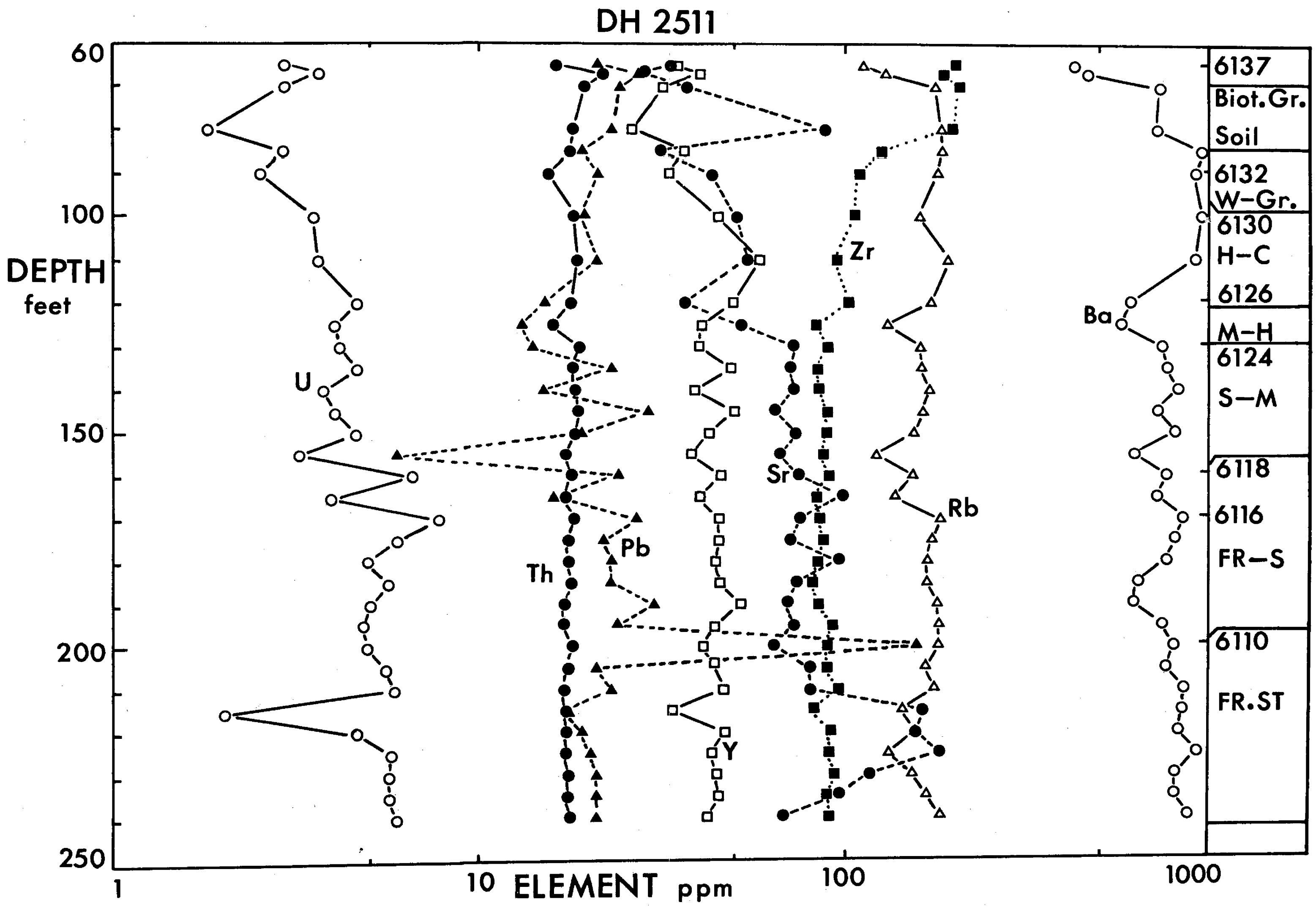

Fig. 21 Trace element variation during weathering of Scamels Granite.

Table 11

Statistical analyses of chemical data for weathered Scamels leucogranite

Variable	Mean[1] $\bar{x}$	Standard Deviation s	Coefficient of Variation C_v
K*	3.16	0.512	16.224
Rb	161	20.297	12.593
Sr	75.9	35.633	46.920
Ba	757	130.133	17.182
Y	42.6	6.346	14.891
Zr	103	36.580	35.357
Pb	24.6	24.188	98.192
U	4.43	1.342	30.334
Th	17.7	1.045	5.902
K/Rb	196	21.320	10.899
K/Ba	42.1	5.658	13.452
Rb/Sr	2.57	1.174	45.753
Ba/Sr	11.8	5.326	45.341
Ba/Rb	4.72	0.759	16.082
U/K	1.41	0.376	26.589
Th/K	5.81	1.346	23.187
Th/U	4.46	1.707	38.311

*Potassium concentration in percent; trace elements in ppm.

[1] Number of samples, n = 33.

A comparison of Tables 10 and 11 reveals a reduction in coefficients of variation for K, Rb and Ba with increases for Sr, Pb, Zr, U, Th and Y. Decreasing coefficients of variation for the alkali elements and Ba are due largely to the absence of pronounced hydrothermal alteration within the weathered granite. The residual enrichment of zirconium in the soil markedly increases the coefficient of variation.

Two samples 6119 and 6110 seriously affect statistical analysis of Pb variation. Small patches of chalcopyrite have been observed in veins and fractures. The high Pb content of sample 6110 may be due to small crystals of galena or a Pb-bearing sulphide. Alternatively this sample has been contaminated during crushing but this is considered very improbable. An adequate mechanism for producing Pb contamination of this magnitude for one only sample cannot be proposed.

Destruction of plagioclase indicated by lower CaO and Na_2O (Chapter 4) is substantiated by lower Sr contents above 130 feet in DH 2511. Evidence for potash feldspar alteration is masked by retention of alkali elements on clay surfaces or in alteration products. Although samples 6137 and 6135 have lower

Ba, K, Rb and Pb contents the influence of residual biotite granite (Chapter 4) within the soil zone is unknown. The mild to marked discontinuity between samples 6133 and 6134 (Fig. 21) is a consequence of change in rock type rather than a weathering trend. Strontium, zirconium, uranium and yttrium show an abrupt break in concentration levels with change to a biotite granite. The weathering trends displayed by the biotite granite and the more leucocratic Scamels granite are similar and the possibility of dual origin for soil samples cannot be rejected.

The behaviour of many elements as hydrated ions differs significantly from their known behaviour in high temperature magmatic processes. Changes in correlation coefficients indicate differences in behaviour of closely associated cations. Weathering is a response to differing chemical conditions and significantly reduces the number of correlations normally encountered in geochemical studies. Of the eighteen significant correlations (Table 9) in the fresh granite only four retain their significance. The four remaining correlations (K-Rb, K-Ba, Rb-Th/K and Ba-Th/K) are all reduced appreciably. Three new correlations are significant for weathered samples, involving Y or Zr and ratios. This group changes from weakly to significantly correlated variables, and is accompanied by a reversal of the correlations, (i.e. from negative to positive or the reverse). These changes are not highly significant but emphasize changing relationships with weathering.

The elements Pb, Ba, Rb and K are frequently located in potash feldspar and biotite of many intermediate to acid rocks. With weathering, close correlations between these elements are either markedly lowered or are no longer significant. Lead correlations with K, Rb and Ba cease to be significant in weathered Scamels granite. Barium correlations show a similar trend although reductions in correlation coefficients are not as pronounced. As potash feldspar and biotite weather, trace elements from either lattice are released and involved in open system conditions. Strontium is removed in solution, however K and Rb are largely retained by adsorption on clays and/or mineral surfaces.

Many ratio and element correlations are changed by weathering processes in an analogous manner to trace element correlations outlined previously. Changes in trace elements are reflected in trace element ratios.

6.3 KHANCOBAN GRANITE

6.3.1 Fresh Rock Variation

Trace element data and elemental ratios are given in Appendix F, Tables F-5 and F-6, with variation versus depth illustrated in Figs. 22 and 23.

Strong positive correlations between K, Rb, Ba and Pb are evident in Fig. 22 with weaker correlations between Y, Th, U and Zr. Statistical analysis of the data detailed in Table 12 confirms these correlations.

Trace element analyses below 200 feet (samples 6222-6243) have been grouped for statistical analysis as fresh rocks although samples between 200 feet and 260 feet are fresh with limonite stained joints. Drill core below 400 feet was not sampled as extensive hydrothermal alteration and faulting were intersected. Aplite dykes frequently intrude the granite and were intersected by DH 2660. In order to have a statistically large sample for treatment data from aplite and granite with limonite stained joints has been grouped as fresh "granite".

The inclusion of aplite and adjacent granite samples increases the range of concentrations and the coefficients of variation for many elements (Fig. 22).

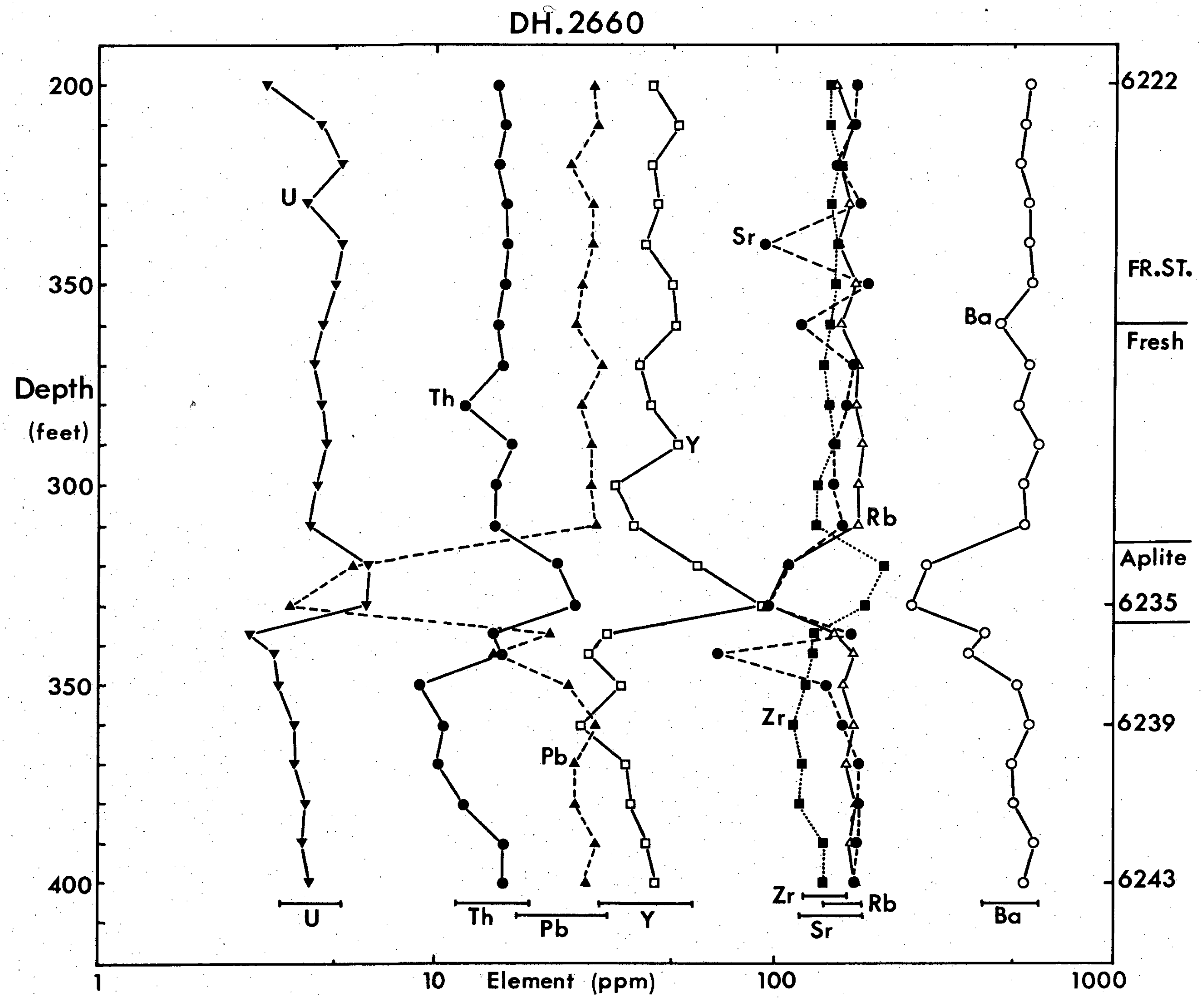

Fig. 22 Trace element variation with depth in DH 2660.

Table 12

Correlations between trace elements and ratios for fresh and weathered Khancoban granite

X	Y	Fresh Granite R[1]	Weathered Granite R[2]
K	Rb	0.901	0.863
K	Ba	0.912	0.139
K	Zr	-0.659	-0.778
K	Pb	0.919	0.772
K	Th	-0.659	-0.802
K	K/Rb	0.296	0.681
Rb	Ba	0.815	-0.177
Rb	Zr	-0.755	-0.806
Rb	Pb	0.834	0.671
Rb	Th	-0.703	-0.764
Rb	K/Ba	-0.506	-0.637
Rb	U/K	-0.851	-0.106
Rb	Th/K	0.873	-0.768
Sr	Ba	0.648	0.822
Sr	U	-0.350	-0.713
Sr	K/Ba	-0.625	-0.710
Sr	Ba/Rb	0.535	0.842
Sr	U/K	-0.508	-0.686
Sr	Th/U	-0.176	0.619
Ba	Pb	0.964	0.047
Ba	U	-0.376	-0.721
Ba	K/Rb	0.282	0.582
Ba	Rb/Sr	-0.215	-0.804
Ba	U/K	-0.741	-0.756
Ba	Th/K	-0.806	-0.268
Y	Zr	0.766	-0.564
Y	U	0.752	0.512
Y	Th	0.819	-0.359

Continued next page

Table 12 (Continued)

Correlations between trace elements and ratios for fresh and weathered Khancoban granite

X	Y	Fresh Granite R[1]	Weathered Granite R[2]
Y	K/Ba	0.256	0.721
Y	Rb/Sr	-0.245	0.598
Y	Ba/Rb	-0.155	-0.560
Y	U/K	0.872	0.320
Y	Th/K	0.856	-0.127
Zr	Pb	-0.656	-0.623
Zr	U	0.819	0.628
Zr	Th	0.873	0.905
Zr	K/Ba	0.419	-0.765
Zr	Rb/Sr	-0.104	-0.685
Zr	U/K	0.863	-0.082
Zr	Th/K	0.825	0.743
Zr	Th/U	0.173	0.567
Pb	K/Ba	0.796	0.495
Pb	Ba/Rb	0.738	-0.031
Pb	U/K	-0.807	-0.295
Pb	Th/K	-0.848	-0.640
U	K/Ba	0.315	0.788
U	Rb/Sr	-0.112	0.756
U	Ba/Rb	-0.108	-0.776
Th	K/Ba	0.466	-0.618
Th	Rb/Sr	0.020	-0.580
Th	U/K	0.832	0.004

[1] Number of samples, n = 22; minimum value of R for significance = 0.72

[2] Number of samples, n = 41; minimum value of R for significance = 0.56.

All elements display greater variability than that accounted for by analytical precision (Table 13). A combination of small sample number (n) and a restricted concentration range for fresh "granite" raises the value of R for which correlations between variables are significant (Table 12). The alkali elements Rb and K closely followed by Zr have the lowest while Y and Pb have the highest coefficients of variation. The K/Rb ratio predictably has the lowest coefficient of variation and Th/K the highest of the ratios.

Trace elements Rb, Ba and Pb substitute for K in potash feldspar and biotite and are therefore strongly correlated. A reduction of potash feldspar and absence of biotite in the "soda-aplite" is correlated with lower K, Rb, Ba, Pb and Sr concentrations. The elements Y, Th, U and Zr are mutually correlated with the exception of U and Th. Uranium is considerably more variable than zirconium (Table 13) suggesting that U is probably located in other sites than zircon (i.e. epidote). A stronger correlation of U with Zr than with Y indicates that relatively more U is located in zircon than apatite.

Table 13

Statistical analyses of chemical data for the Khancoban granite

Variable	Mean[1] $\bar{x}$	Standard Deviation s	Coefficient of Variation C_v
K*	2.57	0.347	13.489
Rb	161	20.869	12.969
Sr	150	32.320	21.530
Ba	503	92.740	18.432
Y	44.2	13.473	30.491
Zr	143	20.999	14.688
Pb	25.1	7.505	29.964
U	4.35	0.883	20.299
Th	15.4	3.740	24.317
K/Rb	160	9.425	5.890
K/Ba	51.9	5.405	10.410
Rb/Sr	1.13	0.352	31.242
Ba/Sr	3.45	0.832	24.081
Ba/Rb	3.11	0.358	11.507
U/K	1.76	0.685	38.888
Th/K	6.31	2.987	47.322
Th/U	3.58	0.735	20.529

*Potassium concentrations in percent; trace elements in ppm.

[1] Number of samples, n = 22.

The lack of large trace element variation is associated with uniformity of major element composition (Chapter 5). The effects of hydrothermal alteration are limited and confined largely to Sr which decreases. In one case Ba also decreases (Fig. 22). Changes in modal mineralogy can account for trace element variability.

The origin of the "soda-aplite" or albitized zone is unknown. This rock probably is hydrothermally altered granite with the addition of later carbonate alteration. The marked increases in U, Y and Zr are possibly due to late stage hydrothermal activity.

6.3.2 Weathering Variation

Trace element contents for the upper 200 feet of DH 2660 are shown in Fig. 23 and a summary of statistical analysis listed in Table 14. Correlation coefficients are given in Table 12 with coefficients for fresh rock samples.

Little change with weathering is shown by a majority of trace elements and ratios. Figure 23 indicates mild U depletion above 100 feet and Sr loss in the uppermost 20 feet. The middle and upper sections of fresh granite with limonite stained joints, display considerable trace element changes reflecting the intrusion of a potash rich aplite and a second

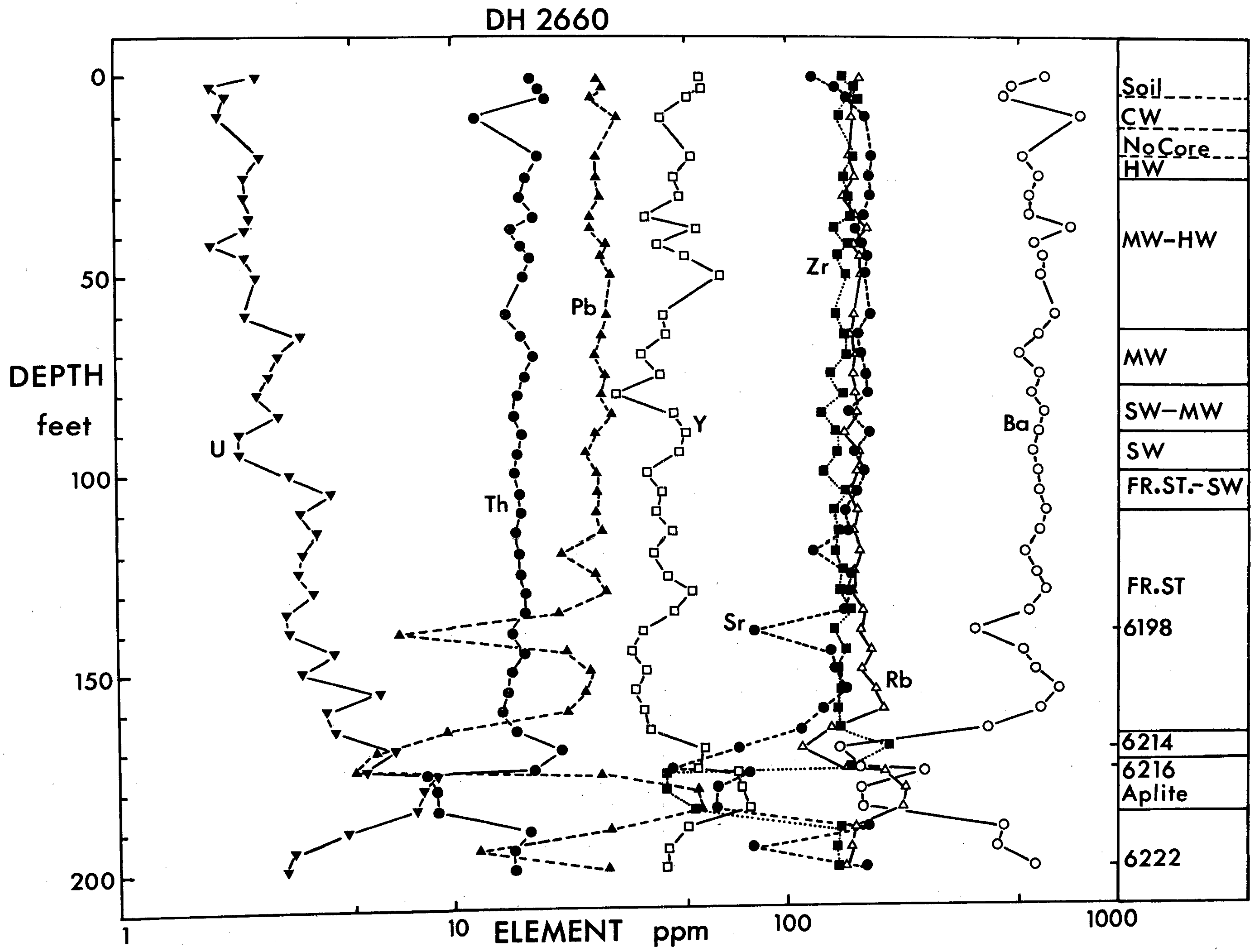

Fig. 23 Trace element variation within weathered Khancoban Granite.

Table 14

Statistical analyses of chemical data for weathered Khancoban granite

Variable	Mean[1] $\bar{x}$	Standard Deviation s	Coefficient of Variation C_v
K*	2.77	0.436	15.739
Rb	164	19.590	11.916
Sr	142	38.777	27.249
Ba	509	145.112	28.493
Y	47.0	10.287	21.889
Zr	140	29.228	20.851
Pb	25.9	9.528	36.727
U	3.62	1.684	46.528
Th	15.6	2.548	16.308
K/Rb	168	15.027	8.932
K/Ba	63.7	42.372	66.563
Rb/Sr	1.33	0.725	54.651
Ba/Sr	3.60	0.689	19.127
Ba/Rb	3.14	0.914	29.142
U/K	1.34	0.744	55.350
Th/K	5.93	2.057	34.706
Th/U	5.12	1.990	38.846

*Potassium concentration in percent; trace elements in ppm.

[1] Number of samples, n = 41.

zone of "soda-rich aplite". SMA geologists made no attempt to separate the two aplites during core logging (Appendix A). Sample 6214 ("soda-aplite") strongly resembles the "aplite" intersected in the fresh granite (samples 6234 and 6235). Similar K, Ba, Rb, Sr and Pb depletions with U, Th, Y and Zr increases are shown by both "soda-aplites". The potash aplite is a normal aplite with higher Rb, K, Pb, U and Y and lower Th, Zr, Ba and Sr contents than the granite. However the two "aplites" differ considerably and strongly influence both correlation coefficients and coefficients of variation.

Comparison of Tables 13 and 14 reveals an absence of significant changes for all trace elements and ratios. Coefficients of variation for all trace elements with the exception of U are relatively unchanged with Y, Th and Rb actually having lower coefficients for weathered granite. The increased U coefficient of variation reflects lower U contents for samples above 100 feet in DH 2660 and the higher U contents of aplite samples.

Small increases are shown by all ratios with the exception of U/K and Th/K. Although both Th/U and Rb/Sr ratios increase with weathering, the K/Rb ratio is insensitive. Weathering intensity is insufficient to achieve preferential retention of Rb over K. The inclusion of aplite analyses in the statistical treatment has distinctly increased the coefficients of variation for K/Ba and Ba/Rb ratios.

Many correlations change despite the low intensity of weathering. The sensitivity of correlations to samples with extreme values relative to a majority of sample data has been mentioned previously. Twenty five significant correlations between elements and ratios in the fresh granite are altered and fourteen become insignificant in the weathered granite (Table 12). Twenty six new and significant correlations are added to the eleven retained from the fresh granite.

Loss of correlation between Ba and K, Rb and Pb and a lowering of correlation coefficients for Pb and alkali elements (K and Rb) support different behaviour for Ba and Pb. Barium is correlated positively with Sr and negatively with U in weathered samples. Potassium, Rb and Pb correlate negatively with Zr but only K and Rb correlate with Th. These correlations demonstrate a marked lowering of the Ba-K, Ba-Rb and Ba-Pb relationships and a strengthening of the Ba-Sr correlation. Once Ba is liberated from K sites in feldspar or biotite it is not adsorbed completely but lost partially in the groundwater.

Separation of the group, U, Th, Y and Zr occurs in that correlations between U and Y and Th and Y are no longer significant in the weathered granite. However, Y and Zr and U and Zr correlations remain significant but change from positive to negative. This reversal is due to two factors; aplites have low Zr and high U and Y contents; and weathering tends to remove U, residually enriching Zr. The lack of samples with low Y and high Zr concentrations reduces the Y and Zr correlation until it is only just significant. Correlations may be interpreted as indicating at least two sites for U and Y. The Zr-Th correlation increases in significance for similar reasons.

CHAPTER 7

WESTERN AUSTRALIA

The Yilgarn block is part of the ancient West Australian Shield and forms an elevated peneplain as a consequence of prolonged erosion. It is underlain by areas of gneisses, granites and undifferentiated granite-gneiss complexes together with greenstones and later dyke swarms. The Darling Scarp, subparallel to the coast and approximately 20 miles inland, marks the western edge of the plateau. The land surface drops from approximately 900 feet to coastal plains just less than 100 feet above sea level.

By the beginning of the Tertiary, deep soil and laterite profiles had formed. Renewed uplift with erosion occurred during the Miocene (Woolnough, 1927), rejuvenating river systems and in part destroying the extensive laterite development. With the onset of arid climatic conditions, rivers became blocked by detritus and broad expanses of salt lakes or shallow drainage basins formed.

The typical truncated laterite profile consists of a layer of concretionary iron-stone or pisolitic laterite, occasionally overlying a sand layer but more commonly a distinctly mottled zone. A pallid horizon of variable depth is developed beneath the former zone (Prider, 1946).

Erosion frequently leads to formation of "breakaways", a term used for cliff-like edges to the higher and older residual plain (Carroll and Jones, 1947). Breakaways range from 50 to 200 feet in height and have a hard indurated ferruginous cap rock overlying soft completely weathered and pallid material. Montgomery (1916) stated:

> The present plain appears to have been excavated to a depth of probably as much as 100 to 200 feet out of a much older plain of which only flat topped portions protected by a hard lateritic covering have survived. Quite similar cliffs with lateritic flat tops to them are seen again some miles north of Mertondale....

This is the only reference in the literature to the geology of the Mertondale region known to the author.

7.1 THE MERTONDALE GRANITE

The Mertondale granite outcrops as a low rise in plain country 29 miles NW of Leonora, W.A. (Fig. 24). Approximately 2½ miles to the NW, a deeply laterized, old land surface forms an escarpment with breakaways. The escarpment varies

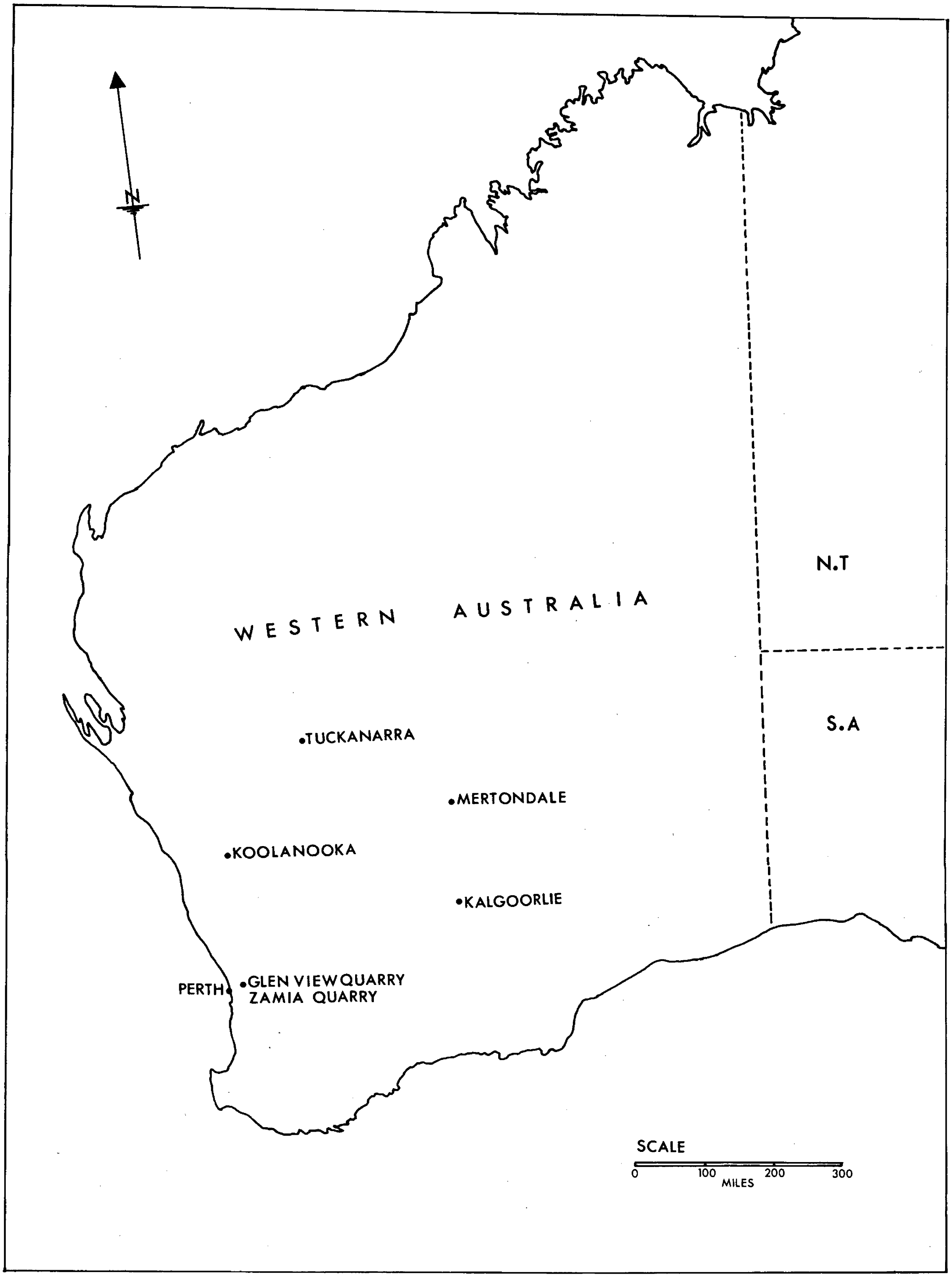

Fig. 24 Localities of samples investigated from Western Australia.

from 100 to 200 feet in height and exposes a deep laterite profile overlying a grey biotite-hornblende granite. The laterite profile does not overlie the Mertondale granite in present exposures, but a pallid zone occurs at the southern end of the exposure and may represent the base of lateritic development. At this point the granite is approximately 150 feet below the ancient land surface.

About 100 yards from the site of the pallid zone, a molybdenite-bearing quartz vein outcrops and has been prospected. A greisen zone occurs within the granite approximately 400 yards to the north of the pallid zone. Diamond drill hole, MD 1 was drilled at the southern edge of the outcrop through the kaolinised zone and into the granite by Western Mining Corporation.

7.2 GLEN VIEW AND ZAMIA QUARRIES

Both quarries are located in the Darling Range close to Perth (Fig. 24). A complex of granitic gneisses, migmatites (hybrid gneiss) and massive granites traversed by aplites, pegmatites and quartz veins is cut by still later basic intrusives. These vary from quartz dolerites to epidiorites (Prider, 1943). Prider found that

> the nature of this granite complex is largely obscured by the weathering of rock outcrops and the accumulation of weathering products and is not fully realized until freshly broken exposures in quarries are available for examination....

In the Zamia Quarry the base of weathering is shown by brown stained weathered "roots" extending downwards into the granite. A selection of fresh granite samples and material from a "weathered root" were collected.

The Glen View Quarry is a clay pit and fresh rock is not exposed. Fresh granite cut by a dolerite dyke, outcrops in a small cutting nearby. Within the quarry a deep truncated laterite profile is exposed for a depth of 150-200 feet. The surface is covered by a concretionary and pisolitic laterite, highly indurated and displaying a variety of nuclei within individual concretions. These vary from iron oxides through quartz to gibbsite and altered, heavily sericitized feldspar. An extensive study of the laterite and sub-lateritic sand was not attempted but a sample of each was analysed for trace elements. Although Terrill (1954) claimed that laterite does not occur west of the vicinity of the Darling Scarp, Prider (1946) examined laterite formed over a ferruginous sandstone which occurs well below the level of the Darling Plateau.

The next major zone below the laterite is a considerable thickness (40-50 feet) of mottled weathered granite. Small and numerous quartz veins appear to have their spatial relationship preserved. This zone merges gradually into the pallid horizon with increasing depth. The base of the pallid zone or horizon is not exposed within the quarry at the present time.

The "contact of the dolerite dyke and granite" can be traced through at least 100 feet by the absence of quartz grains and a pale creamy-yellow colour for the weathered dolerite. Unfortunately the "dolerite dyke" cannot be traced up into the laterite as quarrying activities have obscured the outcrop.

Compston and Arriens (1968) give a revised age of 2700 ± 150 m.y. for the Mundaring Granite, but note that the large range indicates either, a composite age of emplacement, or the opening of some total-rock samples by later metamorphism. The same authors give ages between 590 and 2500 m.y. for different minerals from the granite. With evidence of many intrusive episodes and partial rehomogenization, both the Glen View and nearby Zamia quarries were considered unsuitable for Rb-Sr isotopic studies.

Wilson (1957) has noted that the Boya, Stathams and Gosnells granites are massive although at Mundaring he observed evidence of foliation and structure within the granite. A combination of poor exposure and different weathering intensity has lead to individual discussion of each quarry in Chapters 8 and 9.

7.3 TUCKANARRA QUARRY

A belt of higher ground between Lake Annean and Lake Austin has been stripped of lateritic weathering and now exposes fresh rock.

The Tuckanarra Quarry is located within this belt, approximately 6 miles E of the Tuckanarra Siding on the Mt. Magnet-Cue railway line. Little is known of the geology in this region and there are no former publications.

The Tuckanarra granite outcrops as a gentle rise above the plain and its field relationships are obscured by soil and sand cover. The quarry reveals a grey biotite granite with hydrothermal alteration zones along shears. Xenoliths and/or biotite scheleiren are locally common and may give a streaky appearance to the granite. A small weathering profile (4-5 feet) consisting largely of "rotten rock" is developed above a band of bleached or pale altered granite, which in turn, overlies slightly altered to fresh granite. Pegmatitic stringers and segregations are locally abundant.

A selection of fresh, hydrothermally altered and weathered granite samples were collected along with one sample from a biotite rich xenolith (Chapter 8).

7.4 KOOLANOOKA HILLS, W.A.

7.4.1 Location and Geological Setting

The Koolanooka Hills lie approximately 200 miles north of Perth, W.A. and nearly 13 miles east of the township of Morowa (Fig. 24). They form part of the West Australian shield, lying close to the western margin. Arriens (1963) has described the geological history of the area and only a brief summary will be given here.

To the west, the Koolanooka Hills are bounded by two prominent and parallel NNW trending ridges, rising approximately 300 feet above the surrounding plain. These are formed by vertically dipping jaspilite, and are separated by a large dolerite dyke. Resistant ferruginous laterite caps the flat topped ridges.

To the east of the jaspilite ridges and separated from them by country rocks, low hills of quartz porphyry outcrop. A large crescent shaped band of salt lake country and alluvial plains isolates the Koolanooka Hills from other outcrop areas in the region.

Stream flow is intermittent with the present climate and drains into the salt lake system. Arriens (1963) concludes from bore information, obtained adjacent to the Billeranga Hills, that the salt lakes bury a former river system beneath an alluvial blanket approximately 400 feet deep. Near the northern limit of outcrop in the Koolanooka Hills, 15 feet of alluvium covers the quartz porphyry. Alluvium cannot be very deep adjacent to the jaspilite ridge as outliers of gneiss and granite are visible in cleared land, as far as one or two miles west.

7.4.2 Geology and Intrusive Relationships

Country rock surrounding the quartz porphyry is largely mica schist and quartzite, with minor actinolite schists, hornfelses and jaspilites to the west. These low grade metamorphic rocks have been intruded by acid and basic magmas. Granitic gneisses, concordant with the country rock, have been dated at 2920 ± 220 m.y. (Compston and Arriens,

1968) and are the oldest dated rocks in the area. The intrusion of granites and xenolithic granite porphyrys followed approximately 300 m.y. later (2615 ± 40 m.y.; Compston and Arriens, 1968). The next event was intrusion of the Koolanooka quartz porphyry, dated at 2555 ± 12 m.y. (Arriens *et al.*, 1966) and 2560 ± 15 m.y. (Compston and Arriens, 1968). The last intrusive phase, excluding minor dolerite dykes, was a granite porphyry dated from two highly radiogenic total rock samples at approximately 2290 m.y. (Compston and Arriens, 1968). This last acid intrusive phase is of very minor importance in the Koolanooka Hills. Two periods of dolerite dyke intrusion bring to a close the igneous intrusive activity of the area. A long period of erosion followed by formation of laterite, completes the geological sequence of events of the area.

7.4.3 Koolanooka Quartz Porphyry

The Koolanooka quartz porphyry is a small intrusion exposed over an area of three square miles (Fig. 25). The intrusion has been described as funnel-shaped by Arriens (1963) on the basis of dipping xenoliths around its exposed margins. It is unlike any other intrusive mass known in the West

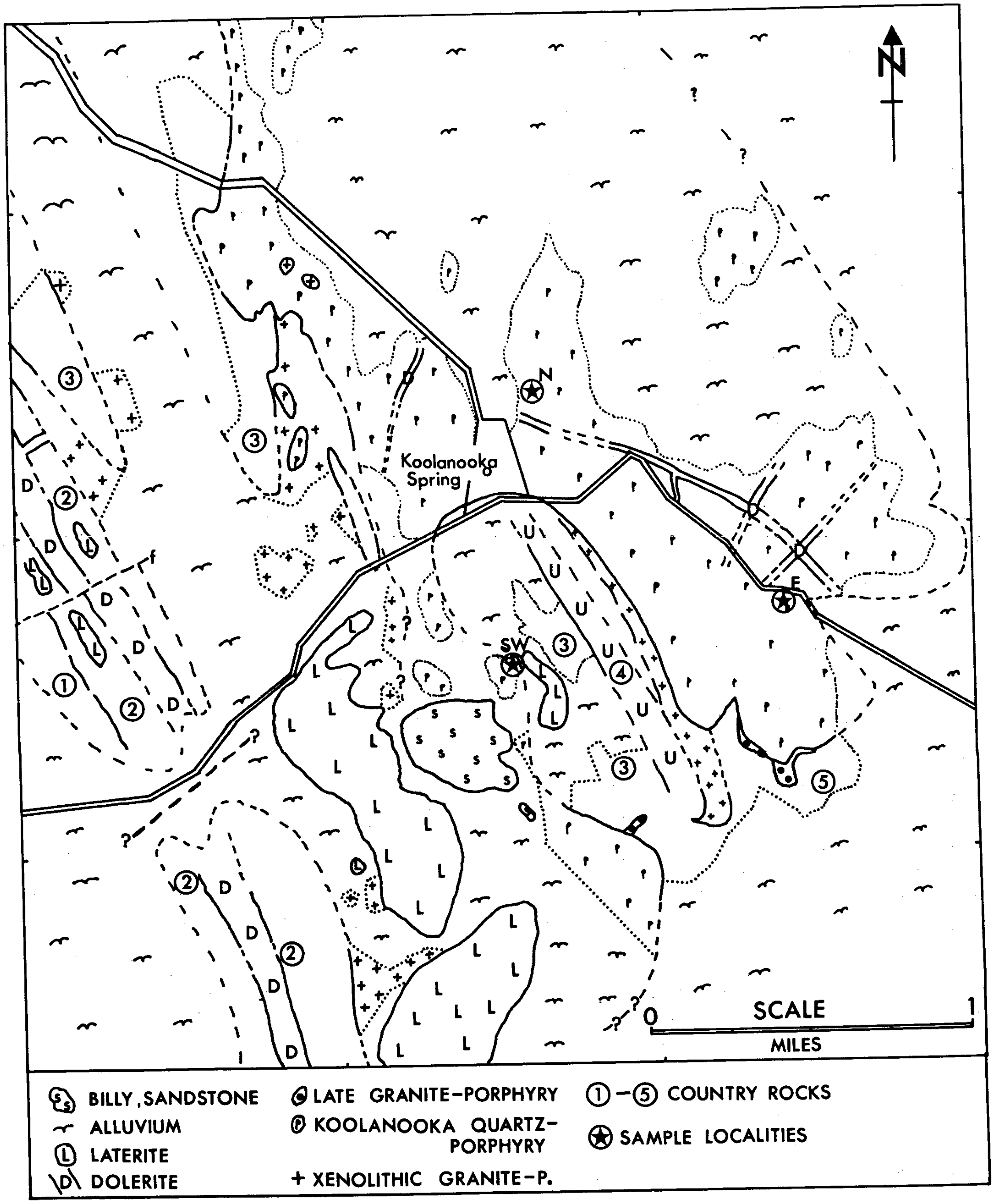

Fig. 25 Geology of the Koolanooka Hills W.A. (after Arriens, 1963).

Australian shield. Xenoliths are numerous at the margins but they are not found far from the contact. Many are biotite hornfelses and further from the margins there are almost no femic minerals. Small phenocrysts of bipyramidal quartz and feldspar in a microcrystalline groundmass of quartz and feldspar can be interpreted as evidence for intrusion into very high levels. The southwestern section of the porphyry is largely covered by laterite or sand preventing interpretation of its structure. Xenoliths are very rare in the southwestern locality and the relationship of this porphyry to the main mass can not be ascertained.

CHAPTER 8

PETROLOGY AND CHEMISTRY OF WEST AUSTRALIAN LOCALITIES

8.1 MERTONDALE GRANITE

8.1.1 Petrography

The Mertondale granite is red, medium to coarse grained (2-5 mm) and leucocratic. Potash feldspar, quartz, plagioclase, muscovite (sericite) and accessory zircon and allanite comprise the granite; it lacks a distinct ferromagnesian mineral. There is extensive evidence of post-emplacement shearing but shears have been healed with muscovite or coarse sericite. Feldspars usually contain heavy pale brown-buff alteration products. Although the lowermost sample from MD.1 (6292) appears fresh with reflective feldspar cleavages, petrographically one can observe the effects of late-stage hydrothermal alteration. Potash feldspar is the dominant mineral varying from approximately 50 to 60% of the granite. It is heavily sericitised, has Carlsbad twins and is coarsely perthitic. Large intergrown crystals (3-7 mm) are frequently rimmed by small plagioclase grains which have apparently exsolved from the host alkali feldspar. Fractured crystals are common with coarse sericitic alteration localised along these zones and in adjacent feldspars.

Quartz ranges from 30 to 35% of the granite and displays undulose extinction. Large anhedral grains are typical but occasionally bipyramidal outlines can be seen where the quartz is partially enclosed by feldspar. A few grains exhibit kink folds (see Chapter 5) suggesting considerable stress and/or deformation after crystallisation.

Plagioclase rarely forms large crystals and usually occurs as exsolved grains either in potash feldspar or as coarse perthite lamellae. The granite probably crystallised one feldspar and exsolved albite during cooling.

Muscovite is present both as large crystals, which are probably primary, and coarse sericite, an alteration product of feldspar.

Accessory minerals include allanite, zircon, an opaque iron oxide and rare fluorite. Allanite is frequently pseudo-hexagonal in fresh samples but may be altered to a brown aggregate.

8.1.2 Chemistry

Analyses of fresh granite and altered variants are listed in Table B-4, Appendix B, together with element ratios. Fig. 26 illustrates the variation in oxides with progressive weathering.

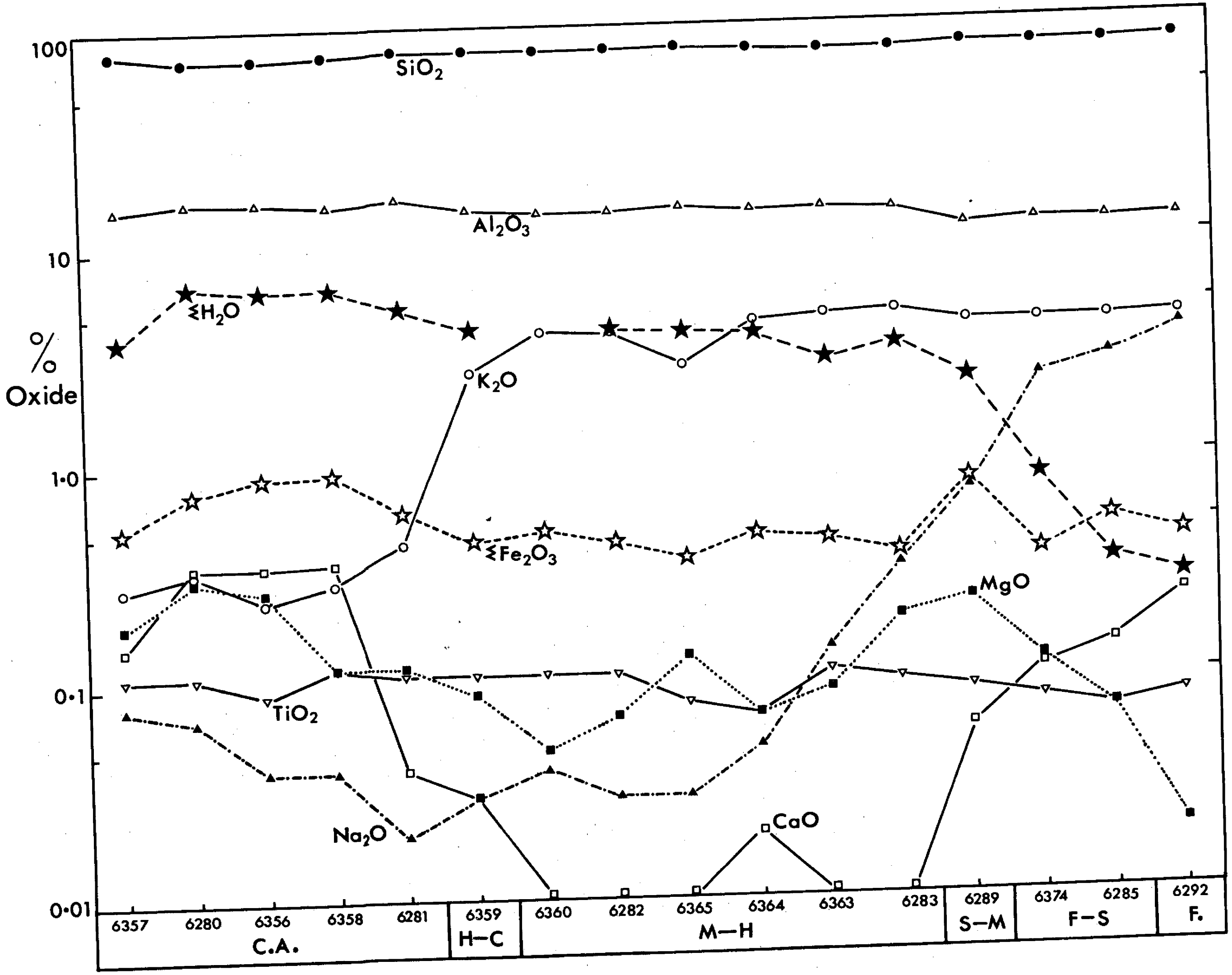

Fig. 26 Oxide variation diagram for altered Mertondale Granite.

High SiO_2 and low ΣFe_2O_3 contents are consistent with the leucocratic character of the granite and a low ΣH_2O content suggests that sample 6292 is unweathered. High Na/Ca and low K/Na ratios demonstrate that the feldspar is soda-rich and that the granite is either a small, extremely fractionated, leucocratic mass, or has aplitic-pegmatitic affinities.

8.2 WEATHERING OF THE MERTONDALE GRANITE

8.2.1 Fresh to Slightly Altered Granite

The alteration of plagioclase, (both as individual grains and perthite lamellae) to kaolinite precedes that of potash feldspar. Cleavage faces are dull, some vugs are visible and the granite is weakened. An increase in total H_2O is accompanied by lower Na_2O and CaO contents (Fig. 26). Oxides other than MgO are unaffected by alteration of the granite. The anomalous increase in MgO may be due to local redistribution by magnesia-saturated groundwater, or else the fresh granite has locally variable MgO contents.

Weathering also results in lower Fe^{++}/Fe^{+++} ratios and higher K/Na and Na/Ca ratios.

8.2.2 Slight to Moderate Alteration

A fine network of muscovite along fractures and in small veins is prominently developed within this interval. Feldspars are heavily altered to pale buff-brown sericite and clay minerals. Occasional small veins of kaolinite are associated with the sericite.

Continued loss of both Na_2O and CaO is more pronounced with concommitant increases in total H_2O, MgO and total iron (Fig. 26). The K/Na ratio increases while the Na/Ca ratio decreases. All changes correlate with greater alteration of plagioclase than potash feldspar.

8.2.3 Moderate to High Alteration

Quartz crystals have corroded edges and are extensively broken, appearing as rather angular fragments. A pale clay frequently surrounds quartz crystals as a clay cutan. Feldspar is practically obscured by alteration products and cut by veins of kaolinite. Muscovite-sericite alteration still predominates over kaolinite.

Nearly complete alteration of plagioclase and initial alteration of both quartz and potash feldspar are reflected in Fig. 26. A slight decrease in SiO_2 accompanies increases in Al_2O_3 and total H_2O, although the latter does not change appreciably throughout this interval. Almost total depletion of CaO and Na_2O suggests complete alteration of plagioclase.

An aplitic phase (sample 6364) is chemically indistinguishable from the granite (Fig. 26) although texturally it is equigranular and finer-grained (<1 mm).

K/Na ratios continue to increase markedly whereas Na/Ca decreases.

8.2.4 Highly to Completely Altered Granite

Microcrystalline carbonate stringers and odd patches traverse sample 6359 but are unrelated to sericitic alteration. Feldspars are totally obscured by alteration products, and it is impossible to assess the extent of alteration. Quartz is shattered, corroded and all fragments are markedly angular. Areas of sericitic alteration are visible within altered feldspars which are veined by kaolinite (?).

Lower K_2O (Fig. 26) substantiates alteration of potash feldspar and marginally higher CaO reflects the addition of carbonate.

The K/Na ratio is unchanged while the Na/Ca ratio has decreased (Table B-4, Appendix B).

8.2.5 Completely Altered Granite

Quartz and kaolinite with subsiduary sericite dominate the mineralogy. Feldspars have been totally altered to kaolinite which occurs as small accordian-like crystals (vermicular kaolinite). Part of the clay appears to lack definite crystallinity and has not been identified. Residual quartz grains are broken and show prominent dissolution effects, particularly when surrounded by clay cutans. Aggregates of sericite or hydromica remain along with residual flakes of muscovite which may be contorted by the encompassing clay. Fine carbonate "stringer veins" are variable from sample to sample. Numerous cavities in the uppermost samples have ferri-argillan cutans which stain the surrounding clay matrix.

The relative amounts of residual quartz, secondary carbonate and clay veins vary considerably. The lower kaolinite/quartz ratio of sample 6357 is reflected by higher SiO_2 and lower Al_2O_3 and total H_2O.

With the exception of quartz-rich sample 6357, SiO_2 and K_2O decrease whereas Al_2O_3, total H_2O, Fe_2O_3, MgO, CaO and Na_2O increase (Fig. 26). TiO_2 does not increase indicating that volume changes are relatively minor during alteration of the granite. Incomplete removal of K_2O substantiates the presence of residual muscovite-sericite or hydromica in quartz-kaolinite assemblages.

8.2.6 Elemental Ratios

Both K/Na and Na/Ca ratios change appreciably although the magnitude of the K/Na change greatly exceeds Na/Ca. Weathering induced variation of the K/Na ratio has been shown in Fig. 27. The K/Na ratio continues to increase through all stages of weathering until the uppermost completely altered zone where it sharply decreases. Total H_2O increases with progressive alteration of the granite. The initial increase in K/Na may be attributed to preferential retention of potash feldspar and muscovite-sericite, however later alteration of the feldspar causes a sharp decrease.

Fe^{++}/Fe^{+++} ratios decrease rapidly during initial weathering but with greater alteration the ratio is highly variable.

Na/Ca ratios decrease during weathering but the addition of secondary carbonate (samples 6280, 6356 and 6358) lowers values below those of other clay residuals (Fig. 28).

8.2.7 X-ray Diffraction Studies (X.R.D.)

The presence of partly disordered (?) kaolinite and quartz in weathered residuals has been confirmed by X.R.D. Kaolinite resulting from feldspar alteration, occurs in slightly to completely altered samples. A micaceous "intermediate" alteration product is suggested by a broad 10Å reflection with a superimposed sharp muscovite peak. Alternatively the mica-like mineral is sericite which has been inherited from the

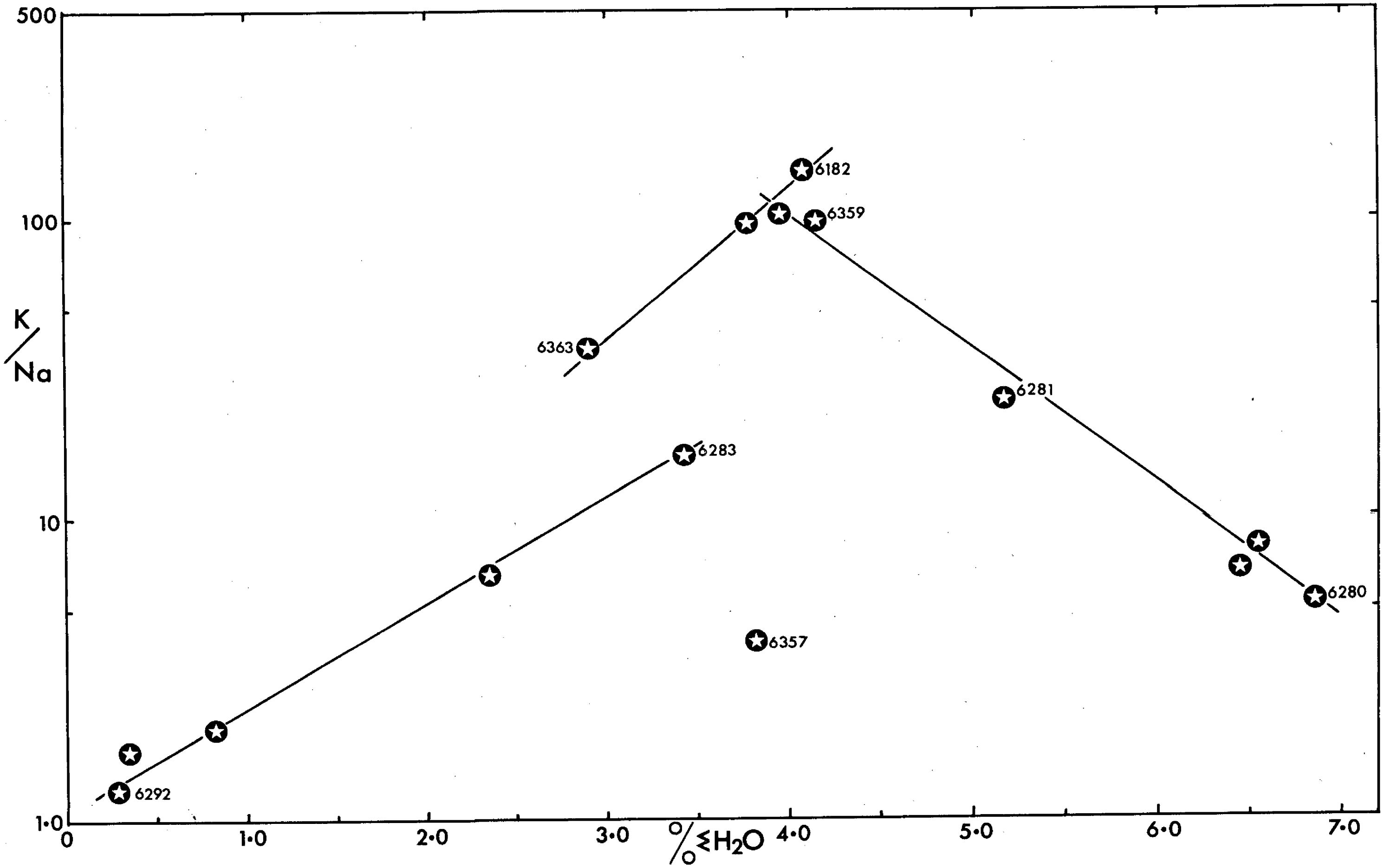

Fig. 27 Total H_2O content and K/Na behaviour during alteration of the Mertondale Granite. (Correction, 6182 replace with 6282.)

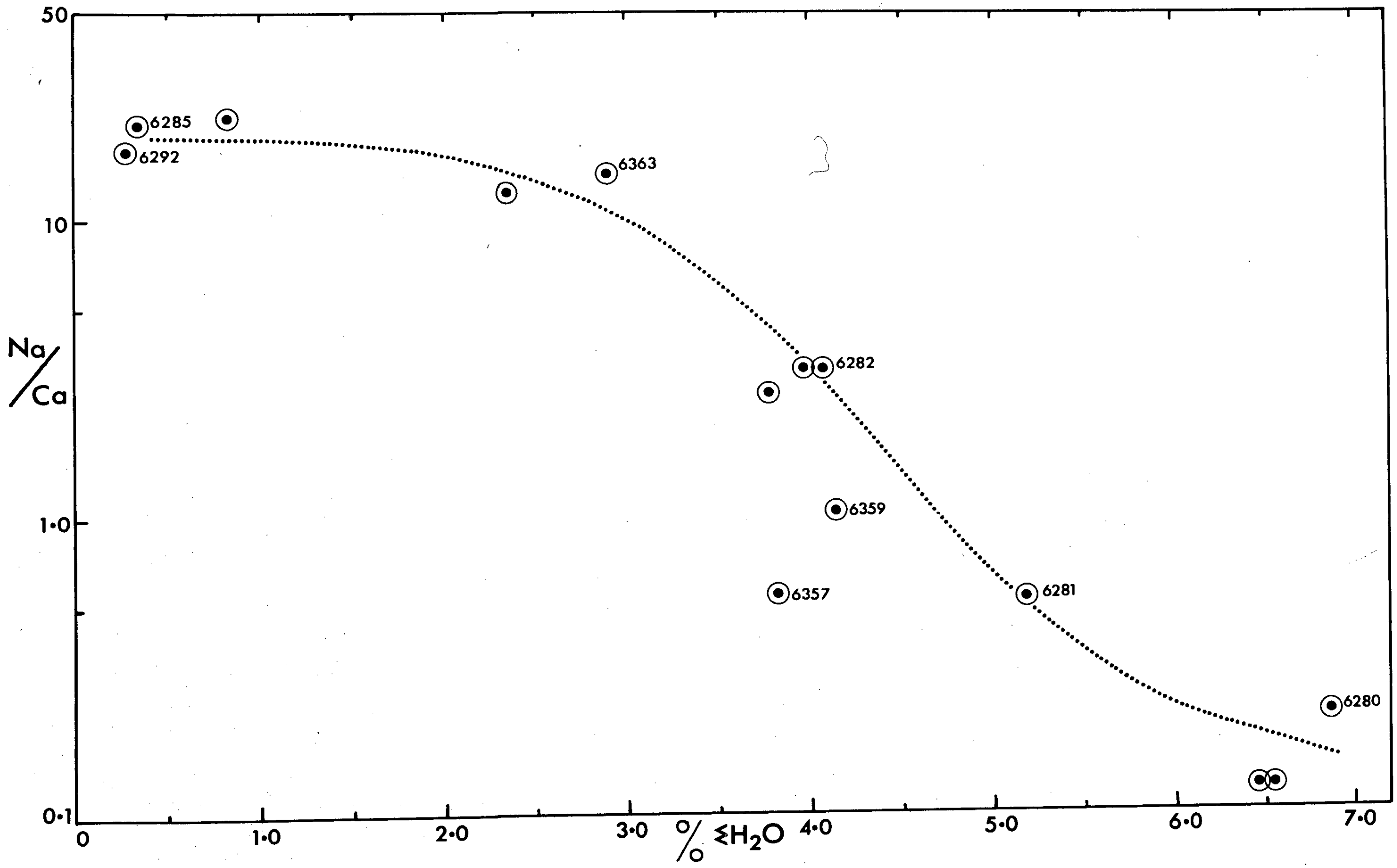

Fig. 28 Total H_2O content and Na/Ca behaviour during alteration of the Mertondale Granite.

parent rock. Sedimentation combined with brief diluted HF acid treatment (Chapter 10) and X.R.D. was employed to demonstrate the presence of sericite and muscovite in sample 6357. Both are considered to be inherited from the parent granite.

8.3 TUCKANARRA GRANITE

8.3.1 Petrography

The Tuckanarra granite is a grey biotite granodiorite which has been hydrothermally altered and bleached adjacent to local shear zones. Plagioclase, quartz, potash feldspar and biotite are the major minerals with accessory magnetite, chlorite, apatite, muscovite, fluorite, carbonate, epidote and rare allanite.

Plagioclase ranges from 35 to 40% of the granite and is the major mineral phase. Large crystals have many inclusions, are twinned and complexely zoned. The cores of zoned crystals are frequently clouded by sericite and may be heavily altered. Unaltered plagioclase is An_{33}.

Quartz commonly constitutes 20 to 25% of the rock. Crystals are large, anhedral and display undulose extinction.

Potash feldspar varies from 20 to 25% and is perthitic.

It is unaltered, has cross-hatched twins and may adjoin small patches of myrmekite/graphic intergrowths.

Biotite constitutes 5 to 8% of the granite but has been partially altered to chlorite. Pleochroism is from reddish-brown to straw yellow-green. Marginal alteration to and odd interleaves of chlorite are frequent particularly when surrounding feldspars have been heavily sericitised.

Accessory minerals are found associated with biotite flakes and opaque grains of magnetite.

Alteration minerals include sericite, epidote and carbonate after plagioclase, epidote and chlorite after biotite and small blades of muscovite.

8.3.2 Chemistry

Hydrothermal and weathering alteration, pegmatitic segregation and fresh granite variability are known at this locality (Chapter 7). Two weathered, one hydrothermally altered and one fresh granite samples were analysed and analyses are given in Table B-5, Appendix B. Analytical data are displayed in Fig. 29. An analysis of sample 6263 has been taken as representative of fresh granite in Fig. 29.

8.4 ALTERATION OF THE TUCKANARRA GRANITE

Late stage hydrothermal alteration has heavily sericitised plagioclase, retrograded biotite to chlorite and epidote and added carbonate. Weathering

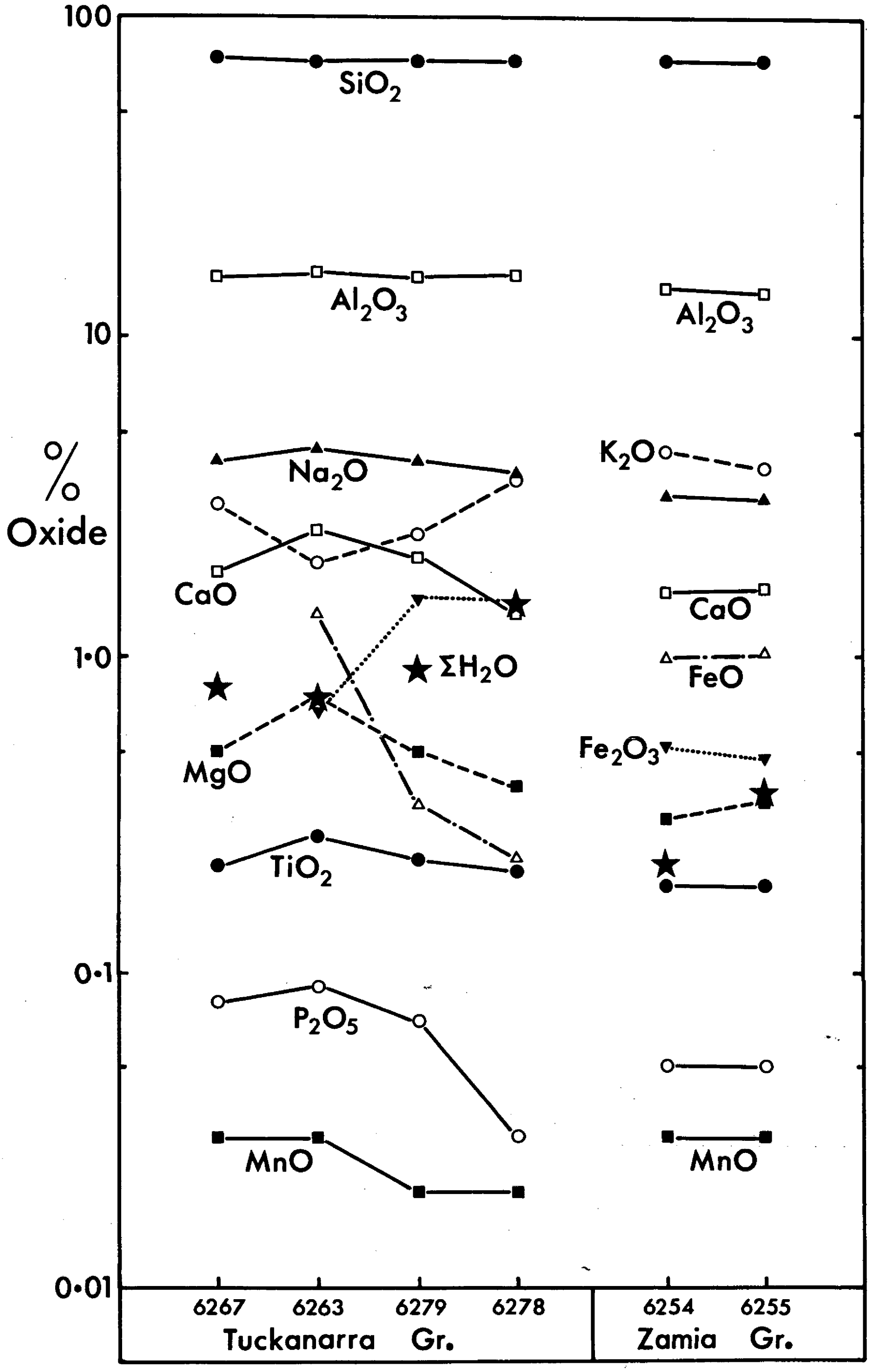

Fig. 29 Oxide variation diagram for samples from Tuckanarra and Zamia Quarries, W.A.

alters biotites by at first causing crystals to swell, liberating iron alteration products, and resulting in exfoliation of flakes; and later by causing brown masses or bleached exfoliated lamellae to form. The liberated iron oxides or hydrated weathering products stain the surrounding groundmass.

Sample 6267 has been mildly affected by hydrothermal processes (relative to sample 6263, fresh granite) and later slightly weathered, yet, changes in major elements are minor (Fig. 29). Surficial alteration (samples 6278 and 6279) is relatively slight, resulting in increasing ΣH_2O and Fe_2O_3 while Na_2O, CaO, FeO, P_2O_5 and MgO decrease. These changes accompany destruction of plagioclase and biotite with migration of iron-rich alteration products.

The Fe^{++}/Fe^{+++} ratio decreases and K/Na, Na/Ca and Fe/Mg ratios increase. Rapid iron oxidation occurs during the initial stages of weathering (Chapter 4) and restricts use of this ratio. The sensitivity of major elements to initial weathering is low although total H_2O and Fe^{++}/Fe^{+++} variations may be used.

8.5 ZAMIA QUARRY GRANITE

8.5.1 Petrography

With the exception of samples 6255 and 6262, all samples are of fresh granite. Late-stage alteration is confined to sericitic "dusting" of plagioclase and epidote alteration of calcic cores of a few plagioclase crystals. The mineralogy consists of potash feldspar, plagioclase, quartz and biotite with minor epidote and accessory chlorite, muscovite, apatite, an opaque mineral and myrmekite.

Potash feldspar comprises approximately 30 to 35% of the rock, is perthitic and displays microcline "cross hatch" twinning. It is unaffected by weathering processes in samples 6255 and 6262.

Plagioclase ranges from 25 to 30%. Zoning and twinning are prevalent, composite crystals are common and the cores of large plagioclases are frequently cracked or fractured. Preferential alteration of more calcic zones occurs and cracks may be stained with limonite.

Quartz makes up approximately 30% of the rock and its large anhedral grains display undulose extinction.

Biotite is commonly 4 to 6% of the granite and is partly chloritised. Raggy crystals have many radioactive halos around small inclusions. Minor weathering is shown by release of iron alteration products from biotite and a change of pleochroism from olive-green to palest straw-brown to dark brown-black to rusty straw. Frequent bands or interlayers of brown alteration products between lamellae may affect the pleochroic scheme although only sample 6262 shows signs of swelling or exfoliation. Chlorite alteration is highly variable within one thin section.

Epidote, an alteration mineral, is formed at the expense of biotite and plagioclase. Muscovite, apatite, titano-magnetite, secondary leucoxene, and possible monazite constitute accessory minerals.

8.5.2 Chemistry

Analyses of one fresh (sample 6254) and one weathered granite (sample 6255) are listed in Table B-5, Appendix B and have been included in Fig. 29 with analyses from the Tuckanarra Quarry. The two analyses are remarkably similar yet indicate minimal weathering of sample 6255. Similar Fe^{++}/Fe^{+++} ratios demonstrate insignificant oxidation and the increase in ΣH_2O is marginal. The low weathering intensity shown by sample 6255 has not affected the major element chemistry.

Analyses of granites from this area have been compiled from various sources and are listed in Table 15. Biotite adamellite (column 3, Table 15) from Mahogany Creek is similar to the Zamia Granite (column 4, Table 15) although K_2O may be marginally higher. The Mundaring granodiorite has distinctly lower SiO_2 and higher Al_2O_3 and CaO and appears to be unrelated to other massive granites. The nearby Glen

Table 15

Analyses of granites and dolerites from the Darling Range, W.A.

	1	2	3	4	5	6	7	8
SiO_2	68.56	73.49	73.36	73.55	75.95	49.13	49.53	47.99
TiO_2	0.24	0.14	0.04	0.19	0.19	1.27	2.13	1.77
Al_2O_3	16.64	14.24	13.88	14.15	13.97	13.13	12.92	13.40
Fe_2O_3	0.89	0.88	0.84	0.52	0.51	3.65	2.60	2.29
FeO	1.77	0.92	0.93	0.99	1.05	8.95	11.40	10.96
MnO	0.03	tr	0.15	0.03	0.02	0.15	0.35	0.22
MgO	0.73	0.43	0.51	0.31	0.40	7.64	6.24	6.94
CaO	2.51	1.84	1.69	1.59	1.71	11.84	10.37	11.47
Na_2O	4.14	3.86	3.22	3.17	3.03	1.72	2.08	1.70
K_2O	3.24	3.42	5.07	4.39	3.97	0.16	0.36	0.32
H_2O^+	0.97	0.55	0.18)	0.22	0.46	1.72	2.21)	1.57
H_2O^-	0.03	0.08	0.11)			0.04	0.09)	
P_2O_5	0.12	0.01	0.07	0.05	0.07	0.14	0.16	0.17
CO_2	nil	0.07	nil	0.09	0.13	-	nil	0.07
Total	99.96	100.01	100.19	99.25	101.46	99.99	100.72	98.87

1. Biotite granodiorite, Mundaring (Simpson, unpublished - cited in Wilson, 1957)
2. Biotite adamellite, Boya (Simpson, unpublished - cited in Wilson, 1957)
3. Biotite adamellite, Mahogany Creek (Simpson, 1916 - cited in Wilson, 1957)
4. Sample 6254, Zamia Quarry
5. Sample 6306, Glen View Quarry (granite)
6. Slightly uralitized quartz dolerite, Toodyay (Prider, 1944 - cited in Wilson, 1957)
7. Uralitized dolerite, Bickley Brook Reservoir, Darling Range (Simpson, unpublished - cited in Wilson, 1957)
8. Sample 6305, Glen View Quarry (dolerite)

View Quarry Granite closely resembles the Zamia granite (Table 15).

8.6 GLEN VIEW QUARRY GRANITE

8.6.1 Petrography

A grey, medium to coarse grained (2-5 mm) and massive granite is exposed in the Glen View Quarry. Late-stage hydrothermal alteration has changed biotite to chlorite and plagioclase to sericite. The mineralogy is typically quartz, plagioclase, potash feldspar, biotite and chlorite with accessory epidote, clinozoisite, muscovite, zircon and an opaque mineral.

Plagioclase is slightly more abundant than potash feldspar ranging from 30 to 35% of the granite. Small laths and large zoned crystals are all sericitised and have epidote-clinozoisit grains as alteration products. Multiple albite twinning may be obscured by alteration products and cracks or fractures infilled with epidote.

Potash feldspar forms large poikilitic crystals enclosing biotite, plagioclase and quartz. Grain size ranges from <1 mm to nearly 5 mm and cross-hatch twinning is well developed. Microcline is mildly perthitic and unaffected by alteration.

Quartz ranges from 30 to 35% of the rock forming occasional large anhedral grains which have undulose extinction, and numerous intergranular aggregates.

Biotite is very largely chloritised although small primary grains remain unaltered. Pleochroism is from slight green-brown to straw and pleochroic halos surround rare inclusions. Complete chloritisation of biotite flakes is more typical than occasional interleaves.

Muscovite forms occasional raggy crystals in addition to coarse sericite.

Chlorite is found filling fractures and as an alteration product of biotite. Large aggregates are sheath-like and associated with epidote.

Accessory minerals include an opaque mineral (magnetite) zircon, epidote, clinozoisite and carbonate.

8.6.2 Chemistry

An analysis of fresh granite (sample 6306) is included in Table 15 and is similar to those of the Zamia Quarry granite. As the quarries are 2 miles apart, both samples may be from the same intrusion.

8.7 WEATHERING OF THE GLEN VIEW QUARRY GRANITE

8.7.1 Petrography and X-ray Diffraction

Both recent weathering of exfoliation surfaces on the granite (sample 6303) and deep lateritic clay alteration (samples 6297, 6299, 6302 and 6310A) were examined. Recent weathering has stained the groundmass of the granite and partially altered plagioclase and biotite. The pleochroic scheme for biotites changes to dark green-opaque to straw and interlayers of red-brown iron oxides/hydroxides are common. Many former biotites have been weathered to either brown limonitic patches or bleached residuals.

The mineralogy of clay residuals was established by X.R.D. and consists of kaolinite, quartz, illite-sericite-muscovite and traces of feldspar except in sample 6310A. The illite-sericite-muscovite component decreases with depth in the profile (i.e. in the sequence 6297>6299>6302). Strong lines at 2.81Å 1.99Å and 1.63Å (possibly halite?) are present in sample 6302 which was collected from the side of a small drainage channel (1 foot wide) at the base of the quarry. Although samples 6310A and 6299 were collected from the same bench level in the quarry, the former is distinctly quartz-rich, illite-sericite-muscovite being greatly reduced and kaolinite possessing lower crystallinity.

8.7.2 Chemistry

Analyses are listed in Table B-6, Appendix B and shown in Fig. 30. Iron staining weathering marginally decreases many oxides with concommittant increase in total H_2O (Fig. 30). The Fe^{++}/Fe^{+++} ratio markedly

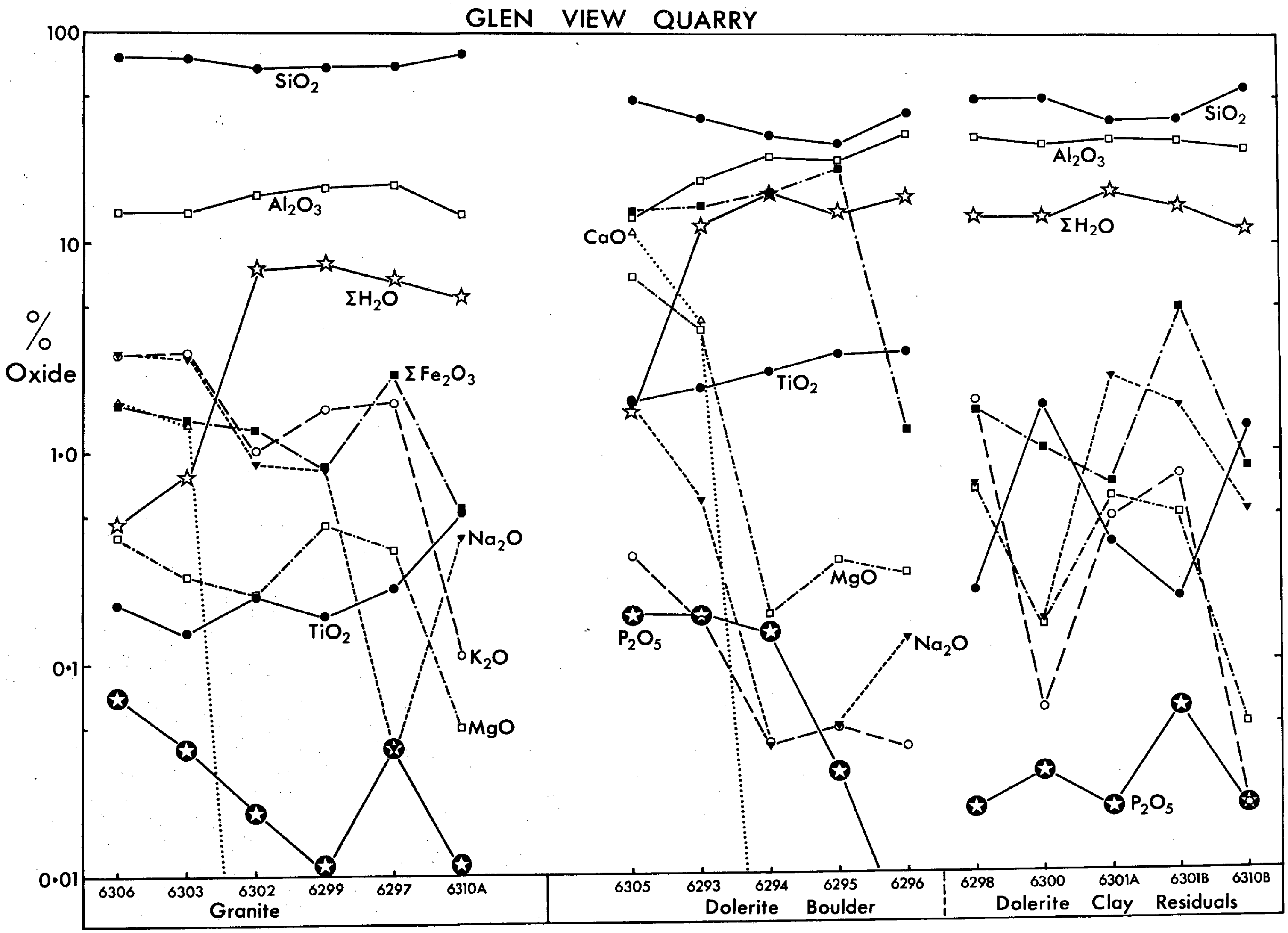

Fig. 30 Oxide variation diagram for weathered granite and dolerite from the Glen View Quarry, W.A.

decreases while other ratios increase slightly.

Kaolinisation has a pronounced effect on the bulk chemistry (Fig. 30). Large decreases in Na_2O, CaO and Fe_2O_3 are accompanied by increases in Al_2O_3 and ΣH_2O. These changes correlate with varying retention of muscovite-sericite and residual feldspar components in addition to different quartz/kaolinite ratios. A low total for the analysis of sample 6302 is due to the presence of halite and to an underestimation of water content. Considerable delay between major element and water determinations may have permitted water loss. The retention of Na_2O suggests that the illite-sericite component must be a soda-rich variety.

Sample 6310A may have anomalous chemistry as it is the granitic portion of a weathered "granite/dolerite contact sample". Higher TiO_2 may be an original feature and not a result of volume changes with residual enrichment.

Fe^{++}/Fe^{+++} ratios are uniformly low for all kaolinite-quartz residuals whereas K/Na and Na/Ca ratios are either erratic or indeterminate.

8.8 GLEN VIEW QUARRY DOLERITE

8.8.1 Petrography

Fresh dolerite is dark grey, fine-grained ($<$1 mm) and consists of a felted mass of amphibole and plagioclase with odd iron ore and epidote grains.

Actinolite varies from 50 to 55% forming felted masses or aggregates which are partially altered. Pleochroism is from blue-green to yellow-green.

Plagioclase ranges from 40 to 45% usually as lath-like twinned crystals. Complex twinning and zoning are shown by large crystals and a pale fawn-pink discolouration is typical.

Iron ore or ilmenite may be heavily altered to leucoxene.

Quartz occurs as odd crystals and as aggregates which are surrounded by altered actinolite masses.

Accessory phases include biotite, chlorite, epidote, apatite and carbonate.

8.8.2 Chemistry

In Table 15 an analysis of fresh dolerite (sample 6305) is compared with analyses of dolerites from the surrounding region: they are generally uniform. The analysis of the Glen View dolerite is intermediate between analyses in Table 15 (columns 6 and 7) suggesting moderate uralitisation of this dyke.

8.9 WEATHERING OF THE GLEN VIEW QUARRY DOLERITE

8.9.1 Petrography and X-ray Diffraction

A residual weathered boulder (samples 6293-6296) within the "dyke" was studied along with other dolerite-derived clay residuals (6298, 6300, 6301A, 6301B and 6310B). Progressive weathering alters the mineralogy, forming iron-rich alteration products and clays (Table 16). Halloysite and a mixed layer micaceous phase are indicated by X.R.D. The outermost rim of the weathered boulder and surrounding clay residuals are bleached and pallid consisting largely of kaolinite and the mixed layer micaceous phase. Very minor quartz is the only residual mineral from the parent dolerite.

8.9.2 Chemistry

Chemical analyses are given in Table B-6, Appendix B and displayed in Fig. 30. Considerable loss of SiO_2, Na_2O, CaO, MnO, FeO, MgO, P_2O_5 and K_2O accompanies marked increases in ΣH_2O, Al_2O_3, TiO_2 and initially, Fe_2O_3. The destruction of dolerite mineralogy and formation of hydrated iron-rich alteration products (samples 6293-6295) results in leaching of many elements and residual enrichment of Al_2O_3, Fe_2O_3 and TiO_2. Poor crystallinity and high iron content prohibit thorough identification of mineral phases by X.R.D. patterns although they and higher H_2O contents indicate halloysite rather than kaolinite as the major clay mineral. Iron alteration products may be appreciably hydrated.

Table 16

Mineralogy of weathered dolerite samples

Sample	Act	Fels	Qtz	Chlor	Mixed Layering (9.3Å - 10.1Å)	Goe	Haem	Kaol	Halloy	Sharp 10Å peak	Hal
6293	X	tr	tr	X	X	tr	-	-	-	X	-
6294	-	-	m	-	X	?	X	?	X	X	-
6295	-	-	tr	-	X	?	X	?	X	m	-
6296	-	-	tr	-	X	-	-	?	X	X	-
6298	-	tr	tr	-	X	-	-	X	-	X	X
6300	-	-	X	-	X	-	-	XX	-	-	-
6301A	-	tr	m-tr	-	X	-	-	XX	-	m	X
6301B	-	tr	m	-	X	-	-	XX	-	m	m-tr
6310B	-	-	X	-	X	-	-	XX	-	-	tr

Act = Actinolite
Fels = Feldspar
Qtz = Quartz
Chlor = Chlorite
Goe = Goethite
Haem = Haematite
Hal = Halite
Halloy = Halloysite
Kaol = Kaolinite
m = minor
tr = trace

Leaching of iron and development of pallid clays has lowered Fe_2O_3 for clay residuals (with the exception of 6301B). SiO_2 and Al_2O_3, but not TiO_2, appear to increase as a consequence of Fe_2O_3 depletion.

Other clay residuals (Fig. 30) have highly variable chemistries which may indicate interaction with the surrounding granitic clays (by means of groundwater transport). High Na_2O and K_2O reflect halite and micaceous components whereas dolerite parentage is demonstrated by high Al_2O_3 and low SiO_2 when compared with "granitic" clay residuals (Fig. 30).

A considerable decrease in Fe^{++}/Fe^{+++} indicates rapid oxidation and the highest iron content (sample 6295) is almost totally Fe_2O_3 (Table B-6, Appendix B). K/Na ratios increase during weathering of the boulder until pallid residuals are formed, beyond which they are erratic. Varying amounts of halite induce erratic behaviour in all ratios involving Na_2O. Fe/Mg ratios increase during weathering of the residual boulder, but other clay residuals have values ranging from lower to greater than those of fresh dolerite.

8.10 THE KOOLANOOKA QUARTZ PORPHYRY

8.10.1 Petrology

The southwestern lobe of the porphyry (Fig. 25) is represented by sample sequence 6311 to 6336 and although this locality differs from that of 94537 (Arriens, 1963) the mineralogy is identical. Fresh porphyry (sample 6311) is free of xenoliths and consists essentially of bipyramidal quartz and microcline phenocrysts (2-3 mm) in a microcrystalline groundmass of quartz and feldspar. Phenocrysts of oligoclase (An_{23}) are sericitised whereas those of quartz are either perfectly formed or corroded with deep embayments of groundmass. Accessory minerals include muscovite, green biotite, tourmaline, fluorite and zircon.

Two other localities from the central northern area (KP-1 of Arriens, 1963) and the eastern section of the porphyry (Fig. 25) were also sampled. The former is represented by samples 6337-6347 with 6337 being the fresh porphyry. This differs slightly from the southwestern porphyry with dark blue-green hornblende, brown biotite and iron ore. Tourmaline is either scarce or absent. Rocks of the eastern locality (samples 6348-6355) resemble those of the northern porphyry although their groundmass is finer, plagioclase phenocrysts are heavily sericitised and all phenocrysts display evidence of resorption. Biotite crystals are extensively chloritized adjacent to heavily sericitised plagioclase. Small microxenoliths are surrounded by groundmass which is almost cryptocrystalline and pronounced development of myrmekite occurs adjacent to these areas.

8.10.2 Chemistry

Analyses of all samples are listed in Table B-7, Appendix B and displayed in Fig. 31. Three fresh porphyries (samples 6311, 6337 and 6348) are compared with analyses from Arriens *et al*. (1966) in Table 17. Significant variations occur only in FeO, Fe_2O_3, CaO, MgO and Na_2O although differences are not great. Oxides which vary are related to ferromagnesian minerals such as hornblende and biotite. SiO_2 and ΣH_2O decrease in the sequence (6311-6348-6347) whereas TiO_2, Fe_2O_3, FeO, CaO, K_2O, P_2O_5 and to a lesser extent MnO and MgO increase. This suggests either progressive contamination during emplacement or a heterogeneous magma chamber and separate pulses of emplacement at slightly different intervals.

8.11 WEATHERING OF THE KOOLANOOKA QUARTZ PORPHYRY

8.11.1 Petrography

Recent iron staining weathering occurs at all localities however alteration is more pronounced on the southwestern variant. Deep lateritic weathering is only preserved at the latter locality.

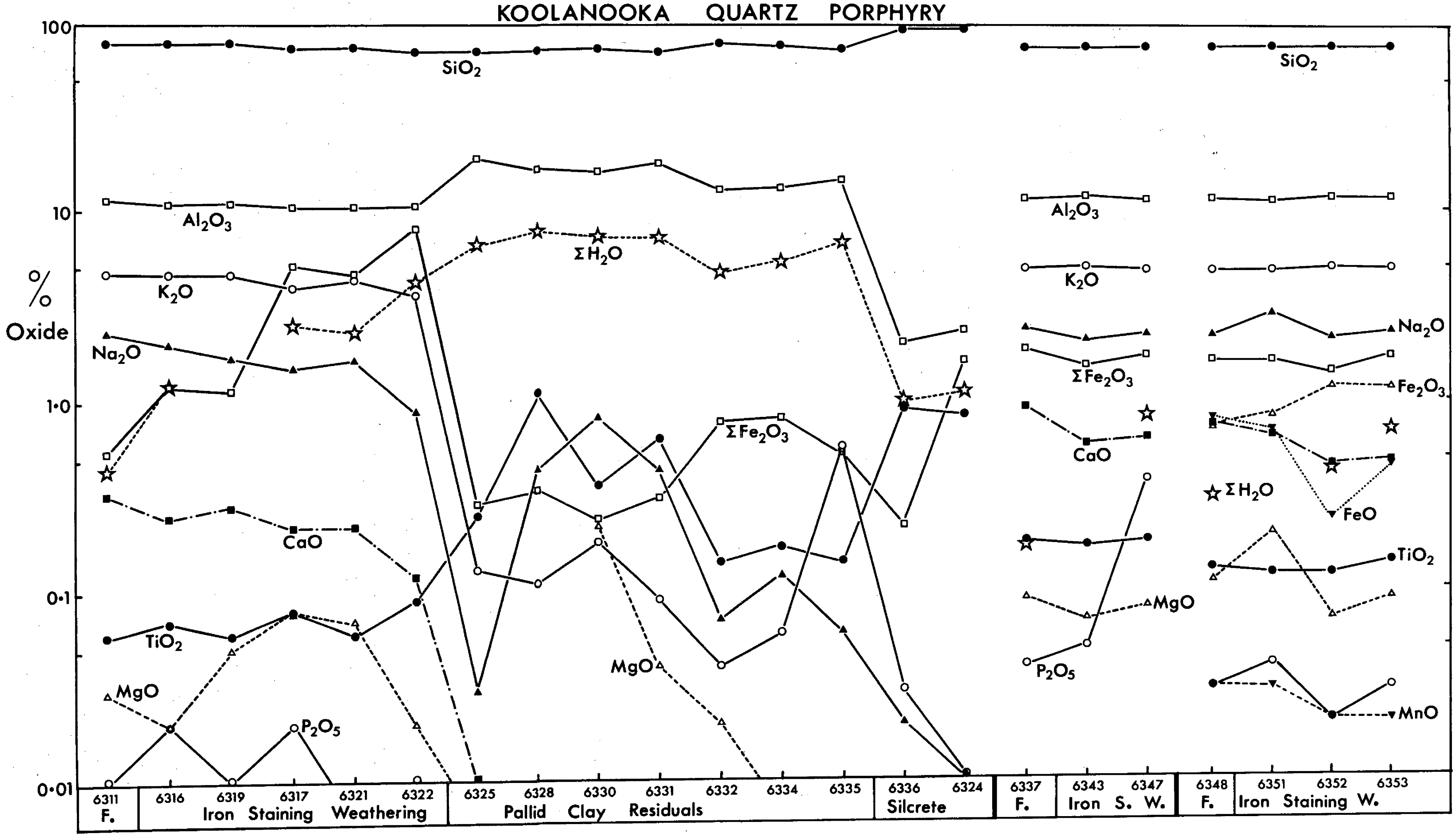

Fig. 31 Oxide variation diagram for weathered quartz porphyry, clay residuals and silcrete from the Koolanooka Hills, W.A.

Table 17

Chemical analyses of Koolanooka Quartz Porphyry

Sample	6311	94537	6337	94539	6348
SiO_2	79.38	77.44	76.46	77.54	77.36
TiO_2	0.06	0.08	0.18	0.20	0.13
Al_2O_3	11.50	11.42	11.52	11.76	11.58
Fe_2O_3	0.30	0.48	0.87	0.53	0.73
FeO	0.23	0.88	0.89	0.98	0.82
MnO	0.01	0.02	0.03	0.03	0.03
MgO	0.03	0.17	0.09	0.02	0.11
CaO	0.33	0.70	0.92	1.06	0.75
Na_2O	2.31	3.61	2.38	3.12	2.20
K_2O	4.73	4.71	4.88	4.56	4.84
H_2O^+	0.44	0.40	0.17	0.33	0.31
H_2O^-		0.02		0.01	
P_2O_5	0.01	0.06	0.04	0.04	0.03
Total	99.39	99.99	98.52	100.17	98.95

Samples 6311, 6337 and 6348 from Table B-7, Appendix B
Samples 94537 and 94539 from Arriens *et al.*, (1966)

At both northern and eastern localities exfoliation slabs and small weathered tors were sampled. Weathering penetration is highly variable but normally is only a few centimetres. Most samples have fresh porphyry at the centre grading outwards through progressively more altered rock. Weathering appears to have two stages; an initial pale cream followed by pale pink to dark red alteration zones. An indefinite boundary separates the two alteration types. At first, feldspar phenocrysts lose reflectivity from crystal cleavages becoming dull and turbid along with the groundmass which may appear cream or "milky" in colour. This stage grades into a pale pink altered zone which darkens in colour to pale red as a result of migrating iron oxides/hydroxides. Fractures develop parallel to the weathering surface, reflecting hydration and expansion. Plagioclase phenocrysts have increased sericitisation and are extensively fractured. Biotites have altered interlayers which are reddish-brown whereas hornblende loses iron and changes from vivid blue-green to straw-green (sample 6343).

Weathering at the eastern locality is less pronounced and confined to limonite staining of the groundmass although biotite in sample 6352 has been leached and displays partial exfoliation.

Weathering of the southwestern variant is more pronounced (samples 6316-6322) with feldspar alteration, fracturing of the rock and extensive limonite staining of the groundmass. Initial ferromagnesian mineral content is only accessory and cannot be the source of iron alteration products. Fractures are open and have been filled by clays. Feldspar phenocrysts become indistinct and quartz phenocrysts are corroded, particularly when surrounded by clay cutans.

Sample 6324 is a quartz residual comprised largely of bipyramidal phenocrysts loosely held together by clays and iron oxides. Variations in iron oxides, clays and films on quartz grains produce a colour banding from red to yellow.

Clay residuals (samples 6325-6335) are from the laterite profile considered to have formed from the porphyry. Quartz phenocrysts are fractured and partly separated by a clay-quartz-sericite matrix. Nearly all quartz grains show signs of corrosion and the main difference between clay residuals is the varying percentage of residual quartz phenocrysts. Thin sections reveal hydromuscovite-sericite in addition to vermicular kaolinite (?) which is present as accordian-like crystals. Tourmaline and muscovite grains are residual. Minor iron staining of the pallid quartz-clay assemblage is related to channelways and voids, but a slightly darker clay (?) appears to form from feldspars.

A hard surface in samples 6328 and 6332 may be due to secondary silicification (chalcedony) and addition of carbonate. The boundary of this layer with the pallid clay is extremely sharp. Prominent development of vermicular kaolinite is lacking in sample 6335 and clay "crystals" or aggregates are larger and splayed or have indistinct outlines. Microcrystalline quartz in the former sample suggests either incomplete alteration of the porphyry or partial resilicification. If the former is correct, this sample must lie near the base of the laterite profile.

A silicified residual (sample 6336) has minor clay and chalcedony filling intergranular areas. Voids with cutans are present and a colour banding is developed as a consequence of variable cementing agents.

8.11.2 Chemistry

Analytical data are listed in Table B-7, Appendix B and illustrated in Fig. 31. At both eastern and northern localities iron staining weathering has produced little chemical change. Increases in ΣH_2O accompany oxidation of ferrous iron. Other ratios are erratic.

In contrast, iron staining weathering of the southwestern variant produces significant changes (Fig. 31). Marked increases in Fe_2O_3 and ΣH_2O occur with decreases in CaO, Na_2O and K_2O during progressive alteration. Addition of limonite weathering products and alteration of feldspars are responsible for the observed changes.

Clay residuals generally have lower SiO_2 and greatly increased ΣH_2O, TiO_2 and Al_2O_3. Alkalis are depleted although samples 6328-6330-6331 have higher Na_2O. The presence of a 2.82 Å reflection suggests halite but the intensity of this peak is considerably less than for Glen View Quarry clay residuals. Fe^{++}/Fe^{+++} ratios are lower and K/Na are generally less than fresh porphyry values. Many Na/Ca and Fe/Mg ratios are indeterminate since Ca and Mg are not major elements for many clay residuals.

Fig. 31 shows strong positive correlations between Al_2O_3 and ΣH_2O whereas SiO_2 appears to be negatively correlated with both. Varying quartz/kaolinite ratios for individual samples are directly reflected by these oxides.

Silcretes or silicified residuals retain total H_2O, Al_2O_3 and SiO_2 correlations observed for clay residuals. The silcrete and quartz residual are remarkably similar, differing only in Fe_2O_3 contents.

CHAPTER 9

TRACE ELEMENT CHEMISTRY

All samples were analysed for the following trace elements: Rb, Sr, Ba, Pb, Y and Zr by X-ray fluorescence spectrometry (X.R.F.) and U and Th by gamma-ray spectrometry.

Insufficient sample prevented determination of U and Th by gamma-ray spectrometry for a few samples. The values determined by this method must be regarded with caution and can be taken as actual U and Th abundances only for samples in which radioactive equilibrium is beyond doubt or has been established by an independent method (Chapter 11, Appendix E).

9.1 MERTONDALE GRANITE

9.1.1 K/Rb Ratios

The fresh granite has a K/Rb of 315, a direct reflection of the high feldspar and low mica contents. Progressive alteration produces no significant change in K/Rb until complete alteration is achieved (Fig. 32, Table F-7 and F-8), as samples that may be grouped as highly to completely altered have virtually retained the initial granite ratio. Although

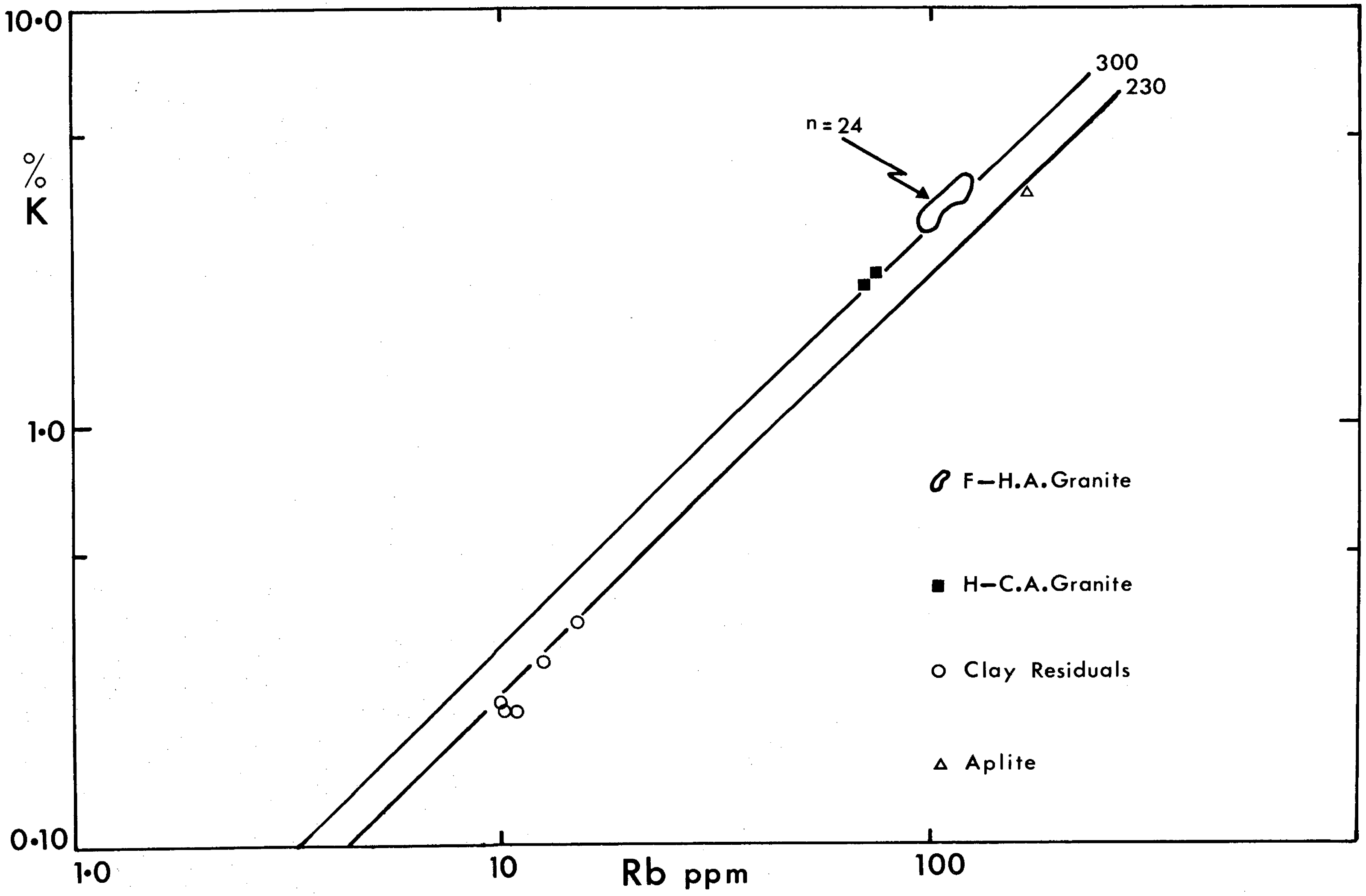

Fig. 32 K/Rb relationships for fresh and altered Mertondale Granite.

depletion in K and Rb occurs, the close coherence of these elements is retained until the mineralogy totally changes. Completely altered samples have K/Rb ratios ranging from 227 to 194, owing to preferential retention of Rb over K in or on the clay minerals. Fig. 32 displays a remarkable degree of internal similarity within the two groups and the lack of any intermediate phase. The destruction of the potassium feldspar lattice coupled with the formation of sericite (retaining nearly all K and Rb) and later kaolinization (with loss of a majority of the K and Rb) readily explains the existence of the two groups. While a detectable feldspar component remains it will effectively control the K/Rb of that sample. The aplitic phase of the granite has a lower K/Rb of 217.

9.1.2 K/Ba Ratios

Fresh granite has a K/Ba of 92 but sericitised granite has a slightly lower value. Kaolinization causes a slight initial loss in K, with relatively larger loss of Ba (Table F-7). Potassium has a lower hydration energy than Ba and will be more acceptable to the new crystal lattice of kaolinite. The completely altered samples appear to reverse this trend with Ba enrichment relative to K.

Secondary addition of carbonate, may have also affected the Ba content of these samples. The fluctuating behaviour of the K/Ba ratio is a result of the interplay of a number of different processes.

9.1.3 Ba/Rb Ratios

Fig. 33 indicates only very minor changes in the Ba/Rb ratio despite destruction of the feldspar lattice and formation of mica and clay possibly at different times. The Ba/Rb ratio is remarkably insensitive to the alteration of this granite, despite depletion of both elements (Table F-8).

9.1.4 Ba/Sr Ratios

Fresh granite has a Ba/Sr of 31.0 and with sericitic alteration this ratio increases to 141, before beginning to fall as kaolinization commences. Completely altered samples have a very low value (2.5), as a result of preferential Ba loss with retention or perhaps slight increase of Sr introduced with secondary carbonate. The strong initial increase in Ba/Sr can be explained as expulsion of Sr from the total rock volume during destruction of feldspar lattices to form sericite (or a fine mica). Sr is generally excluded from the mica lattice at the time of formation.

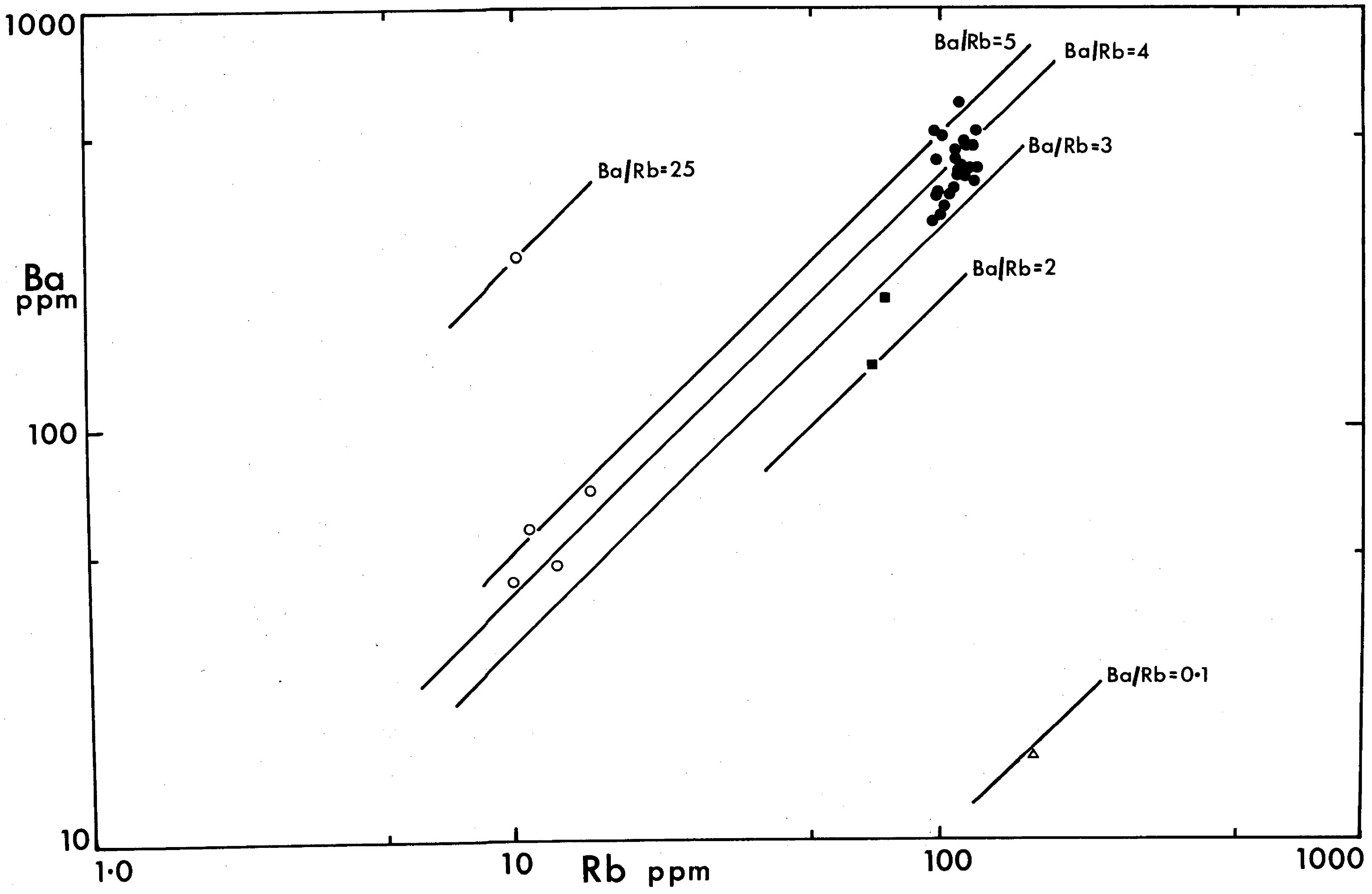

Fig. 33 Ba/Rb relationships for fresh and altered Mertondale Granite.

9.1.5 Rb/Sr Ratios

This ratio contrasts two elements with varying behaviour in different environments. Both enter potassium feldspars with ease but Sr is excluded from micas. Differing hydration energies for each ion, (Rb^+ and Sr^{++}) control adsorption and cation exchange processes which are markedly different from crystal lattice behaviour.

The Mertondale granite has a high Rb/Sr of 9.1 and with sericitisation Sr is lost from the total rock volume; the Rb/Sr ratio then increases to 38.0 (see Chapter 10). Kaolinisation however, causes a sharp drop in the ratio with Rb depletion (Fig. 34). The low initial Sr content limits further large scale removal and, with secondary carbonate addition to the quartz-kaolinite assemblage the Sr content increases. The Rb/Sr then decreases to 0.38, as a consequence of mica formation with feldspar destruction and addition of surficial secondary carbonate. This ratio illustrates the interaction of at least three processes: those previously mentioned and leaching.

9.1.6 K/Pb Ratios

This ratio illustrates the different behaviour of K and Pb during two types of alteration. Secondary mica formation retains K but Pb is progressively lost,

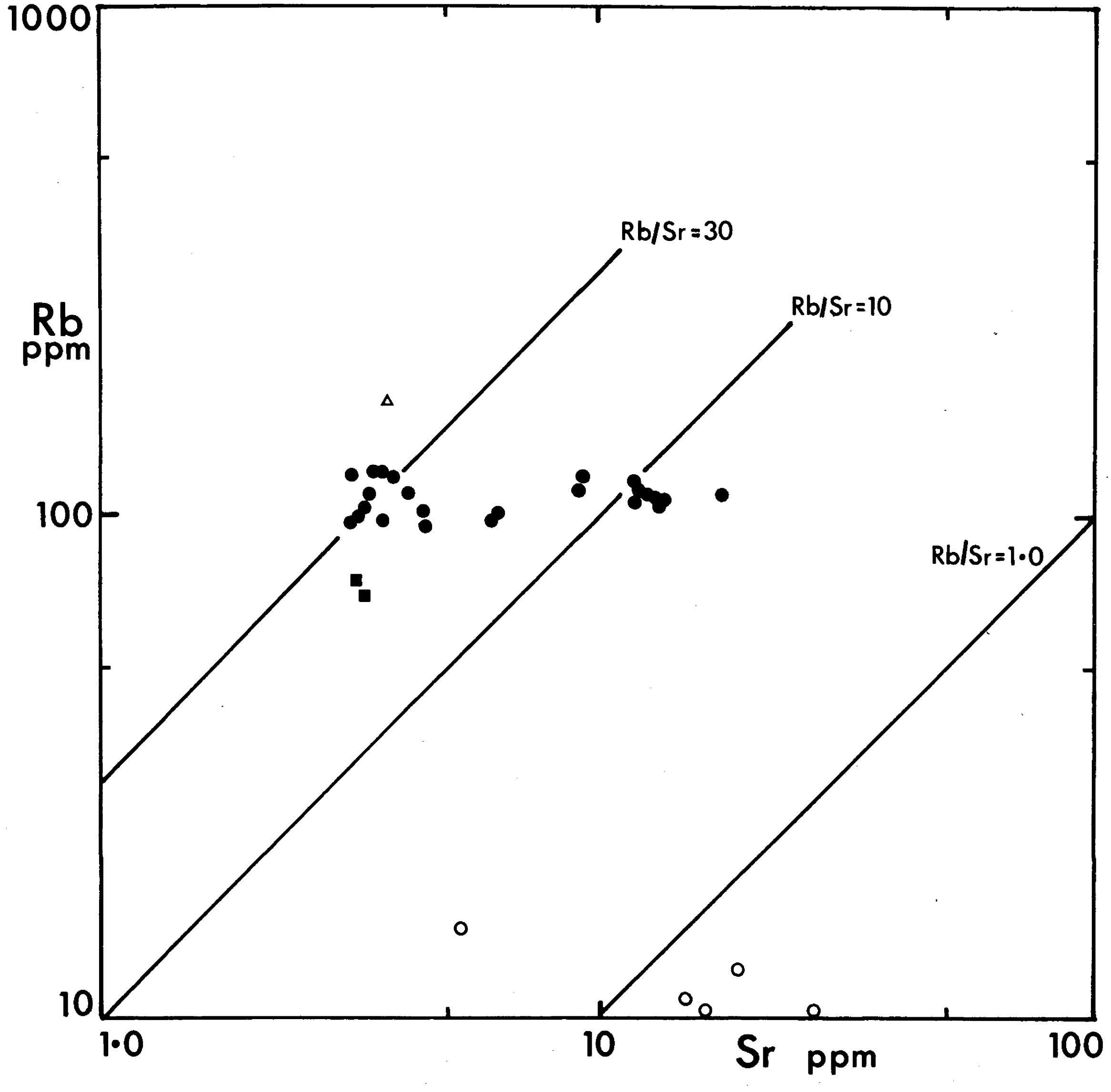

Fig. 34 Rb/Sr relationships for fresh and altered Mertondale Granite.

whereas kaolinization leads to marked depletion of both. Sericitisation alters the K/Pb value from approximately 2 x 10^3 to greater than 2 x 10^4, K remaining nearly constant. Kaolinized samples have K/Pb values similar to those of fresh granite but considerably reduced K and Pb concentrations.

9.1.7 Pb/Sr Ratios

Although there is a range of Pb/Sr ratios from 0.1 to unity, there are no mutually exclusive trends for the processes of sericitisation and kaolinization. Fresh granite with a Pb/Sr of unity changes with secondary mica alteration to lower values of not less than 0.4 with considerable depletion in Pb and Sr. In the three samples with determinable Pb contents, kaolinization lowers the Pb/Sr ratio to approximately 0.1. However, variable Pb contents in fresh to slightly altered samples (ranging from Pb/Sr of 1.0 to 0.1) obscure any trends.

9.1.8 Th/K, U/K and Th/U Ratios

Th/K x 10^4 ratios show no significant departure from fresh granite values of 2.1, until the granite has been totally altered. Such altered samples have markedly higher ratios ranging from 30.9 to 46.1. This is due to K depletion coupled with Th retention, although slight Th enrichment is apparent. The

U/K x 10^4 ratio displays analogous behaviour increasing from 0.5 to 5.7. Th/U ratios of the fresh granite are variable, ranging from 2.96 to 4.2 (Fig. 35). Sericitic alteration has broadened this range to Th/U = 2.0 - 8.29 by leaching of U. The clay residual material has the highest Th/U ratio with values from 9.6 to 11.9.

9.1.9 Yttrium and Zirconium

These elements are normally located in resistant mineral phases and consequently no large scale changes in element concentrations would be expected except residual enrichment. Y is located in allanite in the fresh samples (6291, 6292) and contents are very high, a feature not shown by other samples. These others have lower Y contents and very rare allanite. Zirconium contents are uniform, the only high values determined being for the aplite (6364) and one granite sample (6360).

9.2 TUCKANARRA QUARRY GRANITE

The Tuckanarra quarry exposes a granite with a small recent weathering profile (see Chapter 7). This sampling was intended to trace weathering from the stage exposed in the Zamia Quarry to present day rock decay at the surface. No direct soil profile is

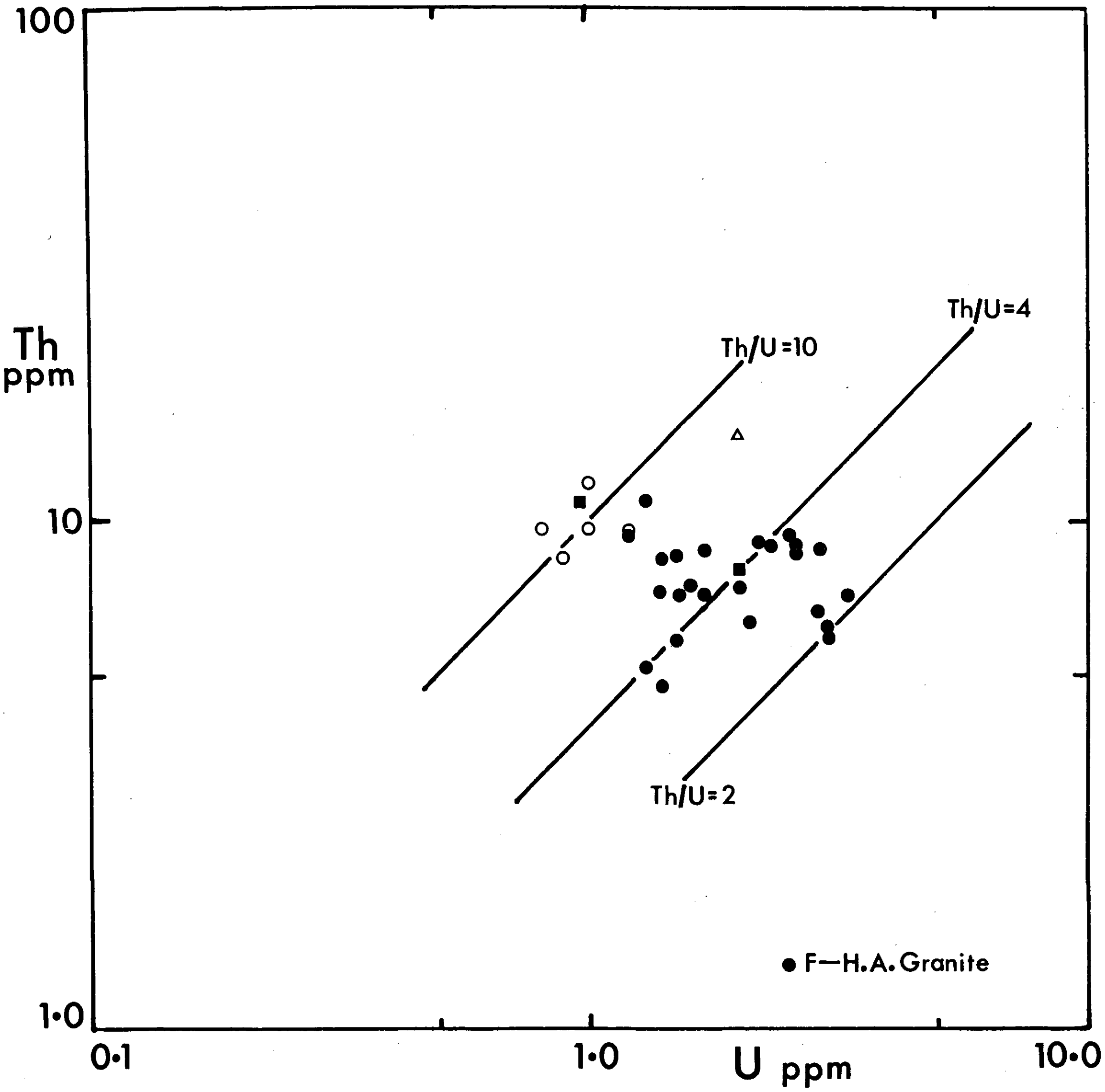

Fig. 35 Th/U relationships for fresh and altered Mertondale Granite.

seen, only decomposed rock at the surface. Unfortunately this granite has considerable evidence of contamination (see Chapters 7 and 10) and late-stage hydrothermal alteration. This alteration is commonly seen petrographically as sericitisation with epidote on feldspars and chloritisation of biotite.

Four samples were of insufficient size after processing to permit gamma-ray spectrometric analysis for Th, U and K. Trace element analyses and ratios are given in Tables F-9 and F-10 in Appendix F.

There is greater variation in analyses of the unaltered granite than between fresh and altered samples, although late stage alteration seems to result in lower K/Rb and higher K/Ba ratios (i.e. samples 6272 and 6273). This alteration has reduced the Ba content relative to K. A plot of Ba versus Rb (Fig. 36) also reveals the uniqueness of these two samples as well as the xenolithic sample 6265. Samples 6272 and 6273 have a Ba/Rb value of approximately 5.0 whereas those of fresh granite range from 6.8-10.9. Weathered samples do not depart from this range and are therefore indistinguishable.

Pb, Y and Zr display no significant changes with weathering. U and Th gamma-ray data show a similar

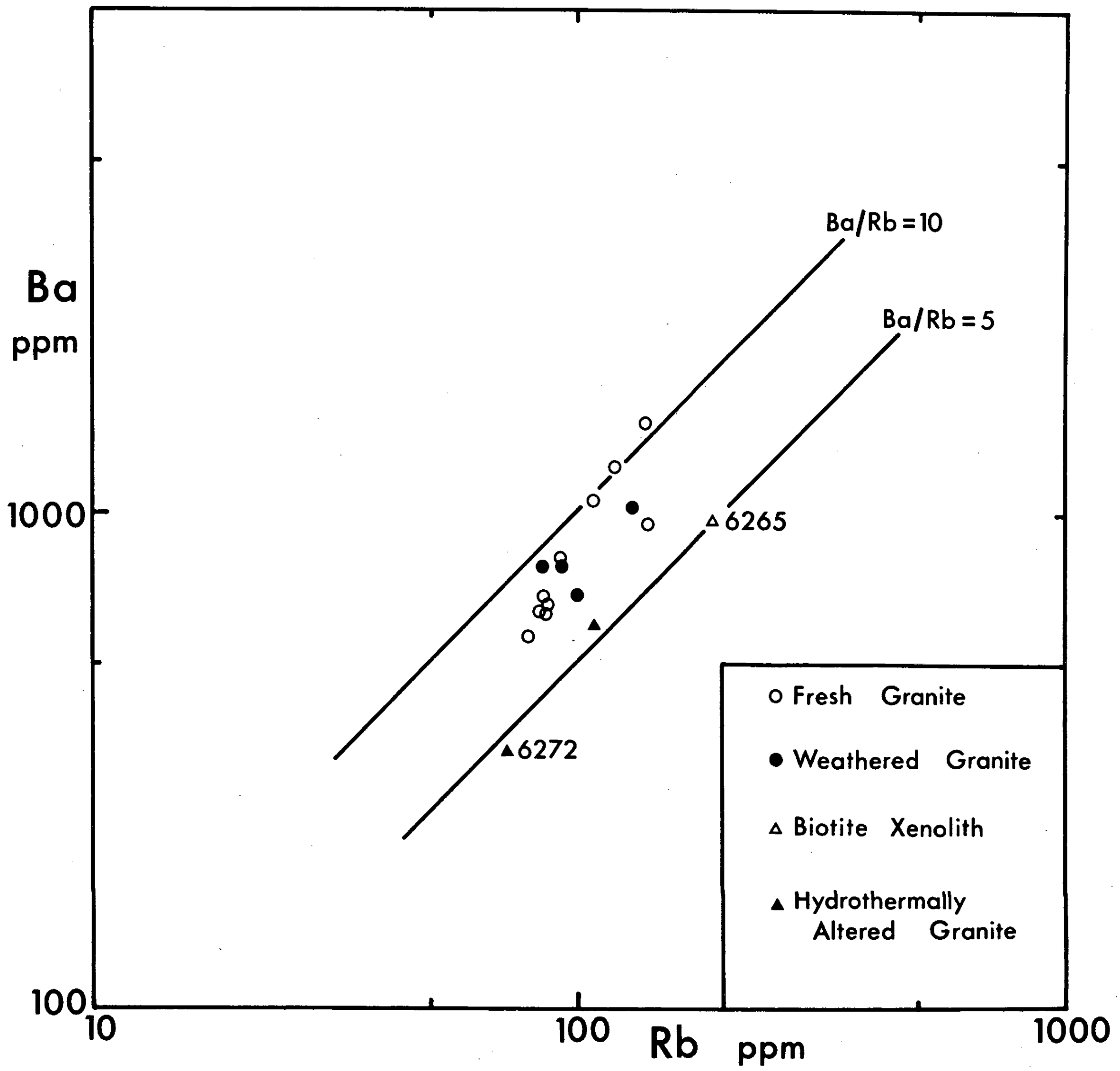

Fig. 36 Ba/Rb relationships for fresh and altered Tuckanarra Granite.

scatter to that of the Zamia Quarry granite and provide no means of separating weathered from fresh granite (Fig. 37).

The initial variations in trace element abundances in the granite are due largely to the assimilation of xenolithic material. This "primary" element dispersion effectively obscures any variations due to surficial weathering alteration.

9.3 ZAMIA QUARRY GRANITE

The very early stages of weathering have been studied in samples from a granite exposed in the Zamia Quarry (see Chapter 7). The grey equigranular granite has an "Fe-stained weathering projection" or "root" from the surface exposed in the quarry and this was sampled (see Chapter 7). Tables F-11 and F-12 in Appendix F detail results for trace elements and their ratios.

K/Rb, K/Ba, Ba/Rb, Ba/Sr, Rb/Sr ratios of the two weathered samples (6255 and 6262) all lie within the scatter of values found for the fresh granite.

Based on the evaluation of γ-ray Th and U data for the Snowy Mountains, U and Th disequilibrium is insignificant and measured gamma-ray U and Th values are therefore reliable. Considerable scatter in

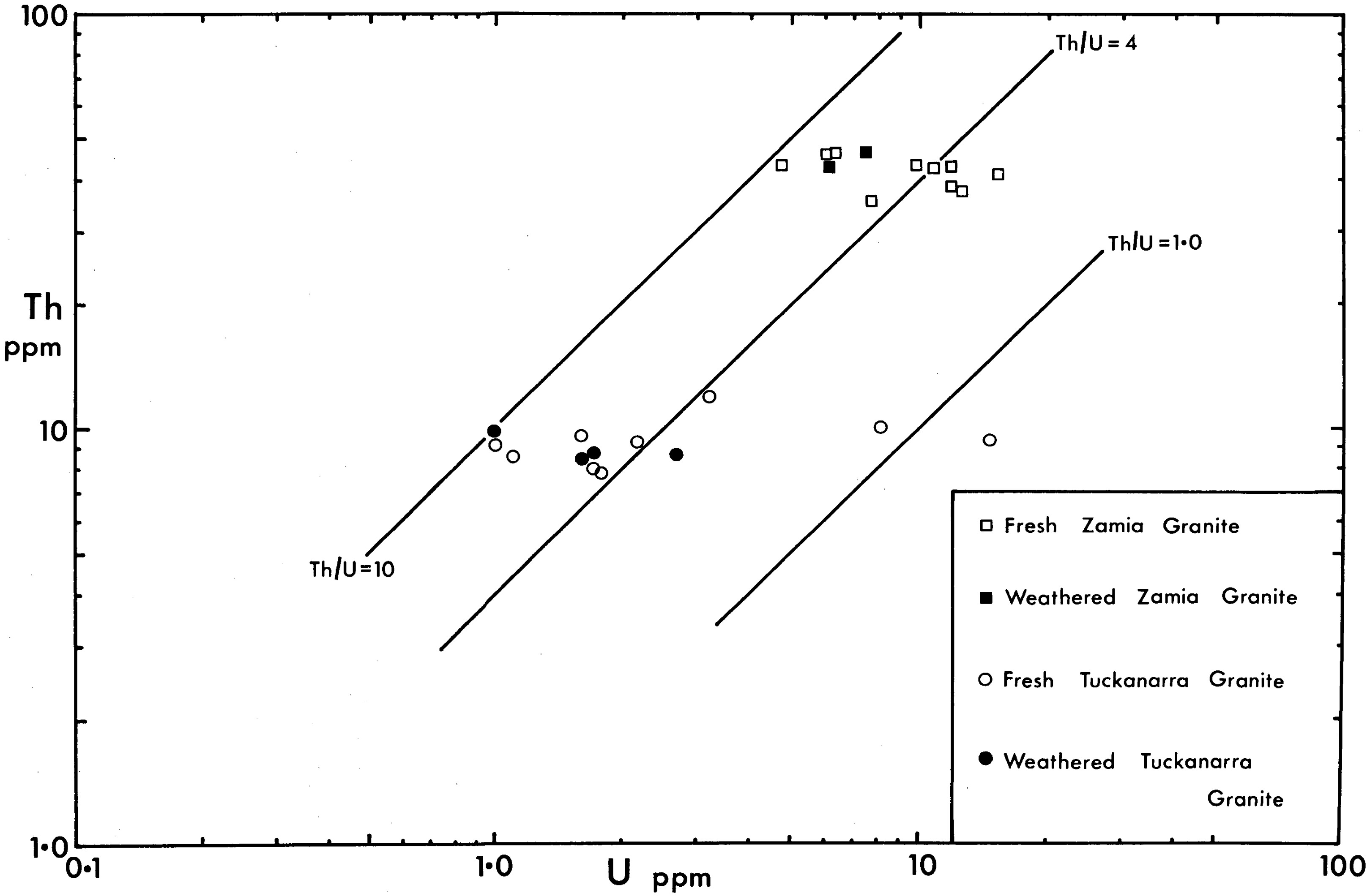

Fig. 37 Th/U relationships for Zamia and Tuckanarra Granites.

fresh rock U concentrations is apparent, resulting in widely varying Th/U ratios (Fig. 37, Table F-12). Samples 6255 and 6262 have Th/U ratios of 6.27 and 7.00 respectively; which are within the range of fresh rock variation. The large dispersion in Th/U ratio was unexpected, although such a variation is common in late stage or high level granites (Whitfield et al., 1959). U/K x 10^4 and Th/K x 10^4 values for the samples investigated also demonstrate no departure from fresh granite data, and neither do Pb, Y and Zr.

9.4 GLEN VIEW QUARRY

The occurrence of both granite and dolerite permits study of their respective weathering and of the extent to which drainage, groundwater flow, and ion exchange/adsorption phenomena may modify their alteration products. For this reason the progressive alteration of granite and dolerite will be considered together under each ratio being discussed.

9.4.1 K/Rb Ratios

Although the fresh dolerite has a K/Rb of 261, it is only 95 in the core of the weathered boulder studied. This core is very weathered and intermediate stages of weathering could not be sampled. K/Rb ratios decrease regularly between core and surface of this boulder (Tables F-13 and F-14 and Fig. 38). These low values are a result of K loss relative to Rb, although both are severely depleted.

The fresh granite has a K/Rb of 257, and very little change is detectable with iron-staining on exfoliation slabs - at most a slight decrease from K/Rb = 257 to 234. Granite clay residuals show a lower K/Rb for two samples (6299, 6302) but it is higher for another (6297). Samples of the laterite (6307) and sub-lateritic sand (6308) have K/Rb values very similar to the two fresh rock types.

Three samples of weathered dolerite have K/Rb values equal to or slightly greater than that of the fresh dolerite, with considerably more K and Rb. It is most likely that these samples have adsorbed K and Rb from the surrounding weathered granite via groundwater. Sample 6301 has two phases, an iron rich and a pallid cream part, but each shows addition of K and Rb.

Weathering has therefore tended to reduce the K/Rb ratio, although ratios of dolerite clay residuals have also been affected by the secondary processes of adsorption from groundwater. There is a tendency for the two clays with different parentage to reach an equilibrium in K and Rb contents.

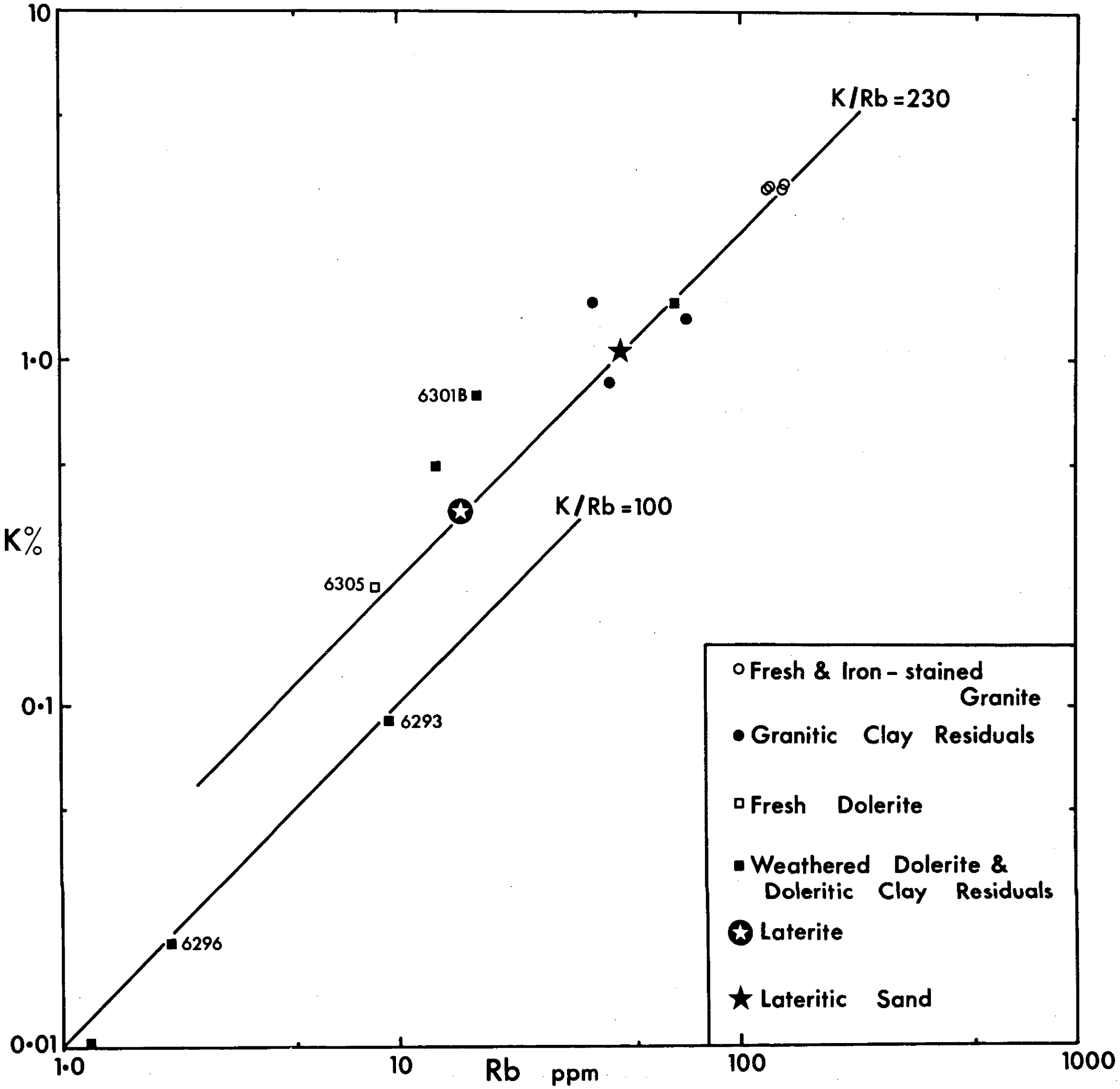

Fig. 38 K/Rb relationships for granite and dolerite from the Glen View Quarry, W.A.

9.4.2 K/Ba Ratios

The K/Ba ratio fluctuates for the weathered dolerite, increasing, decreasing, and finally increasing again. Some weathered dolerite samples reflect the values of the weathered granite clay. No significant changes of K/Ba were found in either iron staining or clay residual weathering of the granite. The behaviour of this ratio is either too erratic or of insufficient magnitude to indicate any distinct trend.

9.4.3 Ba/Rb Ratios

There are definite changes in Ba/Rb ratios during progressive alteration of the dolerite. At first the ratio sharply decreases (from 5.8 to 1.09) then rises to a slightly higher value than that of the fresh dolerite (Fig. 39). Weathered samples not from the residual dolerite boulder have still higher Ba/Rb ratios and higher concentrations of both elements. This ratio also suggests the equilibration of the two clays having different parentage.

Granite alteration produces no significant change. The laterite and sub-lateritic sand once again lie between the two fresh rock types with very similar Ba/Rb ratios (see Fig. 39).

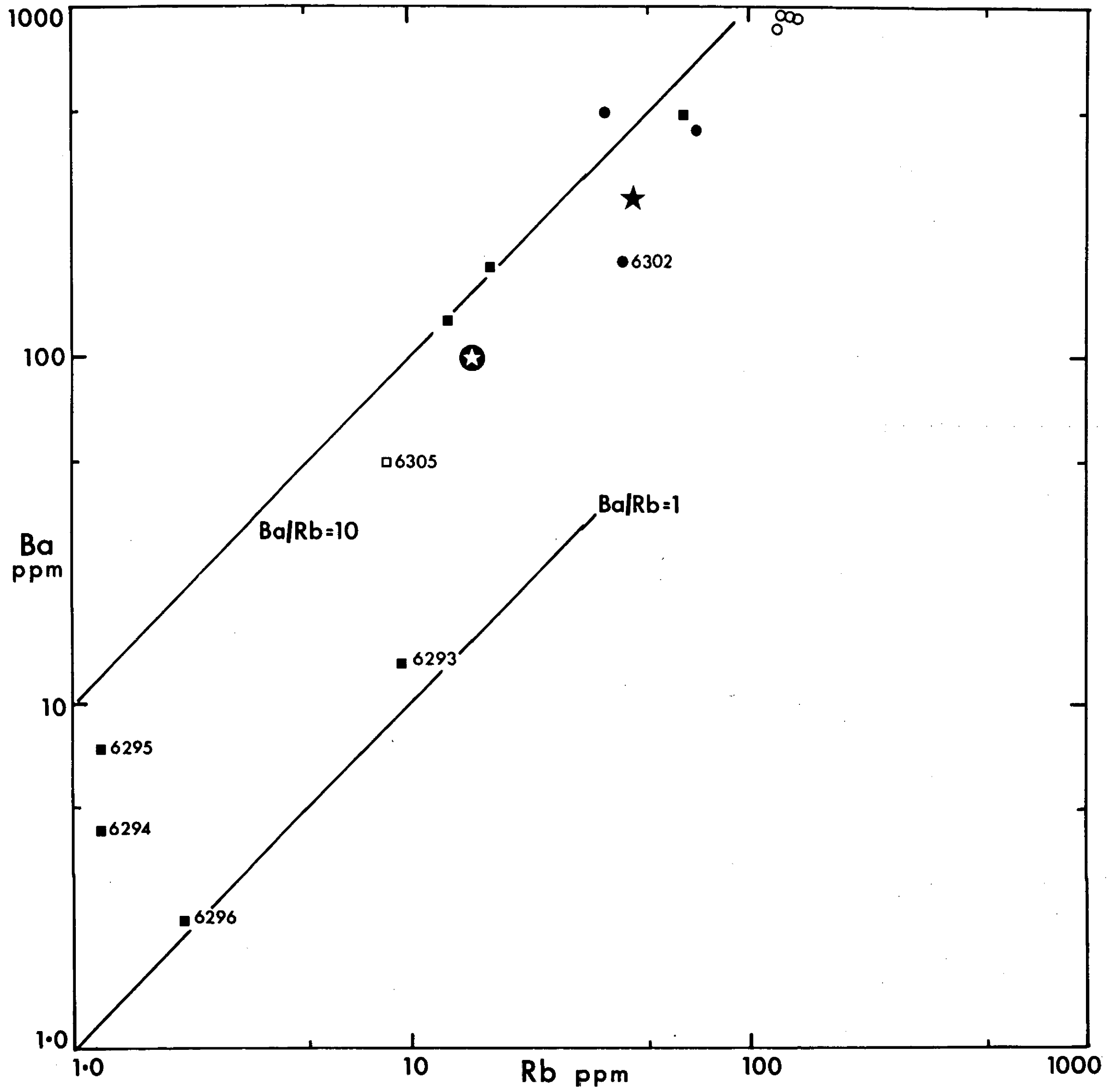

Fig. 39 Ba/Rb relationships for granite and dolerite from the Glen View Quarry, W.A.

9.4.4 Ba/Sr Ratios

This ratio best displays the convergent tendency of weathering for both rock types. Fresh dolerite has a Ba/Sr of 0.29 and with weathering this at first decreases slightly (Ba/Sr = 0.23), then rises tenfold (Fig. 40). This trend is also seen in the residual boulder from the dyke. Other weathered dolerite samples are clearly much higher in Ba and have consequently higher Ba/Sr ratios of approximately 50.0.

The fresh granite has a Ba/Sr of 6.94 which increases slightly with iron staining weathering to 9.29. Clay residual material on the granite has a higher Ba/Sr ranging from 20.3 (sample 6302) to 103 (sample 6297). The increase for samples of granitic parentage is clearly due to loss of Sr relative to Ba. This depletion is probably related to decay of feldspar components forming kaolinite. The similarity of Ba/Sr ratio for both granite-derived and dolerite-derived clays confirms the tendency for equilibration between the two due to cation adsorption (Fig. 40). Both clays have Ba/Sr ratios of approximately 50, representing a 200 fold increase in Ba/Sr ratio relative to fresh dolerite, and almost a 10 fold increase for the granite. The samples of laterite

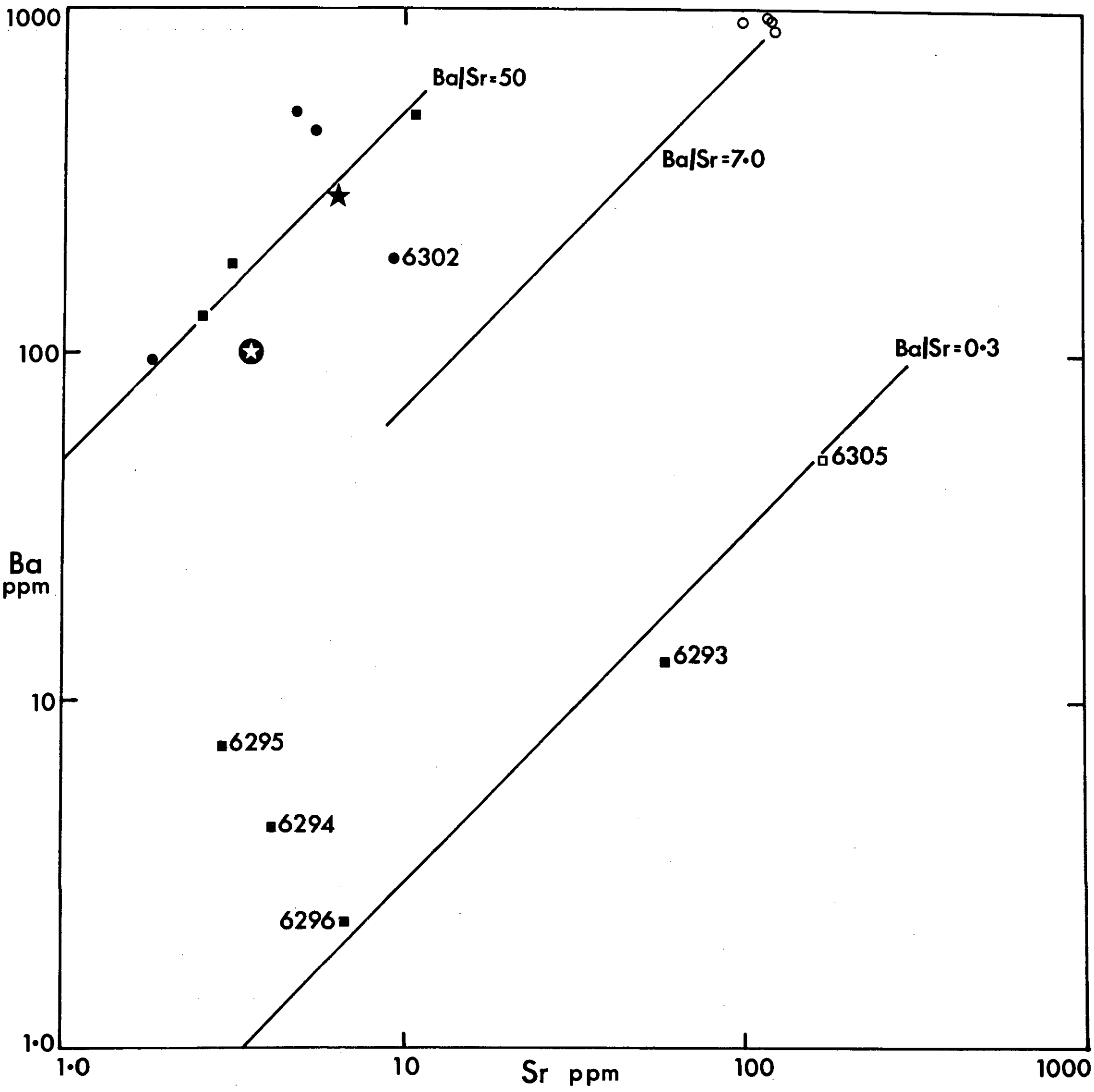

Fig. 40 Ba/Sr relationships for granite and dolerite from the Glen View Quarry, W.A.

and sub-lateritic sand have Ba/Sr ratios which also lie within the field of the residual clays suggesting an origin related to the clays beneath.

9.4.5 Rb/Sr Ratios

Rb/Sr ratios increase during weathering for both rock types (Fig. 41). The fresh dolerite (Rb/Sr = 0.05) weathers progressively in the rotten boulder to an outer rim value of Rb/Sr = 0.42 and other weathered dolerite samples have ratios which are still higher (i.e. Rb/Sr = 5.0 - 6.0). If this represented a residual weathering effect within the dolerite, a hundred fold increase in Rb/Sr would have occurred. This more likely represents adsorbed Rb provided by the circulating groundwater.

The fresh granite has a Rb/Sr of just less than one and a slight increase with iron staining weathering occurs.

Granitic clay residuals have higher Rb/Sr values than those of the fresh rock, varying from 4.55 to 12.8. The laterite and sub-lateritic sand values are similar to those of the altered clays. Weathering has produced changes in the Rb/Sr ratio, Sr loss, and varying degrees of Rb retention or addition from surrounding granitic clays.

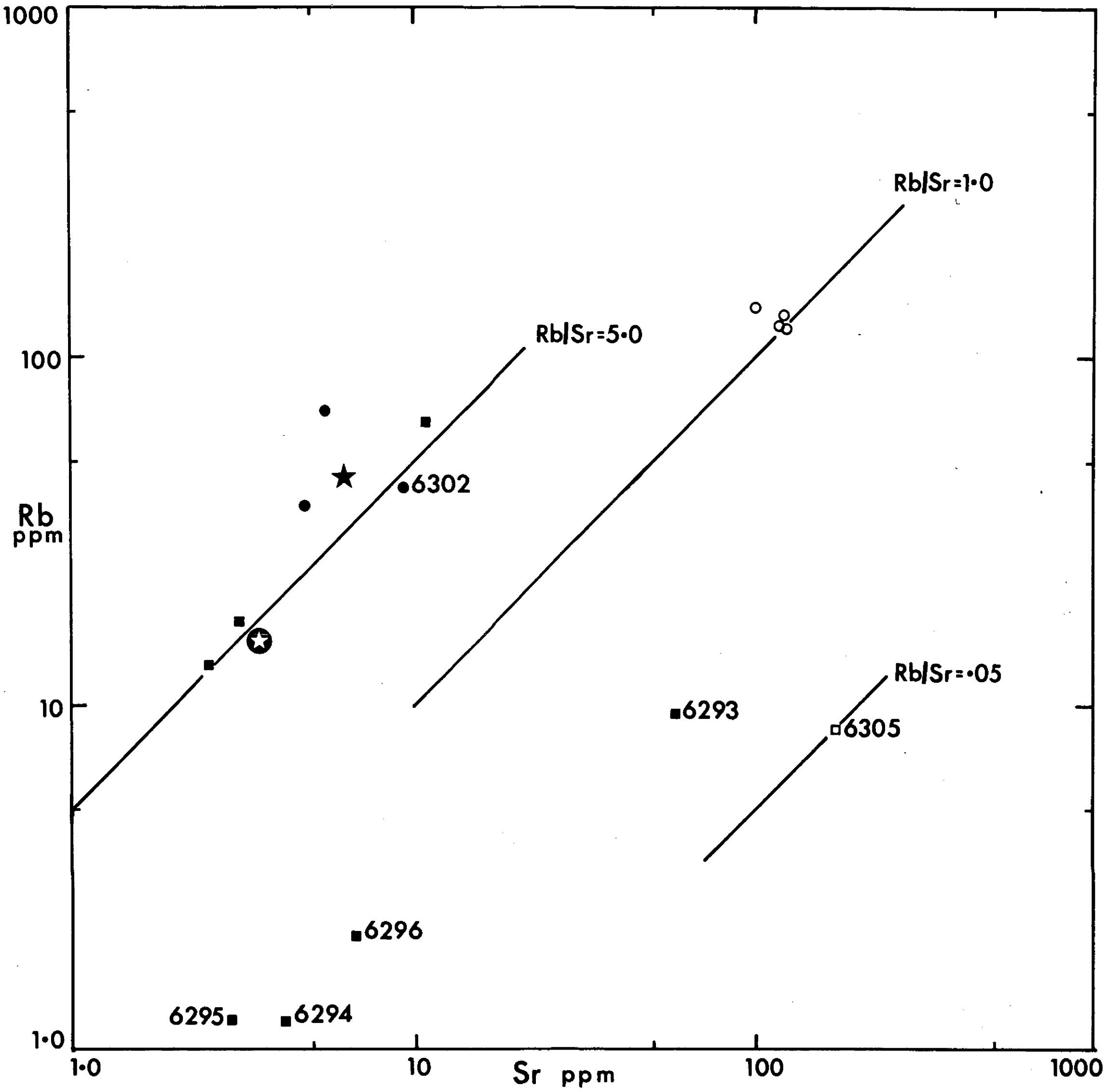

Fig. 41 Rb/Sr relationships for granite and dolerite from the Glen View Quarry, W.A.

9.4.6 K/Pb Ratios

The trend of this ratio is based on few analyses and its significance is accordingly reduced. The weathered dolerite boulder has a much lower K/Pb ratio and higher Pb content. No data are available for other weathered dolerite samples. Mildly weathered exfoliation slabs have slightly lower K/Pb values and more Pb. The only granitic clay residual also displays a lower K/Pb ratio due to lower K content. The trend towards increased Pb contents shown by exfoliation slabs may be due to aerosol fallout from car exhausts, reducing the significance of changes in this ratio. The large increase in Pb for the weathered dolerite kernel cannot be similarly explained. This effect is real and may indicate that the kernel of the weathered dolerite boulder with its high iron content and poorly crystalline mineral phases is a preferred environment for Pb concentration (see Chapter 11).

9.4.7 Pb/Sr Ratios

Although Pb was below the detection limit for many samples, those for which it could be detected demonstrate strong increases in the Pb/Sr ratio relative to the fresh rock. The core of the weathered dolerite boulder is seemingly enriched in Pb (sample

6293), but as weathering causes Pb depletion, many dolerite weathered clays have undetectable Pb. The major control of increasing Pb/Sr ratios, however is Sr loss, with minor Pb enrichment.

Weathering of the granite may also indicate apparent Pb enrichment at first but Sr depletion causes an increase in Pb/Sr ratios. The lateritic samples have similar ratios to the few clays that could be analysed.

9.4.8 Y and Zr

The fresh dolerite has a Y content of 33 ppm but with weathering it decreases to 1.6 ppm (sample 6296). There is large scatter in other weathered samples from the dolerite, (11 ppm - 1.5 ppm), but all are lower than the fresh parent rock. Zr contents for weathered samples are usually higher than the fresh dolerite, although this is only marginally true for some.

The granite has a lower Y content of 14.5 ppm but samples from exfoliation surfaces and weathered granite have higher contents (up to 36.6 ppm in sample 6309). This initial increase occurs with apparent loss of Zr suggesting variability within the granite for both elements. In contrast, granitic clay residuals have higher Zr contents and less Y, If Zr is used as an indicator of volume changes contradictory trends will appear to result with weathering. Sample 6310B, a weathered dolerite clay, has been depleted in many elements, but the Zr content is essentially identical to that of the fresh dolerite. If all trace elements were ratioed to Zr content as a correction for volume change, interpretation will be ambiguous.

Lateritic samples however, have higher Zr contents consistent with their residual origin, (Wolfenden, 1965; Short, 1961).

9.4.9 Th/U, Th/K and U/K Ratios

The degree of alteration and open system conditions casts strong doubt on the assumption of radioactive equilibrium for gamma-ray spectrometric analyses of residual clays. A detailed study of equilibrium and actual U abundances is discussed in Chapter 11, and will not be covered in detail here. The γ-ray results for fresh rock samples of granite and dolerite are acceptable, indicating low Th and U in the dolerite and higher values for the granite (Table F-13). Results from γ-ray spectrometry suggest a considerable increase of U and Th during weathering of the dolerite (weathered boulder) with a later decline in U content in the most weathered dyke material (Fig. 42). Weathering of the granite would result in U loss with almost constant Th if the γ-ray values were accepted. The highly enriched Th content of the laterites is well documented with a Th/U = 14.3. This also supports the residual nature of Th in the laterite and its tendency to be insoluble in weathering solutions.

If the U values can be substantiated by an independent method, (Chapter 11; Appendix E), it would appear that the Fe-rich kernel of the weathered dolerite boulder and its progressively altered zones are favourable environments for U retention and enrichment. Th/K and U/K ratios increase markedly with weathering of the dolerite (Table F-14). The granite shows a similar but much less marked trend towards increased ratios for Th/K, and U/K ratios do not change appreciably.

9.5 KOOLANOOKA QUARTZ PORPHYRY

Arriens (1963) reported remarkable major element uniformity throughout the outcrop area of this intrusive body as would be expected for granites near the ternary minimum in the system SiO_2-$NaAlSiO_4$-$KAlSiO_4$ (Butler et al., 1962). However the trace element concentrations in late stage rocks vary widely and

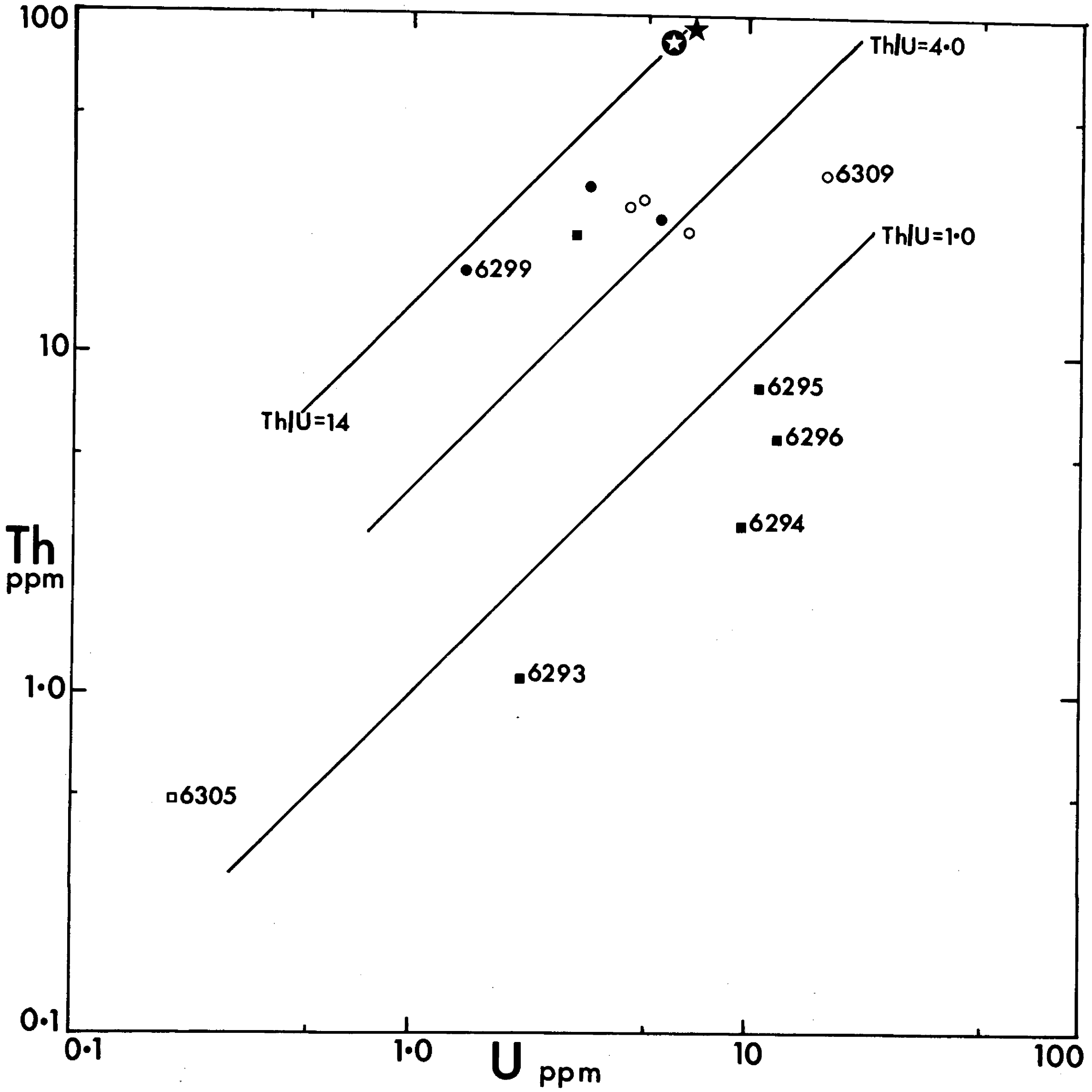

Fig. 42 Th/U relationships for granite and dolerite from the Glen View Quarry, W.A.

suggest a sequence of fractionation or intrusion. Three localities of quartz-porphyry were sampled, one from the southwestern margin (samples 6311-6336), another from the central northern mass (samples 6337-6347) and a third from the eastern part of the outcrop area (sequence 6348-6355). There are significant trace element differences between each locality. These may indicate either that different areas of the one intrusion or separate intrusions are involved, but the outcrop is poor and possible contacts are not exposed. For these reasons each locality will be considered separately under the various element ratios discussed. Analytical data and elemental ratios are given in Tables F-15, and F-16, in Appendix F.

9.5.1 K/Rb Ratios

Fig. 43 reveals a mutually exclusive range of K/Rb values for fresh and iron stained weathered samples from each locality. The central northern locality has K/Rb values varying from 192 to 214, the eastern locality from 151 to 168 and the southwest locality from 97.1 to 115. Weathering of the two northerly localities is represented by exfoliation surfaces and "rotten" weathered boulders (small tors). No change with weathering is detectable for

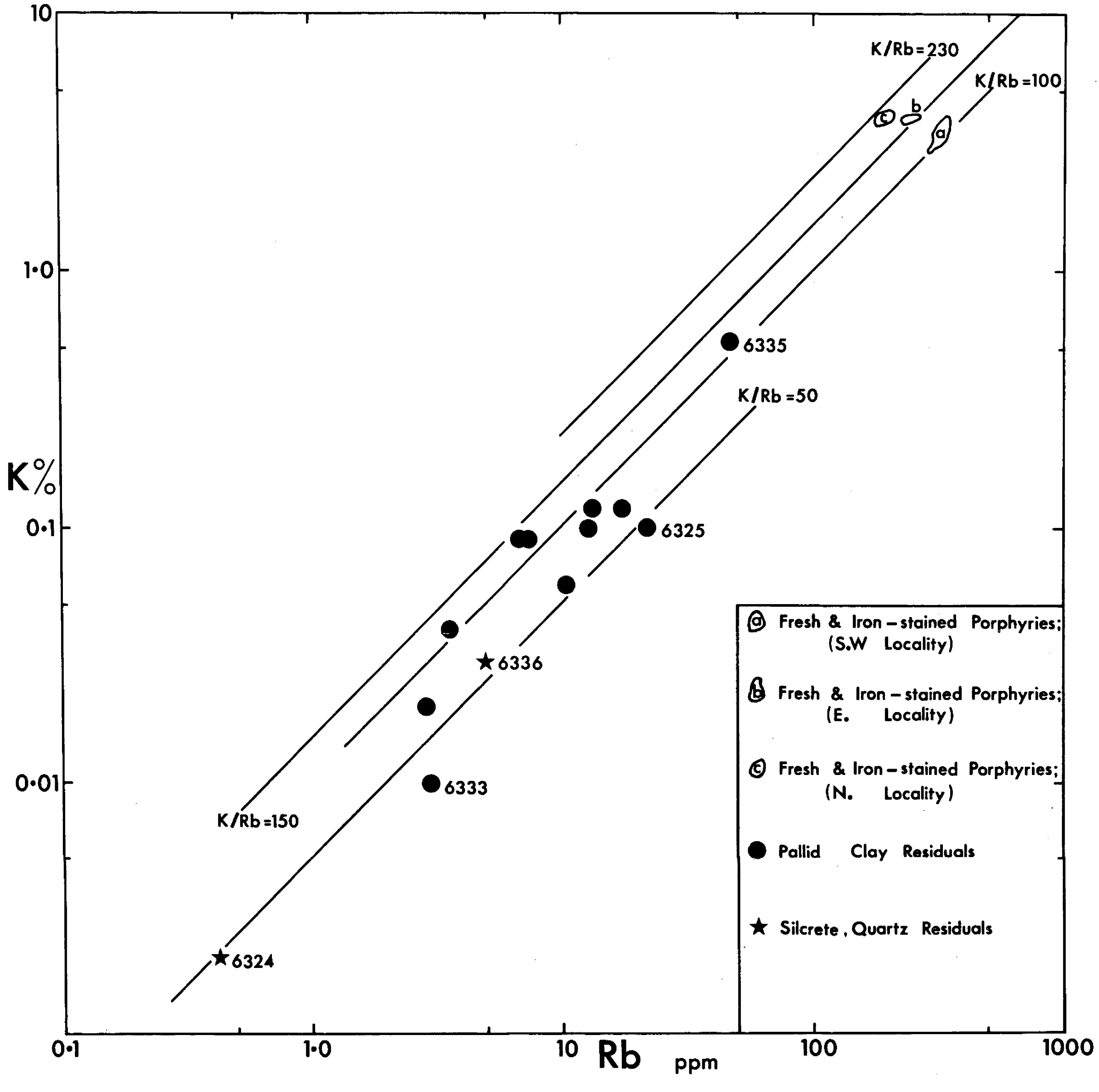

Fig. 43 K/Rb relationships for fresh and weathered quartz porphyry, clay residuals and silcretes from the Koolanooka Hills, W.A.

exfoliation surfaces, although a slight tendency towards lower K/Rb ratios may be present.

The eastern locality has lower K/Rb values. Again there is no change in K/Rb ratios with iron staining weathering for either exfoliation surfaces or weathered tors.

The southwestern locality near the margin of the mapped quartz porphyry (Arriens, 1963) has low K/Rb values as a result of higher Rb contents. Surficially weathered samples display iron staining and varying degrees of lack of cohesion and demonstrate a slight trend towards lower K/Rb values when compared to fresh porphyry from this locality. Clay residual material, available only at or close to this locality, has K/Rb ratios ranging from 46.8 to 124. However, sample 6335 has been partly resilicified, and the presence of montmorillonoid enables retention or adsorption of greater amounts of K and Rb. Montmorillonoids have higher exchange capacities than kaolinite and adsorption will be relatively enhanced (Laudelout _et al_., 1968). The process of secondary surficial silicification has been completed for sample 6336, a silicified remnant, but this sample possesses a K/Rb ratio identical to other clay residuals.

The significance of these changes in K/Rb ratios is dependent on the uniformity of the parent rock within an area. Unfortunately fresh rock is not exposed immediately beneath the clay residual material and in the southwestern locality, variability of the fresh porphyry may exist as a consequence of its marginal location. If the porphyry is considered homogeneous and similar to the analysed fresh porphyry at this locality, then the decrease in K/Rb ratio can be attributed to destruction of potash feldspar and formation of kaolinite with preferential retention of Rb.

9.5.2 K/Ba Ratios

Both northerly localities fail to show any effect of weathering alteration on K/Ba ratios. The central northern locality has K/Ba values of approximately 70 while the eastern has ratios varying from 106 to 134. There is a larger range of K/Ba ratios (315-439) in the southwestern porphyry but iron staining weathering causes a decrease. Exceptions to this trend are samples 6318 and 6322 which have low Ba contents and higher K/Ba ratios. Nearly all clay residuals have K/Ba values less than 100 with the exception of sample 6326. The extremely low Ba content of this clay residual is subject to uncertainty and the K/Ba ratio (2067, Table F-15) will consequently have large error limits. The wide dispersion of K/Ba ratios for clay residuals may be a result of variable cation exchange and adsorption of Ba with a fluctuating groundwater table. The highest K/Ba ratios are characteristic of clays immediately below the cap rock (silcrete) which are noticeably indurated. Lower K/Ba values are common in less indurated clay residuals deeper in the profile. Sample 6335 has a noticeably higher K/Ba ratio, but this sample contains montmorillonoid. The silicified remnant (6336) has a low K/Ba ratio of 11.0.

The wide dispersion of Ba relative to K for iron stained weathered samples demonstrates the difficulty of obtaining a generalised trend for this type of alteration. A majority of weathered samples have lower K/Ba ratios due to higher Ba contents, but the initial Ba content of the southern porphyry may be variable. A decrease in K/Ba ratio is shown by a majority of clay residuals owing to retention of Ba relative to K.

9.5.3 Ba/Rb Ratios

The central northern porphyry has a Ba/Rb of approximately 3 while the eastern porphyry has a lower Ba/Rb ratio of 1.3, but in neither case does this ratio change with alteration.

The southern locality reveals considerable scatter, due to variable Ba contents. Iron-stained weathered samples vary greatly in Ba although all samples have nearly identical Rb contents. Fresh southern porphyry has a Ba/Rb ratio of 0.33 which increases with clay alteration and later secondary silicification.

9.5.4 Ba/Sr Ratios

Little or no change in this ratio is evident in either northern porphyry, although each locality has different Ba and Sr contents. The southern porphyry has a Ba/Sr ratio nearly identical to that of both northern ones, but it can be distinguished from them by Ba and Sr concentrations. The Ba variation again obscures any definite trend for this ratio with iron-staining weathering but most samples display an increase in Ba/Sr ratio. Clay residuals have a wide range in Ba/Sr ratios although most have lower ratios than the fresh porphyry. Both elements are known to vary with porphyry locality but since the initial variation of Ba within the fresh porphyry from the southern locality is not known, the significance of changes in the Ba/Sr ratio is uncertain.

9.5.5 Rb/Sr Ratios

Rb/Sr ratios of the quartz porphyry are between 4 and 40 (Fig. 44). This wide range for total rock samples has enabled a well defined age for this intrusion to be measured (Chapter 10). The central

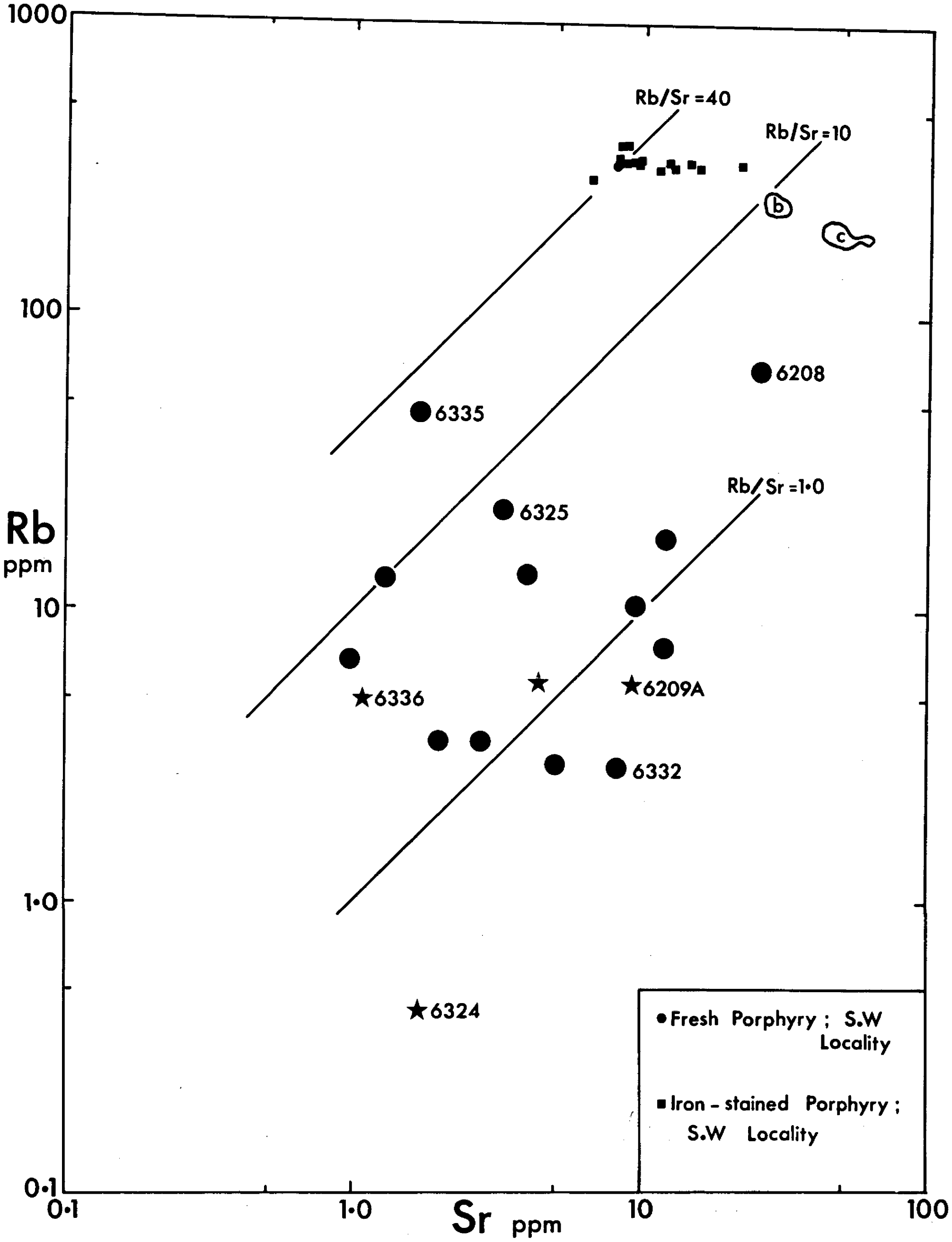

Fig. 44 Rb/Sr relationships for fresh and weathered quartz porphyry, clay residuals and silcretes from the Koolanooka Hills, W.A.

northern porphyry has the lowest Rb/Sr ratios varying from 3.1 to 4.8. This moderate dispersion prevents weathering trend analysis. The eastern locality is distinctly higher in Rb/Sr, varying from 7.37 to 9.62, with higher Rb/Sr ratios for more altered samples. The southern porphyry has still higher Rb/Sr of approximately 42 although it is variable. Iron staining weathering may cause a mild increase in Rb/Sr ratio although the possibility of fresh rock variation cannot be discarded because Arriens et al., (1966) report a quartz porphyry with a ratio lower than that of sample 6311.

If, however, sample 6311 is taken as the fresh rock, the Rb/Sr ratio decreases for many of the iron stained weathered samples. All clay residual and silicified samples have lower Rb/Sr ratios, and display a range of values between 0.35 and 27.6. This large dispersion reflects two possible processes: either residual mica controlling the Rb/Sr ratio, or variable adsorption from a fluctuating groundwater table. The possibility of feldspar relicts is regarded as remote and no evidence for a significant feldspar component is available from X-ray diffraction data.

9.5.6 K/Pb Ratios

K/Pb ratios are nearly uniform for all localities sampled and no definite changes with surficial alteration are observed, although a slight increase in iron-stained weathered samples from the southern locality is suggested. Nearly all clay residuals have undetectable (i.e. <1 ppm) Pb contents. The behaviour of K/Pb ratios with clay alteration is unknown although silicified samples indicate an increase in K/Pb values during silicification.

9.5.7 Pb/Sr Ratios

Although Pb contents are nearly uniform, all three localities can be distinguished by their Sr contents and, hence, Pb/Sr ratios as well. Surficial alteration at both northern localities does not disturb this ratio. Iron staining weathering at the southern locality results in variation of both Pb and Sr contents. The lack of Pb data precludes analysis of effects due to clay alteration. Silicified remnants have highly variable Pb/Sr ratios but contain very small amounts of each element.

9.5.8 Th/K, U/K and Th/U Ratios

Lower Th contents for the central northern porphyry result in lower Th/K ratios when compared to the other two localities for which thorium and

Th/K ratios are essentially identical. Iron staining weathering has not affected Th/K ratios for either northern porphyry but there is a minor increase in the southern variant. Clay alteration, although reducing the Th content, markedly increases the Th/K ratio as a consequence of Th retention (possibly in a resistant mineral phase) relative to K. This discussion assumes radioactive equilibrium for all samples. U/K ratios of the three porphyries are not significantly different. Slightly higher U contents may be found in the northern porphyries but there is no change with surficial alteration. The southwestern porphyry data show marked decreases in U/K ratios with iron staining weathering, but clay alteration produces significantly higher U/K ratios (Table F-16). The southern porphyry has slightly higher Th/U ratios but the three porphyries are only marginally different. Iron staining weathering may cause increases in Th/U ratios for all three porphyries while clay alteration of the southern variant appears to slightly reduce the ratio (Fig. 45).

9.5.9 Y and Zr

Although Y contents are variable it is possible to distinguish between the three sampled localities. Minor depletion of Y may occur with iron staining

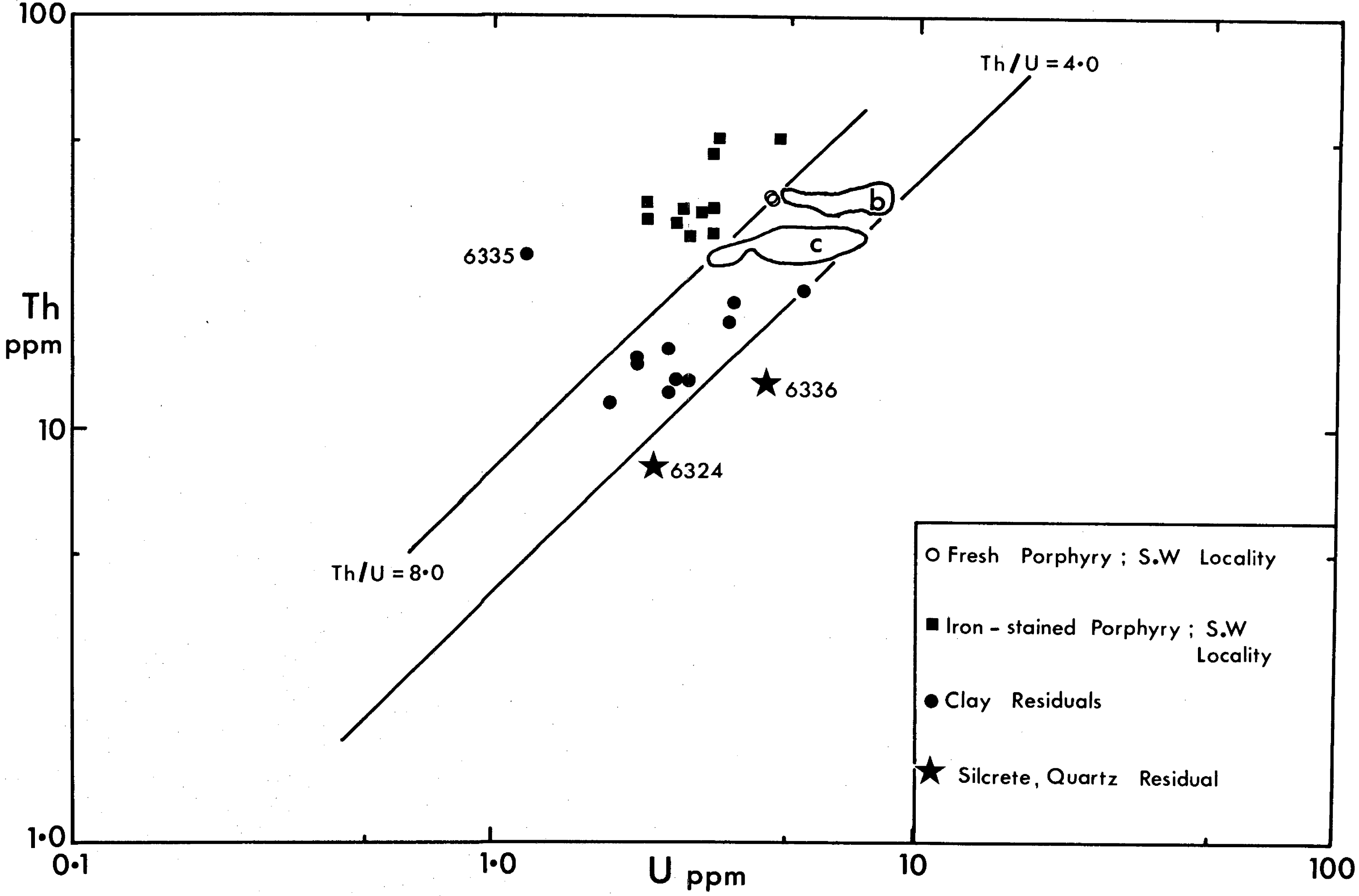

Fig. 45 Th/U relationships for samples from the Koolanooka Hills, W.A.

weathering although initial variation of Y in the fresh porphyry largely obscures any trend. There is no consistent Y variation during clay alteration. In general the behaviour of Zr is analogous to Y except that most clay residuals have higher Zr contents than the fresh porphyry.

These two elements may occur in resistant minerals and their concentrations reflect the behaviour of these phases. The variability of both elements is possibly related to the occurrence of mica clots or small xenoliths in which the minerals apatite, sphene and zircon are common.

9.6 MERTONDALE GRANITE - TRACE ELEMENT SUMMARY

A summary of changes in the ratios is listed in Table 18. Sericitisation and kaolinization are listed separately, and all changes are relative to the initial fresh rock ratio. Sericitisation is represented by the sequence of slight to highly altered samples and kaolinization by completely altered samples (Table 18). This subdivision of samples assumes that alteration was a two stage process with two distinct and consecutive phases. A completely to highly altered sample (6359) is thought to be transitional.

Sericitisation has not changed most of the trace element ratios to any marked degree, with the exception

Table 18

Mertondale Granite: Trace element ratio summary

Alteration	Trace Element Ratio Trend									
	K/Rb	K/Ba	Ba/Rb	Ba/Sr	Rb/Sr	K/Pb	Pb/Sr	Th/K	U/K	Th/U
Sericitisation	=	>	=	+	+	>>	<	=	=	=
Kaolinization	*	<	=	*	*	=	<<	+	+	>>

Key to symbols for Table

=	No change
>	Small increase
>>	Considerable increase
+	Large increase
<	Small decrease
<<	Considerable decrease
*	Large decrease

of Ba/Sr and Rb/Sr. Both increase as a consequence of Sr depletion, but Pb/Sr ratios tend to decrease. This behaviour can be explained by exclusion of Sr from the mica lattice and its removal from the total rock system. The original Sr was largely in potassium feldspar but as this breaks down with formation of a mica lattice, Sr cannot be accommodated. Lead is very similar to Sr in ionic radius and will encounter similar co-ordination problems in micas in addition to bonding difficulties. The slight decrease in the Pb/Sr ratio results from the interplay of these effects.

Kaolinization has involved the formation of simple clay structures. Incorporation of trace elements is restricted and adsorption of ions is limited by the low exchange capacity of kaolinite. Ions with low hydration energies will be preferentially adsorbed exchanging for ions with higher hydration energies (i.e. ion exchange of K or Sr by Rb). Decreases in K/Rb and Ba/Rb ratios and increases in Rb/Sr ratios are predicted but the Ba/Rb ratios are unchanged and the Rb/Sr ratio decreases. This unpredicted behaviour is due to the secondary addition of carbonate and associated Sr and Ba. This has modified ratio trends as follows: K/Ba (slight decrease); Pb/Sr (considerable decrease); K/Pb (constant); and Ba/Sr (large decrease), relative to ratios of the fresh granite. This modification of the kaolinization process adds further complexity to the problem of time of formation and source material for the kaolinite.

The Th/K and U/K ratios display normal increases due to K loss, the magnitude of the increase being relatively insensitive to errors in U and Th measurements (Chapter 11). Similarly, the Th/U ratio tends to increase with preferential retention of Th.

Two alternative hypotheses are available to explain the interrelationship of sericitic and kaolinitic weathering.

i) Consecutive alteration of the granite to lower P-T and pH_2O assemblages shortly after shearing of the granite and possibly related to emplacement of the quartz-molybdenite vein and greisening with subsequent secondary carbonate addition.

ii) Initial hydrothermal and sericitic alteration of the granite shortly after emplacement with kaolinization, a result of weathering, occurring much later. The addition of secondary carbonate is a result of recent weathering (see Chapter 11).

The absence of altered transitional samples, coupled with crystalline kaolinite may be taken to support the first hypothesis, however the second is considered more likely.

9.7 GLEN VIEW QUARRY - TRACE ELEMENT SUMMARY

The trends of various ratios are summarised in Table 19. Each rock type is considered separately and both are further subdivided according to type of weathering alteration and material analysed. All changes are relative to the respective fresh rock ratio. The laterite profile may have formed under different climatic conditions from the present and may exhibit significantly different patterns of ratio behaviour to those of present day weathering. For this reason, alteration of the granite has been divided into two types; iron staining weathering as shown by exfoliation surfaces, and clay residual weathering of the laterite profile. The tendency for approximate equilibration of trace element contents between clay residuals formed from two differing parent rocks adds further complexity. In Table 19, the weathered dolerite boulder sequence is separated from other weathered dolerite samples designated clay residuals. The weathered boulder sequence will indicate a weathering trend for the dolerite, in contrast to equilibration displayed by clay residuals.

Clay residual weathering of the dolerite produces trace element ratios similar to those of granitic clay residuals. The mechanism for this process is groundwater transport and ion exchange or adsorption on clay mineral surfaces.

Table 19

Glen View Quarry: Trace element summary

Alteration	Trace Element Ratio Trend									
	K/Rb	K/Ba	Ba/Rb	Ba/Sr	Rb/Sr	K/Pb	Pb/Sr	Th/K	U/K	Th/U
A. GRANITE										
Iron staining	<	=	=	>	>	<	>	>	<	>
Clay residual	<	=	<	+	+	<<	+	+	<	>>
B. DOLERITE										
Weathered boulder	*	>	*	+	+	*	+	+	+	*
Clay residual	>	<	>>	+	+	n.d.	n.d.	+	>	>>

Key to symbols for Table

=	No change
>	Small increase
>>	Considerable increase
+	Large increase
<	Small decrease
<<	Considerable decrease
*	Large decrease
n.d.	Not determined

Analysis of granite exfoliation slabs reveals little change from fresh granite ratios. Although a comprehensive suite of fresh granite samples was not available from this locality, the minor trends found are probably less than the variability of the original rock, as observed in other localities. Increasing Ba/Sr, Rb/Sr and Pb/Sr ratios indicate early loss of Sr while Th/K and Th/U ratios suggest minor depletion of K and U.

Clay residual material formed from the granite has considerably different trace element ratios from those of the fresh material. There are definite trends in Ba/Sr, Rb/Sr, K/Pb, Pb/Sr, Th/K and Th/U ratios. In every case these are compatible with the initial minor trends found for iron staining weathering. There is strong depletion of Sr indicating destruction of feldspar lattices. Relative retention of Th in resistant minerals coupled with minor depletion of K explain the deviation of other ratios from those of the fresh granite.

The alkali elements are preferentially retained by clay minerals formed and alkaline elements are removed by groundwater. The lack of change in K/Rb, K/Ba and Ba/Rb ratios is remarkable. The close coherence of these elements in silicates and crystal lattices, is usually modified in low temperature hydrated environments (Horstman, 1957; Hart, 1969). The dominant control of these granite weathering processes is the relative stability of different mineral phases (Goldich, 1938).

The dolerite "weathered boulder" sequence shows distinct changes for all ratios except K/Ba. This sequence represents the progressive destruction of a remnant boulder with a dolerite dyke, from the central core to surrounding pallid material. Strong decreases are shown by the K/Rb, Ba/Rb, K/Pb and Th/U ratios. Depletion of K and Ba is quite marked while preferential adsorption or enrichment of U (gamma-ray) and Pb appears to contrast with this trend. This phenomena of higher Pb and "U" contents in weathered material may be due to two different reasons: higher initial contents or the preferential adsorption of Pb and U onto hydrated iron oxide surfaces. The remaining ratios all increase due to loss of Sr and relative retention of Ba, Rb and Pb. Strong increases in the ratios Th/K and U/K are readily explained by K depletion with relative retention of Th and U.

Weathering of the dolerite dyke has produced trends which are remarkably similar to those shown by clay weathering of the granite. The processes of groundwater transport with adsorption on clays has modified the trace element contents of all weathered "doleritic" clays apart from the residual boulder samples.

Consequently the alteration trends shown by the weathered dolerite boulder are either enhanced or reversed. Reversal occurs for the K/Rb, K/Ba, Ba/Rb and Th/U ratio trends indicating adsorption of K, Ba and Rb. Removal of anomalous "U" (the weathered boulder sequence) from the weathered dolerite with leaching of the iron oxides and hydroxides is indicated and return to the normal trend of increasing Th/U ratios with weathering occurs.

Large quantities of Ba seem to have been adsorbed during this equilibration process and consequently all ratios involving Ba display the process clearly. The most remarkable fact to emerge from study of the alteration of both rock types is the degree of similarity in ratios between their respective weathering products.

9.8 KOOLANOOKA QUARTZ PORPHYRY - TRACE ELEMENT SUMMARY

A summary of the alteration displayed by the three porphyries analysed is listed in Table 20. Iron staining weathering is the only type present at both the central northern and eastern localities. Sampling of this type of alteration for bulk analysis has meant inclusion of a large percentage of virtually unweathered rock with the weathered crust or surface. Consequently surface alteration effects have been minimized and perhaps totally camouflaged for many samples. Recent weathering,

Table 20

Koolanooka Quartz Porphyry: Trace element summary

Alteration	Trace Element Ratio Trend									
	K/Rb	K/Ba	Ba/Rb	Ba/Sr	Rb/Sr	K/Pb	Pb/Sr	Th/K	U/K	Th/U
A. CENTRAL NORTHERN PORPHYRY										
Iron staining	=	=	=	=	>	=	=	=	=	>
B. EASTERN PORPHYRY										
Iron staining	<	=	=	>	>	=	=	>	=	>
C. SOUTH WEST PORPHYRY										
Iron staining	<	*	+	>>	=	<	=	>	<	>>
Clay residual	*	*	+	*	*	n.d.	n.d.	+	+	<
Silica residual	*	*	+	+	*	>>	<<	+	+	*

Key to symbols for Table

=	No change
>	Small increase
>>	Considerable increase
+	Large increase
<	Small decrease
<<	Considerable decrease
*	Large decrease
n.d.	Not determined

however, has only affected the Rb/Sr, Th/U and perhaps K/Rb ratios at the central northern locality. The remaining ratios are little different from initial fresh porphyry variation.

The eastern porphyry is analogous to the central northern porphyry in behaviour. The ratios Rb/Sr and Th/U increase slightly, while the K/Rb ratio may marginally decrease. This porphyry shows a mild increase in Ba/Sr ratio with recent weathering and samples from this locality have relatively uniform Ba contents.

The southwestern porphyry is more highly weathered than either of the more northerly areas. Iron staining weathering has progressed to a more advanced stage permitting greater chemical attack by weathering solutions. In Table 20, a large number of ratios display definite trends with more severe weathering. Slight decreases are shown by the K/Rb, K/Pb and U/K ratios, while the K/Ba ratio markedly decreases. Little importance can be attached to ratios involving Ba at this locality owing to variable Ba concentrations. The Ba/Rb ratio increases strongly while the ratios Ba/Sr, Rb/Sr, Th/K and Th/U also increase. Initial leaching of Sr, U, Pb and K is the main cause of changes in ratios but apparent increases in Pb, Ba and Sr occur during advanced alteration.

Two alternative mechanisms can be suggested: addition of Sr, Pb and Ba along with alteration products and secondary carbonate; or large initial variation in the fresh porphyry at this locality. The behaviour of Sr, Ba and Pb is more in accord with the latter. Ratios involving these elements are not typical of weathering, especially as the trend of Rb/Sr apparently decreases. Lower Rb/Sr ratios for increasingly iron-stained weathered materials is more readily explained as an inherited feature of the porphyry. Rb-Sr isotopic analyses of the samples from this locality emphasized the possibility of initial fresh porphyry variation (Chapter 10). Sample 94537 (Arriens, 1963) was reanalysed by the author and proved to have a lower Rb/Sr ratio.

This sample is from the inferred southern extension of the southwest porphyry as laterite obscures the mutual relationship of the outcrops. It is noteable that the addition of a few ppm Sr to the S.W. porphyry will greatly modify the Rb/Sr ratio. The highly variable microxenolith content may critically affect the Rb/Sr ratio if microxenoliths are a source of Sr with predominantly low Rb/Sr ratios (i.e. apatite).

Clay residuals from the southwestern porphyry are subject to the same uncertainty of initial fresh porphyry composition. In Table 20 generalised trends are relative to sample 6311, a typical fresh porphyry. Many clay residuals display decreases in K/Rb, K/Ba, Ba/Sr and Rb/Sr ratios, however the trend of K/Pb and Pb/Sr ratios could not be ascertained. The Pb contents of practically all clay residuals were below the limit of detection. Th/U ratios may decrease slightly, while large increases in Th/K and U/K ratios are suggested. The Ba/Rb ratio increases markedly but initial Ba variation shown by the porphyry must be considered.

Individual samples vary in the amount of residual muscovite, secondary carbonate and silicification shown by exposed surfaces, percentage of inherited quartz phenocrysts, the number and extent of voids, arrangement of channel-ways, and the types of clay mineral present. It is therefore not surprising to find a range of elemental ratios reflecting this variability which is additional to the fresh porphyry diversity.

Trace element behaviour can be explained on the basis of sample variability coupled with different degrees of cation exchange and adsorption.

Both Y and Zr are highly variable for clay residuals reflecting the erratic accessory mineral content and the tendency for many accessory minerals to be resistant to weathering.

Silica residuals probably represent a quartz phenocryst accumulation with secondary chalcedony as a cement, clay and very minor iron oxides. The only difference from clay residual elemental ratios is the increase in Ba/Sr ratios and the decrease of the Th/U ratio. The former reflects preferential retention of Ba with little retention of Sr while the latter appears to represent an increase in U. Sample 6324, a loosely cemented quartz grit composed largely of phenocrystic bipyramidal quartz grains, displays similar although relatively extreme behaviour. It is possible that the uranium is largely associated with the iron oxide cement and in resistant accessory grains. This material has little in common with the porphyry apart from the quartz phenocrysts.

The high degree of scatter of Pb concentrations for silicified residuals is in contrast to the Pb increases found for iron stained weathered samples. Lead is often adsorbed by hydrated iron oxides and hydroxides for these are effective scavengers with large charged surfaces.

CHAPTER 10

RUBIDIUM-STRONTIUM ISOTOPE GEOCHEMISTRY

The behaviour of strontium isotopes in low P-T systems has received little attention despite its importance for geological materials that have passed through the exogenic cycle. Weathering processes may modify Sr isotopic compositions and directly influence ages of exposed rock outcrops. The degree of weathering in Australia makes sampling of fresh rock difficult or in many places impossible. An assessment of weathering processes and the intensity of weathering that will seriously affect or change the age recorded by the total rock system is desirable.

A further implication is the possibility of dating the age of weathering of ancient profiles. Weathering has occurred throughout geological time and if alteration processes can be characterised, relict profiles may be both identified, and dated by Rb-Sr isotopic techniques.

The interpretation of shale ages is largely dependent on knowledge of the effects of weathering, transport and deposition on detritus. If weathering is capable of overprinting the total rock age and shale ages reflect the age of the weathering provenance, shale dating will not give a factual representation of the provenance region.

10.1 INTRODUCTION

Goldich and Gast (1966); Bottino and Fullagar (1968) and Dasch (1968, 1969) have investigated weathering processes with Rb-Sr isotopic techniques. Goldich and Gast (1966) considered the effect of weathering on a biotite and found approximately a 75% loss of Rb-Sr age when compared to the fresh biotite. They suggest that incipient weathering may critically affect the Rb^{87}/Sr^{86} ratio not only for biotites but, by analogy, the feldspar and total rock samples also. Dasch (1968) found that weathering produced an increase in the Rb/Sr ratio and attributed this primarily to loss of strontium. He also showed that for several common rocks the Sr isotopic composition is largely unaffected by weathering, transport and deposition. Bottino and Fullagar (1968) also found an increase of the Rb/Sr ratio for the profiles which they studied.

Two types of weathering alteration, each representing a different climatic regime, can be seen in areas of Western Australia. Extensive development of laterites and lateritic profiles thought to have occurred during Miocene or mid Tertiary times (Woolnough, 1927) cover areas of the West Australian shield. Two clay profiles considered to be from the lower section of the laterite profile were sampled, one at Mertondale and the other from the Koolanooka Hills.

Recent climatic conditions favour iron staining weathering which is normally encountered during sampling in the field. Iron staining weathering was sampled at the Tuckanarra quarry and in the Koolanooka Hills. Fortunately both types of weathering occur within the Koolanooka Hills on the Koolanooka quartz porphyry permitting investigation of both processes on the one parent rock.

10.2 EXPERIMENTAL METHODS

Separation of Rb and Sr from total rock samples and the method of analysis has been described in Appendix C. The graphical display method of Nicolaysen (1961) has been used throughout this study. The slope of the isochron is proportional to the age and the Y intercept of the isochron gives the initial Sr^{87}/Sr^{86}. Statistical treatment is that of McIntyre et al., (1966) modified to enable specification of individual variance estimates in Rb^{87}/Sr^{86} and Sr^{87}/Sr^{86} for each analysed sample (Compston and Chappell (1970), in preparation). The degree of scatter of the data points about the isochron is given by the magnitude of the mean square of weighted deviates (MSWD), a measure of the residual variance. Where the MSWD is less than or equal to unity, all scatter about the fitted line falls within experimental error and the regression program stops at a model 1 fit. If, however, the MSWD value exceeds unity, the regression proceeds allowing alternative weightings to be given to the Sr^{87}/Sr^{86} variance in excess of experimental error. For a model 2 fit, the Sr^{87}/Sr^{86} variance above experimental error is assumed to be related to the value of Rb^{87}/Sr^{86} (X), but a model 3 fit assumes the excess variance in Sr^{87}/Sr^{86} to be independent of Rb^{87}/Sr^{86}. Model 4 represents a compromise in weighting of the excess variance of Sr^{87}/Sr^{86} between models 2 and 3.

Model 2 is appropriate for samples with a real age difference or where subsequent isotopic redistribution has taken place. Model 3 applies to samples with differences in initial Sr^{87}/Sr^{86}.

All tests of significance associated with isochron interpretation are given at the 95% level of confidence.

10.3 THE MERTONDALE GRANITE

10.3.1 Results

Analytical data are detailed in Table 21, and regression analyses for a number of different groupings are given in Table 22. The data are displayed in Figs. 46 and 47.

10.3.2 Regression Analysis

The first regression tests the hypothesis that all samples analysed had the same initial Sr^{87}/Sr^{86} and that

Table 21
Rubidium and Strontium Isotopic Data for the Mertondale Granite and Altered Variants

	X.R.F.		I.D.					
Sample Number	Rb ppm	Sr ppm	Rb ppm	Sr ppm	Rb^{87}/Sr^{86}	Sr^{87}/Sr^{86}	Degree of Alteration*	Rock type
6356	10.2	26.9	10.9	28.7	1.097	0.7449	C.A.	Quartz-kaolinite residual.
6357	10.0	16.4	10.8	17.5	1.785	0.7636	C.A.	" "
6280	12.6	18.9	13.1	19.6	1.944	0.7726	C.A.	" "
6358	10.9	14.9	11.3	16.0	2.052	0.7803	C.A.	" "
6281	15.1	5.3	15.9	7.0	6.714	0.9472	C.A.	" "
6359	69.6	3.4	68.2	4.4	53.49	2.6764	C-H.A.	Altered granite.
6282	97.7	3.7	94.4	4.4	80.66	3.6733	H-M.A.	" "
6372	98.8	3.3	97.0	4.4	83.69	3.7680	H-M.A.	" "
6362	122	3.6	120	4.6	103.5	4.4935	H-M.A.	" "
6283	122	3.7	120	4.5	106.6	4.5953	H-M.A.	" "
6289	118	9.3	116	10.1	37.80	2.0786	M-S.A.	" "
6288	98.1	6.1	96.8	7.0	46.16	2.3687	M-S.A.	" "
6368	110	17.6	109	19.0	17.67	1.3578	S.A.	Slightly altered granite
6374	108	13.4	107	14.5	23.01	1.5607	S.A.	"" " "
6369	113	9.2	111	10.2	35.31	2.0023	S.A.	" " "
6364	167	3.8	164	4.9	147.5	6.1553	Aplitic	Aplite
6291	106	13.2	105	14.9	21.87	1.5112	Fresh	Fresh granite
6292	107	11.8	106	14.7	22.60	1.5493	Fresh	" "
6292 Dup.	107	11.8	106	14.0	23.81	1.5858	Fresh	" "
6357 Quartz	-	-	1.07	0.84	3.700	0.8379	Relic	

*C.A. = completely altered; C-H.A. = completely to highly altered; H-M.A. = highly to moderately altered; M-S.A. = moderately to slightly altered, and S.A. = slightly altered.

Table 22
Regression Analysis of the Mertondale granite data

	Regression	Number of Samples	MSWD	Age (m.y.) $\lambda = 1.39 \times 10^{-11} yr^{-1}$	Initial Sr^{87}/Sr^{86}	Isochron Model
1.	All samples	19	14.32	2596 ± 15	0.7042 ± .0052	4
2.	Fresh samples	7	1.38	2604 ± 38	0.7087 ± .0134	3
				2605 ± 36	0.7086 ± .0123	1
3.	All altered samples	12	20.19	2587 ± 14	0.7018 ± .0048	4
4.	Completely altered samples	5	61.44	2569 ± 172	0.7029 ± .0078	3
5.	Highly-moderately to slightly altered samples	7	1.81	2601 ± 47	0.6880 ± .0434	3
				2604 ± 37	0.6855 ± .0305	1
6.	Completely altered samples and sample 6359	6	48.50	2606 ± 40	0.7016 ± .0042	3
7.	Highly-moderately to slightly altered samples excluding 6359	6	1.10	2605 ± 42	0.6799 ± .0363	3
				2605 ± 40	0.6803 ± .0337	1
8.	All samples excluding completely altered samples	14	2.43	2581 ± 24	0.7143 ± .0117	4
				2580 ± 16	0.7150 ± .0068	1

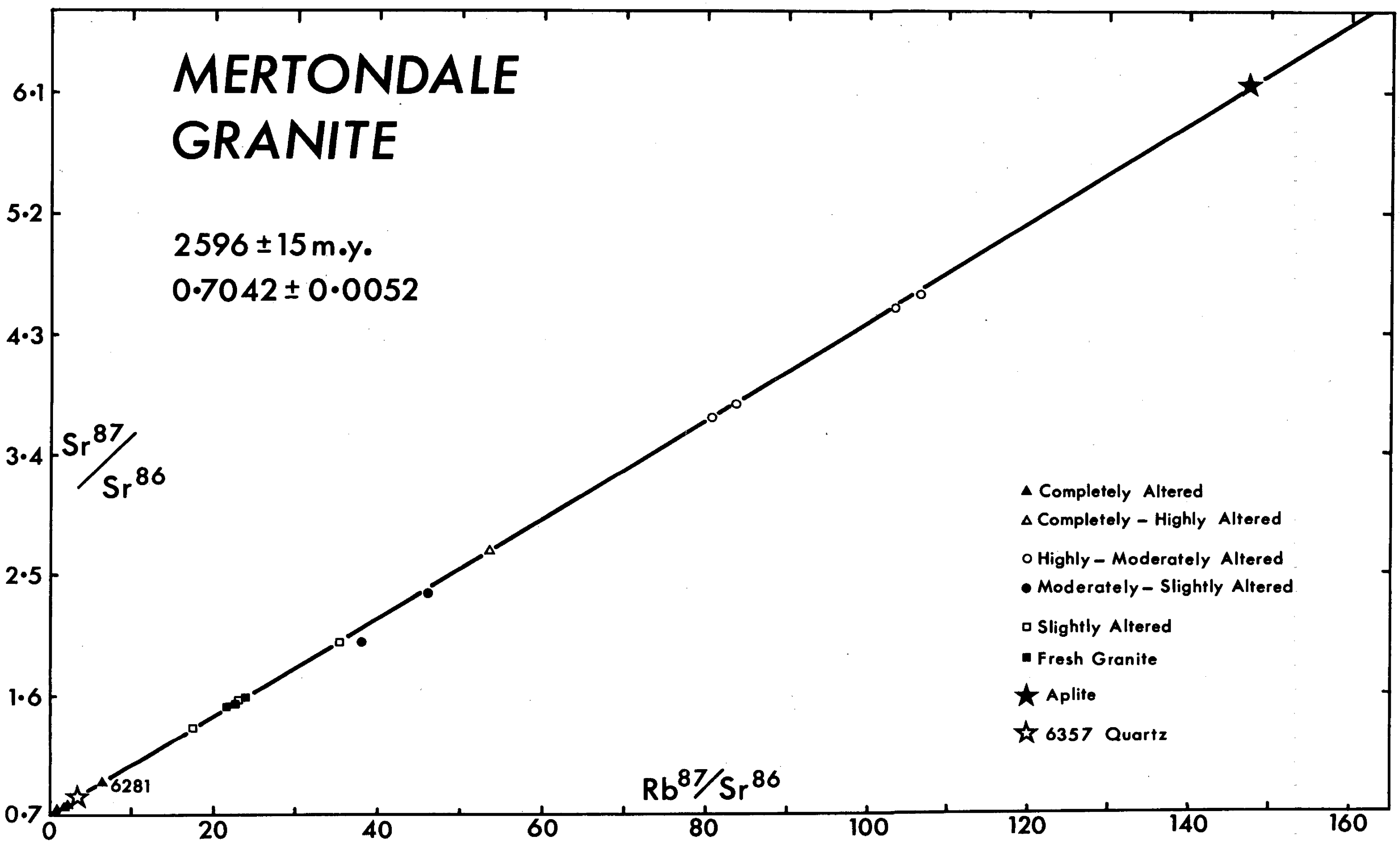

Fig. 46 Rb-Sr isochron plot of total rocks from the Mertondale Granite.

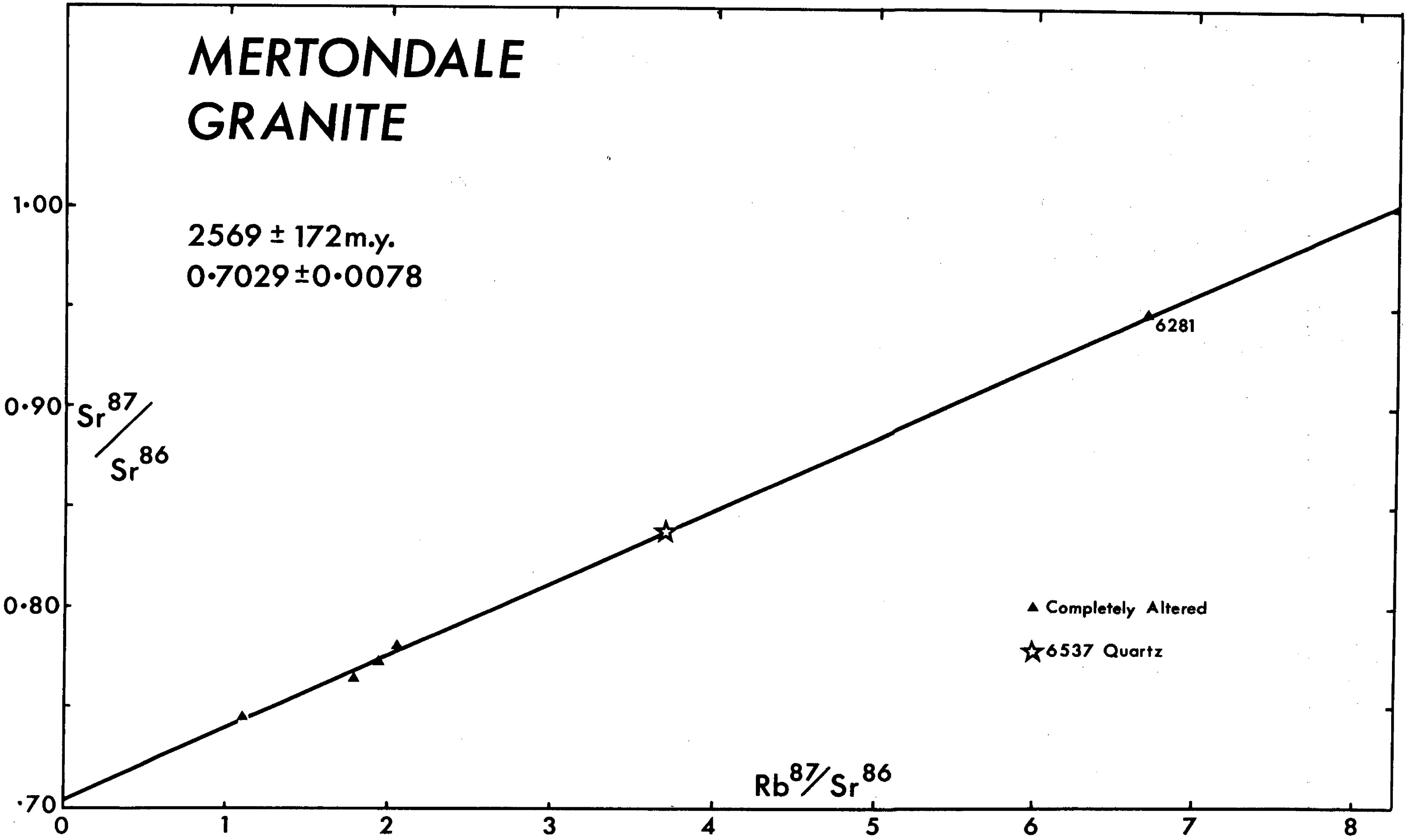

Fig. 47 Rb-Sr isochron plot of clay residuals and quartz from the Mertondale Granite.

all samples became closed systems to Rb and Sr diffusion during a period which is short compared to the experimental precision. This hypothesis will be supported by a value for the Mean Square of Weighted Deviates (MSWD) for the regression which does not statistically exceed unity. All scatter about the isochron could then be assigned to experimental error and yield a McIntyre Model 1 fit.

Geologically this answer implies that the following conditions are upheld:

1. There has been no later event or disturbance of Rb or Sr for any of the samples which could be due to weathering or metamorphism.
2. All samples are cogenetic and uncontaminated by the surrounding country rock during emplacement of the granite.

A negative answer implies that one or both conditions are not true.

Regression one yields a MSWD of 14.32 and is clearly negative.

If smaller groups of samples are regressed it is possible that the excess scatter may be found to associate with one group of samples. If fresh granite samples are regressed separately a low MSWD may be obtained indicating that the granite does uphold the previously mentioned conditions. Regression two (fresh granites only) has a MSWD of 1.38 which is not significantly greater than unity at the 5% point and the model 1 fit is indicated (Table 22). The indicated age does not differ significantly from that given by regression one. The high Rb/Sr ratio and its limited range precludes precise determination of the initial Sr^{87}/Sr^{86}.

If all the altered samples are regressed as one group (regression three), a higher value for MSWD of 20.19 is obtained indicating that the scatter is contained in this grouping. This result is significantly different from a model 1 fit and from regression two, the fresh rock regression. Data from all low Rb samples, those regarded as completely altered, have been pooled in regression four. A value of 61.44 for MSWD is high and includes most of the scatter which influences the MSWD value of regression one. The fifth regression pools the highly to slightly altered samples giving a much lower MSWD of 1.81, which does not significantly differ from a model 1 fit. The parameters of regression two and five do not differ significantly from each other, and both lack precision for the determination of the initial Sr^{87}/Sr^{86}.

On chemical and petrographic evidence, sample 6359 is intermediate between completely and highly altered groupings. Regression six tests the effect of including 6359 with the completely altered samples. The lowered value of 48.50 for the MSWD indicates slightly less scatter; the age is 2605 ± 40 m.y. Exclusion of 6359 from the highly to slightly altered sample grouping yields a lower value for MSWD which does not differ from a model 1 fit. The addition or removal of 6359 from the respective groupings yields no significant change and confirms the intermediate character of the sample. As regressions two and five are not significantly different, regression eight combines the two groups. Although a MSWD value of 2.43 is obtained it is not significantly different from a model 1 fit.

10.3.3 Discussion

The best estimate of the age of the Mertondale granite is given by regression two, Table 22, (2606 ± 36 m.y.) which includes fresh rocks only. This age is in close agreement with the age of granite intrusion around Kalgoorlie, W.A. found by Turek (1966). The period 2600-2750 m.y. includes a major period of granite emplacement in the Yilgarn block (Compston and Arriens, 1968).

The lack of precision in the determination of initial Sr^{87}/Sr^{86} limits its use in the interpretation of clay mineral formation. All regressions yield values for initial Sr^{87}/Sr^{86} that are not significantly different from that of regression two.

Alteration of the granite to a quartz-sericite assemblage was accompanied by an increase in the Rb/Sr ratio. As kaolinite alteration commenced the Rb/Sr ratio decreased. The initial increase of the Rb/Sr is probably related to formation of secondary sericite from K-feldspar during shearing. This involves a slight increase in the Rb content and a considerable decrease in the Sr content (Table 21). Because strontium is preferentially excluded from the mica structure it will migrate out of the system (Taylor, 1966).

Regressions five and two both yield essentially identical ages which would normally be taken to indicate that this process of mild Rb enrichment with strong Sr depletion occurred at the same time. A simple explanation would be that the process in question is late-stage hydrothermal sericitization and kaolinization of feldspars, rather than surficial weathering. The nearby occurrence of greisen represents a localised late-stage alteration.

As alteration proceeds to a quartz-kaolinite residual with minor sericite, the Rb content decreases by one order of magnitude with comparatively little change in the Sr content. However the Sr content of a majority of the completely altered samples is distinctly higher than the sericitised samples, which is possibly related to the occurrence of secondary carbonate as fine stringer veins or fissure fillings. The disequilibrium found in the U^{238} series as shown by the U^{234}/U^{238} ratio (1.58) for sample 6282 indicates present-day open system conditions with respect to the U decay series, (Rosholt et al., 1966). The U^{234} excess is probably related to the recent introduction of secondary carbonate along these fissures. The added Sr will have the Sr^{87}/Sr^{86} ratio of local groundwater, and mixing of this Sr with the original Sr should plot along a line joining both compositions on an isochron plot. Data points for quartz-kaolinite residuals have enriched Sr^{87}/Sr^{86} and plot (Fig. 46) very close to the fresh-rock isochron. Therefore, added Sr must be common Sr with $Sr^{87}/Sr^{86} \sim 0.71$).

It may be considered that the kaolinized rocks, as distinct from the sericitized rocks, are mainly the product of recent weathering. The Rb/Sr ratio should increase during recent weathering (Dasch, 1969; Bottino and Fullagar, 1968). Such a change should be minimal in this instance because the increase is usually based on loss of Sr, and for this granite the Sr content was initially very low. There is no doubt that kaolinization is associated with a strong depletion of Rb which would move the data points for the kaolinized samples to the left hand side of the 2600 m.y. isochron. However, if this depletion was also accompanied by proportional loss of radiogenic Sr^{87}, then the points will remain on the isochron, as they approximately are at present.

The distribution of Rb and Sr in the kaolinite-quartz assemblage is not known. The quartz component contains a negligible amount of Rb and Sr. Table 21 shows that for sample 6357, the quartz which constitutes about 35 wt. % of the total rock, would only contribute approximately 5% of the Rb and less than 2% of the Sr. This is assumed to be true for other samples. Consequently the bulk of the Rb and Sr is in the kaolinite, carbonate and the relict sericite.

The quartz also lies on the 2600 m.y. isochron (Fig. 47). However it contains too little Rb and Sr to account for the location of the total rock, also on the isochron, as a physical mixture of a residual 2600 m.y. quartz with kaolinite and carbonate of zero age. This implies that the quartz-free total rock contains another 2600 m.y. old component, which is either sericite or the kaolinite. The presence of sericite has been verified by separation and X-ray diffraction. (Quartz and kaolinite were removed by heavy liquid and combined sedimentation and limited acid treatment respectively (K. Norrish, pers. comm.)).

A mixture of 2600 m.y. old sericite and zero age kaolinite could explain the linear relation found for totally altered quartz-kaolinite samples. Varying mixtures of both components with secondary carbonate would give an isochron controlled by the age of the residual sericite component.

Late-stage hydrothermal alteration at 2600 m.y. would provide an alternative explanation for nearly all the components of the weathering profile, with the carbonate stringers bearing common Sr as the only recent addition.

The analysis of 6357-quartz, a residual quartz, raises interesting possibilities. This sample gives the fresh rock age, despite the small levels of Rb and Sr present, which suggests a more general use of quartz in geochronology. As a dateable mineral, quartz would have many advantages. It is ubiquitous and normally readily separated in considerable quantity. It is stable up to recrystallisation at 573°C, with a very low diffusion rate for alkalis in the quartz lattice. Any inclusions would act as isolated systems independent of the quartz.

Provenance studies on the source region of detritus may also be possible using different size fractions of quartz. Technically, the analysis of quartz has been made possible by the reduction of contamination to much lower levels as required for the analysis of lunar material.

10.4 TUCKANARRA QUARRY GRANITE

10.4.1 Results

The analytical data for sixteen total rock and three biotite samples are given in Table 23 and regression analysis in Table 24. The data are displayed in Fig. 48 and Fig. 49.

10.4.2 Regression Analysis

The first regression of Table 24 effectively tests for two conditions outlined previously; namely identical initial Sr^{87}/Sr^{86} and a common time of closure to Rb and Sr diffusion shared by all samples analysed. A model 2 McIntyre fit (MSWD = 219.75) is recommended by the regression and supports the presence of geological effect within the data. It is apparent that the conditions detailed above are not upheld and either a real age difference exists or subsequent isotopic redistribution affected the samples. Fig. 48 displays the wide departure of biotite 6272 from the isochron and its exclusion from regressions may be supported both geologically and statistically. This biotite is bleached

Table 23

Rb and Sr isotopic data for the Tuckanarra Granodiorite

Sample	Lithology	ID		Rb^{87}/Sr^{86}	Sr^{87}/Sr^{86}
		Rb ppm	Sr ppm		
6263	Fresh granodiorite	80.9	421	0.5561	0.7261
6265	Biotite rich xenolith from granodiorite	191	313	1.7794	0.7664
6265 dup.	"	192	315	1.7691	0.7668
6266	Mostly fresh granodiorite Partly chloritized biotite	95.4	402	0.6870	0.7278
6267	Slightly altered granodiorite	109	382	0.8269	0.7324
6268	"	87.1	409	0.6149	0.7252
6269	"	136	294	1.3453	0.7532
6270	Fresh granodiorite	141	383	1.0662	0.7422
6271	"	86.6	403	0.6215	0.7271
6272	Slightly altered granodiorite	73.1	423	0.4995	0.7178
6273	Altered granodiorite (No biotite)	107	252	1.2321	0.7442
6275	Slightly altered granodiorite	119	376	0.9208	0.7356
6276	Mildly weathered granodiorite	102	387	0.7637	0.7257
6277	"	93.1	380	0.7086	0.7261
6278	Weathered granodiorite	127	302	1.2191	0.7456
6279	Mildly weathered granodiorite	85.6	376	0.6575	0.7239

Continued on next page

Table 23 (Continued)

Rb and Sr isotopic data for the Tuckanarra Granodiorite

Sample	Lithology	ID		Rb^{87}/Sr^{86}	Sr^{87}/Sr^{86}
		Rb ppm	Sr ppm		
6263-biot.	Fresh granodiorite biotite, minor chlorite interlayers	724	23.4	131.455	5.5168
6265-biot.	Fresh biotite xenolith biotite, minor chlorite interlayers	740	17.9	208.063	8.2618
6272-biot.	Altered granodiorite biotite, bleached red	729	35.9	68.547	2.4491

Table 24

Regression data for the Tuckanarra Granite

Regression	No. of Samples	MSWD	Age (m.y.) $\lambda = 1.39 \times 10^{-11} yr^{-1}$	Initial Sr^{87}/Sr^{86}	Isochron Model
1. All samples	19	219.75	2405 ± 258	0.7037 ± 0.0030	2
2. Fresh rocks without biotites	10	16.87	2478 ± 147	0.7046 ± 0.0023	3
3. Fresh rocks including biotites 6263, 6265	12	16.24	2576 ± 21	0.7032 ± 0.0010	3
4. Samples 6268, 6266, 6267, 6275 and 6265	6	1.34	2524 ± 74	0.7031 ± 0.0010	2
			2526 ± 62	0.7031 ± 0.0009	1
5. Samples 6263, 6271, 6269 and biotites 6263 and 6265	5	6.56	2576 ± 31	0.7048 ± 0.0018	4
			2571 ± 30	0.7050 ± 0.0006	1
6. Weathered samples with biotite 6272	7	156.59	1894 ± 25	0.7076 ± 0.0004	-
7. Weathered samples excluding biotite 6272	6	14.83	2604 ± 381	0.6993 ± 0.0039	2

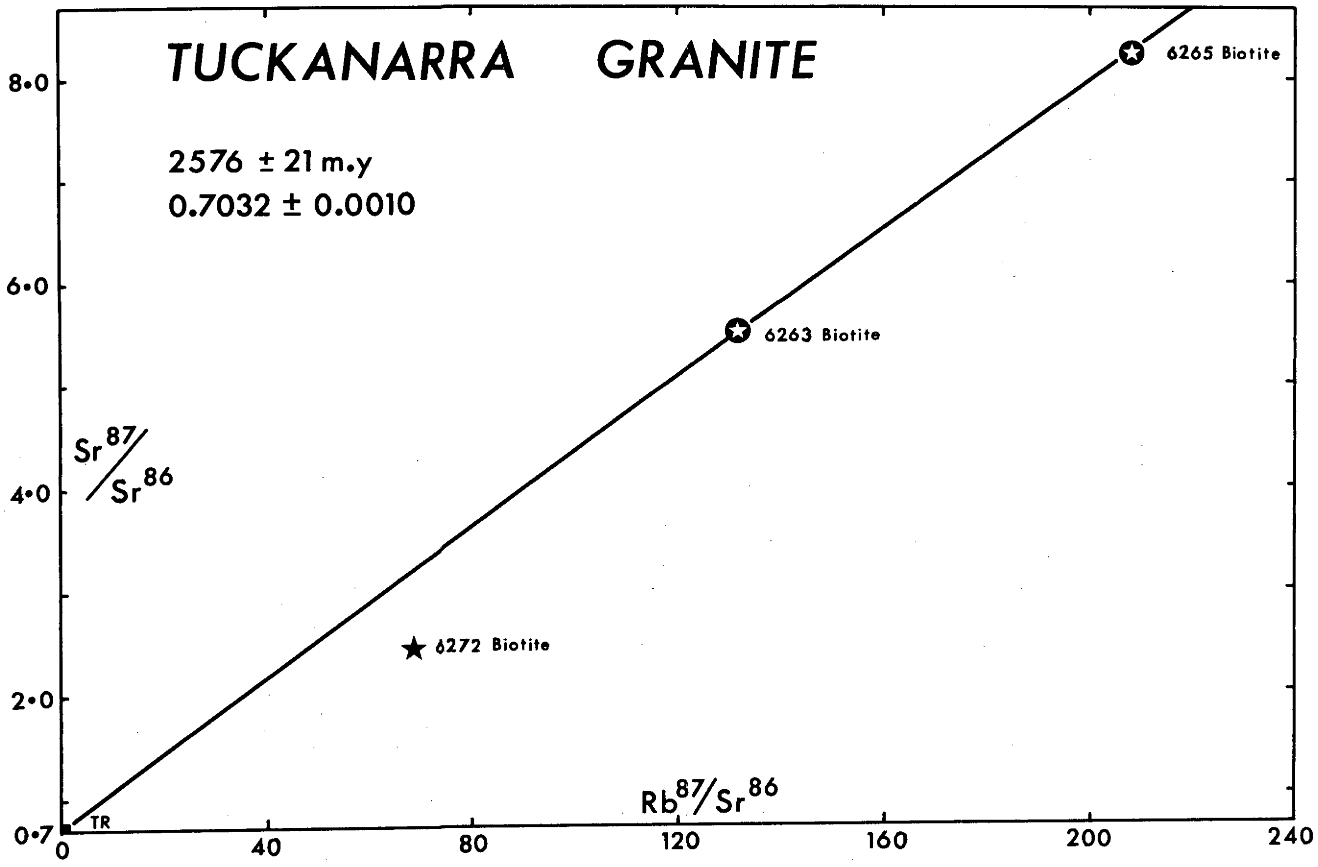

Fig. 48 Rb-Sr isochron plot of total rocks and biotites from the Tuckanarra Granite.

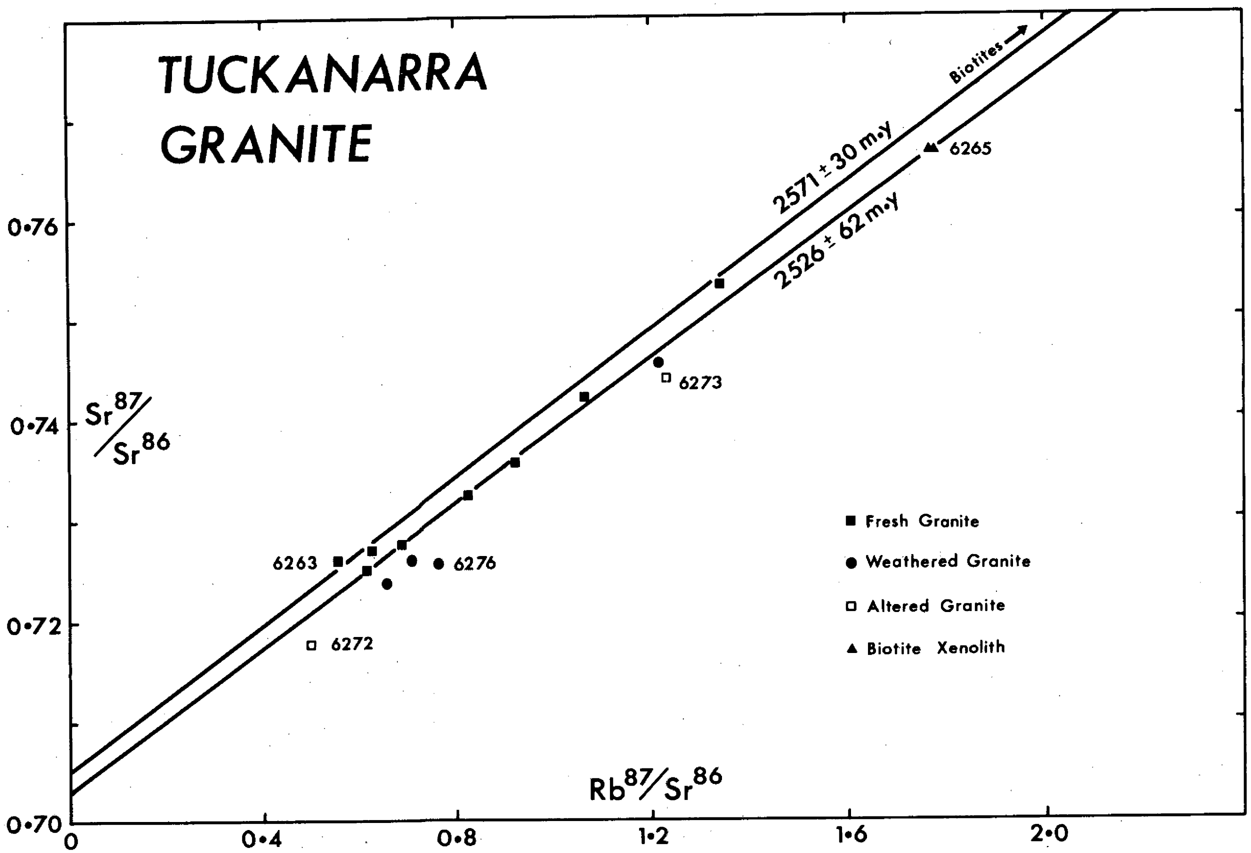

Fig. 49 Rb-Sr isochron plot of total rocks from the Tuckanarra Granite.

and altered in appearance and may be weathered. The total rock points also show considerable scatter and it is possible that the alteration seen petrographically may have been produced by an event which has partially adjusted the Rb-Sr isotopic system. Regression 2 excludes weathered samples and the three biotites and pools all other total rock samples. A model 3 fit is indicated (MSWD = 16.87) and the possibility of differing initial Sr^{87}/Sr^{86} is suggested by the regression. Inclusion of the two fresh biotites overcomes the lack of dispersion in the Rb^{87}/Sr^{86} ratio and may enable a more precise age estimation. Regression 3 (MSWD = 16.24) has a well defined age and a higher precision for the initial ratio but the age is essentially a biotite age. Virtually no change in MSWD and the suggestion of a model 3 fit, confirm the possibility of variable initial Sr^{87}/Sr^{86}. Regressions 4 and 5 represent an attempt to confirm the variation of initial Sr^{87}/Sr^{86} by regressing apparent linear arrays of data points (Fig. 49). Although the ages are not statistically distinct the initial ratios for the two regressions are. Both regressions are also model 1 fits at 95% confidence limits.

If the biotites can be considered to be independent of initial Sr^{87}/Sr^{86} or an initial Sr^{87}/Sr^{86} of 0.704 is taken (regressions 2 and 3), the following ages are given:

6263	biotite	2587 m.y.	(granodiorite)
6265	biotite	2567 m.y.	(biotite xenolith)
6272	biotite	1808 m.y.	(altered granodiorite)

The weathered samples and altered biotite 6272 are regressed in regression 6, giving a high MSWD (156.59) and no recommended model fit.

The age is strongly controlled by the biotite and if it is omitted (regression 7) a much lower MSWD (14.83) and a model 2 fit result. Inclusion of biotite 6272 yields a statistically higher MSWD and its exclusion can be supported on grounds previously outlined. Regression 7 however has much wider uncertainty limits for age and initial ratio and obviously reflects the possibility of a real age difference or subsequent isotopic redistribution. Samples 6272 and 6273 are highly altered but the mode of alteration is in doubt. Complete chloritization of biotite and heavy sericitization of plagioclase is evident in 6273 indicating hydrothermal alteration. Differentiation between weathering and hydrothermal alteration is very difficult and often impossible.

10.4.3 Discussion

The granodiorite has numerous xenoliths and biotite schlieren and may be described as a "streaky" granodiorite. Partly assimilated xenoliths and "smeared-out" contaminated granodiorite has resulted in variable initial Sr^{87}/Sr^{86} ratios. Sample 6265, a biotite rich xenolith, preserves a metamorphic biotite fabric with small scale folds and suggests an earlier metamorphic episode. Considerable retrogression of the biotite to chlorite is evident in part of the xenolith. It is possible that the age recorded by regression 3 and the two biotites is effectively the closure of the rock system to later hydrothermal alteration, demonstrated by chloritization of the biotite and by formation of epidote and sericite on the plagioclase. The most acceptable estimate of the age of the Tuckanarra Granodiorite is given by regression 3, (2576 ± 21 m.y.) and initial Sr^{87}/Sr^{86} of 0.7032 ± 0.0010.

The scatter in age estimation and increased uncertainty in initial Sr^{87}/Sr^{86} may be related to weathering processes, but the shift of the weathered sample data points to the right (higher Rb^{87}/Sr^{86}) may be due to a number of alternatives, acting jointly or separately. These are: Rb gain from surrounding more highly weathered materials, loss of common Sr by leaching and preferential loss of radiogenic Sr^{87} with selective weathering of a highly enriched Sr^{87}/Sr^{86} mineral, i.e. biotite. Of these alternatives Rb gain with slight Sr loss may be likely but the shift to the right on the isochron plot is of insufficient magnitude to be unequivocal and statistically real.

10.5 KOOLANOOKA QUARTZ PORPHYRY

10.5.1 Results

Rb and Sr isotopic analyses of total rock samples and weathered variants are listed in Table 25. Regression analysis of analytical data are tabulated in Table 26 and the data are displayed in Figs. 50 and 51.

10.5.2 Regression Analysis

Analysis of sample data follows the same pattern as outlined in earlier sections. Geological scatter is apparent from the high MSWD value, 281.37, given by regression one, Table 26. The age and initial ratio of the fresh quartz porphyry must be established prior to analysis of any later processes which may have adjusted the Rb-Sr-Sr isotopic system.

Arriens et al. (1966) report an age of 2555 ± 12 m.y. with an initial Sr^{87}/Sr^{86} ratio of 0.707 ± 0.003 ($\lambda = 1.39 \times 10^{-11} yr^{-1}$) for the quartz porphyry. This age estimate was based on duplicate analyses of five quartz porphyry total rocks, one xenolith "total rock" and a biotite from the analysed xenolith. Arriens noted that all total rock samples and the biotite were concordant, but feldspars and fluorite yield discordant ages. A K-Ar age of 2460 ± 55 m.y. for the xenolithic biotite is cited by Arriens (1963).

In Table 26, the second and third regressions are for fresh quartz porphyry total rock samples including

Table 25

Rubidium and strontium isotopic data for the Koolanooka Quartz Porphyry and altered variants

Sample	X.R.F.		I.D.		Rb^{87}/Sr^{86}	Sr^{87}/Sr^{86}	Weathering Type
	Rb	Sr	Rb	Sr			
94537	-	-	351	11.9	121.199	5.0302	Fresh porphyry
94537 dup.	-	-	349	11.9	121.102	5.0605	"
6311	336	8.1	334	9.89	147.182	5.9369	"
6312	333	7.9	335	8.82	177.761	7.0384	"
6313	337	9.5	333	10.7	130.662	5.3766	"
6313 dup.	337	9.5	335	10.7	131.344	5.3715	"
6205	336	9.2	324	9.87	140.309	5.6081	Minor iron staining
6314	340	8.2	333	9.60	152.442	6.0363	"
6315	321	12.7	320	14.2	83.917	3.6329	"
6316	334	14.3	328	15.8	75.025	3.2864	"
6318	336	8.5	333	9.72	147.105	5.6569	"
6319	333	9.4	330	10.6	128.912	5.0731	"
6320	316	11.2	311	12.3	96.428	4.0109	"
6206A	383	8.6	371	8.94	191.009	6.7735	Heavily iron stained, minor clay
6317	323	15.6	324	17.1	64.887	2.6148	"
6321	339	12.3	344	13.7	92.143	3.5086	"
6322	292	6.6	294	7.90	150.496	4.8253	"
6323	331	21.8	333	24.1	45.267	2.1033	"
6325	21.8	3.3	22.3	4.32	15.681	1.2509	Clay residual
6326	13.3	4.0	13.2	4.86	8.039	0.9752	"
6326 dup.	13.3	4.0	13.2	4.72	8.276	0.9800	"
6327	12.9	1.3	14.1	1.95	22.266	1.4353	"
6328	6.8	0.99	7.70	1.73	13.384	1.1204	"
6329	7.5	12.0	8.07	12.9	1.818	0.7744	"
6329 dup.	7.5	12.0	8.05	13.2	1.770	0.7726	"
6330	17.5	12.1	17.6	13.4	3.850	0.8337	"
6331	10.5	9.6	12.0	10.5	3.329	0.8222	"
6332	2.9	8.3	3.89	8.86	1.280	0.7514	"
6333	3.0	5.1	3.86	5.51	2.036	0.7727	"
6334	3.6	2.8	3.88	2.98	3.790	0.8087	"
6335	47.0	1.7	48.4	2.32	73.474	2.9693	"
6207	3.6	2.0	4.64	2.59	5.252	0.8759	"
6208	66.3	25.6	63.1	25.9	7.222	0.9603	"

Continued on next page

Table 26

Regression data for the Koolanooka Quartz Porphyry and altered variants

Regression	No. of Samples	MSWD	Age (m.y.) $\lambda = 1.39 \times 10^{-11} yr^{-1}$	Initial Sr^{87}/Sr^{86}	Isochron Model
1. All samples	45	281.37	2399 ± 78	0.7134 ± 0.0096	4
2. Fresh rocks	13	6.33	2549 ± 11	0.7108 ± 0.0016	1
			2550 ± 26	0.7106 ± 0.0037	2
			2520 ± 15	0.7220 ± 0.0081	3
3. Fresh rocks excluding samples with Rb^{87}/Sr^{86} >30	8	1.51	2595 ± 26	0.7064 ± 0.0044	3
			2591 ± 18	0.7072 ± 0.0021	1
4. All iron-stained samples	16	200.44	2269 ± 121	0.7580 ± 0.0487	2
5. Minor iron-stained samples	10	16.06	2425 ± 50	0.7115 ± 0.0290	4
6. Heavily iron-stained with minor clay	6	129.74	2049 ± 177	0.7971 ± 0.0600	2
7. All clay residuals	15	171.44	2274 ± 136	0.7109 ± 0.0081	4
8. Clay residuals, apparently linear	9	45.00	2368 ± 114	0.7109 ± 0.0051	4
9. Clay residuals, deviant	6	176.31	2238 ± 163	0.7031 ± 0.0215	4
10. Silicified remnants, silcrete	4	18.04	2813 ± 125	0.7097 ± 0.0146	3

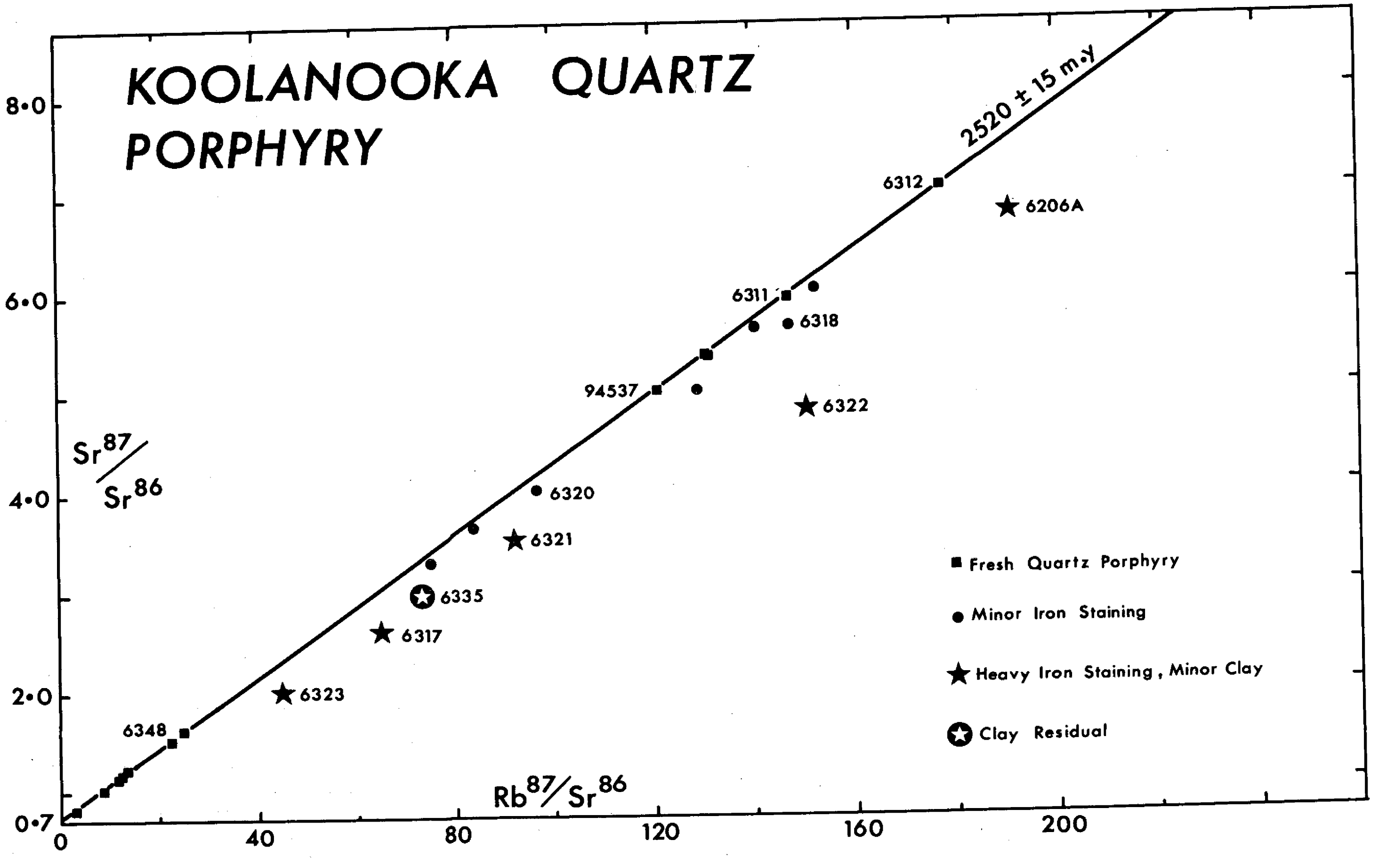

Fig. 50 Rb-Sr isochron plot of total rocks from the Koolanooka Quartz Porphyry.

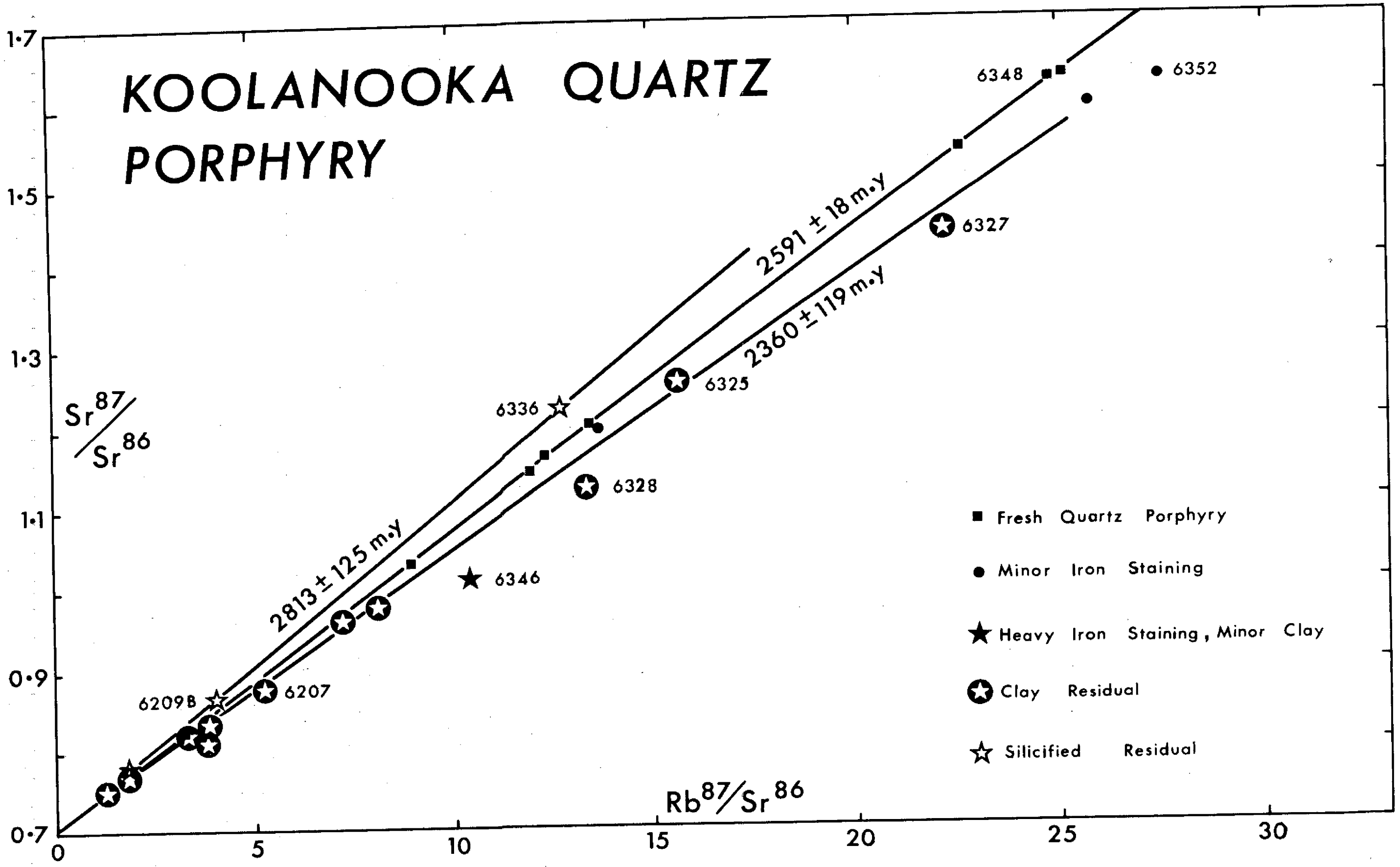

Fig. 51 Rb-Sr isochron plot of total rocks, clay residuals and silcretes from the Koolanooka Quartz Porphyry.

reanalyses of samples 94537 and 94540 (= 5646a) from Arriens et al. (1966). Regression two includes all fresh samples and has a MSWD of 6.33. This regression is significantly different from a model 1 McIntyre fit and therefore indicates the presence of geological effect within the fresh rock data. In this instance, the McIntyre method for regression analysis gives no indication of the possible kind of geological effect. However, visual examination suggests that samples with greatest enrichment of Sr^{87}/Sr^{86} (6311, 6312, 6313 and 94537) may have younger ages than less enriched porphyry samples. Three separate solutions of the McIntyre regression for fresh porphyry are listed in Table 26. Little difference is evident between model 1 and 2 solutions for age and initial Sr^{87}/Sr^{86} but model 3 gives a younger age with a distinctly higher initial Sr^{87}/Sr^{86}.

There are two possible alternatives:

1. Local variations in initial Sr^{87}/Sr^{86} existed within the quartz porphyry intrusion, or
2. A real age difference exists as a consequence of separate magma injections or a later event which has affected one area of the quartz porphyry alone.

Regression 3 excludes samples with $Rb^{87}/Sr^{86} > 30.0$

(namely fresh porphyries from the southwestern locality) and an older age is obtained, (Table 26). The MSWD decreases to 1.51 which is not significantly different from a model 1 fit at the five percent point. The exclusion of samples highly enriched in Sr^{87}/Sr^{86} is supported by regressions 2 and 3 which are significantly different. Many samples give age estimates independent of reasonable variations in the initial Sr^{87}/Sr^{86} ratio. Table 27 lists the individual sample ages for these samples. (An initial Sr^{87}/Sr^{86} ratio of 0.707 has been taken for all samples as a common reference). Samples excluded from regressions 3 have younger ages suggesting that the second alternative of a real age difference is more likely.

Significant contamination of quartz porphyry at the more northerly localities which might produce variation in the initial Sr^{87}/Sr^{86} is not supported by major element chemistry. The quartz porphyry is remarkably uniform although the xenolith content is noticeably higher in the more northerly areas. The occurrence of feldspar discordancy, (Arriens et al., 1966) and possibly later muscovite in samples from the southwest locality prevents discarding the second alternative. A younger age for the southwest porphyry cannot be excluded.

Data for iron-stained weathered samples have been regressed (regression 4) giving a high MSWD of 200.44.

Table 27

Age estimates for enriched samples from the Koolanooka Quartz Porphyry, W.A.

Sample	Age (m.y.)	Weathering Intensity	Sample	Age (m.y.)	Weathering Intensity
94537	2532	Fresh porphyry	6320	2423	Iron stained porphyry
6311	2512	"	6205	2470	"
6312	2518	"	6317	2082	Iron staining, minor clay
6313	2526	"	6321	2154	"
6314	2472	Iron stained porphyry	6322	1942	"
6315	2465	"	6323	2185	"
6316	2432	"	6206A	2248	"
6318	2379	"	6335	2182	Clay residual
6319	2396	"			

A recommended model 2 fit suggests that a range of ages exists within the regressed data. Fig. 50 illustrates variable displacement of weathered porphyry data points away from the fresh rock isochron and Table 27 indicates younger ages for weathered, enriched Sr^{87}/Sr^{86} samples. Although an isochron relationship cannot be predicted for samples which have become open systems to Rb-Sr migration, regressions 5 and 6 attempt to regress iron-stained weathered samples in two groups according to apparent weathering intensity. Moderately weathered samples are included in regression five, with more intensely weathered samples in regression six. A significant lowering of the MSWD to 16.06 (Table 26) for regression 5 confirms the trend towards younger ages with iron staining weathering. Regression 6 also supports this conclusion, and additionally suggests that increased weathering intensity lowers the age even further (Table 26). The use of iron-stained samples in geochronology will always give minimum age estimates.

Data representing clay residuals from the laterite profile on the southwest porphyry have been regressed, (regression 7), giving a high MSWD of 171.44 and a recommended model 4 McIntyre fit. A degree of linearity for many clay residuals is apparent in Fig. 51 with a few samples clearly deviant. Samples with an apparent relationship between radiogenic Sr^{87} and Rb have been regressed separately (regression 8). A significant reduction in MSWD to 45.00 is obtained although a model 4 fit remains and initial Sr^{87}/Sr^{86} and age solutions do not differ from regression seven. The remaining clay residuals have been pooled in regression 9 (Table 26) but estimates of age and initial Sr^{87}/Sr^{86} do not differ from regression eight. Regressions eight and nine are significantly different. The latter regression includes clay residuals immediately beneath the resilicified surface zone. Other clay residual samples appear to retain a younger age than the fresh quartz porphyry.

Table 27, shows an independent age of 2182 m.y. for sample 6335, a clay residual. This sample is sufficiently enriched in Sr^{87}/Sr^{86} to give an age almost independent of initial Sr^{87}/Sr^{86}. Muscovite is a prominent mineral in this clay residual and it is effectively controlling the age given by the sample. Variable Rb^{87}/Sr^{86} and Sr^{87}/Sr^{86} ratios for clay residuals are due to varying amounts of clay, quartz and muscovite, with the first two minerals acting as dilutants. The muscovite controlling the age of clay residuals must have a younger age than the quartz porphyry if clay residuals are viewed as simple mixing of three mineral phases. The occurrence of muscovite at the southwestern locality and the apparently younger ages of fresh porphyries coupled with mineral discordance may be indicating growth of muscovite at approximately 2200 m.y. in response to a localised geological event.

Three analysed silcretes have been regressed in the last regression (10) of Table 26. A moderate MSWD of 18.04 and a recommended model 3 fit are given by the regression. Although variable initial Sr^{87}/Sr^{86} is indicated, the result is statistically distinct and silcretes are apparently older than the fresh porphyry.

10.5.3 Discussion

The age of the Koolanooka quartz porphyry may be slightly different from the age published by Arriens et al. (1966). An apparently older age for most of the exposed porphyry cannot readily be explained as a consequence of contamination with material of lower Sr^{87}/Sr^{86}. The strong similarity of major element chemistry for all sampled localities of the porphyry does not support selective contamination of the more northerly variants. Alternatively the older age is real and the southwestern variant has been affected by a localised later event. The occurrence of granite porphyries around the southern margin of the porphyry, the discordant potassium feldspar age (Arriens et al., 1966), and the apparent younger age of muscovite from this area all support a later thermal event at approximately 2200 m.y. Mineral discordance noted for feldspars from sample 94537 by Arriens et al., (1966) would more readily be explained as formation of a secondary sericite on both feldspar phases in response to this later event. Exchange of Sr and Rb between feldspars as a consequence of local adjustment is more likely a result of the growth of a secondary muscovite/sericite component (Brooks, 1968). The best estimate of the age of the Koolanooka quartz porphyry is regression 3 with an age of 2591 ± 18 m.y. and an initial Sr^{87}/Sr^{86} of 0.7072 ± 0.0021.

Iron staining weathering will result in apparently younger ages and will give minimum ages for a rock formation or intrusion. In general, data in Table 27 support progressively younger ages with increasing weathering intensity. Apparent age loss is related to increased Rb^{87}/Sr^{86} ratio. Low Sr contents for a majority of iron-stained weathered samples are very susceptible to processes that affect Sr concentrations.

Clay residuals can be viewed as mixtures of residual muscovite, quartz and clay. Secondary carbonate introduced by surficial processes may also influence clay residuals but it will form a mixing relationship with muscovite along a mixing line. Clay residuals which do not fit a simple mixing line (regression 9) are from immediately below the silcrete horizon. The apparent increase in Rb^{87}/Sr^{86} shown by these clay samples is complementary to the decrease in Rb^{87}/Sr^{86} shown by silcretes. Preferential Rb adsorption onto the clays as groundwater or pore water rises through capillaries, leaves Sr with silica to precipitate in the surface layer, with evaporation of the pore fluid. In this manner Rb and Sr can be separated, and the relationships between clay residuals and silcretes generated.

10.6 SUMMARY

Iron staining or recent weathering progressively reduces the age of rocks. The magnitude of apparent age loss is related to weathering intensity although parent rock composition and mineralogy exert initial control of any changes.

Weathering of the Tuckanarra granodiorite does not produce a definite trend towards younger ages. Initial Sr^{87}/Sr^{86} variation, a result of contamination during emplacement and later retrogressive events, has affected the granodiorite. Weathering alteration overprints the initial variation and cannot be unequivocally distinguished. However weathering at this locality is largely restricted to disaggregation processes in an arid climate with little chemical attack of silicate minerals.

The Koolanooka quartz porphyry does give apparently lower ages for weathered "total rock" samples. High Rb/Sr ratios and low Sr contents are very sensitive to processes which will change Sr concentrations. The mode of "age loss" is difficult to ascertain but is a result of variations in Sr content. The fresh porphyry is variable in Sr and has no unique Sr content. Strontium loss is regarded as the most likely mechanism producing younger ages (Dasch, 1968, 1969). Samples with visible iron-stained fractures and surface crusts give younger ages and it is evident that even initial weathering processes are capable of reducing the "total rock" age.

Lateritic weathering in the two areas studied is marked by the presence of relict muscovite or sericite. This mineral is very resistant to weathering processes and effectively retains its original age. Varying amounts of relic quartz and muscovite with kaolinite and other clays form mixing isochrons.

Clay alteration of the Mertondale granite has retained the original muscovite and sericitic component of the granite and this phase along with the quartz effectively controls the age recorded for clay residual material.

Deep clay weathering of the Koolanooka quartz porphyry is analogous but here the muscovite has a younger age than the fresh porphyry. The age of muscovite formation is given by clay residuals which have not been affected by secondary silicification processes.

Detritus from clay residual profiles containing muscovite will give the age of the detrital muscovites, providing separation of muscovite from clay does not occur.

It is not known if the presence of muscovite or sericite is rare, or common in clay profiles from lateritic weathering. Significant potassium content in an analysis of a clay residual sample indicates the presence of residual muscovite or sericite (K. Norrish, pers. comm.). The absence of studies on residual clays lacking a mica component does not allow a generalised summary of the effects of lateritic weathering.

CHAPTER 11

GEOCHEMISTRY OF URANIUM AND THORIUM SERIES ISOTOPES

11.1 INTRODUCTION

A study of uranium and thorium series isotopes may permit greater understanding of the complex behaviour of both elements during weathering. The basic assumption of radioactive equilibrium for gamma-ray spectrometry requires examination, particularly if open system conditions can be predicted or suspected i.e. for either recent volcanics or alteration of pre-existing geological materials. The introduction of the parameter of time into weathering processes would be invaluable although it must be remembered that rock decay is a multi-stage event and by no means unidirectional.

Investigations of weathering processes using U and Th isotopes in addition to element concentrations have been few in number, although dating of deep-sea sediments has received considerable attention. Thurber (1962), Rosholt *et al.* (1964), Dooley *et al.* (1966), Rosholt *et al.* (1966), Osmond *et al.* (1968), Sakanoue *et al.* (1968) and Scott (1968) have investigated secondary redistribution of U-ores, sedimentary rocks, stream sediment loads, river waters and weathering processes.

Rosholt _et al_. (1964) found deficiencies of U^{234} in weathered granite samples and noted that

> ... slightly weathered rock is most deficient, suggesting major U^{234} leaching at an early stage in the decomposition....

Very weathered rock had a higher U^{234}/U^{238} ratio but this was attributed to later enrichment of uranium with a higher U^{234}/U^{238}.

Koide and Goldberg (1965) reported ocean water is normally enriched in U^{234} with $U^{234}/U^{238} = 1.14 \pm 0.01$, however surface water samples may display considerably larger enrichments (Cherdyntsev _et al_., 1964).

Rosholt _et al_. (1966) have investigated soil profiles from Minnesota and demonstrated excess of Th^{230} and deficiency of U^{234} compared to U^{238}. Uranium was leached at depth in the profile and possible upward capillary migration of uranium with above normal U^{234}/U^{238} ratios was proposed to explain U^{234}/U^{238} ratios exceeding unity in the upper soil horizons. Scott (1968) examined sediment loads from rivers representing two different weathering regimes. The U^{234}/U^{238} activity ratio was less than unity in sediment derived from well leached soils but greater than unity in organic-rich sediments from surface layers of soil profiles. A majority of fine fractions from sediments had an excess of Th^{230} relative to U^{234} and Scott suggested that this indicated adsorption by clays, complexing with sesqui-oxides or concentration in resistates. Sakanoue et al. (1968) have reported slight deficiencies of U^{234} compared with the radioactive equilibrium value.

The actual location of U and Th in weathered rocks has received little attention. Harriss and Adams (1966) studied the distribution of total radioactivity in both weathered and fresh granites by autoradiography. They were able to demonstrate discrete point sources of radioactivity in fresh granite, however weathered granites revealed a reduction and a more dispersed character for radioactive sources. Small loss of U with little or no loss of Th during weathering has been shown by Adams and Weaver (1958); Pliler and Adams (1962); Richardson and Adams (1963); Rogers et al. (1965) and Harriss and Adams (1966).

11.2 ANALYTICAL TECHNIQUES

The analysis of the isotopic composition of U and Th followed that of Ku (1965) with minor modifications. The chemical procedures have been outlined in Appendix C and U^{234}/U^{238} activity ratios were determined by alpha spectrometry.

An estimate of the Ra^{226}/U^{238} activity ratio was obtained by a comparison between gamma-ray and X.R.F. data.

Although gamma-ray spectrometry measures Bi^{214} in the U^{238} decay series and assumes radioactive equilibrium, extrapolation to at least Ra^{226} is valid if samples have been left for periods of two weeks or longer in sealed cans. Intermediate daughters between Ra^{226} and Bi^{214} have short half-lives and will reach radioactive equilibrium with Ra^{226} during that time. If this procedure is followed, gamma-ray measurements are effectively Ra^{226} determinations and the apparent uranium value is in effect Ra^{226} (U-equivalent units).

Gamma-ray spectrometric analysis of Th employs the gamma spectrum of Tl^{208}, a short-lived daughter near the end of the Th^{232} decay series. All daughter nuclides between Th^{228} and Tl^{208} have short half-lives and hence gamma-ray measurements of Tl^{208} are in effect measurements of Th^{228}.

Th^{230} was determined for three samples only. The very high Al_2O_3 contents of many "lateritic profile" samples (Appendix B) renders the chemical procedure for the isolation of Th cumbersome and impracticable. After the hydroxide precipitate stage of separation a gel frequently forms and effectively adsorbs Th. This suspension "clogs" ion-exchange columns and results in loss of Th during analytical separation procedures. Hexone extractions of the gel fail to recover Th and very low Th yields are obtained (Black, 1969).

All samples were analysed by gamma-ray spectrometry (see Appendix C) for U and Th. These results are discussed separately in Chapters 6 and 9. Approximately forty samples were analysed by X.R.F. for U and Th on a Phillips 1220 semi-automatic X-ray spectrometer, automated to permit repeated analyses of U and Th by recycling. The mean value was taken for a number of different determinations on duplicate pellets of the same sample. This procedure is necessary because of limitations imposed by low count rates (the analytical lines measured were U $L_{\alpha 1}$ and Th $L_{\alpha 1}$).

A comparison of U and Th values determined by both methods is discussed in Appendix E. Data points which clearly deviate from the 45° equivalence line suggest lack of radioactivity equilibrium for those samples.

Alpha spectrometric analyses have been carried out on these samples and a selection of fresh parent rocks. The validity of employing X.R.F. versus gamma-ray spectrometric analyses to assess disequilibrium may be checked by the degree of correlation between X.R.F. and alpha spectrometric analysis. Fig. E-2, Appendix E reveals good agreement between the two independent methods within error limits of ± 5%.

11.3 SNOWY MOUNTAINS REGION

11.3.1 Results

Analytical data for the Snowy Mountains are given in Table 28 and cover the three rock types discussed in Chapters 3 to 6. The analyses of alpha spectrometry have been performed by Dr H.H. Veeh although interpretation is the author's responsibility.

Standard deviations quoted are based on counting statistics and all ratios represent activity ratios. Sampling error will affect X.R.F. determinations and the error in gamma-ray/X.R.F. ratios is believed to be ± 10%. At very low concentrations (<1 ppm) counting statistics will greatly increase error limits for both X.R.F. and gamma-ray determinations.

11.3.2 Discussion

Except for sample 6079, no significant U^{234}/U^{238} disequilibrium was observed for rocks and soils from the Snowy Mountains region. This observation contrasts with conspicuous deficiency and enrichment of U^{234} in soil profiles from North America reported by Rosholt *et al.* (1966), but is similar to the results of Sakanoue *et al.* (1968).

Five of the samples in Table 28 are soils or completely weathered rock, but sample 6079 is hydrothermally altered (see Chapters 4 and 6). The significance of hydrothermal

TABLE 28

Thorium and Uranium Analyses of Fresh and Weathered Rocks from the Snowy Mountains, N.S.W.

Sample No.	Rock Type/Weathering	U ppm (1)	Th ppm (1)	U ppm (2)	Th ppm (2)	U ppm (3)	Th ppm (3)	U^{234}/U^{238} (1)	Th^{230}/U^{238} (1)	Ra^{226}/U^{238} (4)	Th^{228}/Th^{232} (4)
6009	Dioritic Soil, DH 2401, 0" - 6"	1.8	-	1.6	6.3	1.2	7.9	0.99±0.02	-	0.68	1.26
6014	Weathered diorite, DH 2401, 25 feet	1.7	5.4	1.8	5.1	1.4	5.3	0.98±0.03	0.92	0.86	0.98
6019	Weathered diorite, DH 2401, 50 feet	1.1	-	-	-	1.0	3.5	1.01±0.03	-	0.92	-
6021	Weathered diorite, DH 2401, 60 feet	1.5	4.5	-	-	1.2	4.7	0.96±0.04	0.99	0.83	1.04
6170	Soil on granodiorite, DH 2660, 0" - 5"	3.3	-	-	-	2.6	17.4	0.98±0.01	-	0.80	-
6184	Weathered granodiorite, DH 2660, 70 feet	4.0	16.4	-	-	3.0	17.6	1.00±0.02	0.91	0.74	1.07
6137	Granitic Soil, DH 2511, 65 feet	-	-	3.5 4.6[5]	15.4 15.7	2.9	16.2	1.00±0.04	-	-	1.04
6133	Completely weathered granite, DH 2511, 85 feet	5.7	-	4.3 5.5[5]	16.2 17.8	2.9	17.7	0.96±0.03	-	0.51	1.04
6088	Fresh granite, DH 2511, 310 feet	6.0	-	-	-	5.2	17.0	0.98±0.02	-	0.86	-
6079	Hydrothermally altered granite, DH 2511, 355 feet	4.4	-	3.9	15.1	3.6	14.6	0.94±0.02	-	0.82	0.97

(1) Values determined by alpha spectrometry
(2) " " X.R.F.
(3) " " gamma-ray spectrometry
(4) Derived from a comparison between (3) and (1) or (2)
(5) Replicate analyses on separate pellets by (2)

alteration has been outlined in these chapters and is related to shearing, faulting and high secondary carbonate content. Consequently these zones are preferentially weathered to considerable depths and the disturbance of the U^{234}/U^{238} ratio is readily explained by selective leaching of U^{234}.

The radioactive decay of U^{238} to U^{234} is thought to leave U^{234} (Cherdyntsev _et al_., 1955 as discussed in Dooley _et al_., 1966) as a charged (oxidised) ion displayed from the initial location and no longer bonded as the parent U^{238} nuclide was. Thus leaching in mildly oxidising conditions preferentially removes U^{234}, although in highly oxidised environments both U^{234} and U^{238} are leached simultaneously.

There are three alternative explanations for the radioactive equilibrium between U^{234} and U^{238}:

1. Weathering is very minimal and confined largely to physical disintegration of the parent rock. The organic content is correspondingly low.
2. Weathering intensity was high and oxidising conditions were pronounced.
3. Both weathering and soil formation occurred prior to the last million years and the system has subsequently remained closed to U and Th isotopic fractionation.

Supporting major and trace element chemistry (Chapters 3 to 6) suggest a relatively mild weathering intensity without large scale changes. The second alternative is therefore considered improbable. The third alternative is largely dependent on assessment of erosion rates and earlier climatic conditions. An erosion rate of 11 mm per 1,000 years has been estimated for central northern N.S.W. (P. Wellman, pers. comm.) but uplift and warping in the Snowy Mountains region do not permit a similar estimation. The first alternative is therefore considered more likely although the last cannot be disproved. U^{234}/U^{238} ratios less than unity may be due to a combination of low weathering intensity and little organic content.

Without Th^{230} analyses, a detailed examination of uranium isotopic movement for a majority of samples cannot be evaluated.

All Ra^{226}/U^{238} ratios in Table 28 are less than unity and suggest, either leaching of Ra^{226} and daughters intermediate between Ra^{226} and U^{238} or addition of U^{238}. Preferential leaching of U^{234} has not occurred and leaching of Th^{230} is considered improbable (Rosholt _et al._, 1966). Therefore a combination of Ra^{226} leaching and U^{238} enrichment is considered the most likely mechanism to explain the observed ratios. (The possibility of sampling errors must also be considered, Appendix E).

Ra^{228} ($t\frac{1}{2}$ = 5.7 yrs) is an intermediate daughter between Th^{232} and Th^{228} and because Ra is chemically mobile, Ra^{228} may be selectively leached. The Th^{228}/Th^{232} ratios in Table 28 do not differ significantly from unity with the exception of sample 6009. Secondary addition of Th^{228}, through its relatively mobile parent isotope Ra^{228} is considered more likely than preferential leaching of Th^{232} to account for the observed relative excess Th^{228}. A mechanism involving leaching of Ra^{228} from rocks and upwards migration to the soil horizon will effectively add Th^{228} to the upper weathered rock and soil mantle. Th^{228} is probably adsorbed and immobilised immediately after its generation from Ra^{228}.

11.4 WESTERN AUSTRALIA

11.4.1 Results

U and Th concentrations as determined by X.R.F., gamma-ray spectrometry or alpha-spectrometry have been summarized in Appendix E. Owing to the high Al_2O_3 content in most of the samples the chemical isolation of Th is cumbersome and impracticable. Consequently no attempts were made to measure Th isotopes by alpha-spectrometry. The U^{234}/U^{238} ratios in Table 29 were measured directly

TABLE 29

Thorium and Uranium Analyses of Fresh and Weathered Rocks from Western Australia

Sample No.	Rock Type/Weathering	U ppm (1)	Th ppm (1)	U ppm (2)	Th ppm (2)	U ppm (3)	Th ppm (3)	U^{234}/U^{238} (1)	Ra^{226}/U^{238} (4)	Th^{228}/Th^{232} (4)
6356	Clay residual, Mertondale granite	-	-	1.4	9.5	1.2	9.6	-	0.86	1.01
6280	Clay residual, Mertondale granite	-	-	1.4	8.7	0.9	8.5	-	0.64	0.98
6281	Clay residual, Mertondale granite	-	-	1.9	13.6	1.0	11.9	-	0.53	0.88
6282	Weathered Mertondale granite	1.5	-	1.5	8.3	2.6	8.6	1.58 ± 0.01	1.72	1.04
6292	Fresh Mertondale granite	-	-	1.4	6.8	1.7	7.2	-	1.21	1.06
6293	Core, weathered dolerite boulder	8.9	-	8.6	0.2	2.1	1.1	0.82 ± 0.01	0.24	5.24
6294	Outer core, weathered dolerite boulder	14.7	-	16.2	2.7	9.2	3.2	0.99 ± 0.01	0.62	1.19
6295	Inner rim, weathered dolerite boulder	12.9	-	13.2	8.4	10.7	8.1	1.09 ± 0.01	0.83	0.96
6296	Outer rim, weathered dolerite boulder	10.7	-	11.7	4.8	12.3	5.7	1.06 ± 0.01	1.15	1.19
6298	Weathered dolerite Glen View Quarry	2.9	-	2.8	25.6	3.1	22.4	0.84 ± 0.01	1.07	0.88
6299	Weathered granite Glen View Quarry	2.2	-	2.3	19.4	1.4	17.5	0.72 ± 0.01	0.64	0.90
6302	Weathered granitic clay residual	4.9	-	4.8	27.4	5.4	25.0	1.17 ± 0.01	1.10	0.91
6305	Fresh dolerite Glen View Quarry	0.23	-	1.1	0.7	0.2	0.49	1.01 ± 0.01	0.87	0.74
6306	Fresh granite Glen View Quarry	6.2	-	6.9	21.9	6.6	23.2	0.99 ± 0.01	1.07	1.06
6309	Weathered granite Glen View Quarry	16.2	-	19.6	32.5	17.2	34.1	0.97 ± 0.01	1.06	1.05

(1) to (4) as for Table 28.

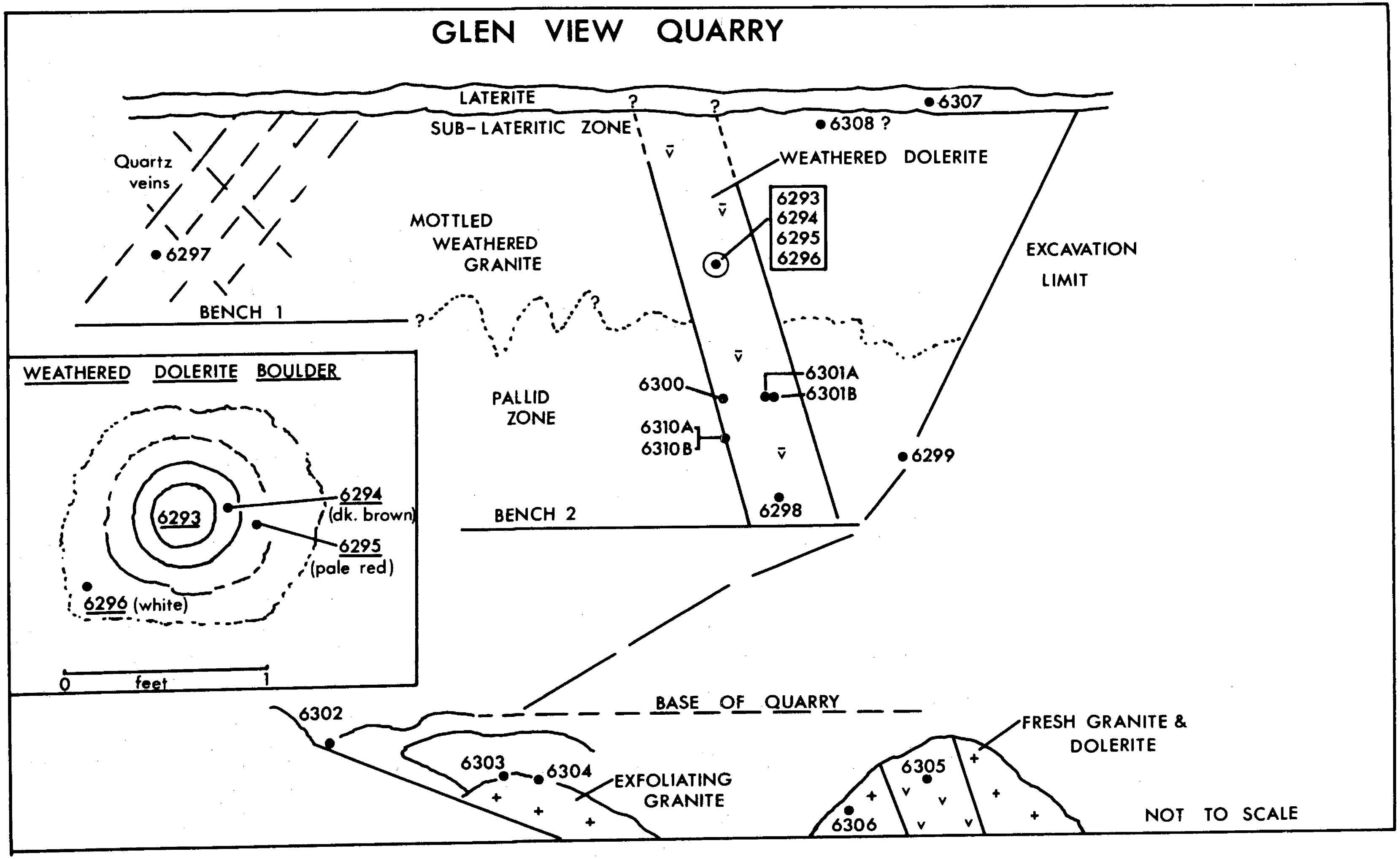

Fig. 52 Geological outline of the Glen View Quarry.

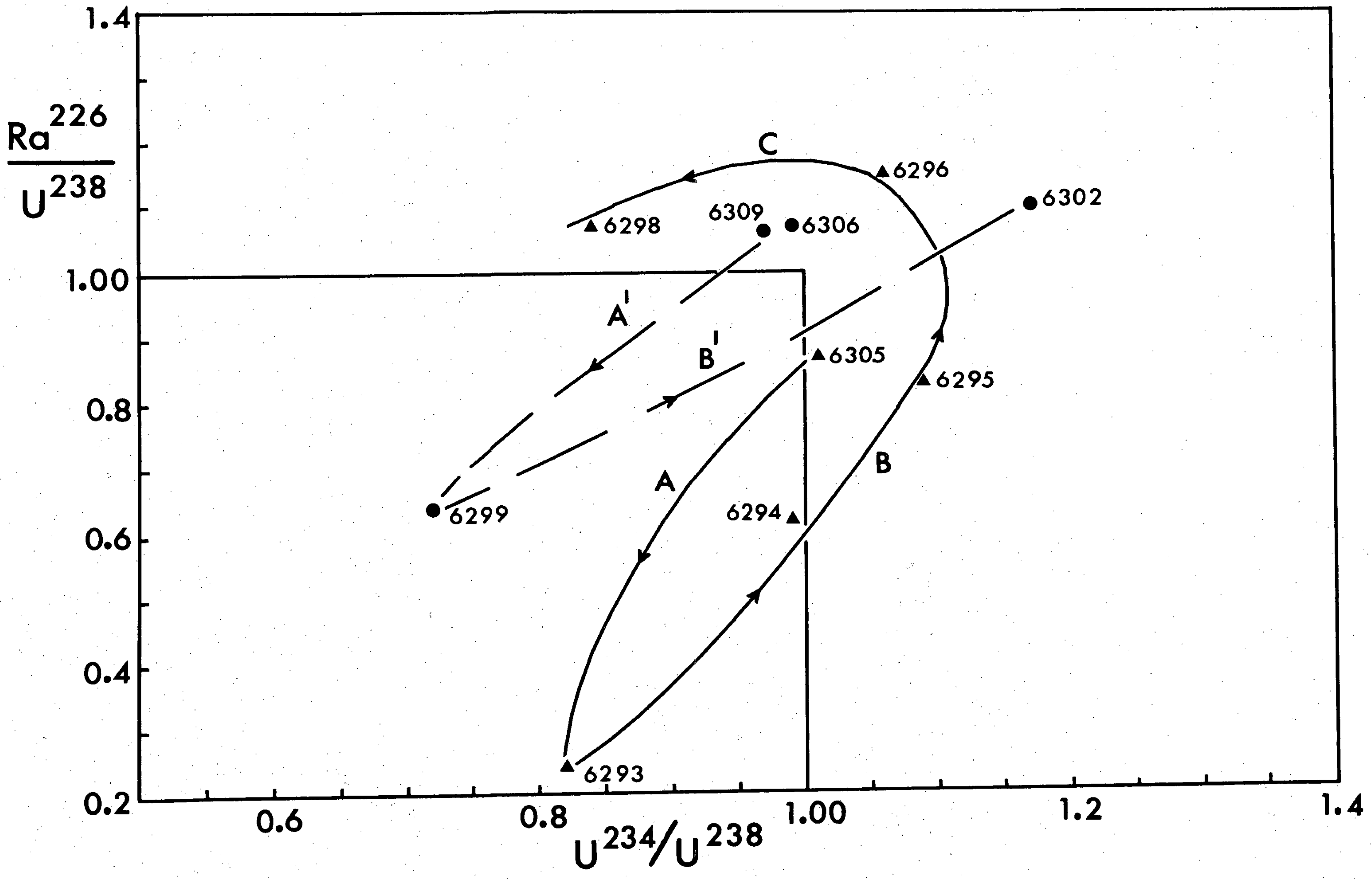

Fig. 53 Ra^{226}/U^{238} and U^{234}/U^{238} variations during weathering.

tend to be >1.0 (Koide and Goldberg, 1965). Stage (C) may be a local aberration because the weathered dolerite dyke is surrounded by weathered granite, a large source of many elements. Alternatively or in addition, a return to pronounced leaching of U occurs and the weathered dolerite and weathered granite converge towards a similar U isotopic composition. Fig. 54 illustrates variation of U^{234}/U^{238} with changing U content of the weathered dolerite boulder sequence. The large enrichment in U^{238} is accompanied initially with a deficiency in U^{234}. If this U came from the surrounding, already weathered granite, the U^{234}/U^{238} ratio should be less than unity (Osmond et al., 1968).

The proposed second stage has involved return to higher U^{234}/U^{238} ratios of just greater than or equal to unity, and a maximum U content. Two alternatives are possible; i.e. considerable time interval with growth of U^{234} and daughters or a contribution from groundwater ($U^{234}/U^{238} > 1$) yielding a total U content with the observed U^{234}/U^{238} ratio. The effective mechanism may lie between these alternatives.

Further leaching (stage C) lowers the U^{234}/U^{238} ratio and U content to values similar to those of the encompassing granite. A combination of time, allowing partial regeneration of daughter isotopes, leaching and

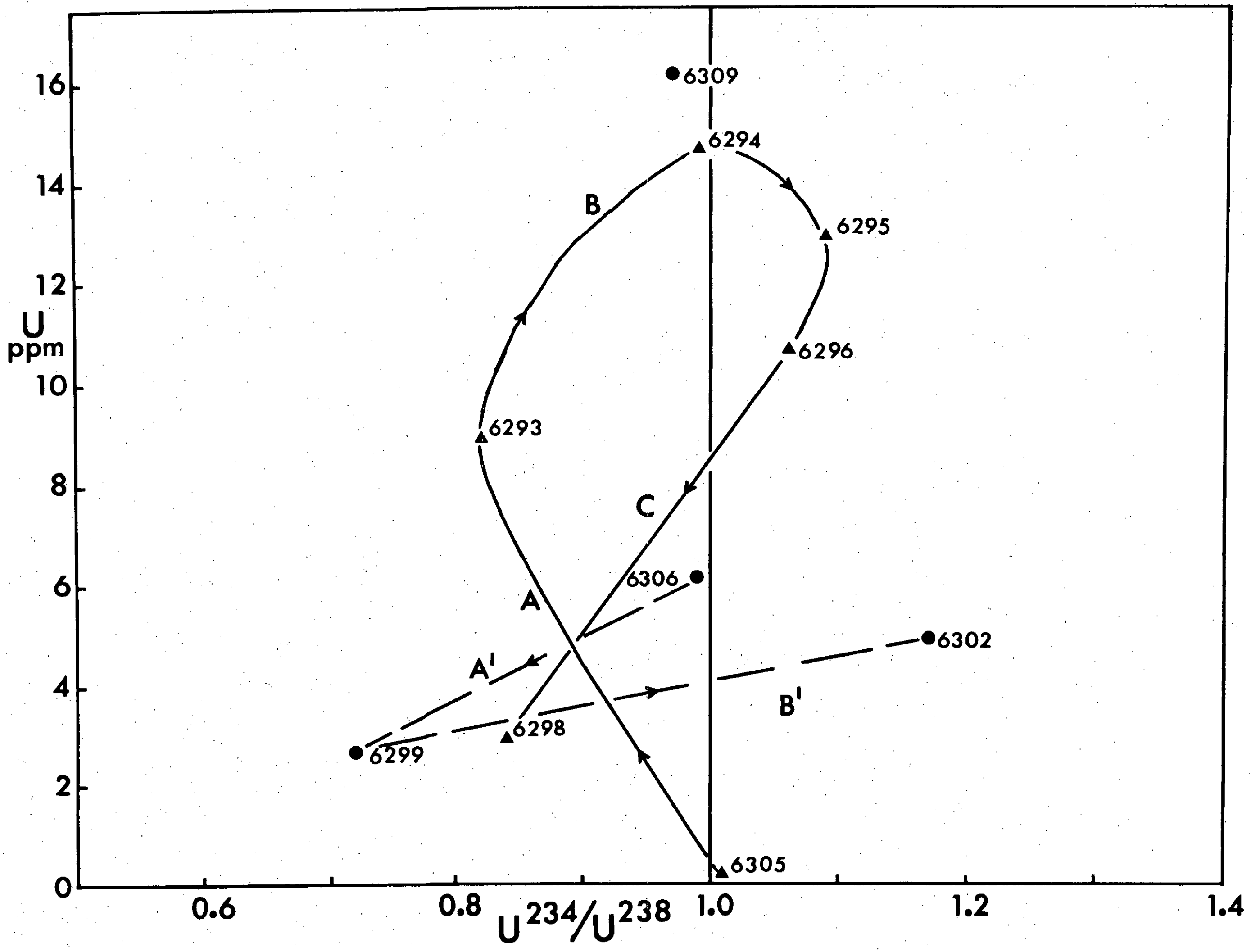

Fig. 54 U^{234}/U^{238} behaviour with varying U content.

groundwater exchange increase the Ra^{226}/U^{238} ratio to greater than unity.

Processes A, B and C may occur simultaneously at different stages of weathering of the one rock mass, however they may also occur at widely separated times.

The behaviour of U and Th is strongly influenced by the ferric iron content of the weathered boulder. Oxidation of iron (Chapter 8) is practically complete in sample 6295 and iron has been leached from samples 6296 and 6298. Ferric hydroxide acts as a scavenger adsorbing ions (i.e. U, Th and Pb). The maximum concentrations of Th and U are consequently related to maximum ferric iron content. A high Th^{228}/Th^{232} ratio for sample 6293 (Table 29) indicates disequilibrium in the Th^{232} series despite large uncertainty in concentration determinations. Local migration of Ra^{228} from the granite via the groundwater to the dolerite is conceivable. The presence of sulphate ions in the weathered dolerite would then cause precipitation of Ra^{228} as an insoluble sulphate. (Many basic rocks carry sulphides, particularly pyrite and pyrrhotite, which indirectly yield sulphate upon weathering.)

At first, addition of Ra^{228} occurred but as weathering and oxidation of ferrous iron progressed, enrichment of Th^{232} became pronounced. The addition of

Th, adsorbed by large surface areas and charge distributions of ferric iron, continued to depress the Th^{228}/Th^{232} ratio (sample 6295). The outer bleached rim (sample 6296) has a lower Th content and a Th^{228}/Th^{232} ratio greater than unity. Sample 6298 is also from the pallid zone of the weathered dolerite dyke however it has considerably more Th (Table 29) and a Th^{228}/Th^{232} ratio less than unity. Active leaching of Ra^{228} probably explains the lower gamma-ray spectrometric value, a conclusion which agrees with a lowered U content and U^{234}/U^{238} ratio of 0.84.

The effects of a multi-stage process during weathering cannot be resolved without complete determination of all significant daughter isotopes and without proper age control.

Weathered granite does not display a regular pattern analogous to the weathered dolerite boulder. A similar pattern is improbable since U and Th in granites are located in different minerals, and possibly a higher percentage of U may occur in mobile sites (i.e. cracks, fractures). Radioactive equilibrium for fresh granite (sample 6306) is indicated by a U^{234}/U^{238} ratio indistinguishable from unity and both Ra^{226}/U^{238} and Th^{228}/Th^{232} ratios approximately unity. Sample 6299 is much higher (150 feet) in the weathered granite than sample 6302 which was sampled in the base of the quarry adjacent to a small drainage channel. The U^{234}/U^{238} value for 6302 is therefore probably close to the U^{234}/U^{238} value of local groundwater. Sample 6309 was collected from a large "rotten" tor in an adjacent quarry. Uranium and thorium contents are different, possibly a consequence of local heterogeneity. In Fig. 53 a weathering sequence from fresh granite (6306) to 6299 and then 6302 has been shown since 6299 will have been continually leached and sample 6302 constantly saturated at the base of the profile.

Weathering in the granite is similar to that in the dolerite, at first decreasing U^{234} and Ra^{226} content with respect to U^{238} (stage A). Subsequent equilibration with groundwater and restoration of the Ra^{226}/U^{238} ratio to approximately unity are identical to stage (B). The third stage is not shown by the granite. Strong leaching of U with slight Th depletion is accompanied by decrease in the U^{234}/U^{238} and Th^{228}/Th^{232} ratios. Equilibration with groundwater ratios may be associated with an increase in Th, although this may reflect an initial nonuniform Th distribution within the granite.

11.5 SUMMARY

In summary, a trend towards lower U^{234}/U^{238}, and Ra^{226}/U^{238} ratios appears to be the predominant result of weathering processes, with preferential leaching of the more mobile U^{234} and Ra^{226}. Subsequent reprecipitation of these isotopes may be affected locally, by chemical changes, controlled by clays and sesquioxides. Other controlling factors include variable rock types, and possibly climate. Consequently the behaviour of U and Th during weathering is difficult to assess without thorough evaluation of local variables.

CHAPTER 12

SUMMARY - CONCLUSIONS

12.1 INTRODUCTION

The geochemistry of weathering has received considerable attention from geologists and pedologists although there has been little collaboration between the two. This study is necessarily biased towards the geological approach as a consequence of the author's background. A discussion of previous weathering studies is given in Appendix H.

Harriss and Adams (1966) summarised the literature on chemical alteration due to weathering and reached the following conclusions: the mobilisation and redistribution of cations is a complex and variable process; the lattice site in which an element occurs primarily controls its relative mobility; the relative importance of environmental factors is difficult to determine and probably locally variable; and practically all data available are for humid-temperate regions.

A fundamental problem in studies of chemical weathering is to establish a basis for comparing the fresh rock composition with its decomposition products. Ruxton (1968) has summarised different methods of displaying weathering effects. Frequently alumina (Al_2O_3) has been assumed to remain constant throughout the weathering profile and has accordingly been used to evaluate element gains or losses (Goldich 1938, and Brewer 1964). However, Al_2O_3 does migrate both as a colloid and in true solution (Sherman 1957 and Pickering, 1962). Veins of aluminium hydrates (gibbsite) occur in some weathering profiles and represent secondarily mobilised alumina (Goldich, pers. comm.). Zircon has been used as an alternative to alumina but there are large uncertainties regarding the initial parent rock content (Haseman and Marshall, 1945 and Brewer, 1964). The variability of zirconium content, has been outlined in Chapters 6 and 9. Volume change is notoriously difficult to quantify (e.g. minor volume alterations indicated by quartz veins which have retained their spatial relationships throughout the weathering profile (Chapter 8)). Because each of these approaches is unsatisfactory, an alternative method was adopted.

Elemental ratios have been used extensively in igneous, metamorphic and sedimentary goechemistry (see review by Taylor 1966). Knowledge of the behaviour of elemental ratios within the exogenic cycle would be useful, as an aid to understanding differences between sedimentary rocks and their source materials. Reiche (1950) has suggested the use of oxide component ratios in both the fresh rock and weathered variant. Ratios have been used extensively throughout this thesis since it is believed they minimise most of the comparison problems inherent in earlier approaches. Use of appropriate ratios has the following advantages:

1. Elements from similar lattice sites are compared,
2. Volume changes do not affect ratios of similar elements;
3. Studies of ratios of a trace element (e.g. Rb) to a major element (e.g. K) in the same lattice site provide a quantitative measure of the relative separation of cations as weathering proceeds,
4. Element ratios frequently change by factors which are large.

12.2 MAJOR ELEMENT RATIOS

A summary of weathering trends for all rock types is shown in Table 30.

Oxidation of iron during all stages of weathering is pronounced and independent of rock type (Table 30). Granitic rocks with low iron contents are oxidised rapidly and complete oxidation normally occurs before advanced chemical weathering. Basic rocks with higher iron contents are also initially oxidised although, complete oxidation only occurs with total alteration of the rock. If

Table 30

Summary of ratio trends during weathering

Rock Type	Weathering	Fe^{++}/Fe^{+++}	K/Na	Na/Ca	Ca/Mg	Fe/Mg
A. SNOWY MOUNTAINS REGION						
Diorite	(Initial	<<	>	=	=	=
	(Advanced	*	>>	<	<	=
Granite	(Initial	*	>	>>	<	n.d.
	(Advanced	*	+	<	*	n.d.
Adamellite	(Initial	n.d.	=	=	=	>>
	(Relatively- (advanced	n.d.	>	=	=	>>
B. WESTERN AUSTRALIA						
Adamellite	Initial	<	>	>	n.d.	>
Granite	Advanced	*	+	>	n.d.	*
Dolerite	Advanced	*	+	>	n.d.	+
Granite	(Initial	*	>	>	n.d.	>
	(Advanced	*	n.d.	n.d.	n.d.	>
Quartz-Porphyry	(Initial	*	>	>	n.d.	+
	(Advanced	*	<	n.d.	n.d.	n.d.

=	No change
>	Slight increase
>>	Considerable increase
+	Large increase
<	Slight decrease
<<	Considerable decrease
*	Large decrease
n.d.	Not determined

oxidising conditions are maintained during weathering the Fe^{++}/Fe^{+++} ratio is a sensitive parameter of initial rock decay.

Increases in K/Na ratios are consistent with predictions based on the respective hydration energies (Lebedev, 1957). Potassium is retained relative to Na within the weathered rock by two mechanisms; the preferential retention of potash relative to soda feldspar and by incorporation of K into new low temperature mineral phases or adsorption on to charged surfaces of clays and colloids. Sodium will be rapidly hydrated after liberation from a mineral lattice and remain dissolved in the groundwater.

Many clay residuals from deep laterite profiles do not show the normal pattern of K/Na increase and display lower K/Na ratios than those of the parent rock (Chapter 8). Groundwaters permeating through the pallid horizons are frequently hard and very mineralised (Woolnough, 1918). Higher Na_2O contents and identification of halite in XRD patterns indicates secondary deposition of this mineral during the dry summer months. (West Australian laterite profiles were sampled at the end of summer). Variable halite contents mask the actual Na_2O content of residual phases and restrict the usefulness of K/Na and Na/Ca ratios.

Na/Ca ratios normally increase with weathering (Table 30) although the relative stability of minerals may exert temporary control of changes. Decreasing ratios were found in weathered diorite and leucogranite from the Snowy Mountains region. In the former, retention of hornblende after destruction of plagioclase results in lower Na/Ca ratios whereas a lower hornblende content in soil formed from the diorite is accompanied by a higher Na/Ca ratio. Probable contamination from the biotite granite boulder and/or secondary addition of carbonate leached from the overlying slopewash (Appendix A) may explain the reversal noted for granitic soil.

Relative retention of iron with loss of Mg by leaching increases Fe/Mg ratios for all but pallid clay residuals which have been markedly depleted in iron. Ca/Mg ratios decrease which may reflect a combination of mineralogical control and marginal adsorption advantage of Mg over Ca (Bear, 1960).

A preferential order of retention; K>Na>Ca<Mg<Fe is indicated by the ratios investigated. This sequence reflects the relative stability of minerals during weathering and relative cation adsorption tendencies.

An identical retention sequence can be derived from the data of Goldich, Brock, Short and Harriss and Adams (op. cit.) although temporary mineralogical control is shown by the early behaviour of Fe, Mg and Ca.

12.3 TRACE ELEMENT BEHAVIOUR

The trends for all ratios incorporating trace elements are listed in Table 31.

K/Rb ratios always decrease during weathering although later processes of ion exchange and groundwater transport may produce ratios higher than those of the parent rock (Glen View Quarry dolerite, residual clays - Table F-14). The early attack of plagioclase by weathering solutions may not significantly affect the K/Rb ratio as both elements occur dominantly in potash feldspar and biotite. An initial enrichment of these minerals as a consequence of alteration of less stable components (i.e. plagioclase) affects both elements equally. Horstman (1957) however, has shown that leaching of K exceeds that of Rb.

K/Ba ratios do not change significantly except for the southernmost Koolanooka quartz porphyry. Considerable variability of Ba reduces the significance of the indicated trend at this locality. K/Ba ratios of basic rocks appear to increase whereas those of granitic rocks decrease during weathering (Table 31).

The lower hydration energy of K compared with Ba favours retention by adsorption onto clays and alteration products.

Ba/Rb ratios decrease or remain constant with some exceptions due to anomalous Ba contents in the Koolanooka

Table 31

Trace element ratio trends

Alteration	K/ Rb	K/ Ba	Ba/ Rb	Ba/ Sr	Rb/ Sr	K/ Pb	Pb/ Sr	Th/ K	U/ K	Th/ U
Khancoban Granite	=	=	=	>	>	=	>	>	<	>>
Windy Creek Diorite	*	>	<<	>>	+	>	=	>	<	>
Scamels Granite	<<	=	<	>>	>	>	>>	>	=	>
Mertondale Ser.	=	>	=	+	+	>>	<	=	=	=
Kaol.	*	<	=	*	*	=	<<	+	+	>>
G.V.Q. Granite Initial	<	=	=	>	>	<	>	>	<	>
Clay Res.	<	=	<	+	+	<<	+	+	<	>>
Dolerite Boulder	*	>	*	+	+	*	+	+	+	*
Clay Res.	>	<	>>	+	+	n.d.	n.d.	+	>	>>
Koolanooka Porphyry										
Central N	=	=	=	=	>	=	=	=	=	>
Eastern	<	=	=	>	>	=	=	>	=	>
South-Initial	<	*	+	>>	=	<	=	>	<	>>
Clay Res.	*	*	+	*	*	n.d.	n.d.	+	+	<
Silcrete	*	*	+	+	*	>>	<<	+	+	*

= No change
\> Slight increase
\>> Considerable increase
\+ Large increase
< Slight decrease
<< Considerable decrease
* Large decrease
n.d. Not determined

quartz porphyry (see above) and clay residuals formed from dolerite in the Glen View Quarry (see Chapter 9). A reduction of the Ba/Rb ratio is predicted by hydration energy differences.

Ba/Sr ratios, except in clay residuals from Mertondale and Koolanooka, increase uniformly. Secondary addition of carbonate bearing Sr reverses a well established trend towards higher ratios. Barium occurs in potassium sites and together with K will be residually enriched as plagioclase (with Sr) weathers preferentially. After liberation from crystal-lattice sites Ba will be selectively adsorbed relative to Sr, thus further increasing the Ba/Sr ratio.

Rb/Sr ratios increase as do Ba/Sr ratios. The same exceptions noted for the latter decrease Rb/Sr ratios for similar reasons. This ratio is considerably more affected by weathering processes in all rock types than any other. Rb-Sr geochronology is therefore susceptible to errors induced by weathering (see Chapter 10).

The behaviour of K/Pb and Pb/Sr ratios is variable and may be subject to factors other than weathering. A combination of secondary processes affecting Pb and Sr at different localities tends to obscure changes of either ratio due to weathering.

Th/K ratios uniformly increase wherever there has been significant weathering. This probably reflects residual enrichment of Th relative to K in resistant accessory minerals (zircon, monazite etc.).

U/K ratios tend to decrease suggesting leaching of U from non-lattice sites (fractures, cracks etc.). Where the U/K ratio increases secondary processes related to groundwater transport or residual enrichment of U-bearing accessory minerals may have increased U contents.

Th/U ratios generally increase except for those of the Koolanooka residual clays and silcretes and the Glen View Quarry residual boulder. The latter has been extensively discussed in Chapter 11 where U and Th migration from the surrounding granite via groundwater was shown to be adsorbed by iron hydroxide surfaces within the weathered dolerite boulder. Without disequilibrium control for clay residuals from the Koolanooka quartz porphyry, definite explanations for this decrease cannot be proposed. Table F-15 suggests that Th has been leached relative to U, but as all measurements were made by gamma-ray spectrometry, this problem cannot be resolved without analyses by an independent method.

12.4 SUMMARY OF RATIO BEHAVIOUR

Rb/Sr, Th/U and Fe^{++}/Fe^{+++} ratios are generally the most affected by weathering processes. K/Rb and Ba/Sr ratios are slightly less responsive to alteration processes.

Previous investigations rarely combined trace and major element chemistries. Trace element determinations were measured by optical spectrography and without assessment of parent rock heterogeneity. Evaluation of published studies is therefore unreliable and difficult, reflecting poor precision for optical spectrography and unknown initial rock variability.

12.5 MINERALOGICAL CONTROL

Chemical changes which result from weathering of three different rock types in the Snowy Mountains are minimal. Parent rock mineralogical heterogeneity is the dominant chemical variable until the majority of minerals are destroyed or altered. Complete destruction of the parent rock is restricted to thin soils. Weathering products are dominated by illite, chlorite-vermiculite, montmorillonoids and hydrated iron oxides which, together with residual phases, make up the soils of this region. This suggests a relatively low chemical weathering intensity with significant physical breakdown.

Most sediments are deposited in geosynclines adjacent to uplifted sediment sources. Such sediments frequently consist of greywackes and rock types with a high percentage of unstable components (i.e. incompletely weathered minerals such as feldspar). Relative weathering intensities must be low at their source and may resemble highland weathering within the Snowy Mountains area. Griffin et al., (1968) studied the distribution of chlorite, montmorillonite, kaolinite and illite in the less than 2 micron size fraction of sediments from all world oceans. They found a zone of high chlorite content off S.E. Australia which can be related to the formation and retention of chlorite in soils from the Southern highlands of N.S.W.

~~This would indicate that~~ a majority of sediments contain significant amounts of detrital phases which are variably altered parent rock minerals. The alteration of these phases will be generally slight because of mild chemical weathering in the source region. Weathering, therefore, does not significantly separate elements under these conditions.

Present day weathering in Western Australia as shown by iron-stained surfaces resembles that of the Snowy Mountains region although secondary iron oxides are relatively more abundant. Deep lateritic weathering of pre(?) to middle Tertiary (?) has drastically affected the chemistry of residual phases when these are compared with the parent rock. Complete removal of unstable minerals and the formation of kaolinite was associated with high weathering intensities under warm-moist climates. Erosion was limited and deep leaching occurred at or near base level (Woolnough, 1927). Under these conditions sedimentation in adjacent ocean basins must have been limited and probably confined largely to kaolinite.

The Indian Ocean adjacent to Western Australia was shown to have high kaolinite contents and to be relatively deficient in chlorite (Griffin et al., op. cit.). They stated:

> The rather high kaolinite concentrations in the East and West Indian Ocean indicate a source area with an intense chemical weathering environment not favourable for the preservation of the less resistant and more easily altered chlorite.

12.6 FRESH ROCK VARIATION

Fresh rock variation was extensively investigated in the Snowy Mountains region for the three rock types. Significant changes in major element chemistry are directly related either to changing mineralogy (Chapter 3) or to the extent of late-stage hydrothermal alteration (Chapter 4). The latter is highly significant and must be distinguished from weathering processes. The degree of fresh rock variation is surprisingly large (Chapters 3-6) and this fact should engender caution when interpreting elemental changes. Trace elements are more sensitive to late-stage hydrothermal and weathering alteration than major elements (Chapter 6). The behaviour of Sr, Ba and Pb (Chapter 6) may be used to indicate the type of alteration providing the distribution of these elements has been accurately assessed for a particular rock mass being investigated.

12.7 WEATHERING EFFECTS IN THE Rb-Sr-Sr ISOTOPE SYSTEM

Mild iron staining and present day weathering will result in minimum ages due to increased Rb/Sr ratios and should be avoided during sampling for geochronological studies. No evidence for selective movement of Sr^{87} was found. The magnitude of apparent age loss is roughly proportional to the degree of weathering and it is evident that even initial weathering is capable of reducing the total-rock age.

In contrast, deep lateritic weathering at the localities studied has not altered ages significantly from that shown by the parent rock. Residual minerals including muscovite, sericite and quartz were found at these localities but it is not known if this is common to all such profiles. These minerals effectively control the age of the clay residual.

Pedogenic processes such as silicification, secondary surficial alteration and possible reconversion of kaolinite to montmorillonite can alter the age of residual weathering products. Further examination of these processes is warranted although it will have restricted application to thin, intensely weathered clay sediments.

The presence of significant detrital phases in weathering profiles has important implications for geochronological studies. The amount of sediments derived from areas of intense chemical weathering is probably small but may be stratigraphically important (i.e. flat-lying platform sediments). Detrital quartz and muscovite will preserve the related fresh rock age until metamorphic rehomogenisation occurs, and they may be useful in provenance studies. The use of quartz as a dateable mineral phase may have many implications for sedimentary geochemistry. In areas of lower chemical weathering intensity, (i.e. Snowy Mountains) a large proportion of the detritus may be residual or slightly altered phases from many rock masses. Analysis of such intimately mixed detritus will be complex and may await further studies on simpler systems of intense weathering. The Rb-Sr method cannot date the commencement of weathering but may prove useful in examination of detrital phases. Shales will therefore have a range of ages representing different source regions.

12.8 U-Th ISOTOPIC STUDIES

Without Th^{230} analyses, a time control for weathering cannot be evaluated by studies involving U-Th series isotopes. However, disequilibrium (i.e. U^{234}/U^{238} ratios departing from unity) indicates that open system conditions have existed during the last one million years. Uranium is very mobile and has been leached to considerable depths. Pedogenic processes of adsorption onto clays and colloids, complexing with sesquioxides or concentration in resistant minerals can alter U^{234}/U^{238} ratios by groundwater migration and thus overprint geological weathering processes (Chapter 11).

The existence of significant disequilibrium in W.A. restricts use of gamma-ray spectrometry to fresh rocks from this area.

U^{234}/U^{238} ratios equal unity in the Snowy Mountains and reflect the mild chemical weathering intensity relative to that of W.A.

Further studies of U-Th isotopic behaviour under different climatic conditions and with local control are necessary, before an evaluation of the relative influence of climate and other interrelated factors is possible.

12.9 CONCLUSIONS

Rocks from the Snowy Mountains with compositions typical of the upper crust were examined. Mild weathering of these rocks in upland regions results in little chemical change. One of the principal conclusions of this thesis is the surprisingly low degree of chemical alteration within the upper sections of weathered rock from the Snowy Mountains. Detritus from this area may form typical geosynclinal sediments with a high proportion of slightly weathered mineral phases. Under these conditions, the separation of elements during weathering is restricted to the alkali and alkaline earth metals and its importance in producing highly fractionated material is minimal.

In areas of high chemical weathering intensity, erosive forces are normally restricted and a limited supply of detritus will reach off-shore areas. Sediments formed from detritus of this type will be of limited importance and will not quantitatively affect considerations of overall crustal evolution.

Chemical separation of elements within the exogenic cycle probably occurs during transportation and deposition, and not as a consequence of weathering.

The relative stability sequence proposed by Goldich (1938) is generally observed. Exceptions may occur during the initial stages of weathering. However, with increased alteration mineral retention reverts to that proposed by Goldich.

REFERENCES CITED

ADAMS, J.A.S., WEAVER, C.E. (1958) Thorium to uranium ratios as indicators of sedimentary processes: example of concept of geochemical facies. Bull. Amer. Ass. Pet. Geol., 42, p. 387-430.

ALDRICH, L.T., WETHERILL, G.W., TILTON, G.R. and DAVIS, G.L. (1956) Half life of ^{87}Rb. Phys. Rev., 103, p. 1045-1047.

ANDERSON, D.H. and HAWKES, H.E. (1958) Relative mobility of the common elements in weathering of some schist and granite areas. Geochim. et Cosmochim. Acta, 14, p. 204-210.

ARRIENS, P.A. (1963) The petrology and geochronology of the Koolanooka Hills, Western Australia. Unpub. Ph.D. Thesis, University of Cambridge.

ARRIENS, P.A., BROOKS, C., BOFINGER, V.M. and COMPSTON, W. (1966) The discordance of mineral ages in granitic rocks resulting from the redistribution of rubidium and strontium. J. Geophys. Res., 71, p. 4981-4994.

ARRIENS, P.A. and COMPSTON, W. (1968) A method for isotopic ratio measurement by voltage peak switching, and its application with digital output. J. Mass Spectrometry and Ion Physics, 1, p. 471-481.

BARTH, T.F.W. (1961) Abundance of the elements, areal averages and geochemical cycles. Geochim. Cosmochim. Acta, 23, p. 1-8.

BEAR, F.E. (1960) Chemistry of the soil. Reinhold Pub. Corp. New York, Monograph Series No. 126.

BLACK, L.P. (1969) Isotopic relationships in the Chillagoe-Herberton Area, North Queensland. Unpub. Ph.D. Thesis, A.N.U. Canberra, Australia.

BOTTINO, M.L. and FULLAGAR, P.D. (1968) Effects of weathering on whole-rock Rb-Sr ages of granitic rock. Amer. J. Sci., 266, p. 661-670.

BREWER, R. (1964) Fabric and mineral analysis of soils. John Wiley and Sons, New York.

BROCK, R.W. (1943) Weathering of igneous rocks near Hong Kong. *Geol. Soc. Amer. Bull.*, *54*, p. 717-738.

BROOKS, C. (1968) Relationship between feldspar alteration and the precise post-crystallization movement of rubidium and strontium isotopes in a granite. *J. Geophys. Res.*, *73*, p. 4751-4757.

BUTLER, J.R. (1953) The geochemistry and mineralogy of rock weathering: 1. The Lizard area, Cornwall. *Geochim. et Cosmochim. Acta*, *4*, p. 157-178.

BUTLER, J.R. (1954) The geochemistry and mineralogy of rock weathering: 2. The Nord marka area, Oslo. *Geochim. et Cosmochim. Acta*, *6*, p. 268-281.

BUTLER, J.R., BOWDEN, P. and SMITH, A.Z. (1962) K/Rb ratios in the evolution of the Younger Granites of Northern Nigeria. *Geochim. et Cosmochim. Acta*, *26*, p. 89-100.

CARROLL, D. and JONES, N.K. (1947) Laterite developed on acid rocks in Southwestern Australia. *Soil Sci.*, *64*, p. 1-15.

CHAPPELL, B.W., COMPSTON, W., ARRIENS, P.A. and VERNON, M.J. (1969) Rubidium and strontium determinations by X-ray fluorescence spectrometry and isotope dilution below the part per million level. *Geochim. et Cosmochim. Acta*, *33*, p. 1002-1006.

CHERDYNTSEV, V.V., MALYSHEV, Z.A., SOKOLOVA, I.N., KAZACHEVSKII and BORISOV, I.V. (1964) Isotopic composition of uranium and thorium in the supergene zone. *Geochem. Internat.*, No. 3, p. 398-401.

CLARK, S.P., PETERMAN, Z.E. and HEIER, K.S. (1966) Abundances of uranium, thorium and potassium. *Geol. Soc. Amer. Mem.* *97*, Handbook of Physical Constants, ed. S.P. Clark.

COMPSTON, W. and ARRIENS, P.A. (1968) The Precambrian geochronology of Australia. *Can. J. Earth Sci.*, *5*, p. 561-583.

COMPSTON, W. and CHAPPELL, B.W. (1970) Rb-Sr geochronology by combined mass- and X-ray spectrometry. (In preparation)

COMPSTON, W., LOVERING, J.F. and VERNON, M.J. (1965) The rubidium-strontium age of the Bishopville aubrite and its component enstatite and feldspar. Geochim. et Cosmochim. Acta, 29, p. 1085-1099.

COOPER, J.A. (1963) The flame photometric determination of potassium in geological materials used for potassium-argon dating. Geochim. et Cosmochim. Acta, 27, p. 525-546.

DASCH, E.J. (1968) Strontium isotopes in weathering profiles, deep-sea sediments, and sedimentary rocks. Unpub. Ph.D. Dissertation, Yale University.

DASCH, E.J. (1969) Strontium isotopes in weathering profiles, deep sea sediments and sedimentary rocks. Geochim. et Cosmochim. Acta, 33, p. 1521-1552.

DENNEN, W.H. and ANDERSON, P.J. (1962) Chemical changes in incipient rock weathering. Geol. Soc. Amer. Bull., 73, p. 375-384.

DOOLEY, J.R., GRANGER, H.C. and ROSHOLT, J.N. (1966) Uranium-234 fractionation in the sandstone-type uranium deposits of the Ambrosia Lake district, New Mexico. Econ. Geol., 61, p. 1362-1382.

EVERNDEN, J.F. and RICHARDS, J.R. (1962) Potassium-argon ages in eastern Australia. J. geol. Soc. Aust., 9, p. 1-49.

FIELDS, M. and SWINDALE, L.D. (1954) Chemical weathering of silicates in soil formation. N.Z. J. Sci. Technol. (B) 36, p. 140-154.

FLEISCHER, M. (1965) Summary of new data on rock samples G-1 and W-1, 1962-1965. Geochim. et Cosmochim. Acta, 29, p. 1263-1283.

GOLDICH, S.S. (1938) A study in rock weathering. J. Geol., 46, p. 17-58.

GOLDICH, S.S. and GAST, P.W. (1966) Effects of weathering on the Rb-Sr and K-Ar ages of biotite from the Norton Gneiss, Minnesota. Earth Plan. Sci. Letters, 1, p. 372-375.

GORDON, M. and MURATA, K.J. (1952) Minor elements in Arkansas bauxite.
Econ. Geol., 47, p. 169-179.

GRIFFIN, J.J., WINDOM, H., GOLDBERG, E.D. (1968) The distribution of clay minerals in the World Ocean.
Deep Sea Res., 15, p. 433-459.

GRIM, R.E. (1953) Clay mineralogy.
McGraw-Hill, New York, N.Y. 384 p.

GULSON, B.L. (1968) The evolution of dioritic rocks - with special reference to the high potassium diorites of the Yeoval igneous complex, N.S.W.
Unpub. Ph.D. Thesis, A.N.U. Canberra, Australia.

GUY, B.B. (1969) Granitic development and emplacement in the Tumbarumba-Geehi district, N.S.W.
(ii) The massive granites.
J. Proc. R. Soc. N.S.W., 102, p. 149-156.

HARRISS, R.C. and ADAMS, J.A.S. (1966) Geochemical and mineralogical studies on the weathering of granitic rocks.
Amer. J. Sci, 264, p. 146-173.

HART, S.R. (1969) K, Rb, Cs contents and K/Rb, K/Cs ratios of fresh and altered submarine basalts.
Earth Planet. Sci. Letters, 6, p. 295-303.

HASEMAN, J.F. and MARSHALL, C.E. (1945) The use of heavy minerals in studies of the origin and development of soils.
Missouri Agr. Exp. Sta. Res. Bull., 387.

HEIER, K.S. and ROGERS, J.J.W. (1963) Radiometric determination of thorium, uranium and potassium in basalts and in two magmatic differentiation series.
Geochim. et Cosmochim. Acta, 27, p. 137-154.

HORSTMAN, E.L. (1957) The distribution of lithium, rubidium and caesium in igneous and sedimentary rocks.
Geochim. et Cosmochim. Acta, 12, p. 1-28.

JAKEŠ, P. (1970) Analytical and experimental geochemistry of volcanic rocks from Island Arcs.
Unpub. Ph.D. Thesis, A.N.U. Canberra, Australia.

JOPLIN, GERMAINE A. (1942) Petrological studies in the Ordovician of New South Wales. I. The Cooma complex. Proc. Linn. Soc. N.S.W., 67, p. 156-196.

JOPLIN, GERMAINE, A. (1958) Basic and ultrabasic rocks near Happy Jacks and Tumut Pond in the Snowy Mountains of New South Wales. J. Proc. R. Soc. N.S.W., 91, p. 120-141.

JOPLIN, GERMAINE, A. (1964) A petrography of Australian igneous rocks. Angus and Robertson, Sydney.

KELLER, W.D. (1955) The principles of chemical weathering. Columbia, Missouri, Lucas Brothers, 189 p.

KELLY, W.C. and ZUMBERGE, J.H. (1961) Weathering of quartz diorite at Marble Point, McMurdo Sound, Antarctica. J. Geol., 69, p. 433-446.

KISS, E. (1967) Chemical determination of some major constituents in rocks and minerals. Anal. Chim. Acta, 39, p. 223-234.

KOIDE, M. and GOLDBERG, E.D. (1965) Uranium-234/Uranium-238 ratios in seawater. In. Progress in Oceanography, 3, Pergamon Press, London, p. 173-177.

KOLBE, P. and TAYLOR, S.R. (1966) Geochemical investigation of the granitic rocks of the Snowy Mountains area, New South Wales. J. Geol. Soc. Aust., 13, p. 1-25.

KU, T. (1965) An evaluation of the U^{234}/U^{238} method as a tool for dating pelagic sediments. J. Geophys. Res., 70, p. 3457-3474.

LAMBERT, I.B. (1963) The geology of the Berridale district, New South Wales. B.Sc. Hons. Thesis, A.N.U. Canberra, Australia (unpubl.

LAMBERT, I.B. (1967) Investigations of high grade regional metamorphic and associated rocks. Unpub. Ph.D. Thesis, A.N.U. Canberra, Australia.

LAMBERT, I.B. and WHITE, A.J.R. (1965) The Berridale Wrench Fault, a major structure in the Snowy Mountains of New South Wales.
J. Geol. Soc. Aust., 12, p. 25-33.

LAUDELOUT, H., van BLADEL, R., GILBERT, M. and CREMERS, A. (1968) Physical chemistry of cation exchange clays.
Trans. 9th Congr. Int. Soil Sci. Soc., Adelaide, 1, p. 565-575.

LEBEDEV, V.I. (1957) Some factors in the migration of alkali and alkali earth elements in the supergene zone.
Geokhimiya, 1957, p. 508-517.

MONTGOMERY, A. (1916) The significance of some physiographical characteristics of Western Australia.
J. Roy. Soc. W.A., 2, p. 59-96.

MORGAN, J.W. and HEIER, K.S. (1966) Uranium, thorium and potassium in six U.S.G.S. standard rocks.
Earth Plan. Sci. Letters, 1, p. 158-160.

MOYE, D.G. and SHARP, K.R. (1961) Report on the geology of Murray 1 project and associated works.
Snowy Mountains Hydro-Electric Authority, Cooma, Australia.

MOYE, D.G., SHARP, K.R. and STAPLEDON, D.H. (1963) Geology of the Snowy Mountains Region.
Geological Report of the Snowy Mountains Hydro-Electric Authority, Cooma, Australia.

McINTYRE, G.A., BROOKS, C., COMPSTON, W. and TUREK, A. (1966) The statistical assessment of Rb-Sr isochrons.
J. Geophys. Res., 71, p. 5459-5468.

McLAUGHLIN, R.J.W. (1955) Geochemical changes due to weathering under varying climatic conditions.
Geochim. et Cosmochim. Acta, 8, p. 109-130.

McLAUGHLIN, R.J.W. (1959) The geochemistry of some kaolinitic clays.
Geochim. et Cosmochim. Acta, 17, p. 11-16.

NICOLAYSEN, L.O. (1961) Graphic interpretation of discordant age measurements on metamorphic rocks.
Ann. N.Y. Acad. Sci., 91, Pt. II, p. 198-206.

NORRISH, K. and CHAPPELL, B. (1967) X-ray fluorescence spectrography.
In. Physical Methods in determinative mineralogy. ed. J. Zussman, Academic Press, New York.

NORRISH, K. and HUTTON, J.T. (1964) Preparation of samples for analysis by X-ray fluorescent spectrography
I. Fusion in borate glass
II. Powder samples
C.S.I.R.O. Aust. Div. Soils, Div. Rep. No. 3/64

NORRISH, K. and HUTTON, J.T. (1969) An accurate X-ray spectrographic method for the analysis of a wide range of geological samples.
Geochim. et Cosmochim. Acta, 33, p. 431-453.

OSMOND, J.K., RYDELL, H.S. and KAUFMAN, M.I. (1968) Uranium disequilibrium in groundwater: an isotope dilution approach in hydrologic investigations.
Science, 162, 3857, p. 997-999.

PACKHAM, G.H. (1960) Sedimentary history of part of the Tasman Geosyncline in southeastern Australia.
Rep. 21, Int. geol. Congr., 12, p. 74-83.

PACKHAM, G.H. (1969) The geology of New South Wales.
J. Geol. Soc. Aust., 16, p. 1-654.

PICKERING, R.J. (1962) 1. Some leaching experiments on three quartz-free silicate rocks and their contribution to an understanding of laterization.
Econ. Geol., 57, p. 1185-1206.

PIDGEON, R.T. and COMPSTON, W. (1965) The age and origin of the Cooma granite and its associated metamorphic zones, New South Wales.
J. Petrology, 6, p. 193-222.

PLILER, R. and ADAMS, J.A.S. (1962) The distribution of thorium and uranium in a Pennsylvanian weathering profile.
Geochim. Cosmochim. Acta, 26, p. 1137-1146.

PRIDER, R.T. (1943) Granitic rocks from Canning Dam.
J. Roy. Soc. W.A., 24, p. 137-147.

PRIDER, R.T. (1946) The geology of the Darling Scarp at Ridge Hill.
J. Roy. Soc. W.A., 32, p. 105-129.

REICHE, P. (1950) A survey of weathering processes and products. Albuquerque, New Mexico, New Mexico Univ. Pubs. Geology. 95 p.

RICHARDSON, K.A. and ADAMS, J.A.S. (1963) Effect of weathering on radioactive elements in the Conway granite of New Hampshire. *Geol. Soc. Amer. Spec. Paper*, *76*, p. 137A.

RILEY, J.P. (1958) Simultaneous determination of water and carbon dioxide in rocks and minerals. *The Analyst*, *83*, 982, p. 42-49.

ROGERS, J.J.W., ADAMS, J.A.S. and GATLIN, B. (1965) Distribution of thorium, uranium, and potassium concentrations in three cores from the Conway Granite, New Hampshire, U.S.A. *Amer. J. Sci.*, *263*, p. 817-822.

ROSHOLT, J.N., DOE, B.R., TATSUMOTO, N. (1966) Evolution of the isotopic composition of uranium and thorium in soil profiles. *Bull. Geol. Soc. Am.*, *77*, p. 987-1004.

ROSHOLT, J.N., GARNER, E.L. and SHIELDS, W.R. (1964) Fractionation of uranium isotopes and daughter products in weathered granites and uranium-bearing sandstone, Wind River basin region, Wyoming. *U.S. Geol. Survey Prof. Paper* 501-B, p. B84-B87.

RUXTON, B.P. (1968) Measures of the degree of chemical weathering of rocks. *J. Geol.*, *76*, p. 518-527.

SAKANOUE, M., YONEDA, S., ONISHI, K., KOYAMA, K., KOMURA, K. and NAKANISHI, T. (1968) Alpha radioactive nuclides of uranium, protactinium and thorium in uranium deposits. *Geochem. J.*, *2*, p. 71-86.

SANTOS-YNIGO, L. and ESGUERRA, F.B. (1961) Geology and geochemistry of the nickeliferous laterites of Nonoc and adjacent islands, Surigao Province, Phillippines. *Philippines Bur. of Mines Spec. Projects Series*, Pub. No. 18, 90 p.

SCOTT, M.R. (1968) Thorium and uranium concentrations and isotope ratios in river sediments. Earth. Plan. Sci. Letters, 4, p. 245-252.

SHARP, K.R., BOUCAUT, W.R.P. and SVENSON, D. (1963) Report on the geology of Khancoban project and associated works. Snowy Mountains Hydro-Electric Authority, Cooma, Australia.

SHERMAN, G.D. (1957) Formation of gibbsite aggregates in latosols developed on volcanic ash. Science, 125, p. 1243-1244.

SHIELDS, W.R. and GARNER, E.L. (1963) Survey of Rb^{85}/Rb^{87} in minerals. J. Geophys. Res., 68, p. 2331-2334.

SHORT, N.M. (1961) Geochemical variations in four residual soils. J. Geol., 69, p. 534-571.

SNELLING, N.J. (1960) The geology and petrology of the Murrumbidgee Batholith. Q. Jl. geol. Soc. Lond., 116, p. 187-217.

TAYLOR, S.R. (1966) The application of trace element data to problems in petrology. Physics and Chemistry of the Earth, 6, Pergamon Press, Oxford.

TAYLOR, S.R. (1968) Geochemistry of andesites. Origin and Distribution of the Elements. Ed. L.H. Ahrens, Pergamon Press, Oxford, p. 559-583.

TAYLOR, S.R. and WHITE, A.J.R. (1966) Trace element abundances in andesites. Bull. Volcan., 29, p. 177-194.

TERRILL, S.E. (1954) Laterite and materials of similar appearance in south-western Australia. J. Roy. Soc. W.A., 40, p. 4-14.

THURBER, D.L. (1962) Anomalous U^{234}/U^{238} in nature. J. Geophys. Res., 67, p. 4518-4520.

TUREK, A. (1966) Rb-Sr isotopic studies in the Kalgoorlie-Norseman Area, Western Australia. Unpub. Ph.D. Thesis, A.N.U. Canberra, Australia.

VALLANCE, T.G. (1953) Studies in the metamorphic and plutonic geology of the Wantabadgery-Adelong-Tumbarumba district, N.S.W. Pt. III The granitic rocks.
Proc. Linn. Soc. N.S.W., *78*, p. 197-220.

VALLANCE, T.G. (1960) Notes on metamorphic and plutonic rocks from the Wantabadgery-Adelong-Tumbarumba district, N.S.W.
Proc. Linn. Soc. N.S.W., *85*, p. 94-104.

WAHLSTROM, E.E. (1948) Pre-Fountain and recent weathering in Flagstaff Mountain near Boulder, Colorado.
Geol. Soc. Amer. Bull., *59*, p. 1173-1190.

WELBY, C.W. (1958) Occurrence of alkali elements in some Gulf of Mexico sediments.
J. Sed. Petr., *28*, p. 431-452.

WHITFIELD, J.M., ROGERS, J.J.W., and ADAMS, J.A.S. (1959) The relationship between the petrology and the thorium and uranium contents of some granitic rocks.
Geochim. et Cosmochim. Acta, *17*, p. 248-271.

WILSON, A.F. (1957) Advances in the knowledge of the structure and petrology of the Pre-Cambrian rocks of South-western Australia.
J. Roy. Soc. W.A., *41*, p. 57-83.

WOLFENDEN, E.B. (1965) Geochemical behaviour of trace elements during bauxite formation in Sarawak, Malaysia.
Geochim. et Cosmochim. Acta, *29*, p. 1051-1062.

WOODHAMS, D.J. (1965) Report on the geology of Murray 2 project.
Snowy Mountains Hydro-Electric Authority, Cooma, Australia.

WOOLNOUGH, W.G. (1918) The physiographic significance of laterite in Western Australia.
Geol. Mag., p. 385-393.

WOOLNOUGH, W.G. (1927) The duricrust of Australia.
J. Proc. Roy. Soc. N.S.W., *61*, p. 17-53.

YAMASAKI, K., IIDA, C. and YOKOI, H. (1955) A spectrographic determination of the distribution of trace elements in a granodiorite and in its weathering products.
Nagoya Univ. Jour. Earth. Sci, *3*, p. 58-64.

APPENDIX A

Geological Logs for Diamond Drill Holes 2401, 2511 and 2660 from the Snowy Mountains, N.S.W.

<u>Sources</u>

1. DH 2401 (Windy Creek Diorite) and DH 2511 (Scamels Granite);
   Moye, D.G. and Sharp, K.R. (1961). Report on the Geology of Murray 1 project and Associated works. Snowy Mountains Hydro-Electric Authority, Cooma, Australia.
2. DH 2660 (Khancoban Granite);
   Woodhams, D.J. (1965). Report on the Geology of Murray 2 project. Snowy Mountains Hydro-Electric Authority, Cooma, Australia.

SNOWY MOUNTAINS HYDRO-ELECTRIC AUTHORITY

GEOLOGICAL LOG OF DRILL HOLE

PROJECT SNOWY – GEEHI FEATURE TUNNEL
HOLE No. 2401 CO-ORDINATES: E 289 M 4667·0 , N 141 M 1623·4 R.L. GROUND 3490·3
LOCATION GEEHI RESERVOIR ANGLE FROM HORIZONTAL 40° DIRECTION 096°

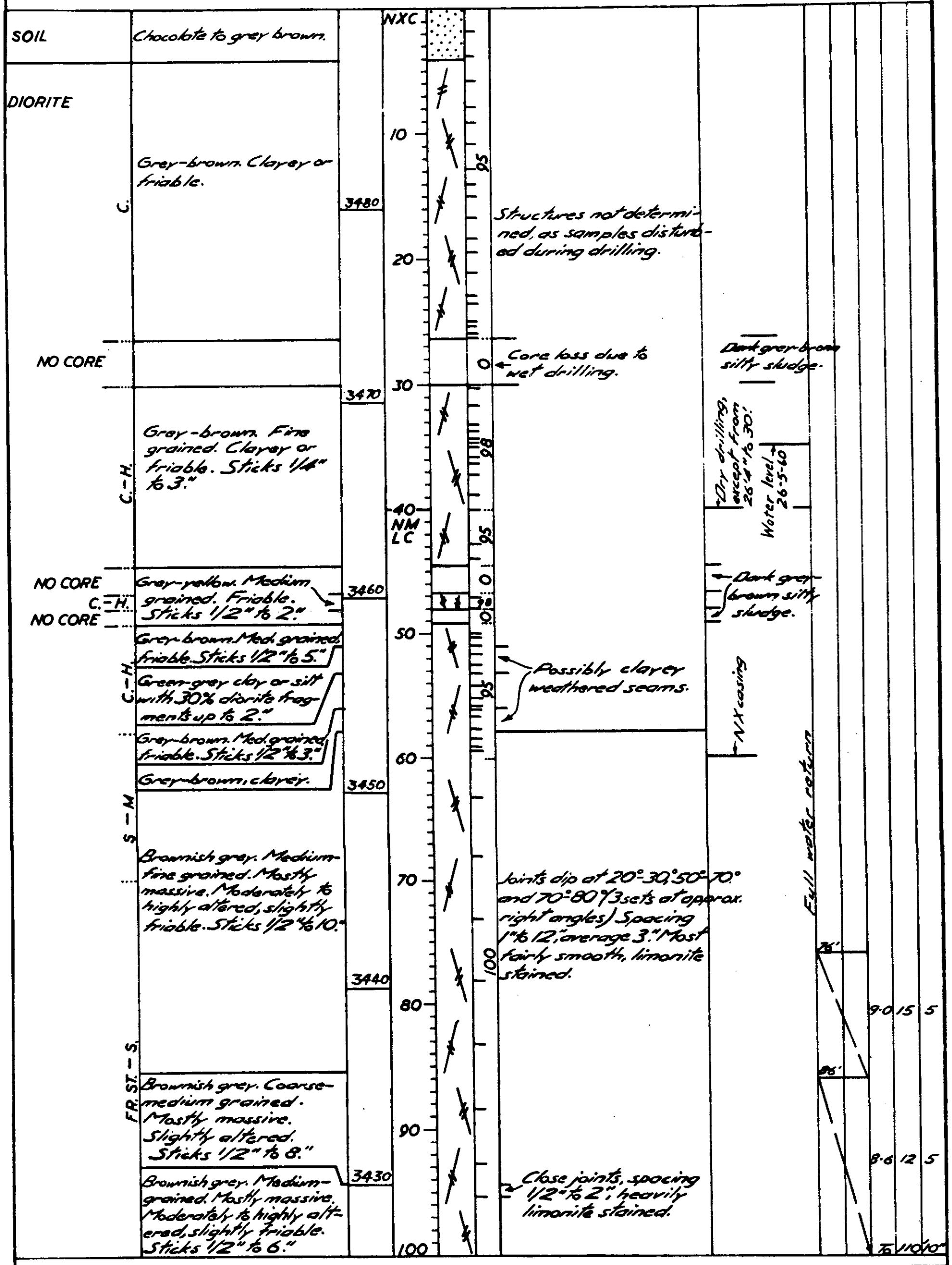

ROCK TYPE & DEGREE OF WEATHERING SHOWN IN CORE	DESCRIPTION	R.L.	DEPTH & SIZE OF CORE	LIFT & CORE RECOVERY (%)	STRUCTURES JOINTS, VEINS, SEAMS FAULTS, CRUSHED ZONES	NOTES WATER LEVEL (DATE) DRILLING WATER RETURN CHARACTER OF DRILL CUTTINGS
SOIL	Chocolate to grey brown.		NXC			
DIORITE C.	Grey-brown. Clayey or friable.	3480	10 20	95	Structures not determined, as samples disturbed during drilling.	
NO CORE				0	Core loss due to wet drilling.	Dark grey-brown silty sludge.
C.-H.	Grey-brown. Fine grained. Clayey or friable. Sticks 1/4" to 3."	3470	30 40 NM LC	98 95		Dry drilling, except from 26'4" to 30'. Water level 26-5-60
NO CORE		3460		0		Dark grey-brown silty sludge.
C.-H.	Grey-yellow. Medium grained. Friable. Sticks 1/2" to 2."			98		
NO CORE				0		
C.-H.	Grey-brown. Med. grained, friable. Sticks 1/2" to 5."		50	95	Possibly clayey weathered seams.	NX casing
	Green-grey clay or silt with 30% diorite fragments up to 2."					
	Grey-brown. Med. grained, friable. Sticks 1/2" to 3."		60			
	Grey-brown, clayey.	3450				
S.-M.	Brownish grey. Medium-fine grained. Mostly massive. Moderately to highly altered, slightly friable. Sticks 1/2" to 10."	3440	70 80	100	Joints dip at 20°-30°, 50°-70° and 70°-80° (3 sets at approx. right angles) Spacing 1" to 12", average 3." Most fairly smooth, limonite stained.	Full water return
FR. ST.-S.	Brownish grey. Coarse-medium grained. Mostly massive. Slightly altered. Sticks 1/2" to 8."		90			
	Brownish grey. Medium-grained. Mostly massive. Moderately to highly altered, slightly friable. Sticks 1/2" to 6."	3430	100		Close joints, spacing 1/2" to 2", heavily limonite stained.	

PERCOLATION TEST

DEPTH (FT) FROM	TO	LOSS IN G.P.M.	PRESSURE (P.S.I.)	LENGTH OF TEST (MIN)
76'		9·0	15	5
86'		8·6	12	5
	To	110	10	10"

DRILL No. 6 – A – 18
TYPE BOYLES
DRILLER S · M · A
COMMENCED 28 · 3 · 60
COMPLETED 14 · 4 · 60

EXPLANATION
C.= COMPLETE.
H.– HIGH.
M.– MODERATE.
S.– SLIGHT.
FR.ST.– FRESH, STAINED JOINTS.
FR.– FRESH.

ENGINEERING GEOLOGY BRANCH
LOGGED W. E. BAMFORD
SHEET No.
DRAWN G. Bee
CHECKED
SUBMITTED

VERT. SCALE 1" = 10'
SHEET 1 OF 3
DRAWING No. M5/11

SNOWY MOUNTAINS HYDRO-ELECTRIC AUTHORITY

GEOLOGICAL LOG OF DRILL HOLE

PROJECT SNOWY – GEEHI FEATURE TUNNEL
HOLE No. 2401 CO-ORDINATES: E 289 M 4657·0, N 141 M 1623·4 R.L. GROUND 3490·3
LOCATION GEEHI RESERVOIR ANGLE FROM HORIZONTAL 40° DIRECTION 096°

ROCK TYPE & DEGREE OF WEATHERING SHOWN IN CORE	DESCRIPTION	R.L.	DEPTH & SIZE OF CORE	LIFT & CORE RECOVERY (%)	STRUCTURES JOINTS, VEINS, SEAMS FAULTS, CRUSHED ZONES	NOTES WATER LEVEL (DATE) DRILLING WATER RETURN CHARACTER OF DRILL CUTTINGS
	As above.		NMLC		Probable completely altered zone.	Caving from 100 to 110 ft.
NO CORE				0		
FR.ST. – S.	Brownish grey. Mainly massive. Medium-fine grained. Moderately to highly altered, slightly friable. Sticks 1/2" to 7."	3420	110		Joints dip at 20°-30°; 40°-60° and 70°-80°. (3 sets striking 0°-60° to each other) Spacing 1" to 10" average 3." Some smooth, some fairly rough. Thin limonite stains on 60%, other clean.	
	Grey. Fine and coarse grained. Mostly massive. Slightly altered. Sticks 1" to 9."					
DIORITE	Grey, mostly fine grained. Massive. Sticks 1" to 14."	3410	120			
FR.ST.	Dark grey. Mostly medium-coarse grained. Massive. Sticks 1" to 16."	3400 3390	130 140 150 160	100	Joints dip at 20°-40° and 50°-60°. (strike 150° to each other.) Spacing 1" to 15" average 5." Most fairly rough, some smooth. Most have thin limonite stains. Joints dip mainly at 40°-60°, a few at 20°-30° and 70°-80°. Spacing 1/2" to 6" average 2." Most fairly smooth, limonite stained. Joints dip at 10°-25°, 40°-60° and 80°-90°. Spacing 1" to 15" average 5." Most fairly smooth, 70% thinly limonite stained, others have thin calcite coatings	Water return
BASIC DYKE	Greenish-black. Fine grained.	3380	170		Contact dips at 10°. 3" of irregular frags. 1/10" to 1/2". 30% yellow-brown clay, at 20°? Rough irregular joints 1/4" to 3," earthy limonite coated.	
FR.ST. – S.					2" sheared zone, completely weathered, clayey, at 30° Heavily stained joints at 60°, 1/2" to 2," with up to 1/10" earthy limonite.	
FR.ST.		3370	180 190		Joints dip at 20°-50°, a few at 70°-80°. Spacing 1/2" to 12" average 3." Some rough, some fairly smooth. Limonite stained, some earthy.	
FR.			200		See below.	

PERCOLATION TEST

DEPTH (FT) FROM	TO	LOSS IN G.P.M.	PRESSURE (P.S.I.)	LENGTH OF TEST (min)
100'	10"			
		0·4	25	
		0·5	50	5
		0·8	75	
		1·4	100	
110'	10"			
		1·0	20	
		2·2	60	5
		3·0	80	
		4·6	120	
119'2"				
	121'7"			
		1·4	40	
		3·3	80	5
		5·7	130	
129'	6"			
		2·0	25	
		3·5	50	5
		4·3	75	
		6·1	100	
138'1"				
	139'			
		1·1	25	
		1·9	50	
		2·7	75	5
		4·2	100	
		7·1	125	
147'2"				
	148'			
		2·7	25	
		3·9	50	
		5·1	75	5
		6·1	100	
		7·4	125	
	157'2"			
157'10"				
		0·6	25	
		1·4	50	
		2·0	75	5
		2·6	100	
		3·4	125	
		4·6	150	
167'	10"			
		0·4	25	
		1·0	50	
		1·2	75	5
		1·6	100	
		2·3	125	
		4·8	150	
180'	4"			
		0·4	25	
		0·6	50	
		0·9	75	5
		1·1	100	
		1·2	125	
190'	4"			
		0·4	25	
		0·5	50	
		0·7	75	5
		0·6	100	
		0·7	125	
	To 210'4"			

DRILL No. 6 – A – 18
TYPE BOYLES
DRILLER S·M·A
COMMENCED 28·3·60
COMPLETED 14·4·60

ENGINEERING GEOLOGY BRANCH
LOGGED W.E. BAMFORD
SHEET No.
DRAWN G. Bonomi
CHECKED
SUBMITTED

VERT. SCALE 1" = 10'
SHEET 2 OF 3
DRAWING No. M5/11

SNOWY MOUNTAINS HYDRO-ELECTRIC AUTHORITY

GEOLOGICAL LOG OF DRILL HOLE

PROJECT SNOWY – GEEHI FEATURE TUNNEL
HOLE No. 2401 CO-ORDINATES: E 289 M 4657·9, N 141 M 1623·4 R.L. GROUND 3490·3
LOCATION GEEHI RESERVOIR ANGLE FROM HORIZONTAL 40° DIRECTION 096°

ROCK TYPE & DEGREE OF WEATHERING SHOWN IN CORE	DESCRIPTION	R.L.	DEPTH & SIZE OF CORE	LOG	LIFT & CORE RE-COVERY (%)	STRUCTURES JOINTS, VEINS, SEAMS FAULTS, CRUSHED ZONES	NOTES WATER LEVEL (DATE) DRILLING WATER RETURN CHARACTER OF DRILL CUTTINGS
DIORITE FRESH	Dark grey. Mostly medium-fine grained. Massive. Sticks 3" to 4ft	3360 3350 3340 3330 3320	NM LC 210 220 230 240 250 260 270		100	Joints dip at 30°-60°. Spacing 3" to 12 ft. average 14". Some smooth, slightly slickensided, others rough, stepped. Most have thin calcite coatings, a few with traces of pyrite.	Water return

PERCOLATION TEST

DEPTH (FT) FROM	TO	LOSS IN G.P.M.	PRESSURE IN P.S.I.	LENGTH OF TEST (MIN)
	210'4"	0·4	25	5
		0·5	50	
		0·7	75	
		0·6	100	
		0·7	125	
238'4"		0·2	25	5
		0·4	50	
		0·4	75	
		0·6	100	
		1·4	125	
		1·4	150	

Not tested due to caving of hole at 100 to 110 ft.

END OF HOLE AT 278' 4".

NOTE: TERMS SUCH AS "HIGHLY ALTERED" REFER TO ROCK WEAKENED BY CHEMICAL (OR HYDROTHERMAL) ALTERATION, HAVING A STRENGTH COMPARABLE WITH HIGHLY WEATHERED ROCK.

DRILL No. 6-A-18
TYPE BOYLES
DRILLER S.M.A
COMMENCED 28·3·60
COMPLETED 14·4·60

ENGINEERING GEOLOGY BRANCH
LOGGED W.E. BAMFORD
SHEET No.
DRAWN G. Bono
CHECKED
SUBMITTED

VERT. SCALE 1" = 10'
SHEET 3 OF 3
DRAWING No. M5/11

P 477

SNOWY MOUNTAINS HYDRO-ELECTRIC AUTHORITY

GEOLOGICAL LOG OF DRILL HOLE

PROJECT MURRAY I
FEATURE PRESSURE TUNNEL
HOLE No. 2511
CO-ORDINATES: E 286 M 2741·8, N 144 M 1270·3
R.L. GROUND
LOCATION BOGONG CREEK
ANGLE FROM HORIZONTAL 40°
DIRECTION 311°

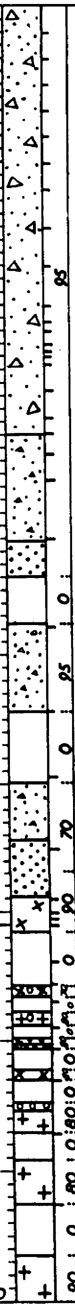

ROCK TYPE & DEGREE OF WEATHERING SHOWN IN CORE		DESCRIPTION	R.L.	DEPTH & SIZE OF CORE	LIFT & CORE RE-COVERY (%)	STRUCTURES JOINTS, VEINS, SEAMS FAULTS, CRUSHED ZONES	NOTES WATER LEVEL (DATE) DRILLING WATER RETURN CHARACTER OF DRILL CUTTINGS	PERCOLATION TEST
SOIL AND SLOPEWASH	C.—M.	Brown-red soil with quartzite and spotted siltstone fragments. 30% rock fragments up to 2"	3600 3590	NXC 10 20 30	95	Not determined.		NOT TESTED
CLAY OR SILT.		Yellow-brown, with 20% quartzite and spotted siltstone fragments up to 1."		40			← Water level 18/11/59 during drilling	
SANDY CLAY		Soft, pale brown-grey.	3580					
NO CORE					0			
	C.—H.	Yellow-brown with 20% quartzite fragments up to 1."		50	95			
NO CORE					0			
	C.—M.	Chocolate-brown, with 10% quartzite frgments up to 1/4."	3570	60	70			
GRANITIC SOIL?	C.—M.	Reddish-brown, friable. Pale grey, well cemented.			90		← Dry drilling tungsten bit.	
RIVER GRAVEL M-H AND BOULDERS	C.	Granite boulders from 6" up to possibly 5 ft. including pink granite and medium-coarse grained biotite granite. Rounded quartzite pebbles up to 3." Small amounts of interstitial silt.	3560	70 NMLC	0		Pale brown sandy cuttings	
NO CORE	C.—H.			80	70, 0, 70, 0, 70, 0, 80, 0, 80, 0		Grey-brown sandy cuttings	
GRANITE		bedrock(?) Medium coarse grained, leucocratic, sticks up to 3."	3550	90	80		Water return	
NO CORE →					0		Yellow-brown sandy cuttings	
	H-C.			100	90			

DRILL No.	6 – A – 22
TYPE	MINDRILL A2000
DRILLER	S.M.A
COMMENCED	30 · 10 · 59
COMPLETED	18 · 11 · 59

EXPLANATION

C. = COMPLETE.
H. = HIGH.
M. = MODERATE

ENGINEERING GEOLOGY BRANCH

LOGGED	W.E. BAMFORD
SHEET No.	
DRAWN	G. Bonomi
CHECKED	W.E. Bamford
SUBMITTED	

VERT. SCALE 1" = 10'
SHEET 1 OF 5
DRAWING No. M7/42

SNOWY MOUNTAINS HYDRO-ELECTRIC AUTHORITY

GEOLOGICAL LOG OF DRILL HOLE

PROJECT MURRAY I FEATURE PRESSURE TUNNEL
HOLE No 2511 CO-ORDINATES E 286 M 2741·8, N 144 M 1270 3 R.L. GROUND 3608·8
LOCATION BOGONG CREEK ANGLE FROM HORIZONTAL 40° DIRECTION 311°

ROCK TYPE & DEGREE OF WEATHERING SHOWN IN CORE	DESCRIPTION	R.L.	DEPTH & SIZE OF CORE	LOG	LIFT & CORE REC. (%)	STRUCTURES JOINTS, VEINS, SEAMS FAULTS, CRUSHED ZONES	NOTES WATER LEVEL (DATE) DRILLING WATER RETURN CHARACTER OF DRILL CUTTINGS	PERCOLATION TEST
	As above		NM LC	+ +		2" gravel. "caving."		
GRANITE H-M	Medium grained leucocratic, sticks 2" to 8."			+ +	100	Joints 30°-40° and 60°-80°. Spacing 2" to 8", average 4½", limonite stained, smooth or slickensided	Yellow-brown sandy cuttings	
NO CORE		3540			0			
S-M	Yellow-brown silt, (river deposit ?) sub-rounded siliceous granite fragments. 50% sub-rounded slickensided silicified fragments up 3½" 50% granite sand.		110	+ +	95			112'0"
SILT					0		Pale yellow-brown sandy cuttings.	
NO CORE					10	Close slickensided joints, ¼" to 1" ½" clay seam at 40°.		
C.-H.			120	+ +				
M-M	Fine-medium grained. Yellow-pink and green feldspars. 40% quartz and 5-10% black biotite flakes. Sticks ½" to 4"	3530		+ +	80	Joints mostly 30°-40°, others 60°-80°. Spacing ½" to 5" average 2", limonite stained, slickensided. Associated with greenish alteration.	NX casing	7·3 25 5 10·4 50
	Medium-coarse grained. Predominantly yellow pink but also green feldspars. 40% quartz. No biotite. Sticks ½" to 8."		130	+ +		4" of sheared joints at 25° greenish alteration		
		3520		+				
S-M	Medium-coarse grained approx. 50-50% of grey-white and yellow-pink feldspars. 40% quartz 5-10% black biotite. Sticks 1" to 12." Greenish alteration		140	+ +		Clayey sheared joints at 20°	Full water return	142'0"
GRANITE		3510	150	+ + +		Joints at 30°-40° and 50°-60° with a few at 80°-90°. Spacing 1" to 12" average 3½" 70% limonite stained many slickensided others smooth.		2·0 25 2·2 50 2·2 75 5 2·4 100 5·0 150
	Fine-medium grained. Yellow-pink and green feldspars 40% quartz. Practically all biotite has been hydrothermally altered. Sticks 1" to 10."	3500	160	+ +				
FR.ST.-S			170	+ +		Joints 20°-45°. Spacing 1" to 3 ft. average 6½" 30% limonite stained others with chlorite or calcite. Most slickensided or smooth.		172'0"
	Fine-medium grained, yellow-pink and green feldspars, many phenocrystic. 40% quartz, 5-10% biotite. Sticks ½" to 14"	3490	180	+ +	100			0·8 25 0·4 50 1·0 100 5 2·8 125 1·7 150
			190	+ +		6" of sheared clayey joints, ¼" to 2"		
			200	+		Joints 20-40° and 60°-80° Spacing 1" to 9", average 3½" Most limonite stained, clayey. Most smooth or slickensided.		5 222'10"

DRILL No 6-A-22 TYPE MINDRILL A·2000	**EXPLANATION**	ENGINEERING GEOLOGY BRANCH	VERT. SCALE 1"=10'
DRILLER S·M·A	C. = COMPLETE. H. = HIGH. M. = MODERATE. S. = SLIGHT. FR.ST. = FRESH, STAINED JOINTS.	LOGGED M.E. BAMFORD SHEET No. DRAWN G. Bo... CHECKED M.E. Bamford SUBMITTED	SHEET 2 OF 5
COMMENCED 30·10·59 COMPLETED 18·11·59			DRAWING No

SNOWY MOUNTAINS HYDRO-ELECTRIC AUTHORITY

GEOLOGICAL LOG OF DRILL HOLE

PROJECT MURRAY I FEATURE PRESSURE TUNNEL
HOLE No. 2511 CO-ORDINATES: E 286 M 2741·8 , N 144 M 1270·3 R.L. GROUND 36
LOCATION BOGONG CREEK ANGLE FROM HORIZONTAL 40° DIRECTION 311°

ROCK TYPE & DEGREE OF WEATHERING SHOWN IN CORE	DESCRIPTION	R.L.	DEPTH & SIZE OF CORE	LOG	LIFT & CORE RECOVERY (%)	STRUCTURES JOINTS, VEINS, SEAMS FAULTS, CRUSHED ZONES	NOTES WATER LEVEL (DATE) DRILLING WATER RETURN CHARACTER OF DRILL CUTTINGS
GRANITE FRESH — FRESH, STAINED JOINTS FRESH	Mainly fine-medium grained, sticks 1" to 50". Alternate zones of different appearance, width 1 to 28 ft. average 10 ft., approx. 55% yellow-pink feldspars, 30% grey-white feldspars, 15% green feldspars. Approx. 40% quartz, 10% black biotite flakes. Numerous dark grey fine grained zones 1/2" to 3" wide at 0°-40°.	3480 3470 3460 3450 3440 3430 3420	NM LC 210 220 230 240 250 260 270 280 290 300	+	100	Joints 45°-55°, 0°-30° and 60°-80°. Spacing 1" to 16" average 6." Most slightly slickensided. 30% are limonite stained, others have thin calcite or chlorite veneers, some are slightly clayey. Open stained joints at 80°, 1" spacing. 3" rough, slightly slickensided, earthy limonite stained joints at 30° and 50°, spacing 1/4" to 1/2." Joints 0°-30° and 50°. Spacing 1" to 21" average 10" most are fairly rough, some slightly slickensided. Most are clean, but some have thin calcite veneers. 20% are limonite stained. Base of limonite staining. 3" irregular fragments, 1/50" to 1/4", clayey sheared joints at 50°-70°. Joints 20°-30° and 40°-50°. Spacing 1" to 21" average 6." Most rough or slightly polished. Most clean but some have thin calcite veneers. 1/2" quartz vein at 50°. Joints 10°-40°, a few at 60°. Spacing 3" to 4 1/2 ft., average 11." Most smooth, slightly polished. Thin calcite veneers. Joints 10°-40° and 50. Spacing 1" to 12" av. 5," smooth, slightly polished. Thin calcite veneers, some slightly clayey. 8" clayey slickensided joints, 1/2" to 2" at 20° and 60°.	Water return

PERCOLATION TEST

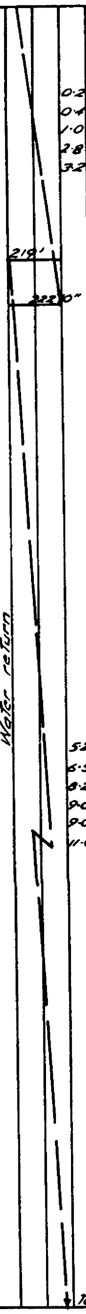

DEPTH (FT) FROM	TO	LOSS IN G.P.M.	PRESSURE (P.S.I.)	TIME OF TEST (MIN)
219'	222'0"	0·2	25	
		0·4	50	
		1·0	100	5
		2·8	125	
		3·2	150	
	To 319'	5·2	25	
		6·5	50	
		8·2	75	5
		9·0	100	
		9·0	125	
		11·0	150	

DRILL No. 6-A-22
TYPE MINDRILL A2000
DRILLER S·M·A
COMMENCED 30·10·59
COMPLETED 18·11·59

ENGINEERING GEOLOGY BRANCH
LOGGED W·E·BAMFORD
SHEET No.
DRAWN G. Bono
CHECKED W.E. Bamford
SUBMITTED

VERT. SCALE 1" = 1
SHEET 3 OF 5
DRAWING No. M7/4

SNOWY MOUNTAINS HYDRO-ELECTRIC AUTHORITY

GEOLOGICAL LOG OF DRILL HOLE

PROJECT MURRAY I
FEATURE PRESSURE TUNNEL
HOLE No. 2511
CO-ORDINATES: E286 M 2741·8, N144 M 1270·3
R.L. GROUND 360[illegible]
LOCATION BOGONG CREEK
ANGLE FROM HORIZONTAL 40°
DIRECTION 311°

ROCK TYPE & DEGREE OF WEATHERING SHOWN IN CORE	DESCRIPTION	R.L.	DEPTH & SIZE OF CORE	LOG	LIFT & CORE RECOVERY (%)	STRUCTURES JOINTS, VEINS, SEAMS FAULTS, CRUSHED ZONES	NOTES WATER LEVEL (DATE) DRILLING WATER RETURN CHARACTER OF DRILL CUTTINGS	PERCOLATION TEST DEPTH (FT) FROM	TO	LOSS IN GPM	PRESSURE (P.S.I.)	LENGTH OF TEST (MIN)
GRANITE FRESH		3410	NM LC	+		Joints 10°-40° and 60°,(2 sets striking 60° apart) Spacing 2" to 16" average 6." Most slightly polished. Thin calcite veneers, some with chlorite.	Water return			5·2 6·5 8·2 9·0 9·0 11·0	25 50 75 100 125 150	5
	Medium-coarse grained Sticks 1" to 28." Alternate zones of different appearance, widths 1 to 15 ft. average 6 ft. Approx. 45% yellow-pink feldspars, 30% green feldspars, 25% grey-white feldspars. Approx. 40% quartz, 10% black biotite flakes but 3 zones totalling 9 ft. are without any dark minerals. Numerous dark grey fine grained zones 1/2" to 4" wide at 10°-40°.		310	+		Joints mostly at 45°-65.° Spacing 8" to 3 ft. average 13." Most polished slightly slickensided. Calcite veneers with chlorite.		319'				
		3400	320	+		Joints mostly at 45°-60.° (2 set striking 90° apart) Spacing 1/2" to 6" av. 5." Most rough, slightly slickensided. Thin calcite veneers, slightly clayey.				2·0 2·4 3·0 3·8 4·2 4·4	25 50 75 100 125 150	5
		3390	330 340	+		Joints 10°-30° and 50°-60.° Spacing 1" to 25" av. 10." Most smooth, slightly polished, thin calcite veneers.		339'				
		3380	350	+	100	1/2" breccia on slickensided joints at 70°-80.°	No water return			1·0 1·4 1·5 1·7 2·2 3·5	25 50 75 100 125 150	5
	Medium-coarse grained, 50-50% yellow-pink and green feldspars. 40% qtz. Practically all biotite has been hydrothermally altered. Sticks 1" to 16."		360	+		Many open clayey joints, some vughs open up to 1/2" with well developed pyramidal quartz crystals.		359'		7·9 9·9 10·9 11·5 12·2	25 50 75 100 125	5
	3 dark grey fine grained zones, 3/4" to 2," at 10°-15.°	3370	370	+		Joints mostly at 10°-40° and 50°-60.° Spacing 1/2" to 16" average 4." Many joints open up to 1/2." Most smooth or slickensided, some rough. Calcite veneers, many clayey.		379'				
	3 dark grey, fine grained zones, 3/4" to 1 1/2" at 10° and 40.°	3360	380 390 400	+		4" polished irregular fragments, 1/8" to 1." 4" polished irregular fragments, 1/4" to 1," slightly clayey. 2" polished irregular fragments, 1/16" to 1/2." 3" of slickensided irregular fragments 1/50" to 1/2."	Water return	399'	To 419'	8·0 8·3 8·1 9·7 10·9 11·7	25 50 75 100 125 150	5

DRILL No. 6 - A - 22	ENGINEERING GEOLOGY BRANCH
TYPE MINDRILL	LOGGED W.E. BAMFORD
DRILLER S.M.A	SHEET No.
COMMENCED 30·10·59	DRAWN G. Bo[illegible]
COMPLETED 18·11·59	CHECKED W.E. Bamford
	SUBMITTED

VERT. SCALE 1" = 10'
SHEET 4 OF 5
DRAWING No. M7/42

SNOWY MOUNTAINS HYDRO-ELECTRIC AUTHORITY

GEOLOGICAL LOG OF DRILL HOLE

PROJECT MURRAY I FEATURE PRESSURE TUNNEL
HOLE No. 2511 CO-ORDINATES: E 286 M 2741·8, N 144 M 1270·3 R.L. GROUND 36
LOCATION BOGONG CREEK ANGLE FROM HORIZONTAL 40° DIRECTION 311°

ROCK TYPE & DEGREE OF WEATHERING SHOWN IN CORE	DESCRIPTION	R.L.	DEPTH & SIZE OF CORE	LOG	LIFT & CORE RECOVERY (%)	STRUCTURES JOINTS, VEINS, SEAMS FAULTS, CRUSHED ZONES	NOTES WATER LEVEL (DATE) DRILLING WATER RETURN CHARACTER OF DRILL CUTTINGS	PERCOLATION TEST DEPTH (FT) FROM	TO	LOSS IN GPM	PRESSURE (P.S.I.)	LENGTH OF TEST (min)
GRANITE FRESH	Medium-coarse grained mainly green with lesser yellow-pink feldspars. 40% quartz. Practically no biotite. Sticks 1" to 10"	3350	NM LC	+ + +	100	Joints 10°-30°, 50°-60° and 80° spacing 1/2" to 10" av. 5" Most are slickensided. Calcite coatings, some slightly clayey.	Full water return			1·0 1·2 1·3 0·1 0·3 1·8	25 50 75 100 125 150	5
	Med-coarse grained, mainly yellow-pink, also green feldspars. 40% quartz, 5% black biotite flakes. Sticks 1" to 23."	3340	410	+ +		Joints at 10°-40°. Spacing 2" to 2 ft. average 10." Mostly polished. Calcite veneers.						
						END OF HOLE AT 419'0".						

DRILL No.	6 - A - 22
TYPE	MINDRILL A2000
DRILLER	S·M·A
COMMENCED	30·10·59
COMPLETED	18·11·59

ENGINEERING GEOLOGY BRANCH

LOGGED	W·E·BAMFORD
SHEET No.	
DRAWN	G. Boronni
CHECKED	W.E. Bamford
SUBMITTED	

VERT. SCALE 1" = 10'
SHEET 5 OF 5
DRAWING No. M7/42

SNOWY MOUNTAINS HYDRO-ELECTRIC AUTHORITY

GEOLOGICAL LOG OF DRILL HOLE

PROJECT MURRAY 2
FEATURE POWER STATION-ALIGNMENT D
HOLE No. 2660
CO-ORDINATES: E280M 3146·8 N145 M 1635·6
R.L. GROUND 1853·3
LOCATION WESTERN FOOTHILLS OF CLEW'S RIDGE
ANGLE FROM HORIZONTAL 90°
DIRECTION —

ROCK TYPE & DEGREE OF WEATHERING SHOWN IN CORE		DESCRIPTION OF CORE OR CUTTINGS WHERE CORE LOST	R.L. CASING	DEPTH SIZE OF CORE	LIFT & CORE RECOVERY %	STRUCTURES JOINTS, VEINS, SEAMS, FAULTS, CRUSHED ZONES
SLOPEWASH		Granitic soil	1850	NXC	95	No structures observed
BIOTITE GRANITE	C.W.	Buff to grey, clayey, friable		10	90	
NO CORE			1840	NMLC	0	
BIOTITE GRANITE	H.W.	As from 24 to 38 feet		20	95	As from 24 to 38 feet
NO CORE			1830		0	
BIOTITE GRANITE (KHANCOBAN GRANITE)	H.W.-M.W.	Pale grey to buff, medium to coarse grained, mostly in 3 to 12 inch sticks.	1820	30	95	Joint spacing mainly from 4 inches to 2 feet. Fractures and very rough joints at 30° and 50°. Limonite coated joint at 75°
NO CORE				40	0	
BIOTITE GRANITE	M.W.-H.W.	As from 24 to 38 feet	1810		98	As from 24 to 38 feet
Alternating NO CORE and BIOTITE GRANITE	M.W.-H.W.	As from 24 to 38 feet Aplite fragments mainly granite fragments	1800 1790	50 60	0 80 0 98 98 0 60 60 0	As from 24 to 38 feet Limonite coated joints at 35° to 65°. Some crushed rock.
BIOTITE GRANITE	M.W. S.W.-M.W. S.W.	Core in fragments Pale grey to buff, medium to coarse grained, in 1 to 17 inch, but mainly 2 to 10 inch sticks.	1780 1770 1760	70 80 90 100	50 99 100	Joint spacing 2 to 12 inches. Joints at 20° and 50° to 65°, Smooth or rough, limonite stained or coated. 1/8 inch pink, altered seam at 20°. Joint spacing mainly from 2 to 8 inches. Joints at 35°, 55° and 75°. Most joints smooth, some are rough. Limonite stained or coated.

NX-Casing to 80 ft.
BX-Casing to 523 ft.

WATER LEVEL: Full water return
Groundwater level during drilling from 160 to 470 feet

WATER PRESSURE TEST GALLONS PER MINUTE LOSS 5 10
Not tested

TEST PRESSURES SHOWN IN POUNDS PER SQ INCH MEASURED AT GROUND SURFACE

DRILL No. 6-A-6
TYPE A 3000
DRILLER S.M.A.
COMMENCED 6 Sep. 60
COMPLETED 19 Dec. 60

EXPLANATION

CASING IN HOLE DURING DRILLING ▌
WATER LEVEL IN DRILL HOLE ◄ (DATE)

C.W. = Completely weathered
H.W. = Highly "
M.W. = Moderately "
S.W. = Slightly "

ENGINEERING GEOLOGY BRANCH
LOGGED BY D.J.W.
DRAWN BY
CHECKED BY
SHEET 1 OF 10
DRAWING No M 10/81

$\frac{P}{E.G.}$ 489

SNOWY MOUNTAINS HYDRO-ELECTRIC AUTHORITY

GEOLOGICAL LOG OF DRILL HOLE

PROJECT MURRAY 2
FEATURE POWER STATION – ALIGNMENT D
HOLE No. 2660
CO-ORDINATES: E 280 M 3146·8, N 145 M 1635·6
R.L. GROUND. 1853·3
LOCATION WESTERN FOOTHILLS OF CLEW'S RIDGE
ANGLE FROM HORIZONTAL 90°
DIRECTION —

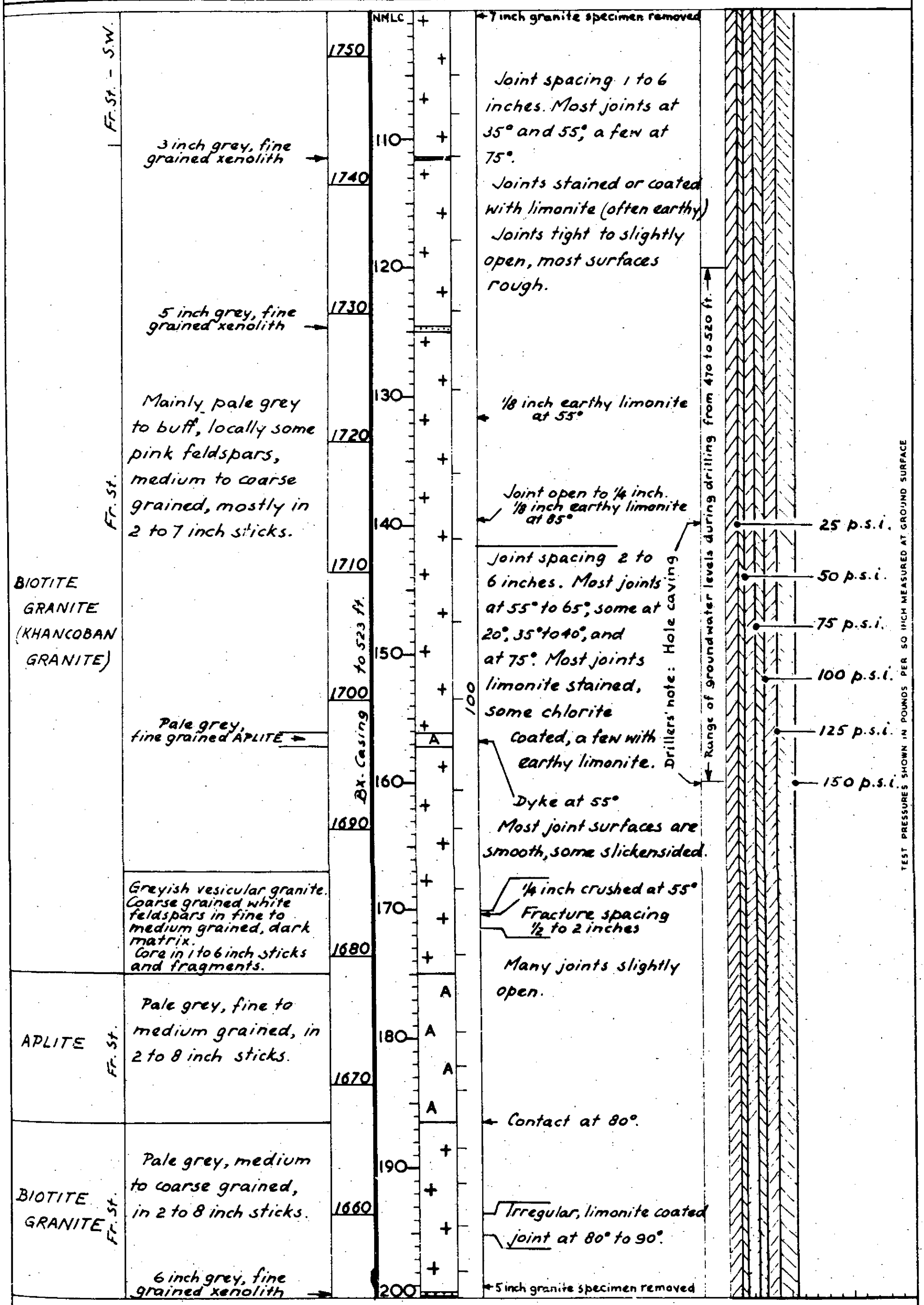

Rock type

Fr. St. – S.W.

BIOTITE GRANITE (KHANCOBAN GRANITE) Fr. St.

APLITE Fr. St.

BIOTITE GRANITE Fr. St.

Description of core

3 inch grey, fine grained xenolith

5 inch grey, fine grained xenolith

Mainly pale grey to buff, locally some pink feldspars, medium to coarse grained, mostly in 2 to 7 inch sticks.

Pale grey, fine grained APLITE

Greyish vesicular granite. Coarse grained white feldspars in fine to medium grained, dark matrix. Core in 1 to 6 inch sticks and fragments.

Pale grey, fine to medium grained, in 2 to 8 inch sticks.

Pale grey, medium to coarse grained, in 2 to 8 inch sticks.

6 inch grey, fine grained xenolith

Structures

7 inch granite specimen removed

Joint spacing 1 to 6 inches. Most joints at 35° and 55°, a few at 75°.

Joints stained or coated with limonite (often earthy)

Joints tight to slightly open, most surfaces rough.

1/8 inch earthy limonite at 55°

Joint open to 1/4 inch. 1/8 inch earthy limonite at 85°

Joint spacing 2 to 6 inches. Most joints at 55° to 65°, some at 20°, 35° to 40°, and at 75°. Most joints limonite stained, some chlorite coated, a few with earthy limonite.

Dyke at 55°

Most joint surfaces are smooth, some slickensided.

1/4 inch crushed at 55°

Fracture spacing 1/2 to 2 inches

Many joints slightly open.

Contact at 80°.

Irregular, limonite coated joint at 80° to 90°.

5 inch granite specimen removed

DRILL No 6-A-6 TYPE A 3000	EXPLANATION CASING IN HOLE DURING DRILLING | WATER LEVEL IN DRILL HOLE ◄ (DATE)	ENGINEERING GEOLOGY BRANCH
DRILLER S.M.A. COMMENCED 6 Sep. 60 COMPLETED 19 Dec. 60	S.W. = Slightly weathered Fr. St. = Fresh, joints limonite stained.	LOGGED BY D.J.W. DRAWN BY CHECKED BY SHEET 2 OF 10 DRAWING No M 10/81

P/E.G. 489

SNOWY MOUNTAINS HYDRO-ELECTRIC AUTHORITY

GEOLOGICAL LOG OF DRILL HOLE

PROJECT **MURRAY 2**　FEATURE **POWER STATION–ALIGNMENT D**
HOLE No. **2660**　CO-ORDINATES E280M 3146·8　N145M 1635·6　R.L. GROUND 1853·3
LOCATION **WESTERN FOOTHILLS OF CLEW'S RIDGE**　ANGLE FROM HORIZONTAL 90°　DIRECTION —

ROCK TYPE & DEGREE OF WEATHERING SHOWN IN CORE	DESCRIPTION OF CORE OR CUTTINGS WHERE CORE LOST	R.L. CASING	DEPTH SIZE OF CORE	LOG	LIFT & CORE RECOVERY %	STRUCTURES JOINTS, VEINS, SEAMS, FAULTS, CRUSHED ZONES	WATER LEVEL	WATER PRESSURE TEST GALLONS PER MINUTE LOSS

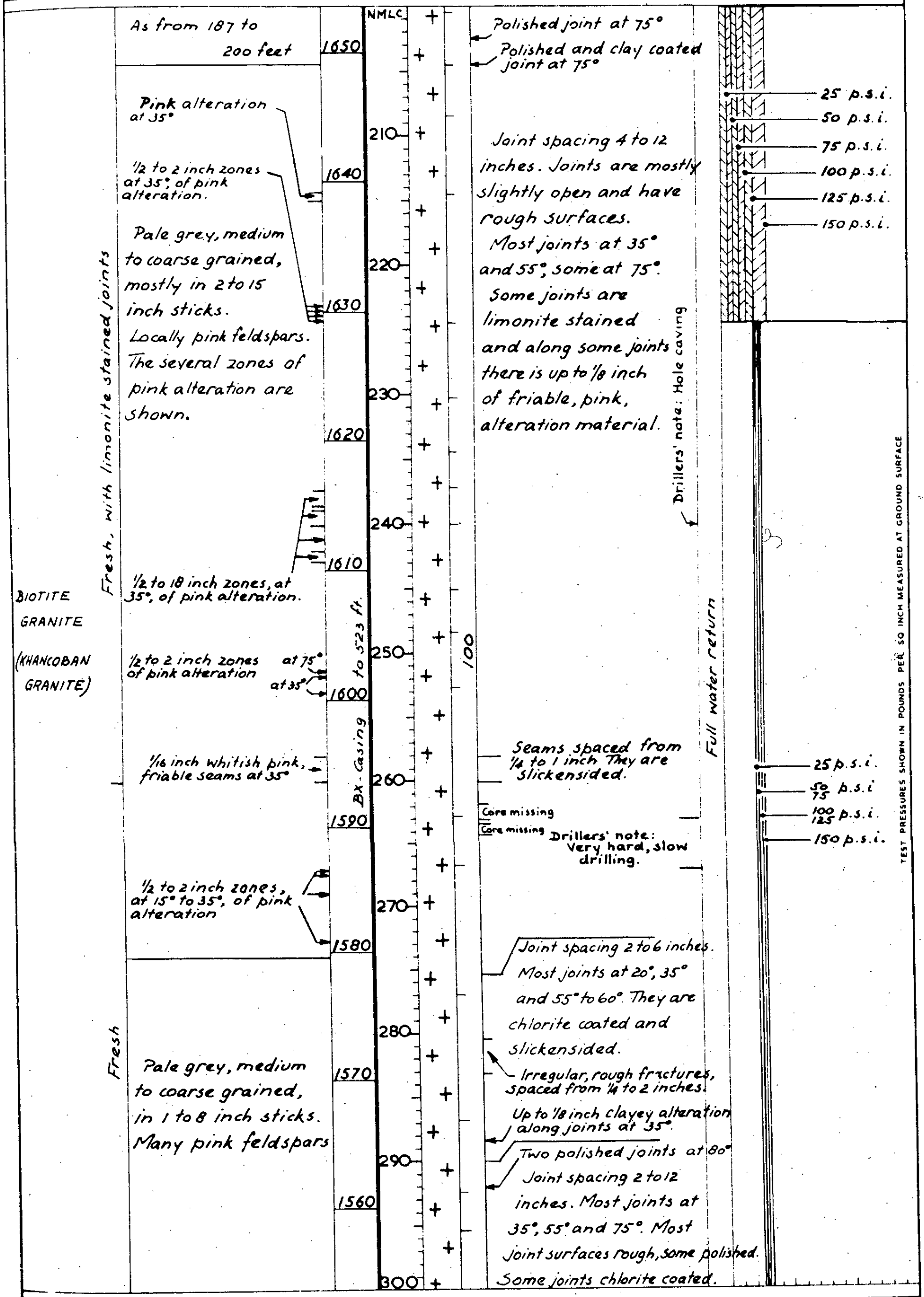

BIOTITE GRANITE (KHANCOBAN GRANITE)

As from 187 to 200 feet

Pink alteration at 35°

½ to 2 inch zones at 35°, of pink alteration.

Pale grey, medium to coarse grained, mostly in 2 to 15 inch sticks. Locally pink feldspars. The several zones of pink alteration are shown.

½ to 18 inch zones, at 35°, of pink alteration.

½ to 2 inch zones of pink alteration at 75° at 35°

1/16 inch whitish pink, friable seams at 35°

½ to 2 inch zones, at 15° to 35°, of pink alteration

Pale grey, medium to coarse grained, in 1 to 8 inch sticks. Many pink feldspars

Polished joint at 75°

Polished and clay coated joint at 75°

Joint spacing 4 to 12 inches. Joints are mostly slightly open and have rough surfaces. Most joints at 35° and 55°, some at 75°. Some joints are limonite stained and along some joints there is up to 1/8 inch of friable, pink, alteration material.

Seams spaced from ¼ to 1 inch They are slickensided.

Core missing

Core missing

Drillers' note: Very hard, slow drilling.

Joint spacing 2 to 6 inches. Most joints at 20°, 35° and 55° to 60°. They are chlorite coated and slickensided.

Irregular, rough fractures, spaced from ¼ to 2 inches.

Up to 1/8 inch clayey alteration along joints at 35°.

Two polished joints at 80°

Joint spacing 2 to 12 inches. Most joints at 35°, 55° and 75°. Most joint surfaces rough, some polished. Some joints chlorite coated.

DRILL No 6–A–6 TYPE A 3000	EXPLANATION CASING IN HOLE DURING DRILLING ▌ WATER LEVEL IN DRILL HOLE ◄ (DATE)	ENGINEERING GEOLOGY BRANCH	
DRILLER S.M.A. COMMENCED 6 Sep. 60 COMPLETED 19 Dec. 60		LOGGED BY	D. J. W.
		DRAWN BY	
		CHECKED BY	
		SHEET 3 OF 10	
		DRAWING No M 10/81	

P/E.G. 489

SNOWY MOUNTAINS HYDRO-ELECTRIC AUTHORITY

GEOLOGICAL LOG OF DRILL HOLE

PROJECT MURRAY 2
FEATURE POWER STATION–ALIGNMENT D
HOLE No. 2660 CO-ORDINATES: E 280 M 3146·8, N 145 M 1635·6 R.L. GROUND 1853·3
LOCATION WESTERN FOOTHILLS OF CLEW'S RIDGE ANGLE FROM HORIZONTAL 90° DIRECTION —

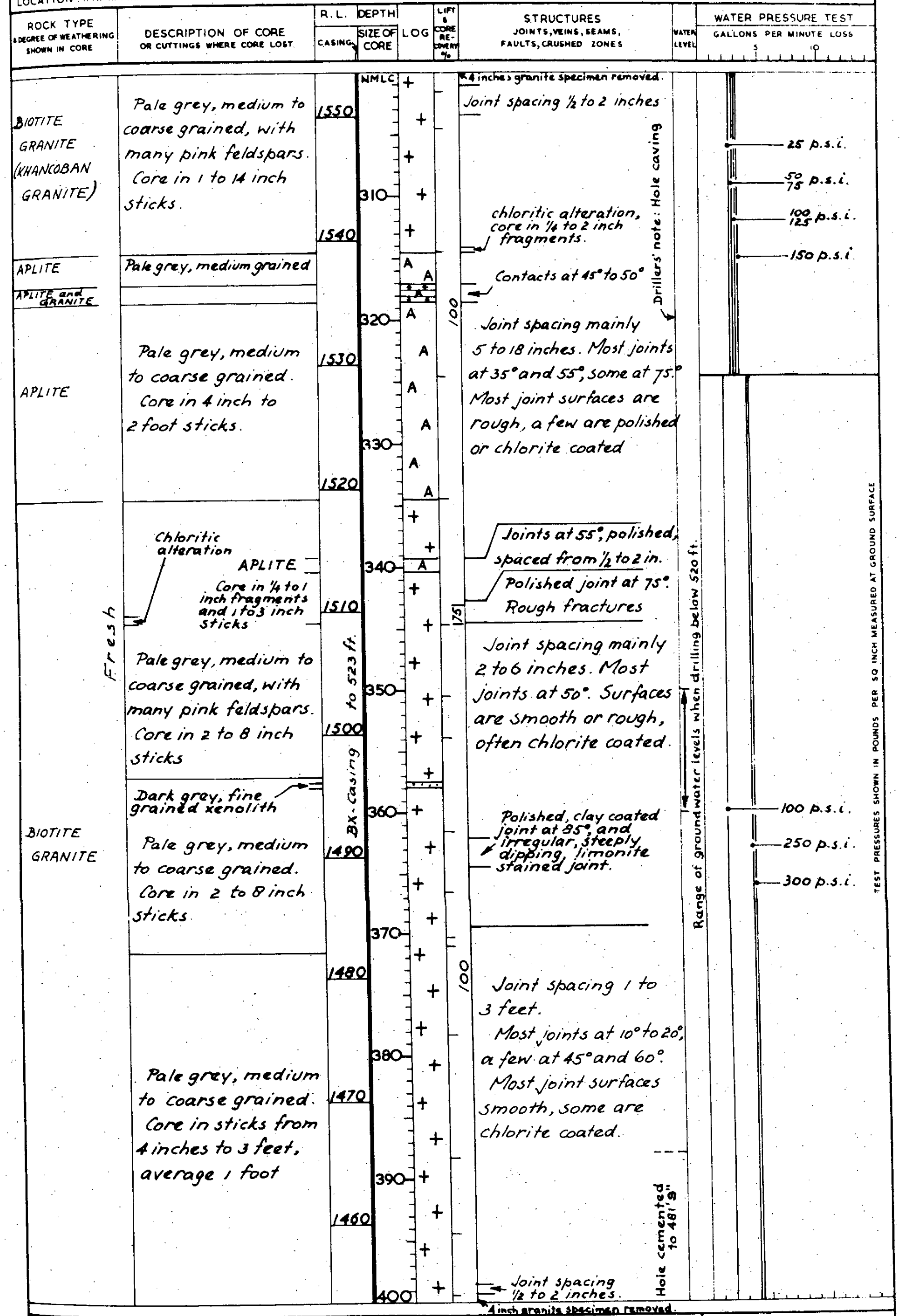

ROCK TYPE & DEGREE OF WEATHERING SHOWN IN CORE	DESCRIPTION OF CORE OR CUTTINGS WHERE CORE LOST	STRUCTURES JOINTS, VEINS, SEAMS, FAULTS, CRUSHED ZONES
BIOTITE GRANITE (KHANCOBAN GRANITE)	Pale grey, medium to coarse grained, with many pink feldspars. Core in 1 to 14 inch sticks.	4 inches granite specimen removed. Joint spacing ½ to 2 inches chloritic alteration, core in ¼ to 2 inch fragments.
APLITE	Pale grey, medium grained	Contacts at 45° to 50°
APLITE and GRANITE		
APLITE	Pale grey, medium to coarse grained. Core in 4 inch to 2 foot sticks.	Joint spacing mainly 5 to 18 inches. Most joints at 35° and 55°, some at 75°. Most joint surfaces are rough, a few are polished or chlorite coated
BIOTITE GRANITE Fresh	Chloritic alteration APLITE Core in ¼ to 1 inch fragments and 1 to 3 inch sticks	Joints at 55°, polished, spaced from ½ to 2 in. Polished joint at 75°. Rough fractures
	Pale grey, medium to coarse grained, with many pink feldspars. Core in 2 to 8 inch sticks	Joint spacing mainly 2 to 6 inches. Most joints at 50°. Surfaces are smooth or rough, often chlorite coated.
	Dark grey, fine grained xenolith	
	Pale grey, medium to coarse grained. Core in 2 to 8 inch sticks.	Polished, clay coated joint at 85°, and irregular, steeply dipping, limonite stained joint.
	Pale grey, medium to coarse grained. Core in sticks from 4 inches to 3 feet, average 1 foot	Joint spacing 1 to 3 feet. Most joints at 10° to 20°, a few at 45° and 60°. Most joint surfaces smooth, some are chlorite coated. Joint spacing ½ to 2 inches. 4 inch granite specimen removed.

DRILL No 6-A-6
TYPE A 3000
DRILLER S.M.A.
COMMENCED 6 Sep. 60
COMPLETED 19 Dec. 60

EXPLANATION
CASING IN HOLE DURING DRILLING ▌ WATER LEVEL IN DRILL HOLE ◄ (DATE)

ENGINEERING GEOLOGY BRANCH
LOGGED BY D.J.W.
DRAWN BY
CHECKED BY
SHEET 4 OF 10
DRAWING No M10/81

P/E.G. 489

APPENDIX B

Major element analyses and elemental ratios for samples

TABLE B-1

Chemical Analyses and Element ratios of Windy Creek Diorite, Dh 2401

	6065	6156	6061	6059	6055	6054	6050	6049	6048	6046	6045	6044	6043	6041	6038	6037	6034
SiO_2	60.23	58.74	59.80	59.59	59.96	59.03	60.64	61.92	59.53	58.50	59.51	59.32	59.73	59.74	60.24	61.03	60.00
TiO_2	1.27	1.13	1.14	1.09	1.15	1.08	1.11	0.82	1.20	1.10	0.87	1.00	1.10	1.13	0.89	0.94	1.22
Al_2O_3	15.66	16.23	15.85	18.05	16.06	16.57	16.38	18.87	16.19	17.23	17.47	17.05	16.97	16.56	17.49	16.49	15.60
Fe_2O_3	1.68	1.69	1.19	1.57	1.67	1.26	1.05	1.87	1.59	2.45	1.68	1.97	1.24	0.91	1.24	1.34	1.85
FeO	6.82	7.62	7.53	6.16	7.17	7.92	6.87	6.05	6.80	6.95	7.21	6.72	6.76	7.17	6.46	6.23	6.50
MnO	0.16	0.18	0.17	0.16	0.18	0.18	0.16	0.15	0.15	0.19	0.14	0.16	0.15	0.15	0.13	0.13	0.14
MgO	2.29	1.81	2.19	1.46	1.98	1.71	2.22	1.30	2.40	1.74	1.15	1.86	2.04	2.22	1.58	2.05	2.54
CaO	5.76	5.64	5.64	5.85	5.82	5.62	5.66	5.16	5.95	5.26	5.23	4.05	5.77	5.76	5.50	5.53	5.95
Na_2O	4.01	4.13	4.28	4.72	4.34	4.26	4.37	4.87	4.32	4.38	4.45	4.44	4.54	4.19	4.48	4.40	4.01
K_2O	0.83	0.96	0.74	0.73	0.62	0.94	0.94	1.09	0.84	1.09	0.64	1.14	0.65	0.72	0.98	1.03	0.96
P_2O_5	0.41	0.48	0.41	0.41	0.48	0.46	0.37	0.23	0.40	0.31	0.28	0.30	0.37	0.37	0.26	0.28	0.38
H_2O^+	1.13	1.01	-	-	-	-	-	-	-	-	-	-	-	-	1.05	-	-
H_2O^-	0.20	0.21	0.17	0.13	0.17	0.19	0.15	0.22	0.23	0.33	0.54	0.46	0.23	0.17	0.19	0.13	0.25
CO_2	0.20	<0.02	-	-	-	-	-	-	-	-	-	-	-	-	<0.02	-	-
	100.65	99.67													100.49		
ΣFe_2O_3	9.26	10.16	9.56	8.41	9.63	10.06	8.68	8.59	9.15	10.17	9.69	9.44	8.75	8.87	8.41	8.26	9.07
Fe^{++}/Fe^{+++}	4.51	5.01	7.02	4.37	4.78	6.99	7.30	3.60	4.75	3.15	4.78	3.79	6.07	8.77	5.80	5.18	3.91
Na/K	4.32	3.86	5.18	5.78	6.26	4.06	4.16	3.98	4.60	3.60	6.23	3.49	6.25	4.32	4.09	3.82	3.74
ΣH_2O	1.33	1.22	-	-	-	-	-	-	-	-	-	-	-	-	1.24	-	-
Na/Ca	0.72	0.76	0.79	0.84	0.77	0.79	0.80	0.98	0.75	0.86	0.88	1.14	0.82	0.76	0.85	0.83	0.70
Ca/Mg	2.98	3.69	3.05	4.75	3.48	3.89	3.02	4.61	2.94	3.58	5.39	2.58	3.35	3.07	4.12	3.20	2.78
Fe/Mg	4.69	6.51	5.06	6.68	5.64	6.82	4.53	7.66	4.42	6.78	9.77	5.89	4.97	4.63	6.17	4.67	4.14

TABLE B-1 (continued)

Chemical Analyses and Element Ratios of Windy Creek Diorite, DH 2401

	6033	6032	6031	6029	6028	6027	6025	6023	6022	6021	6020	6019	6018	6017	6016	6015	6014	6013	6012	6011	6010	6127	6009
SiO_2	59.54	58.72	62.02	59.87	58.49	58.75	59.57	59.29	62.29	60.65	59.46	59.89	59.23	58.38	61.73	60.46	61.41	57.84	54.67	55.01	54.07	50.90	56.18
TiO_2	1.21	1.13	1.10	0.93	1.00	0.86	0.95	0.92	0.54	0.66	1.03	0.99	1.18	1.08	0.75	0.81	0.84	0.99	1.22	1.18	1.09	1.31	1.13
Al_2O_3	15.56	14.78	15.48	15.90	16.13	16.46	15.69	16.19	15.98	16.37	16.43	17.02	15.75	15.73	16.07	15.11	16.36	16.18	16.50	16.89	17.23	17.99	18.46
Fe_2O_3	2.02	2.26	2.14	3.82	3.85	3.97	4.54	2.78	2.81	3.10	4.72	4.26	4.28	4.78	4.56	4.62	5.56	6.24	5.15	4.91	6.26	5.42	7.80
FeO	6.84	6.56	5.60	5.92	6.16	6.11	5.53	5.60	3.52	3.90	4.22	4.10	4.95	4.63	2.85	2.73	1.98	4.13	5.26	5.59	5.05	6.08	1.69
MnO	0.15	0.15	0.12	0.19	0.18	0.20	0.21	0.15	0.11	0.13	0.14	0.13	0.15	0.16	0.12	0.13	0.13	0.19	0.17	0.16	0.17	0.19	0.13
MgO	2.42	2.42	1.96	1.53	1.88	1.53	1.55	2.50	2.89	2.97	1.85	1.62	2.34	2.18	1.92	2.62	2.21	2.16	3.75	3.23	2.60	3.79	1.49
CaO	6.00	5.45	5.17	5.22	4.54	5.25	5.03	5.79	5.31	5.80	5.20	5.27	5.79	4.98	4.37	4.19	3.61	3.94	4.89	4.97	4.27	4.75	1.08
Na_2O	4.07	3.85	4.01	4.08	5.18	4.15	3.82	4.22	3.86	3.80	3.48	3.75	3.30	3.08	3.22	2.47	2.30	2.02	1.55	1.75	1.80	1.46	0.57
K_2O	0.95	1.03	0.80	0.81	0.84	0.99	1.07	0.93	1.02	0.98	1.21	1.09	1.23	1.12	1.26	1.42	1.53	1.35	1.26	1.22	0.97	1.13	1.04
P_2O_5	0.39	0.34	0.33	0.39	0.37	0.33	0.41	0.25	0.17	0.19	0.36	0.25	0.38	0.38	0.21	0.21	0.24	0.28	0.23	0.21	0.35	0.14	0.14
H_2O^+	-	-	-	-	-	-	-	-	1.26	-	-	-	-	0.85	-	2.25	3.03	-	3.86	-	4.03	3.91	4.37
H_2O^-	0.24	0.38	0.36	0.45	0.55	0.57	0.52	0.38	0.49	0.59	0.76	0.61	0.64	0.76	0.67	0.85	0.98	1.24	1.58	1.39	1.86	1.81	3.76
CO_2	-	-	-	-	-	-	-	-	0.17	-	-	-	-	0.58	-	0.39	0.54	-	0.58	-	0.63	0.77	1.39
									100.42					98.69		98.26	100.72		100.67		100.38	99.65	99.23
ΣFe_2O_3	9.62	9.55	8.36	10.39	10.69	10.76	10.69	9.00	6.72	7.43	9.40	8.82	9.78	9.92	7.73	7.65	7.75	10.83	11.00	11.12	11.87	12.18	9.68
Fe^{++}/Fe^{+++}	3.77	3.22	2.91	1.72	1.78	1.71	1.35	2.24	1.39	1.40	0.99	1.07	1.29	1.08	0.69	0.66	0.40	0.74	1.13	1.27	0.90	1.25	0.24
Na/K	3.84	3.33	4.49	4.51	5.53	3.76	3.20	4.07	3.39	3.48	2.58	3.08	2.41	2.45	2.29	1.56	1.34	1.34	1.10	1.28	1.65	1.16	0.49
ΣH_2O	-	-	-	-	-	-	-	-	1.76	-	-	-	-	1.61	-	3.09	4.01	-	5.44	-	5.89	5.72	8.12
Na/Ca	0.70	0.73	0.81	0.81	1.18	0.82	0.79	0.76	0.75	0.68	0.69	0.74	0.59	0.64	0.76	0.62	0.66	0.53	0.33	0.37	0.44	0.32	0.55
Ca/Mg	2.94	2.67	3.13	4.04	2.86	4.07	3.85	2.74	2.18	2.31	3.33	3.85	2.93	2.71	2.70	1.89	1.94	2.16	1.55	1.82	1.95	1.49	0.86
Fe/Mg	4.61	4.58	4.95	7.87	6.59	8.16	8.00	4.17	2.70	2.90	5.89	6.31	4.85	5.28	4.67	3.39	4.07	5.81	3.40	3.99	5.29	3.73	7.53

TABLE B-2

Chemical Analyses and Element Ratios of Scamels Granite, DH 2511

	6068	6070	6074	6079	6081	6082	6085	6088	6092	6094	6098	6101	6102	6104	6105	6107	6110
SiO_2	76.85	76.26	75.91	78.57	76.22	76.39	76.30	76.10	76.69	77.02	76.71	76.25	76.61	76.95	77.04	77.35	76.55
TiO_2	0.06	0.07	0.06	0.05	0.06	0.07	0.07	0.06	0.07	0.07	0.07	0.06	0.06	0.06	0.06	0.06	0.06
Al_2O_3	12.96	12.74	12.43	10.63	12.94	12.89	12.96	12.84	12.65	13.01	12.99	12.79	13.00	12.95	12.85	12.98	13.05
Fe_2O_3	0.25	-	-	0.39	-	-	-	-	-	-	-	-	-	-	-	-	-
FeO	0.87	-	-	0.60	-	-	-	-	-	-	-	-	-	-	-	-	-
MnO	0.03	0.04	0.04	0.04	0.03	0.03	0.04	0.03	0.03	0.03	0.02	0.04	0.03	0.03	0.02	0.02	0.05
MgO	<0.01	0.18	0.08	0.38	0.01	<0.01	0.10	<0.01	0.08	<0.01	0.06	0.03	<0.01	0.05	<0.01	0.03	<0.01
CaO	0.66	1.55	1.84	2.07	0.83	0.77	0.66	0.70	0.76	0.64	1.31	0.68	0.59	0.78	0.87	0.54	0.54
Na_2O	3.84	4.11	3.68	3.38	3.84	3.71	3.80	3.70	3.62	3.91	4.96	3.36	3.84	4.00	4.06	3.99	3.78
K_2O	4.34	1.82	1.79	1.50	3.39	3.99	4.33	4.21	4.26	4.22	2.04	4.33	4.32	3.86	3.60	3.65	4.28
P_2O_5	0.02	0.02	0.02	0.02	0.02	0.02	0.02	0.01	0.03	0.02	0.02	0.01	0.02	0.02	0.01	0.02	0.02
H_2O^+	0.19	-	-	0.82	-	-	-	0.44	-	-	0.57	-	-	-	-	-	-
H_2O^-	0.18	0.19	0.17	0.19	0.20	0.17	0.20	0.15	0.12	0.13	0.15	0.13	0.13	0.15	0.09	*0.17	0.17
CO_2	0.43	-	-	2.10	-	-	-	0.55	-	-	0.83	-	-	-	-	-	-
	100.78			100.80				100.07			100.76						
ΣFe_2O_3	1.22	1.34	1.41	1.05	1.58	1.47	1.32	1.28	1.51	1.29	1.03	1.84	1.26	1.29	1.17	1.23	1.40
ΣH_2O	0.37	-	-	1.01	-	-	-	0.60	-	-	0.72	-	-	-	-	-	-
K/Na	1.27	0.50	0.54	0.50	0.99	1.20	1.27	1.27	1.32	1.21	0.46	1.44	1.26	1.08	0.99	1.02	1.27
Na/Ca	6.06	2.75	2.08	1.70	4.79	5.03	6.01	5.52	4.96	6.38	3.93	5.15	6.80	5.36	4.84	7.63	7.34
Ca/Mg	-	10.2	27.3	6.45	98.3	-	7.82	-	11.3	-	25.9	26.9	-	18.5	-	21.3	-
Fe^{++}/Fe^{+++}	3.91	-	-	1.72	-	-	-	-	-	-	-	-	-	-	-	-	-

TABLE B-2(continued)

Chemical Analyses and Element Ratios of Scamels Granite, DH 2511

	6111	6112	6116	6117	6118	6119	6120	6122	6124	6125	6126	6128	6130	6132	6133	6134	6136	6135	6137
SiO_2	76.92	77.09	76.30	77.97	76.91	78.82	77.04	76.90	77.62	78.75	75.96	76.10	76.03	76.12	74.29	67.82	69.55	71.16	71.79
TiO_2	0.06	0.05	0.06	0.06	0.06	0.06	0.06	0.06	0.06	0.06	0.08	0.07	0.08	0.13	0.21	0.72	0.62	0.38	0.48
Al_2O_3	13.14	13.08	13.08	12.51	12.96	12.81	13.10	12.78	13.12	12.48	13.90	13.03	13.97	12.80	14.30	14.89	14.67	17.48	15.25
Fe_2O_3	0.40	-	-	-	-	-	0.69	1.24	0.65	1.16	2.02	0.88	1.24	1.77	1.71	1.81	2.80	1.41	3.21
FeO	0.62	-	-	-	-	-	0.30	0.06	0.06	0.09	0.10	0.33	0.10	0.26	0.49	3.46	2.06	0.13	0.22
MnO	0.03	0.03	0.03	0.02	0.03	0.02	0.02	0.03	0.01	0.03	0.07	0.03	0.02	0.03	0.06	0.06	0.06	0.01	0.02
MgO	0.04	<0.01	0.09	0.17	0.03	<0.01	0.09	<0.01	0.12	0.17	0.21	0.21	0.08	0.27	0.46	1.98	1.52	0.22	0.41
CaO	0.41	0.35	0.55	0.83	0.52	0.10	0.35	0.19	0.17	0.10	0.10	0.37	0.10	0.12	0.09	1.17	0.34	0.02	0.05
Na_2O	3.91	3.58	3.61	3.42	3.85	3.81	3.87	3.67	3.28	3.19	1.94	3.55	1.65	1.67	0.58	1.36	0.51	0.08	0.09
K_2O	4.07	4.27	4.42	3.27	4.26	2.61	4.29	4.30	4.16	2.88	3.50	4.51	4.05	4.45	4.10	3.38	3.17	2.43	2.02
P_2O_5	0.01	0.01	0.02	0.01	0.02	0.02	0.01	0.02	0.01	0.01	0.01	0.02	0.01	0.03	0.04	0.15	0.11	0.03	0.06
H_2O^+	0.47	-	-	-	-	-	-	0.76	-	1.09	2.00	-	1.64	1.61	2.85	2.13	3.28	4.95	4.78
H_2O^-	0.23	0.22	0.21	0.16	0.14	0.16	0.17	0.16	0.24	0.22	0.44	0.31	0.68	0.62	0.79	1.27	1.13	2.05	2.01
CO_2	0.33	-	-	-	-	-	-	0.14	-	<0.02	0.14	-	0.22	0.25	0.46	<0.02	0.21	0.10	0.54
	100.71							100.31		100.24	100.49		99.88	100.16	100.49	100.58	100.26	100.46	100.95
ΣFe_2O_3	1.09	1.15	1.31	0.91	1.20	0.97	1.03	1.30	0.72	1.26	2.14	1.25	1.35	2.06	2.26	5.65	5.09	1.55	3.45
ΣH_2O	0.70	-	-	-	-	-	-	0.92	-	1.31	2.44	-	2.32	2.23	3.64	3.41	4.40	7.00	6.79
K/Na	1.16	1.33	1.37	1.07	1.24	0.77	1.24	1.31	1.42	1.01	2.02	1.42	2.75	2.98	7.91	2.78	6.97	34.3	25.1
Na/Ca	9.90	10.6	6.87	4.26	7.76	41.0	11.4	20.0	19.9	33.1	20.9	9.90	17.5	14.0	6.94	1.20	1.54	3.69	1.81
Ca/Mg	12.1	-	7.24	5.79	20.5	-	4.61	-	1.68	0.70	0.56	2.09	1.48	0.53	0.23	0.70	0.27	0.11	0.14
Fe^{++}/Fe^{+++}	1.71	-	-	-	-	-	0.48	0.05	0.11	0.09	0.06	0.41	0.09	0.16	0.32	2.12	0.81	0.10	0.08

TABLE B-3

Chemical Analyses and Element Ratios for the Khancoban Granite, DH 2660

241	6240	6239	6238	6237	6236	6235	6234	6233	6232	6231	6230	6229	6228	6227	6226	6225
70.27	73.32	70.97	70.43	70.61	69.05	57.71	55.06	71.22	71.47	70.85	70.39	70.24	70.47	70.39	69.35	70.44
0.29	0.27	0.25	0.25	0.26	0.40	0.37	0.40	0.27	0.27	0.29	0.27	0.26	0.28	0.29	0.29	0.29
13.90	14.33	13.77	13.85	14.19	14.27	18.08	19.57	14.05	14.04	14.27	14.14	14.16	14.10	14.29	13.86	14.38
3.28	3.12	3.04	3.10	2.48	4.20	3.91	5.58	3.26	3.11	3.30	3.18	3.03	3.13	3.31	3.28	3.31
0.06	0.06	0.06	0.05	0.04	0.07	0.04	0.06	0.06	0.06	0.06	0.06	0.06	0.06	0.06	0.06	0.06
0.71	1.04	0.82	0.85	0.97	1.09	1.86	2.15	0.70	0.83	1.16	0.77	0.62	1.51	0.74	0.81	1.10
2.53	2.31	2.16	2.14	2.63	3.01	2.26	1.74	2.32	2.12	2.34	2.38	2.30	2.06	2.42	1.79	2.50
2.23	2.45	2.36	2.18	1.56	2.70	5.84	5.81	1.52	2.23	1.57	2.70	2.72	2.66	1.67	2.91	1.57
3.24	3.30	3.57	2.95	2.92	2.55	1.82	2.20	3.35	3.43	3.40	3.20	3.51	2.91	3.16	3.19	3.29
0.10	0.11	0.10	0.10	0.10	0.13	0.15	0.16	0.10	0.11	0.12	0.12	0.11	0.12	0.11	0.12	0.11
-	-	-	1.86	-	-	1.37	-	-	1.06	-	-	-	-	-	1.86	-
-	-	-	0.35	-	-	4.03	-	-	0.06	-	-	-	-	-	<0.02	-
			98.11			97.44			98.79						97.52	
1.63	1.51	1.64	1.46	2.09	1.06	0.35	0.42	2.47	1.72	2.42	1.33	1.44	1.22	2.12	1.23	2.34
0.91	1.10	1.13	1.06	0.62	0.93	2.68	3.47	0.68	1.09	0.70	1.18	1.23	1.34	0.72	1.69	0.65
4.22	2.63	3.12	2.98	3.21	3.27	1.44	0.96	3.93	3.03	2.39	3.66	4.40	1.15	3.87	2.62	2.69
5.36	3.48	4.30	4.23	2.96	4.47	2.44	3.01	5.40	4.34	3.30	4.79	5.67	2.40	5.19	4.70	3.49

TABLE B-3 (continued)

Chemical Analyses and Element Ratios for the Khancoban Granite, DH 2660

23	6222	6221	6220	6217	6216	6215	6214	6213	6212	6211	6210	6199	6198	6197	6196	6195	6194
.65	72.26	71.71	70.08	74.67	74.85	72.65	57.62	70.51	70.82	71.57	70.90	71.04	71.35	74.29	70.44	71.57	70.39
.27	0.28	0.28	0.28	0.05	0.04	0.30	0.38	0.27	0.27	0.28	0.27	0.29	0.27	0.29	0.30	0.29	0.27
.86	14.37	13.87	14.37	14.43	14.83	14.51	20.15	13.04	14.14	14.85	14.18	14.44	14.38	15.13	14.74	14.22	13.96
.12	3.17	3.56	3.19	0.81	0.89	3.46	4.14	3.56	3.13	3.40	3.14	3.21	3.98	3.38	3.40	3.21	3.17
.06	0.06	0.04	0.05	0.03	0.01	0.03	0.03	0.03	0.03	0.05	0.04	0.03	0.02	0.02	0.04	0.06	0.03
.68	1.17	1.25	0.83	0.12	0.35	1.47	1.66	1.24	1.02	0.81	0.85	1.08	1.27	0.83	1.26	0.77	1.04
.33	2.48	0.31	2.57	0.62	0.21	0.60	1.70	0.22	0.37	0.90	1.46	0.73	0.20	0.77	1.25	1.93	0.75
.48	2.52	2.85	2.72	3.23	3.67	3.84	6.72	2.73	1.60	2.54	2.50	2.64	2.80	2.66	1.62	2.62	2.60
.44	3.15	3.25	3.05	4.77	4.15	2.02	1.72	2.80	3.86	3.64	3.44	3.58	2.97	3.61	3.42	3.16	3.54
.11	0.11	0.10	0.10	0.09	0.09	0.11	0.16	0.11	0.11	0.11	0.11	0.11	0.11	0.12	0.12	0.11	0.11
-	-	-	-	0.72	-	-	-	-	-	-	-	-	-	-	-	-	-
-	-	-	-	<0.02	-	-	-	-	-	-	-	-	-	-	-	-	-
				99.54													
.55	1.40	1.28	1.25	1.65	1.27	0.59	0.29	1.15	2.70	1.60	1.54	1.52	1.19	1.52	2.36	1.35	1.52
.10	1.05	9.54	1.10	5.41	18.1	6.64	4.10	12.9	4.49	2.93	1.78	3.75	14.5	3.59	1.35	1.41	3.60
.06	2.51	0.29	3.67	6.12	0.71	0.48	1.21	0.21	0.43	1.32	2.04	0.80	0.19	1.10	1.18	2.97	0.85
.32	3.14	3.30	4.46	7.83	2.95	2.73	2.89	3.33	3.56	4.87	4.28	3.45	3.63	4.72	3.13	4.83	3.53

TABLE B-3 (continued)

Chemical Analyses and Element Ratios for the Khancoban Granite, DH 2660

	6193	6192	6191	6190	6189	6188	6187	6186	6185	6184	6183	6182	6181	6180	6179	6178	6177	6176	6175
SiO_2	69.16	70.16	71.39	70.20	71.61	73.37	70.26	70.42	70.30	70.23	70.74	70.04	71.53	70.83	70.23	70.07	70.48	71.94	71.55
TiO_2	0.28	0.28	0.27	0.27	0.27	0.26	0.25	0.27	0.26	0.28	0.26	0.26	0.28	0.27	0.28	0.26	0.30	0.28	0.28
Al_2O_3	14.25	13.85	14.61	14.41	14.56	14.86	14.11	14.08	14.20	14.44	13.85	13.77	14.76	14.10	14.01	14.09	14.40	14.43	14.51
ΣFe_2O_3	3.12	3.13	3.13	3.08	3.33	3.29	2.90	3.17	3.05	3.16	3.02	3.08	3.24	3.17	3.25	3.04	3.42	3.25	3.24
MnO	0.05	0.05	0.04	0.05	0.04	0.05	0.05	0.05	0.05	0.05	0.05	0.05	0.06	0.05	0.05	0.05	0.06	0.05	0.05
MgO	1.20	0.83	0.80	0.87	0.74	0.52	0.96	0.60	0.60	0.70	0.52	0.51	0.88	0.46	0.43	0.54	0.45	0.33	0.58
CaO	1.65	1.96	1.78	2.28	1.48	1.86	2.01	2.14	2.31	2.08	2.12	2.27	2.44	2.42	2.40	1.53	2.59	2.49	2.56
Na_2O	1.53	1.52	2.83	2.86	2.75	2.56	2.63	2.84	1.55	1.82	2.30	2.08	2.25	2.24	1.83	2.04	2.05	2.11	2.24
K_2O	3.32	3.48	3.36	3.42	3.48	3.25	3.52	3.22	3.37	3.18	3.37	3.41	3.54	3.48	3.19	3.94	3.07	3.26	3.20
P_2O_5	0.11	0.12	0.11	0.12	0.11	0.11	0.11	0.12	0.12	0.12	0.12	0.11	0.12	0.12	0.12	0.11	0.13	0.12	0.11
ΣH_2O	-	-	-	-	1.65	-	-	-	-	-	1.56	-	-	-	-	1.75	-	-	-
CO_2	-	-	-	-	<0.02	-	-	-	-	-	<0.02	-	-	-	-	<0.02	-	-	-
Total					100.02						97.91					97.42			
K/Na	2.43	2.56	1.33	1.34	1.42	1.42	1.50	1.27	2.43	1.96	1.64	1.83	1.76	1.74	1.95	2.16	1.68	1.73	1.60
Na/Ca	0.96	0.81	1.65	1.30	1.93	1.43	1.36	1.38	0.70	0.91	1.13	0.95	0.96	0.96	0.79	1.38	0.82	0.88	0.91
Ca/Mg	1.63	2.80	2.64	3.11	2.37	4.24	2.48	4.23	4.56	3.52	4.83	5.27	3.29	6.23	6.61	3.36	6.82	8.94	5.23
Fe/Mg	3.01	4.37	4.54	4.11	5.22	7.34	3.50	6.13	5.89	4.51	6.73	7.00	4.27	7.99	8.76	6.53	8.81	11.42	6.48

TABLE B-3 (continued)

Chemical Analyses and Element Ratios for the Khancoban Granite, DH 2660

	6174	6173	6172	6171	6170
SiO_2	70.35	71.09	67.65	69.63	67.93
TiO_2	0.30	0.28	0.31	0.30	0.31
Al_2O_3	14.53	14.06	14.39	15.19	15.37
ΣFe_2O_3	3.48	3.24	3.60	3.49	3.57
MnO	0.06	0.05	0.06	0.06	0.04
MgO	0.53	0.44	0.70	0.53	0.51
CaO	2.76	2.03	2.25	1.97	1.26
Na_2O	2.76	2.00	2.00	1.85	1.37
K_2O	3.18	3.63	2.73	2.99	3.29
P_2O_5	0.12	0.11	0.11	0.07	0.06
ΣH_2O	0.99	-	2.63	3.35	3.26
CO_2	<0.02	-	0.05	<0.02	0.40
Total	99.06		96.48	99.43	97.37
K/Na	1.29	2.03	1.53	1.81	2.69
Na/Ca	1.04	1.02	0.92	0.97	1.13
Ca/Mg	6.17	5.47	3.80	4.40	2.93
Fe/Mg	7.61	11.8	5.96	7.64	8.12

TABLE B-4

Chemical Analyses and Element Ratios of the Mertondale Granite

	6280	6281	6282	6283	6285	6289	6292	6356	6357	6358	6359	6360	6363	6364	6365	6374
SiO_2	74.25	78.45	77.67	76.87	78.71	79.31	79.73	74.09	80.54	75.93	78.12	77.93	76.73	77.06	77.84	78.12
TiO_2	0.11	0.11	0.11	0.10	0.07	0.09	0.08	0.09	0.11	0.12	0.11	0.11	0.11	0.07	0.08	0.08
Al_2O_3	16.50	16.57	14.22	14.00	11.91	11.66	12.06	16.29	15.41	15.65	14.79	14.23	14.28	14.13	14.69	12.15
Fe_2O_3	0.62	0.49	0.26	-	0.32	0.57	0.21	0.85	0.49	-	0.40	0.45	-	-	-	0.32
FeO	0.13	0.11	0.16	-	0.18	0.21	0.20	0.05	0.03	-	0.04	0.04	-	-	-	0.05
MnO	0.01	<0.01	<0.01	<0.01	0.01	0.01	0.01	<0.01	<0.01	0.01	<0.01	<0.01	<0.01	<0.01	<0.01	0.01
MgO	0.30	0.12	0.07	0.19	0.07	0.23	0.02	0.27	0.19	0.12	0.09	0.05	0.09	0.07	0.13	0.12
CaO	0.35	0.04	0.01	<0.01	0.14	0.06	0.23	0.35	0.15	0.36	0.03	0.01	0.01	0.02	0.01	0.11
Na_2O	0.07	0.02	0.03	0.33	2.81	0.72	3.79	0.04	0.08	0.04	0.03	0.04	0.14	0.05	0.03	2.34
K_2O	0.33	0.44	3.90	4.75	4.25	4.23	4.27	0.24	0.28	0.29	2.66	4.02	4.63	4.36	2.79	4.25
P_2O_5	<0.01	0.01	0.01	0.01	0.02	0.01	0.01	<0.01	0.01	0.01	0.01	0.01	0.01	0.01	0.01	0.01
ΣH_2O	6.86	5.17	4.08	3.43	0.34	2.35	0.28	6.45	3.82	6.55	4.15	-	2.90	3.78	3.96	0.82
CO_2	0.25	0.13	0.10	0.10	<0.01	0.08	0.13	0.45	0.15	0.24	0.13	-	0.19	0.11	0.10	0.15
Total	99.78	101.66	100.62	-	98.83	99.53	101.02	99.17	101.26		100.56					98.53
ΣFe_2O_3	0.76	0.62	0.44	0.38	0.52	0.81	0.43	0.90	0.52	0.93	0.45	0.50	0.44	0.47	0.37	0.37
Fe^{++}/Fe^{+++}	0.23	0.25	0.68	-	0.63	0.41	1.06	0.07	0.07	-	0.11	0.10	-	-	-	0.17
K/Na	5.27	24.6	145	16.1	1.69	6.57	1.26	6.71	3.92	8.11	99.2	112	37.0	97.6	104	2.03
Na/Ca	0.21	0.52	3.11	-	20.8	12.5	17.1	0.12	0.55	0.12	1.04	4.15	14.5	2.60	3.11	22.1
Fe/Mg	2.94	5.99	7.29	2.32	8.61	4.08	24.9	3.87	3.17	8.99	5.80	11.6	5.67	7.79	3.30	3.58

TABLE B-5

Chemical Analyses and Element Ratios for Zamia and Tuckanarra Granites

	Zamia Quarry		Tuckanarra Quarry			
	6254	6255	6263	6267	6278	6279
SiO_2	73.55	73.47	72.37	73.75	73.26	73.35
TiO_2	0.19	0.19	0.27	0.22	0.21	0.23
Al_2O_3	14.15	13.84	15.80	15.35	15.58	15.28
Fe_2O_3	0.52	0.48	0.67	-	1.49	1.51
FeO	0.99	1.03	1.36	-	0.23	0.34
MnO	0.03	0.03	0.03	0.03	0.02	0.02
MgO	0.31	0.35	0.74	0.50	0.39	0.50
CaO	1.59	1.64	2.49	1.84	1.36	2.04
Na_2O	3.17	3.12	4.47	4.08	3.76	4.11
K_2O	4.39	3.90	1.96	3.01	3.54	2.41
P_2O_5	0.05	0.05	0.09	0.08	0.03	0.07
ΣH_2O	0.22	0.37	0.73	0.79	1.45	0.90
CO_2	0.09	0.01	0.08	0.09	0.15	0.08
Total	99.25	98.48	101.06	-	101.47	100.84
ΣFe_2O_3	1.62	1.62	2.18	1.86	1.75	1.89
Fe^{++}/Fe^{+++}	2.12	2.38	2.26	-	0.17	0.25
K/Na	1.55	1.40	0.49	0.83	1.05	0.66
Na/Ca	2.07	1.97	1.86	2.30	2.87	2.09
Fe/Mg	6.06	5.37	3.42	4.31	5.20	4.38

TABLE B-6

Chemical Analyses and Elemental Ratios for Dolerite and Granite from the Glen View Quarry

	Dolerite										Granite					
	6293	6294	6295	6296	6298	6300	6301A	6301B	6310B	6305	6297	6299	6302	6303	6306	6310A
SiO_2	40.34	33.19	30.13	42.23	48.17	50.48	39.32	40.52	55.77	47.99	70.20	69.00	67.44	75.23	75.95	80.08
TiO_2	2.06	2.45	2.96	3.06	0.22	1.71	0.37	0.20	1.34	1.77	0.23	0.17	0.21	0.14	0.19	0.52
Al_2O_3	20.21	26.31	25.02	33.58	32.67	30.01	31.74	31.29	28.37	13.40	19.15	18.55	17.08	13.98	13.97	13.84
Fe_2O_3	9.67	17.43	22.50	1.22	1.51	1.04	-	-	-	2.29	2.13	0.74	1.19	0.82	0.51	-
FeO	5.01	0.17	0.12	0.05	0.07	<0.02[1]	-	-	-	10.96	0.21	0.07	0.09	0.55	1.05	-
MnO	0.12	0.03	0.02	0.01	<0.01	<0.01	<0.01	0.01	<0.01	0.22	0.01	<0.01	<0.01	0.02	0.02	<0.01
MgO	3.88	0.17	0.31	0.27	0.67	0.15	0.61	0.51	0.05	6.94	0.35	0.46	0.21	0.26	0.40	0.05
CaO	4.29	<0.01	<0.01	0.01	<0.01	<0.01	<0.01	<0.01	<0.01	11.47	<0.01	<0.01	<0.01	1.37	1.71	<0.01
Na_2O	0.59	0.04	0.05	0.13	0.71	0.16	2.31	1.67	0.52	1.70	0.04	0.83	0.88	2.84	3.03	0.40
K_2O	0.16	0.04	0.05	0.04	1.78	0.06	0.49	0.78	0.02	0.32	1.75	1.62	1.03	4.00	3.97	0.11
P_2O_5	0.17	0.14	0.03	<0.01	0.02	0.03	0.02	0.06	0.02	0.17	0.04	0.01	0.02	0.04	0.07	0.01
ΣH_2O	12.11	17.33	14.39	16.64	13.57	13.54	17.87	15.33	11.73	1.57	6.78	8.23	7.58	0.78	0.46	5.63
CO_2	0.02	0.12	0.21	0.16	0.06	<0.01	0.26	0.26	0.10	0.07	0.27	0.21	0.21	0.11	0.13	0.10
Total	98.63	97.42	95.79	97.40	99.45	97.18	-	-	-	98.87	101.16	99.89	95.94	100.14	101.46	-
ΣFe_2O_3	15.24	17.62	22.63	1.28	1.59	1.04	0.72	4.91	0.83	14.47	2.36	0.81	1.29	1.43	1.68	0.49
Fe^{++}/Fe^{+++}	0.58	0.01	0.006	0.05	0.05	-	-	-	-	5.32	0.11	0.11	0.08	0.75	2.29	-
K/Na	0.30	1.12	1.12	0.34	2.81	0.42	0.24	0.52	0.04	0.21	49.0	2.18	1.31	1.58	1.47	0.31
Na/Ca	0.14	-	-	13.5	-	-	-	-	-	0.15	-	-	-	2.15	1.84	-
Fe/Mg	4.55	120	84.7	5.50	2.75	8.04	1.37	11.2	19.2	2.42	7.82	2.04	7.12	6.38	4.87	11.4

[1] FeO below detection

TABLE B-7

Chemical Analyses and Elemental Ratios for Koolanooka Porphyry and Altered Variants

	6311	6316	6317	6319	6321	6322	6324	6325	6328	6330	6331	6332	6334	6335	6336	6337	6343	6347	6348	6351	6352	6353
SiO_2	79.38	79.42	74.98	80.06	76.35	72.05	94.26	71.75	73.08	74.58	72.27	80.44	78.52	74.79	94.28	76.46	76.83	76.36	77.36	77.16	77.50	77.39
TiO_2	0.06	0.07	0.08	0.06	0.06	0.09	0.84	0.25	1.12	0.36	0.64	0.14	0.17	0.14	0.90	0.18	0.17	0.18	0.13	0.12	0.12	0.14
Al_2O_3	11.50	11.12	10.61	11.22	10.62	10.74	2.33	19.46	16.86	16.47	18.19	13.01	13.28	14.70	2.03	11.52	11.98	11.47	11.58	11.42	11.84	11.73
Fe_2O_3	0.30	1.02	4.96	0.98	4.47	7.94	1.38	0.18	-	0.19	-	0.71	-	-	0.16	0.87	-	0.91	0.73	0.83	1.18	1.17
FeO	0.23	0.18	0.21	0.16	0.18	0.17	0.22	0.10	-	0.04	-	0.06	-	<0.04	0.06	0.89	-	0.72	0.82	0.71	0.24	0.46
MnO	0.01	<0.01	0.01	0.01	0.01	0.01	<0.01	0.01	0.01	<0.01	<0.01	<0.01	<0.01	<0.01	<0.01	0.03	0.02	0.02	0.03	0.03	0.02	0.02
MgO	0.03	0.02	0.08	0.05	0.07	0.02	<0.01	<0.01	<0.01	0.22	0.04	0.02	<0.01	0.16	<0.01	0.09	0.07	0.08	0.11	0.20	0.07	0.09
CaO	0.33	0.25	0.22	0.28	0.22	0.12	<0.01	0.01	<0.01	<0.01	0.01	0.01	<0.01	<0.01	<0.01	0.92	0.59	0.63	0.75	0.66	0.46	0.48
Na_2O	2.31	2.00	1.51	1.70	1.66	0.87	0.01	0.03	0.44	0.83	0.44	0.07	0.12	0.61	0.02	2.38	2.07	2.21	2.20	2.85	2.14	2.28
K_2O	4.73	4.68	3.95	4.70	4.35	3.62	0.01	0.13	0.11	0.18	0.09	0.04	0.06	0.58	0.03	4.88	4.99	4.84	4.84	4.87	4.98	4.92
P_2O_5	0.01	0.02	0.02	0.01	<0.01	0.01	<0.01	0.01	0.01	0.01	0.01	<0.01	<0.01	<0.01	<0.01	0.04	0.05	0.38	0.03	0.04	0.02	0.03
ΣH_2O	0.44	1.23	2.53	-	2.32	4.28	1.11	6.72	7.75	7.37	7.25	4.73	5.48	6.88	0.99	0.17	-	0.83	0.31	-	0.44	0.70
CO_2	0.06	0.21	0.34	-	0.07	0.30	0.22	0.20	0.38	0.17	0.34	0.04	0.52	0.23	0.13	0.09	-	0.20	0.06	-	0.10	0.06
Total	99.39	100.22	99.50	-	100.38	100.22	100.38	98.85	-	100.42	-	99.27	-	-	98.60	98.52		98.83	98.95		99.11	99.47
ΣFe_2O_3	0.55	1.22	5.19	1.16	4.67	8.13	1.63	0.29	0.34	0.24	0.31	0.78	0.82	0.53	0.22	1.86	1.52	1.71	1.64	1.62	1.44	1.68
Fe^{++}/Fe^{+++}	0.85	0.20	0.05	0.18	0.04	0.02	0.18	0.62	-	0.23	-	0.09	-	-	0.42	1.14	-	0.88	1.25	0.95	0.23	0.44
K/Na	2.29	2.62	2.93	3.09	2.93	4.66	1.12	4.85	0.28	0.24	0.23	0.64	0.56	1.06	1.68	2.29	2.70	2.45	2.46	1.91	2.60	2.41
Na/Ca	7.27	8.30	7.13	6.30	7.83	7.53	-	3.11	-	-	45.7	7.3	-	-	-	2.69	3.64	3.64	3.05	4.48	4.83	4.93
Fe/Mg	21.3	70.7	75.2	26.9	77.4	471	-	-	-	1.27	8.98	45.2	-	3.84	-	24.0	25.2	24.8	17.3	9.39	23.9	21.6

APPENDIX C

ANALYTICAL PROCEDURES

C.1 SAMPLE PREPARATION

C.1.1 Snowy Mountains Region, N.S.W.

Three diamond drill cores were obtained from the Snowy Mountains Authority, SMA DH 2401, DH 2511 and DH 2660 (see Appendix A). These were chosen to represent different chemical compositions and the most complete percentage recovery of core from the critical weathered zones. Core recovery is incomplete in all cores studied from this region.

Core footage was selected at five foot intervals but if core gaps were present at the specified sampling point the closest footage was taken. Sample sizes were in the range 1½-2 Kg.

Samples were passed through both coarse and fine jaw crushers. All samples were passed through the fine jaw crusher twice ensuring that all material was less than 1 cm in size. The sample was then quartered and two separate fractions taken.

The first fraction of less than 100 g was crushed in a Siebe Technik tungsten carbide vibratory grinding mill until a uniform fine powder (~40 microns) was obtained. This comprised the bulk chemical sample used for all determinations other than γ-ray spectrometry.

The second fraction of approximately 700 g was passed between revolving steel plates effectively reducing the grainsize to that of a coarse sand. This sample was then used for gamma-ray spectrometric determination of Th, U and K.

The remaining sample was set aside in plastic bags. The crushing procedure employed will give Fe and Mn contamination from the jaw crushers and W, Mo, Co and Ni from the tungsten carbide mill. Levels of Fe and Mn contamination will not be significant for the interpretation of the results obtained in this work.* The other elements contributed by the Siebe Technik mill were not determined in this study. The large size of the γ-ray spectrometric sample minimises any minor contamination.

C.1.2 West Australia

Only one diamond drill core, (Mertondale DDH.1) was sampled following procedures described previously, although limited footage and irregular sections prevented use of a regular sampling interval.

---

*Lambert (1967) and Gulson (1968) independently checked for Fe and Mn contamination from the jaw crushers, Lambert (1967) found contamination insignificant and Gulson (1968) undetectable.

All other samples were from surface outcrop, from quarries and clay pits or small cliff erosion profiles exposed along dry watercourses.

Bulk chemical analysis samples were prepared as previously described. However, γ-ray spectrometric samples were passed through a roller mill in place of the rotating steel plates to reduce contamination levels. After measurements by γ-ray spectrometry the large sample was used for mineral separations for the small number of minerals analysed.

C.2 CHEMISTRY - X-RAY FLUORESCENCE SPECTROMETRY

Samples were analysed for major elements by the following techniques: Si, Al, Ti, Mn, total Fe as Fe_2O_3, Mg, Ca, K and P by X-ray fluorescence spectrometry (Norrish and Chappell, 1967; Norrish and Hutton, 1969); Fe^{++} following the method of Kiss (1967) using end point detection by voltametry with Pt/Pt-Rh (20%) electrode system in conjunction with a Metrohm automatic potentiograph; Na by flame photometry (Cooper, 1963); total H_2O and CO_2 by heating in a tube furnace at 1150°C for 30 minutes in a stream of dry argon (Riley, 1958); H_2O^- as weight loss after heating for two hours at 110°C, and K additionally by gamma-ray spectrometry (see section C.3, this Appendix).

Potassium was determined by X.R.F. only for West Australian samples; all remaining K determinations were measured by gamma-ray spectrometry.

Crushed rock powders were fused with a lithium tetraborate flux and cast as glass discs. This preparation removes grain-size problems, minimizes matrix effects (by dilution) and yields a sample with minimum surface area to volume relationships. The last mentioned fact is important and reduces H_2O and CO_2 absorption by the glass. Fusion discs had been considered stable and satisfactory for analysis until one year after preparation (K. Norrish, pers. comm.). However, preparation and measurement of fusion discs of standards and unknown samples should be made within one month (B. Chappell, pers. comm.). Irregular totals, especially for Khancoban granite analyses (Table B-3, Appendix B) reflect this previously unsuspected effect. West Australian analyses have been measured relative to standard FS 28 obtained from Dr K. Norrish, C.S.I.R.O., Division of Soils, Adelaide, S.A. Earlier analyses were calibrated against recommended values for rock standards (Table C-1).

Trace elements Rb, Sr, Pb, Ba, Y and Zr were also determined by X.R.F., employing techniques outlined by Norrish and Hutton (1964) and Norrish and Chappell (1967).

Table C-1

Standards used for X-ray fluorescence spectrometry

Oxide/Element	Standard	Accepted Value[1]
SiO_2	G-1	72.52%
Al_2O_3	W-1	14.94%
TiO_2	W-1	1.08%
Fe_2O_3[2]	W-1	11.10%
MnO	W-1	0.17%
MgO	W-1	6.52%
CaO	W-1	10.92%
P_2O_5	Phosphate Rock	34.4 %
Rb[3]	G-1	210 ppm
Sr[3]	G-1	247 ppm
Pb	G-1	49 ppm
Ba[4]	G-1	1030 ppm
Zr	G-1	210 ppm
Y	G-1	13 ppm

1. Major oxides and trace elements based on values of Fleischer (1965)
2. Total Fe as Fe_2O_3
3. Rb and Sr based on isotope dilution analyses (W. Compston, Department of Geophysics and Geochemistry, ANU)
4. Ba based on value from K. Norrish (pers. comm.)

Corrections for counting losses, spectral interferences, X-ray tube contaminants, non-linear backgrounds and absorption by the sample have been made. In general, counts were accumulated for 200 seconds on the K_α line and for 100 seconds at each of two background positions, on either side of the peak position. All trace element determinations (with the exception of U and Th measurements by X.R.F. (see Appendix E)) were made on PW 1540 Phillips manual spectrometer necessitating tail corrections between adjacent peaks (i.e. Rb and Sr).

Collimators used on the PW 1540 spectrometer contain Pb and corrections have been applied which were derived from measuring apparent Pb contents in pure SiO_2 Herasil glass. Mass absorption coefficients have been measured directly for all trace elements other than Ba which was determined by the peak to background method. Lower limits of detection for elements determined by X.R.F. employing all correction procedures are listed in Table C-2. A granitic composition (G-1) has slightly lower limits of detection than a diabase composition (W-1) as a result of the influence of A (the mass absorption coefficient). All values are calculated for a standardised counting time of peak = 200 seconds and backgrounds = 100 seconds each. The value of LLD may be lowered by increased counting times or by increasing the value of m (see Table C-2).

Table C-2

X.R.F. lower limits of detection (LLD)[1] for trace elements (ppm)

	Sr	Rb	Pb	Y	Zr
G-1	0.4	0.4	1.9	1.2	2.3
W-1	0.5	0.5	2.0	1.2	2.3

1. LLD = $\frac{4}{m}\sqrt{Cb/T}$ where m = cps. ppm^{-1}

Cb = cps at the background position and

T = total analysis time split equally between background and peak. Estimate of LLD is ± 2 standard deviations.

Replicate analyses were determined on separate pellets of each standard and are listed in Table C-3. The number of determinations is indicated below values for the mean and standard deviation. Only four determinations of Rb and Sr in GSP-1 were made.

Computer programs were written for correction procedures by the author, however Dr P. Arriens has written programs for Rb and Sr measurements. These programs were used for X-ray fluorescence and isotope dilution analyses of Rb and Sr. Dr K. Norrish (C.S.I.R.O., Division of Soils, Adelaide) supplied a program for major element absorption corrections.

C.3 GAMMA-RAY SPECTROMETRY

Potassium, uranium and thorium were determined by γ-ray spectrometry using essentially the method described by Whitfield *et al*. (1959) and Heier and Rogers (1963). Uranium and thorium are determined indirectly assuming that radioactive equilibrium exists in both decay series for all samples.

Thorium was determined from the 2.62 MeV peak (the Tl^{208} photo peak in the thorium-232 series), uranium from the 1.76 MeV peak (the Bi^{214} photo peak of the uranium-238 series) and potassium from the 1.47 MeV photo peak.

Table C-3

X.R.F. precision estimates based on replicate analyses of separate pellets of standard rocks

Standard Rock	Element					
	Rb ppm	Sr ppm	Pb ppm	Ba ppm	Zr ppm	Y ppm
G-1[1]	210	247	49	1030	210	13
W-1	22.1±0.2	187±0.6	8.1±1.1	198± 6.2	92±1.1	29.5±1.5
G-2	169 ±0.4	472±1.9	33.6±0.8	1738±16	307±3.6	9.2±0.4
AGV-1	67.4±0.4	650±2.0	36.7±1.0	1195±12	233±4.0	23.2±1.3
GSP-1	248	232	60.7±1.5	1255±10	521±5.1	29.7±0.9
BCR-1	47.0±0.3	322±0.9	15.8±0.6	734± 8.3	189±2.2	48.4±2.3
PCC-1	-	-	8.1±1.0	-	-	-
DTS-1	-	-	8.7±1.0	-	-	-
S-1	-	-	-	315± 6.9	3095±15.7	600 ±34
Number of determinations						
W-1	24	24	18	25	10	19
G-2	18	18	16	29	14	19
AGV-1	19	19	17	22	12	13
GSP-1	4	4	17	23	13	10
BCR-1	18	18	17	24	13	18
PCC-1	-	-	17	-	-	-
DTS-1	-	-	17	-	-	-
S-1	-	-	-	5	10	10

1. Accepted values for G-1 (see Table C-1)

A 5" x 4" Tl activated NaI crystal with photomultiplier and a 200 channel model 34-8 R.I.D.L. pulse height analyser with typewriter readout was used. Later the 5" detector crystal was linked to a 400 channel model 24-2 R.I.D.L. pulse height analyser with Punch-type matrix 99-24A; ADC model 23-4 and an I.B.M. typewriter output.

K was standardised against Analar KBr and U and Th against standards of known U and Th concentrations supplied by the American Atomic Energy Commission.

All crushed samples were packed into perspex containers, sealed and left for at least two weeks prior to measurement. All samples were counted twice, a few being measured up to four times and the average of all determinations taken. Two standards, U.S.G.S. samples G-2 and AGV-1, were run at regular intervals as monitor standards and to check calibration of the equipment.

Morgan and Heier (1966) compared γ-ray spectrometric and neutron activation analyses of Th and U on the U.S.G.S. standards AGV-1, BCR-1 and G-2. A composite table of their results and those of the author is given in Table C-4.

The limits quoted for γ-ray determinations are for one standard deviation calculated from repetitive measurements on the same sample.

Table C-4

Sample	Uranium p.p.m.			Thorium p.p.m.		
	N.A	γ-ray	This work γ-ray	N.A	γ-ray	This work γ-ray
AGV-1	2.17	1.9±0.2	1.8±0.1*	6.47	6.4±0.4	6.4±0.2*
BCR-1	1.81	1.6±0.1		6.00	6.1±0.4	
G-2	2.16	2.1±0.3	2.0±0.1+	24.1	25.7±0.5	25.8±0.6+

*Number of determinations, n = 20

+Number of determinations, n = 16

C.4 Rb-Sr ANALYSIS BY ISOTOPE DILUTION

All samples analysed by isotope dilution, except for three biotites, were analysed beforehand by X-ray fluorescence spectrometry and the results used to determine sample size and the most suitable tracer.

Rubidium and strontium were separated from bulk rock powders using the method of Compston et al. (1965) with minor alterations. Sample size varied from 0.5 to 1.0 g but for samples with low Rb and Sr contents larger amounts of sample were processed. For samples containing less than 10 ppm Rb and low Sr, separate dissolutions were used for Rb and Sr and a double tracer (Sr^{84} and Sr^{86}) used for Sr determinations. For low level Sr samples a small amount of radioactive $*Sr^{85}$ yield tracer was added and used to monitor the ion-exchange process. In all other cases a single tracer Sr^{84} was used.

The volume of perchloric acid used was kept to a minimum (0.5 - 1.0 ml) as this reagent has the highest blank.

For samples with low (<5 ppm) Rb, the alkalis were separated initially from the bulk of the sample by hydroxide precipitation following the method of Chappell et al. (1969).

Rb and Sr blanks were measured and found to be 0.0095 µg per dissolution for Rb and 0.0169 µg per dissolution for Sr. These values were measured for the largest reagent volumes used for a dissolution, and for the complete analytical procedure followed. Hence, these are total blanks for the largest amount of contamination expected. For a dissolution of 0.7 g the calculated blank values, based on individual measured reagent blanks, were 0.0022 μg per dissolution Rb and 0.0138 μg per dissolution Sr. Whenever the ratio of blank to sample exceeds 0.5% for Sr and 0.1% for Rb, blank corrections have been made to the measured concentrations and the Sr^{87}/Sr^{86} variance. The blank variability has been assessed in variance estimates for the Sr^{87}/Sr^{86} value for each sample following the method of Compston and Chappell (in preparation).

All samples were run as chlorides using a triple rhenium filament technique.

Strontium isotope ratios and isotope dilution analyses were measured using a twelve-inch 60 degree sector mass-spectrometer, with Faraday-cup collector, vibrating reed electrometer and digital output, under the following operating conditions: Sr^{88} beam intensity at least 2×10^{-11} amperes; Rb^{87} not more than 2 per cent of the total mass 87; cross-contamination under mass 87 less than 0.02% of mass 87; and coefficient of variation for a single ratio observation, better than 0.03 per cent.

Data were taken by magnet-field switching and reduced as described by Arriens and Compston (1968). Sr^{87}/Sr^{86} was normalized to 8.3752 for Sr^{88}/Sr^{86}. The ratio of normal Rb^{85}/Rb^{87} was taken as 2.600 (Shields and Garner, 1963) and the decay constant (λ) used for Rb^{87} is 1.39 x 10^{-11}yr (Aldrich et al., 1956). Rubidium isotope dilution analyses were measured using a six inch 90 degree sector mass spectrometer, with Faraday-cup collector, vibrating reed electrometer and digital output. Beam intensities varied from 2 to 7 x 10^{-11} amperes and the coefficient of variation for a single ratio observation was better than 0.08 per cent.

C.5 ALPHA-SPECTROMETRIC ANALYSIS

Analytical procedures are based on those of Ku (1965) and Rosholt et al. (1966) with minor modifications. Sample size ranged from 5 to 12 gms using the gamma-ray spectrometric determinations as an approximate guide to the Th and U concentrations.

Measurement of uranium isotopes was made by an isotope dilution technique using a U^{232} tracer calibrated gravimetrically against a uranium salt. Activity ratios were determined by alpha-particle spectrometric analysis. Separation and purification of U was achieved by ion exchange and solvent extraction procedures.

The samples were completely dissolved in HF, HCL and HNO_3 and the U^{232} tracer (100λ) added. Evaporation to dryness with $HClO_4$ ensured equilibration between the tracer and U in the sample. This was followed by dissolution in 8N HCl and loading onto an anion exchange column (Dowex AG-1x8, 100-200 mesh). The uranium was eluted from the column with water and further purified from iron by isopropyl ether extraction. After conversion to the nitrate form, the sample was dissolved in a saturated $Al(NO_3)_3$ solution and a hexone (iso-butyl methyl ketone) extraction carried out. The uranium is stripped from the nitrate phase into the hexone and then back extracted into the aqueous phase. The processed U was further purified by an additional ether extraction if any iron was present and then loaded in 8N HCl onto a small anion exchange column (Dowex AG-1x8). The final elutant, after destruction of any organic matter with HNO_3 and $HClO_4$ is dissolved in 2N NH_4Cl, adjusted to a pH of 2.2 and electroplated at 8V for 30 minutes, on stainless steel planchets. Each planchet is washed with acetone and briefly flamed after electroplating and prior to counting.

The electroplated samples were counted by an alpha spectrometer consisting of a silicon diode solid-state detector (ORTEC), a low noise amplifier system (ORTEC 101/201), and a 400 channel model 24-2 R.I.D.L. pulse height analyser with typewriter readout.

Alpha resolution of the detector and counting system used in this study was within 60 keV. The isotopic composition was determined directly from integrating all counts under the peaks of the α-particle energy spectrum. The background was negligible and a minimum of 10^4 counts for the smallest peak was counted in all cases usually requiring counting times of 2-4 days. A majority of analyses accumulated 2 x 10^4 counts. The U content of U.S.G.S. standard G-2 was determined at 1.97 ppm with a U^{234}/U^{238} ratio indistinguishable from unity (H. Veeh, pers. comm.).

APPENDIX D

COMPARISON OF RUBIDIUM AND STRONTIUM RESULTS OBTAINED BY X-RAY FLUORESCENCE SPECTROMETRY AND ISOTOPE DILUTION

Comparisons of Rb and Sr values are listed in Table D-1, and displayed in figures D-1 and 2. All comparisons are for total rock samples.

There is good agreement between the two methods for Rb over the concentration range 350 ppm - > 10 ppm (Fig. D-1). The small degree of scatter about the 45° equivalence line is due to slight variations in the calibration of the XRF data as the samples were processed in batches, each being calibrated separately. Below 10 ppm agreement is less ideal and can be attributed to three factors.

1. Imprecision due to low count rates. Longer counting times would improve the precision and extend the limit of detection.
2. Virtually all samples (excluding 6336) with less than 50 ppm Rb are clays with variable water content which will adjust to atmospheric humidity during sample preparation. Consequently the mass

Table D-1

Comparison of rubidium and strontium results
obtained by X-ray fluorescence spectrometry
and isotope dilution

Sample	Rb		Sr	
	XRF	ID	XRF	ID
6280	12.6	13.1	18.9	19.6
6281	15.1	15.9	5.3	7.0
6283	122	120	3.7	4.5
6288	98.1	96.8	6.1	7.0
6357	10.0	10.8	16.4	17.5
6359	69.6	68.2	3.4	4.4
6364	167	164	3.8	4.9
6368	110	109	17.6	17.7
6263	79.6	80.9	407	421
6265	189	191	304	313
6267	108	109	371	382
6270	140	141	374	383
6277	92.9	93.1	367	380
6208	66.3	63.2	25.6	25.9
6315	321	320	12.7	14.2
6321	339	344	12.3	13.7
6322	292	294	6.6	7.9
6325	21.8	22.3	3.3	4.3
6326	13.3	13.2	4.0	4.8
6328	6.8	7.7	0.99	1.7
6329	7.5	8.1	12.0	12.9
6330	17.5	17.6	12.1	13.4
6331	10.5	12.0	9.6	10.5
6332	2.9	3.9	8.3	8.9
6333	3.0	3.9	5.1	5.5
6335	47.0	48.4	1.7	2.3
6336	5.0	4.2	1.1	2.5
6343	207	210	43.4	46.5
6348	245	250	28.7	31.7
6351	236	242	27.1	30.2
6352	261	265	27.2	30.4
5646A	141	138	120	124

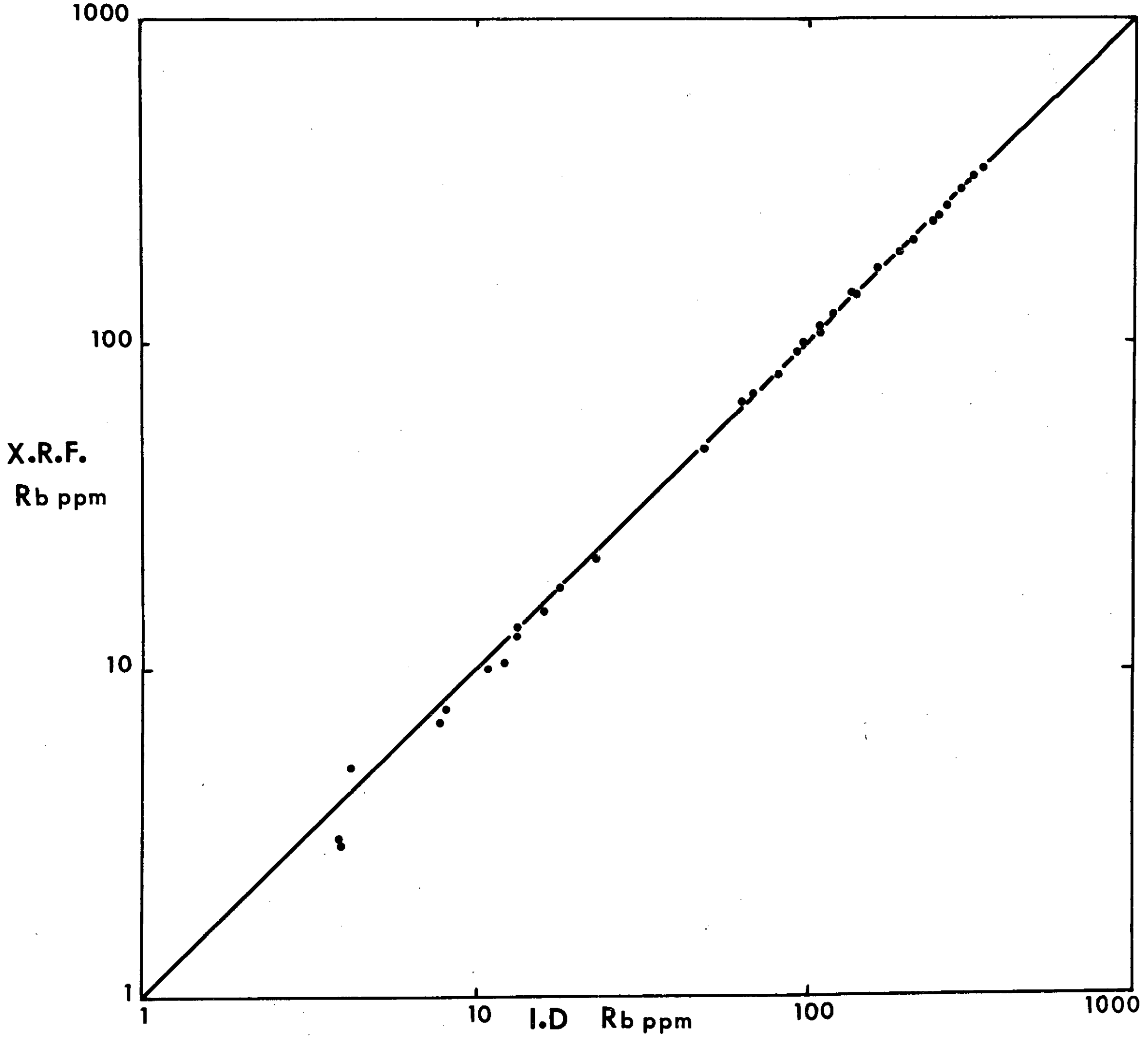

Fig. D-1 Comparison of Rb determinations by X.R.F. and I.D.

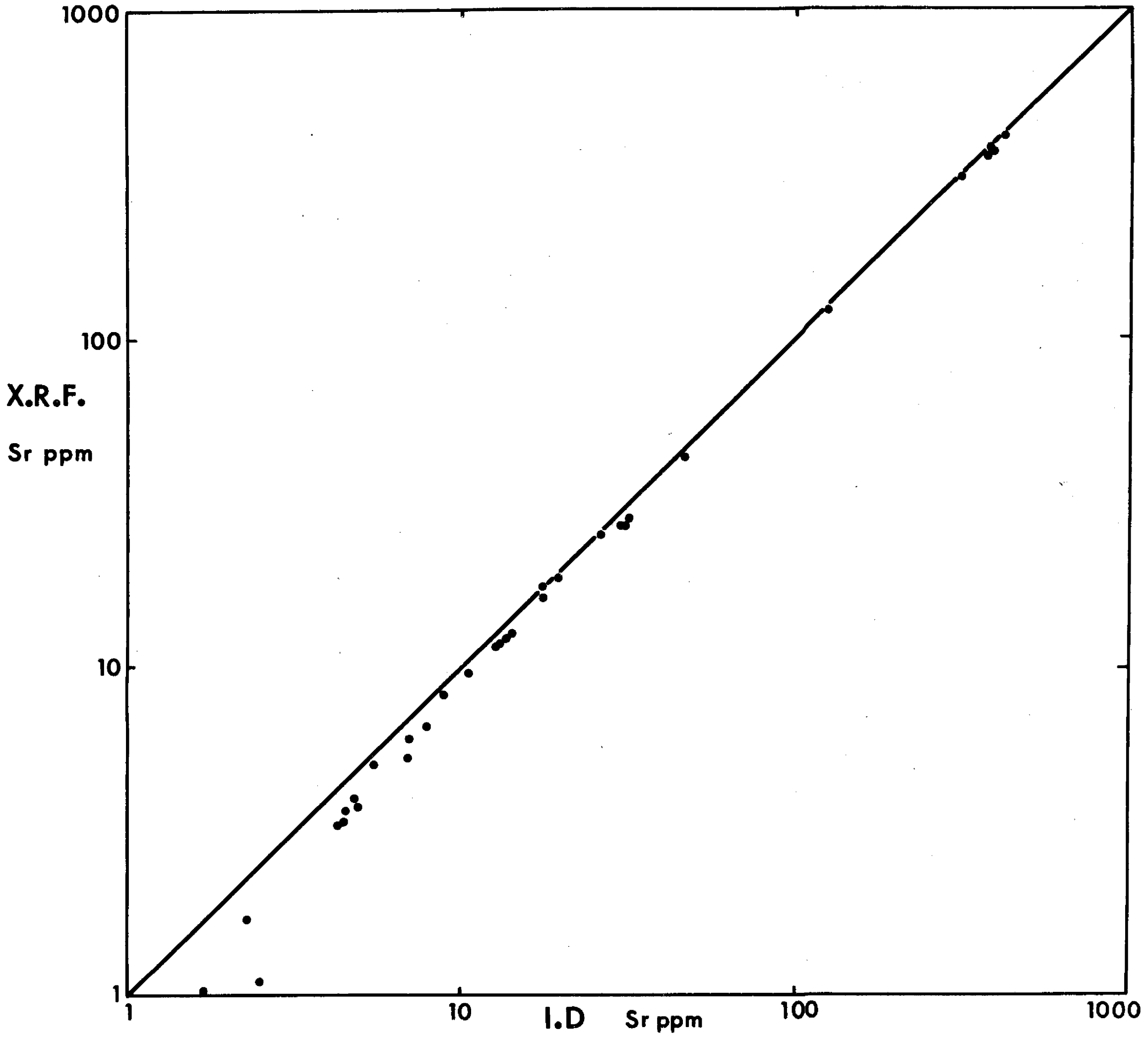

Fig. D-2 Comparison of Sr determinations by X.R.F. and I.D.

absorption coefficient for XRF procedures will vary and the weighing error for isotope dilution will be variable.

3. Blank corrections for isotopic dilution procedures vary and their significance increases for lower concentrations. (If the ratio of blank determined to sample handled exceeds 0.1% for Rb, and 0.5% for Sr, blank corrections have been applied.)

Fig. D-2 relates Sr concentrations determined by the two methods. After allowance has been made for the factors just discussed, a systematic difference exists over the range 5 to 500 ppm. Blank corrections have been applied for samples whose f_c exceeds or equals 0.5% but these are not of sufficient magnitude to shift points back to the 45^o equivalence line. The XRF determinations are regarded as systematically lower than the I.D. values due to calibration error. Below 5 ppm Sr, error in tail corrections (a feature of the resolution of the Phillips PW 1540 X-ray spectrometer and the LiF (200) crystal combination), coupled with possible error in assessment of backgrounds may combine to produce apparently much lower Sr values.

APPENDIX E

COMPARISON OF THORIUM AND URANIUM CONCENTRATIONS DETERMINED BY X-RAY FLUORESCENCE, GAMMA-RAY AND ALPHA SPECTROMETRY

Values of U and Th are given in Table E-1 and displayed in Figures E-1, E-2 and E-3. The lower limit of detection for gamma-ray spectrometry is approximately 0.1 ppm for U and 0.5 ppm for Th employing counting times not exceeding 40 hours. Although counting statistics may be improved by counting for longer periods, background fluctuations become significant. Counting statistics likewise impose detection limits on measurements by X-ray fluorescence spectrometry (X.R.F.). The statistical lower limit of detection (L.L.D.) is given by the relationship:

L.L.D. ($\pm$ 2 standard deviations) $= 4/m \sqrt{C_b/T}$

where, m = cnts sec^{-1} ppm^{-1}; C_b = average background cnts sec^{-1} and T = total counting time split equally between peak and background measurements. The L.L.D. in this study by X.R.F. for both elements is

U = 0.5 ppm and Th = 0.6 ppm for T = 800 secs.

The lower level of detection by alpha spectrometry is several orders of magnitude lower. The technique

Table E-1

Comparison of uranium and thorium determinations by X-ray fluorescence, gamma-ray and alpha spectrometry

Sample No.	Thorium			Uranium		
	XRF	γ-ray	α-spec	XRF	γ-ray	α-spec
6280	8.7	8.5	-	1.4	0.9	-
6281	13.6	11.9	-	1.9	1.0	-
6282	8.3	8.6	-	1.5	2.6	1.5
6292	6.8	7.2	-	1.4	1.7	-
6293	0.2	1.1	-	8.6	2.1	8.9
6294	2.7	3.2	-	16.2	9.2	14.7
6295	8.4	8.1	-	13.2	10.7	12.9
6296	4.8	5.7	-	11.7	12.3	10.7
6298	25.6	22.4	-	2.8	3.1	2.9
6299	19.4	17.5	-	2.3	1.4	2.2
6302	27.4	25.0	-	4.8	5.4	4.9
6305	0.7	0.5	-	1.1	0.2	0.23
6306	21.9	23.2	-	6.9	6.6	6.2
6309	32.5	34.1	-	19.6	17.2	16.2
6356	9.5	9.6	-	1.4	1.2	-
6009	6.3	7.9	-	1.6	1.2	1.8
6127	4.2)) 3.7[1])	3.7	-	2.3)) 1.3)	0.8	-
6014	5.1	5.3	5.4	1.8	1.4	1.7
6017	4.3	5.0	-	2.9	1.1	-
6019	-	3.5	-	-	1.0	1.1
6021	-	4.7	4.5	-	1.2	1.5
6032	4.3	4.5	-	2.5	1.5	-
6033	3.1	2.3	-	0.8	0.8	-
6056	4.3	4.0	-	2.6	1.6	-
6058	1.8	2.2	-	1.3	0.8	-

Continued on next page

Table E-1 (Continued)

Comparison of uranium and thorium determinations by X-ray fluorescence, gamma-ray and alpha spectrometry

Sample No.	Thorium			Uranium		
	XRF	γ-ray	α-spec	XRF	γ-ray	α-spec
6064	4.4 2.7[1]	3.8	-	1.8 1.5[1]	1.5	-
6066	16.4	17.0	-	5.1 6.3	5.3	
6068	15.2	17.4	-	5.9	6.6	-
6079	15.1	14.6	-	3.9	3.6	4.4
6089	17.8 16.7[1]	17.3	-	5.3 5.0[1]	4.9	-
6098	17.9	17.8	-	5.2	4.6	-
6107	17.8	17.7 16.4	-	2.5	2.0	-
6116	19.1	18.2	-	7.6	7.7	-
6120	17.0	18.4	-	6.0	4.6	-
6125	16.4	15.7	-	5.3	4.0	-
6130	19.8	18.3	-	5.8	3.5	-
6132	15.9	15.4	-	4.7	2.5	-
6133	16.2 17.8[1]	17.7	-	4.3 5.5[1]	2.9	5.7
6134	16.5	18.1	-	2.2	1.8	-
6135	21.3	21.4	-	4.8	3.6	-
6137	15.4 15.7[1]	16.2	-	3.5 4.6[1]	2.9	-
6170	-	17.4	-	-	2.6	3.3
6184	-	17.6	16.4	-	3.0	4.0
6088	-	17.0	-	-	5.2	6.0

---

[1] Replicate analyses on separate pellets.

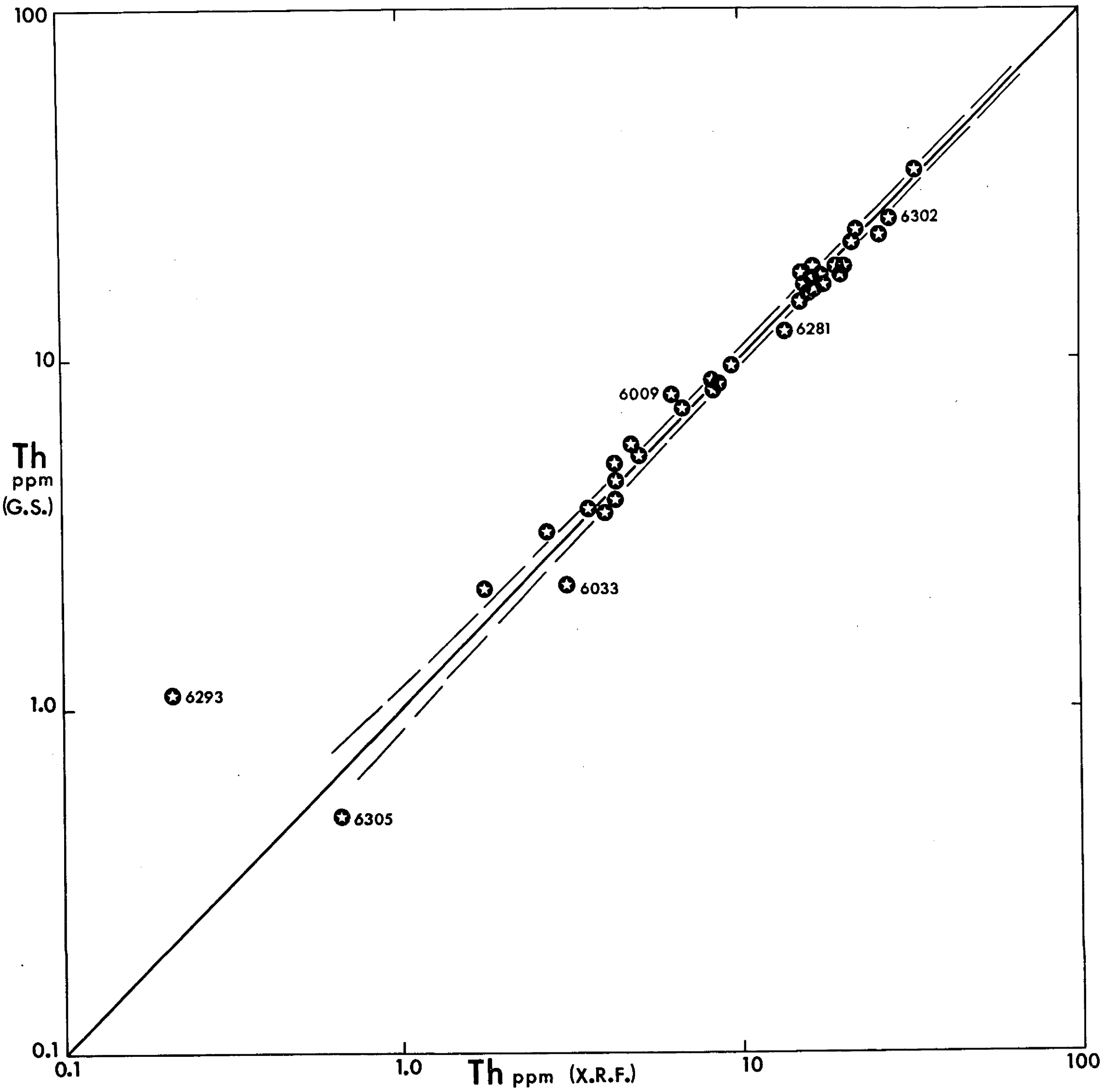

Fig. E-1 Comparison of Th determinations by X.R.F. and gamma-ray spectrometry (G.S.).

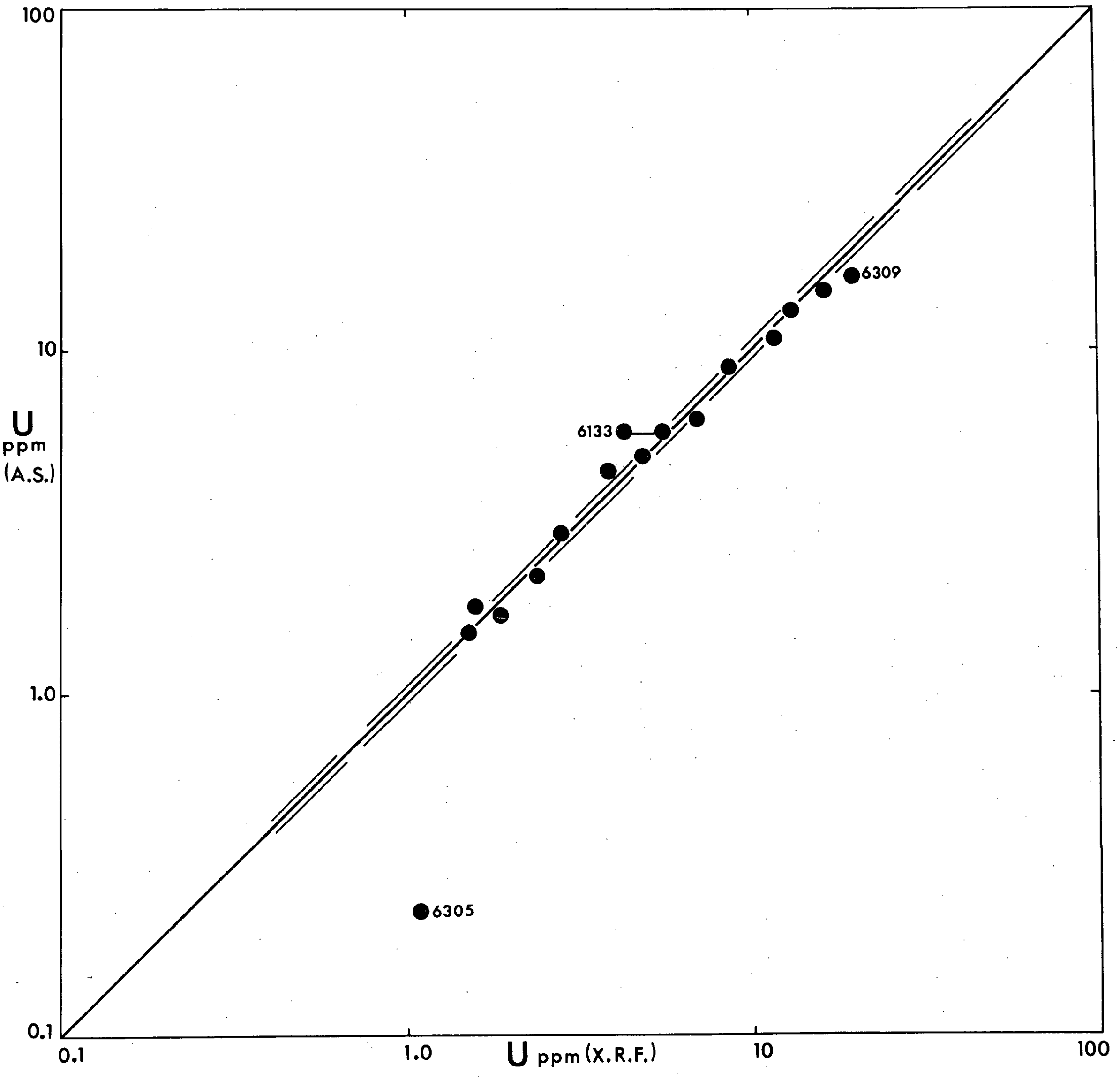

Fig. E-2 Comparison of U determinations by X.R.F. and alpha-spectrometry (A.S.).

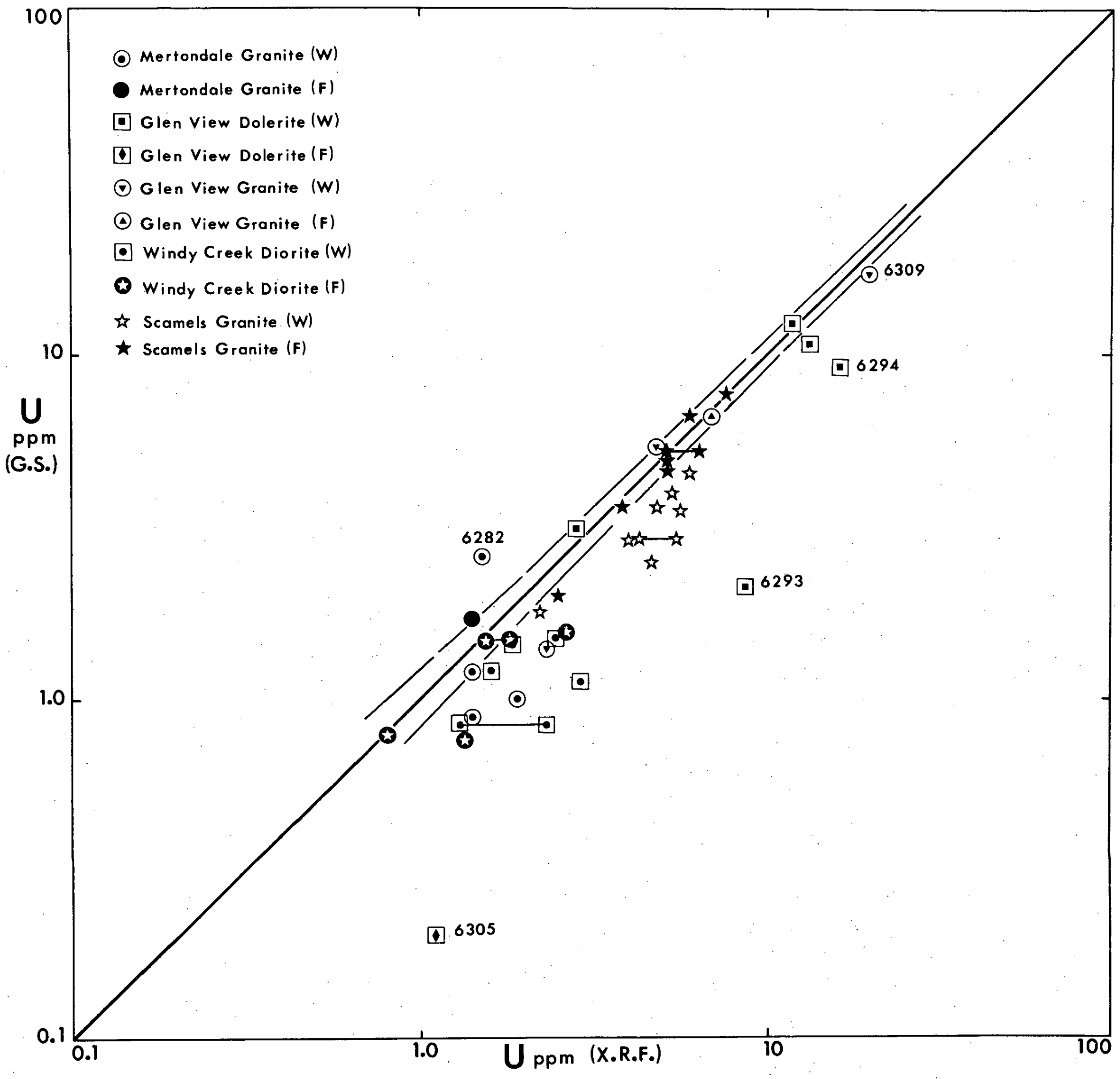

Fig. E-3 Comparison of U determinations by X.R.F. and gamma-ray spectrometry (G.S.).

used (Ku, 1965) involves isotope dilution and has much higher sensitivity.

A comparison of Th concentrations determined by gamma-ray and X.R.F. (Fig. E-1) reveals good agreement for concentrations above 3 ppm. Limiting values shown on Fig. E-1 have been derived from precision estimates of Th determinations by gamma-ray spectrometry for USGS standards G-2 and AGV-1 (± 2 standard deviations). At 1 ppm Th the precision is probably ± 10% rapidly deteriorating with decreasing Th contents. Replicate analyses by gamma-ray spectrometry on the same sample are indicated by a vertical line joining the two values while replicate analyses on separate pellets of the same sample by X.R.F. are indicated by a horizontal line connecting each determination.

Sample 6305 may be considered to lie within the expected precision limits when consideration has been given to both sampling errors and the restrictions of the L.L.D. inherent in both X.R.F. and gamma-ray analyses. Sampling error in addition to counting statistics has caused the variation in X.R.F. values shown by samples 6127, 6064 and 6133. (Nearly all thorium and uranium contents were determined from replicate analyses on duplicate pellets by X.R.F.)

Sample 6293 is clearly deviant from the 45° equivalence line. In addition to sampling error and counting statistics, lack of equilibrium in the Th^{232} series may cause the displacement of this data point.

There are insufficient Th determinations by alpha spectrometry to permit comparison with either X.R.F. or gamma-ray measurements. However, agreement is within ± 10% (Table E-1).

Both alpha spectrometric and gamma-ray spectrometric U values have been plotted against X.R.F. values in Figs. E-2 and E-3. Despite the smaller number of alpha spectrometric analyses agreement is good within the range 1 ppm to 14 ppm (Fig. E-2). At higher concentrations, alpha spectrometric analyses are lower than X.R.F. concentrations, suggesting incomplete dissolution of uranium bearing minerals (i.e. zircon). Below 1 ppm U, X.R.F. precision is poor. Two replicate analyses of separate pellets of sample 6133 illustrate the influence of sampling error and counting statistics. Error limits of ± 5% are indicated in Fig. E-2.

Uranium determinations by gamma-ray spectrometry are subject to disequilibrium uncertainties

(Chapter 11). However, comparison with X.R.F. values reveals good agreement (± 2 standard deviations) for fresh rock samples (Fig. E-3) with values above 2 ppm U. These precision estimates are from USGS standards, G-2 and AGV-1, by gamma-ray spectrometry. Practically all weathered samples have lower "gamma-ray U" contents, a result of disequilibrium in the U^{238} series (Chapter 11). The high gamma-ray U value for sample 6282 is also caused by disequilibrium. The anomalous X.R.F. value for sample 6305 (Table E-1) reflects sampling difficulties and poor counting statistics.

There is good agreement between X.R.F. and alpha spectrometric analyses except for very low concentrations where counting statistics, limits of detection and sampling error restrict X-ray analysis. Gamma-ray measurements and X.R.F. values show less correlation (Fig. E-3). Weathering processes initiate open system conditions destroying radioactive equilibrium in both the U^{238} and Th^{232} decay series. The assumption of radioactive equilibrium is fundamental to gamma-ray spectrometric analysis and consequently restricts the application of this method to fresh rock samples.

APPENDIX F

Trace element analyses and elemental ratios for samples:

(p.p.m.)[1]	Trace elements in parts per million, i.e. Rb^+ = Rb ppm etc.;
K^+(%)	K percent as metal determined by gamma-ray spectrometry;
eTh^{4+} and eU^{4+}	U ppm and Th ppm determined by gamma-ray spectrometry;
n.d.	not detected; - not determined.

TABLE F-1

Windy Creek Diorite, Geehi Damsite, N.S.W.

PART I: Trace Elements (p.p.m.)[1]

Sample	Rb^+	Ba^{2+}	K^+(%)	Pb^{2+}	Sr^{2+}	eTh^{4+}	eU^{4+}	Y^{3+}	Zr^{4+}
6009	54.3	291	0.88	n.d[1]	64.6	7.9	1.2	39.5	162
6127	44.0	295	0.96	1.5	127	3.7	0.84	30.5	65
6010	45.2	372	0.82	5.3	163	3.5	1.1	39.1	90
6011	41.0	423	1.03	7.2	174	4.1	1.1	32.5	81
6012	49.4	399	1.06	8.1	154	4.9	1.2	34.6	91
6013	46.6	429	1.13	8.3	194	4.5	1.3	35.8	95
6014	63.0	427	1.28	9.7	219	5.3	1.4	31.7	94
6015	60.0	385	1.19	2.6	242	4.7	1.0	33.7	76
6016	47.0	362	1.05	7.2	306	3.4	1.1	26.5	105
6017	37.9	335	0.94	7.9	300	5.0	1.1	27.3	72
6018	41.9	315	1.02	8.1	318	4.8	1.2	66.1	85
6019	35.5	336	0.90	6.1	385	3.5	0.97	26.3	208
6020	43.9	395	1.00	7.7	371	4.4	1.2	29.2	111
6021	29.0	315	0.81	5.9	320	4.7	1.2	24.5	109
6022	29.0	352	0.85	6.3	343	3.4	0.77	25.3	118
6023	26.8	338	0.77	6.2	340	4.1	1.2	33.3	108
6024	26.8	376	0.75	6.1	421	3.4	0.94	16.2	289
6025	44.4	357	0.89	5.6	374	3.2	1.2	30.5	144
6026	36.4	354	0.86	5.4	395	2.7	0.89	29.8	89
6027	27.9	388	0.82	6.9	423	3.3	0.99	37.3	102
6028	18.9	272	0.70	5.1	259	3.1	0.94	40.2	100
6029	29.4	336	0.67	3.9	384	3.1	0.80	35.3	102
6030	30.7	325	0.78	6.4	404	3.1	0.88	31.2	117
6031	24.8	313	0.67	6.4	341	4.3	1.1	34.9	120
6032	28.6	361	0.86	7.2	339	4.5	1.5	37.6	143
6033	23.2	366	0.79	6.3	366	2.3	0.79	46.2	69
6034	23.7	357	0.80	7.2	354	3.4	1.1	41.4	95
6035	26.0	377	0.83	6.1	369	2.9	1.1	42.9	81
6036	19.2	354	0.66	5.8	375	3.0	0.95	44.2	81
6037	27.8	417	0.86	7.4	409	3.7	1.1	30.4	149
6038	26.0	444	0.81	7.8	453	3.6	1.1	25.7	107
6039	22.7	341	0.73	6.8	412	3.9	1.1	37.7	197
6040	19.2	352	0.62	5.0	401	3.2	1.2	41.3	145
6041	17.4	360	0.60	6.5	413	3.8	1.2	25.2	146
6042	15.8	278	0.54	6.3	390	3.6	1.2	34.2	150
6043	14.0	245	0.54	8.0	443	4.2	1.3	33.5	202
6044	33.5	407	0.94	7.4	472	3.2	1.1	25.0	92
6045	16.0	274	0.53	6.6	453	2.8	1.0	30.2	35
6046	27.6	356	0.91	7.6	421	2.5	0.79	24.1	206
6047	25.7	360	0.85	6.6	489	2.8	1.1	16.3	298
6048	24.3	343	0.70	5.9	385	2.3	0.85	56.8	145
6049	31.9	412	0.90	6.7	489	3.1	1.2	14.3	414
6050	26.0	350	0.78	7.2	395	2.3	1.2	50.7	150
6051	29.4	366	0.89	5.1	424	2.9	1.2	37.9	106
6052	20.5	338	0.70	6.1	448	2.6	1.1	37.0	249
6053	24.6	354	0.78	4.9	423	3.2	1.3	41.0	90
6054	23.7	348	0.78	6.0	427	3.2	1.3	39.2	98
6055	13.2	304	0.51	4.8	408	3.0	1.2	39.3	95
6056	15.5	333	0.61	6.7	429	4.0	1.6	37.2	64
6057	25.2	341	0.94	6.1	393	3.3	1.3	37.5	114
6058	20.6	335	0.73	6.5	419	2.2	0.76	32.3	50
6059	17.0	324	0.61	6.4	502	3.0	1.0	28.1	86
6060	18.5	408	0.71	6.3	413	3.2	1.1	42.4	68
6061	13.5	373	0.61	6.0	402	3.2	1.3	48.4	52
6062	16.7	349	0.67	5.7	406	3.9	1.3	47.1	92
6063	17.2	375	0.71	6.2	371	3.9	1.6	39.5	190
6064	14.3	354	0.55	6.4	413	3.8	1.5	44.0	109
6065	17.7	344	0.69	5.9	411	3.6	1.4	47.2	102
6151	27.8	392	0.85	7.1	421	2.7	1.3	36.9	184
6152	21.5	361	0.71	6.8	410	2.4	1.1	42.4	135
6153	23.3	356	0.72	5.4	428	2.5	1.1	45.4	102
6154	26.4	380	0.81	4.8	442	2.9	1.3	37.9	118
6155	26.8	359	0.84	5.4	435	2.5	1.1	35.4	94
6156	26.3	360	0.80	5.7	419	2.8	1.3	39.6	89
6157	24.8	360	0.81	5.3	420	2.9	1.4	36.0	99
6158	22.6	377	0.72	6.1	451	3.3	1.4	26.8	116
6159	13.1	310	0.53	6.2	399	3.1	1.4	37.7	64
6160	13.9	330	0.54	7.0	420	2.8	1.1	38.2	48
6161	17.3	352	0.61	7.8	470	4.8	1.6	27.3	123
6162	19.7	324	0.69	6.0	404	3.9	1.5	38.5	86
6163	19.8	309	0.72	5.6	416	2.9	1.1	43.4	130
6164	22.3	355	0.73	7.0	413	2.1	0.91	32.9	73
6165	18.9	324	0.62	6.6	577	3.6	1.3	8.2	203
6166	20.4	368	0.71	7.5	441	2.4	0.91	31.1	76
6167	14.6	379	0.58	6.1	415	3.7	1.4	47.1	80
6168	15.2	402	0.62	8.7	390	3.5	1.2	47.1	124
6169	17.6	353	0.65	7.4	406	2.8	1.3	42.9	103

TABLE F-2

Windy Creek Diorite, Geehi Damsite, N.S.W.

PART II: Trace Element Ratios

Sample	K/Rb	K/Ba	Ba/Rb	Ba/Sr	Rb/Sr	$Th/K \times 10^4$	$U/K \times 10^4$	Th/U
6009	163	30.4	5.36	4.51	0.84	8.9	1.4	6.50
6127	217	32.4	6.71	2.33	0.35	3.8	0.88	4.36
6010	182	22.2	8.23	2.29	0.28	4.3	1.3	3.21
6011	251	24.3	10.3	2.43	0.24	4.0	1.0	3.83
6012	215	26.6	8.08	2.60	0.32	4.6	1.1	4.19
6013	242	26.3	9.21	2.21	0.24	4.0	1.1	3.60
6014	203	30.0	6.78	1.95	0.29	4.1	1.1	3.67
6015	199	30.9	6.42	1.59	0.25	3.9	0.86	4.51
6016	223	28.9	7.70	1.18	0.15	3.2	1.1	3.06
6017	248	28.0	8.85	1.12	0.13	5.3	1.2	4.42
6018	243	32.3	7.53	0.99	0.13	4.7	1.2	3.89
6019	254	26.9	9.47	0.87	0.09	3.8	1.1	3.56
6020	229	25.4	9.00	1.07	0.12	4.4	1.2	3.73
6021	281	25.8	10.9	0.99	0.09	5.7	1.5	3.75
6022	292	24.1	12.1	1.03	0.08	4.0	0.91	4.40
6023	288	22.8	12.6	0.99	0.08	5.4	1.6	3.39
6024	279	20.0	14.0	0.89	0.06	4.6	1.3	3.66
6025	199	24.8	8.04	0.95	0.12	3.7	1.3	2.78
6026	237	24.4	9.72	0.90	0.09	3.2	1.0	3.08
6027	293	21.1	13.9	0.92	0.07	4.1	1.2	3.36
6028	370	25.8	14.4	1.05	0.07	4.4	1.3	3.24
6029	229	20.0	11.5	0.87	0.08	4.6	1.2	3.89
6030	253	23.9	10.6	0.80	0.08	4.0	1.1	3.56
6031	269	21.3	12.6	0.92	0.07	6.5	1.6	3.94
6032	302	23.9	12.6	1.07	0.08	5.3	1.8	3.00
6033	339	21.5	15.8	1.00	0.06	2.9	1.0	2.86
6034	337	22.4	15.1	1.01	0.07	4.2	1.3	3.13
6035	319	22.0	14.5	1.02	0.07	3.5	1.3	2.78
6036	345	18.6	18.5	0.94	0.05	4.6	1.4	3.19
6037	309	20.6	15.0	1.02	0.07	4.3	1.3	3.34
6038	313	18.3	17.1	0.98	0.06	4.4	1.3	3.30
6039	320	21.3	15.0	0.83	0.06	5.3	1.5	3.46
6040	321	17.6	18.3	0.88	0.05	5.2	1.9	2.73
6041	344	16.6	20.7	0.87	0.04	6.3	2.0	3.21
6042	344	19.5	17.6	0.71	0.04	6.6	2.2	3.06
6043	386	22.0	17.6	0.55	0.03	7.8	2.5	3.13
6044	281	23.2	12.1	0.86	0.07	3.4	1.1	3.00
6045	333	19.5	17.1	0.60	0.04	5.3	1.9	2.80
6046	328	25.5	12.9	0.85	0.07	2.8	0.87	3.20
6047	330	23.6	14.0	0.74	0.05	3.3	1.3	2.60
6048	287	20.4	14.1	0.89	0.06	3.3	1.2	2.73
6049	284	21.9	12.9	0.84	0.07	3.4	1.4	2.48
6050	300	22.3	13.5	0.89	0.07	2.9	1.5	1.92
6051	302	24.2	12.5	0.86	0.07	3.3	1.4	2.43
6052	340	20.6	16.5	0.75	0.05	3.7	1.5	2.45
6053	317	22.0	14.4	0.84	0.06	4.2	1.7	2.42
6054	327	22.3	14.7	0.82	0.06	4.1	1.6	2.55
6055	391	16.9	23.1	0.75	0.03	5.8	2.4	2.44
6056	392	18.3	21.4	0.78	0.04	6.6	2.6	2.54
6057	373	27.6	13.5	0.87	0.06	3.5	1.4	2.57
6058	352	21.6	16.3	0.80	0.05	3.1	1.1	2.92
6059	358	18.8	19.0	0.65	0.03	4.9	1.7	2.89
6060	382	17.3	22.1	0.99	0.04	4.5	1.6	2.92
6061	454	16.4	27.7	0.93	0.03	5.2	2.1	2.45
6062	400	19.1	20.9	0.86	0.04	5.9	2.0	2.99
6063	413	18.9	21.8	1.01	0.05	5.5	2.3	2.42
6064	384	15.6	24.7	0.86	0.03	6.8	2.7	2.53
6065	388	20.0	19.4	0.84	0.04	5.2	2.0	2.54
6151	305	21.9	14.1	0.93	0.07	3.2	1.5	2.15
6152	331	19.7	16.8	0.88	0.05	3.4	1.6	2.18
6153	311	20.3	15.3	0.83	0.05	3.4	1.5	2.30
6154	307	21.3	14.4	0.86	0.06	3.6	1.6	2.26
6155	312	23.3	13.4	0.83	0.06	3.0	1.3	2.33
6156	302	22.1	13.7	0.86	0.06	3.5	1.6	2.20
6157	326	22.5	14.5	0.86	0.06	3.5	1.7	2.09
6158	319	19.1	16.7	0.84	0.05	4.6	1.9	2.47
6159	405	17.1	23.8	0.78	0.03	5.8	2.6	2.24
6160	385	16.3	23.7	0.79	0.03	5.3	2.0	2.64
6161	351	17.2	20.4	0.75	0.04	8.0	2.7	3.00
6162	352	21.4	16.4	0.80	0.05	5.6	2.2	2.58
6163	364	23.3	15.6	0.74	0.05	4.0	1.6	2.54
6164	330	20.7	16.0	0.86	0.05	2.9	1.2	2.33
6165	326	19.0	17.1	0.56	0.03	5.8	2.2	2.68
6166	346	19.2	18.1	0.83	0.05	3.3	1.3	2.58
6167	396	15.2	26.0	0.91	0.04	6.4	2.3	2.73
6168	407	15.3	26.5	1.03	0.04	5.6	2.0	2.88
6169	369	18.4	20.1	0.87	0.04	4.3	2.0	2.16

TABLE F-3

Scamels Leucogranite, SMA, NSW

PART I - Trace Elements (p.p.m.)

Sample	Rb^+	Ba^{2+}	K^+(%)	Pb^{2+}	Sr^{2+}	eTh^{4+}	eU^{4+}	Y^{3+}	Zr^{4+}
6066	155	723	3.00	16	93.8	17.0	5.3	43.0	92
6067	173	766	3.40	22	71.3	18.7	5.8	42.2	93
6068	181	797	3.56	24	62.2	17.4	6.6	41.6	85
6069	99.1	480	1.78	7.3	113	18.1	5.6	45.4	89
6070	90.2	335	1.50	4.1	102	17.2	4.9	42.6	87
6071	120	570	2.33	8.8	116	18.5	5.6	45.1	96
6072	127	458	1.97	4.2	102	17.4	5.3	43.1	84
6073	112	479	1.89	7.2	109	18.4	5.1	43.6	96
6074	102	321	1.47	3.3	100	16.8	5.3	46.0	89
6075	115	614	2.13	9.0	90.9	18.5	4.2	33.2	96
6076	99.9	551	1.85	4.9	116	17.5	4.6	32.1	84
6077	146	431	1.99	5.9	46.9	16.0	4.2	28.2	82
6078	93.4	379	1.32	2.8	80.5	16.2	3.6	35.7	82
6079	84.2	313	1.23	2.4	71.1	14.6	3.6	34.0	75
6080	112	540	1.85	6.2	101	17.9	4.7	36.5	82
6081	139	656	2.78	14	111	17.1	3.7	39.6	85
6082	171	943	3.28	22	88.8	18.7	5.2	42.0	94
6083	158	803	2.85	16	86.8	18.7	5.5	39.5	89
6084	75.8	810	3.10	20	78.9	18.0	5.1	41.1	91
6085	172	944	3.55	23	71.3	17.0	4.8	39.3	86
6086	162	863	3.33	19	93.3	18.0	5.6	40.9	93
6087	161	927	3.52	18	85.7	16.6	4.8	38.3	85
6088	171	826	3.46	23	72.3	17.0	5.2	41.8	92
6089	167	882	3.48	23	73.4	17.3	4.9	38.6	90
6090	181	862	3.63	23	71.4	18.3	5.6	41.4	90
6091	167	825	3.24	20	71.2	18.1	6.0	39.0	96
6092	174	964	3.50	19	122	17.6	5.0	39.7	89
6093	169	864	3.54	22	76.3	18.4	4.6	41.1	92
6094	170	866	3.47	22	73.2	17.4	5.5	39.5	93
6095	148	940	3.02	20	125	17.7	5.2	41.0	93
6096	157	854	3.24	20	88.5	17.2	5.7	41.9	93
6097	161	813	3.35	21	95.9	17.1	5.1	42.4	93
6098	100	507	1.68	10	180	17.9	4.6	40.5	87
6099	167	814	3.22	21	93.1	18.2	6.3	41.4	93
6100	181	810	3.56	21	71.4	17.4	6.0	43.1	94
6101	193	815	3.56	18	76.0	16.7	5.7	39.8	89
6102	182	872	3.55	21	67.4	17.6	5.9	42.7	89
6103	165	798	3.45	21	96.4	17.4	5.6	45.1	89
6104	152	808	3.17	21	116	17.5	5.6	44.4	93
6105	131	918	2.96	20	180	17.2	5.7	42.8	89
6106	155	818	2.96	19	155	17.3	4.6	47.2	90
6107	142	842	2.99	17	163	17.1	2.0	33.7	81
6108	176	852	3.34	23	80.5	17.0	5.8	46.5	96
6109	165	755	3.26	21	79.5	17.5	5.5	44.5	88
6110	179	792	3.51	157	63.4	17.9	4.9	40.7	88
6111	181	738	3.34	24	72.3	17.1	4.8	43.9	92
6112	178	612	3.50	30	70.3	17.0	5.0	51.9	84
6113	167	630	3.58	23	74.0	17.8	5.6	45.4	81
6114	167	760	3.19	23	96.0	17.5	4.9	44.1	84
6115	173	802	3.67	22	71.5	17.5	5.9	45.2	87
6116	181	839	3.63	27	76.0	18.2	7.7	45.1	85
6117	136	707	2.68	16	99.0	17.2	3.9	39.9	83
6118	153	756	3.50	24	74.2	17.8	6.6	45.6	90
6119	122	616	2.14	5.9	66.3	17.2	3.2	37.8	86
6120	154	813	3.52	19	73.0	18.4	4.6	42.0	89
6121	163	711	3.52	29	64.4	18.7	4.0	49.7	88
6122	168	817	3.53	15	71.2	18.4	3.7	38.6	85
6123	162	762	3.28	23	70.5	17.8	4.6	48.3	84
6124	161	738	3.41	14	72.2	18.7	4.1	39.5	89
6125	129	567	2.36	13	51.8	15.7	4.0	40.6	83
6126	171	607	2.88	15	36.3	17.7	4.6	48.9	103
6128	192	917	3.71	21	54.1	18.5	3.6	58.1	93
6130	158	955	3.34	19	50.4	18.3	3.5	44.6	105
6132	177	914	3.66	21	43.1	15.4	2.5	32.6	108
6133	184	965	3.38	19	31.1	17.7	2.9	46.4	125
6134	183	711	2.80	23	88.0	18.1	1.8	25.9	196
6136	175	726	2.63	24	37.0	19.4	2.9	31.5	205
6135	128	458	2.03	27	27.8	21.4	3.6	39.8	186
6137	111	417	1.69	21	33.3	16.2	2.9	33.4	203

TABLE F-4

Scamels Leucogranite, S.M.A. N.S.W.

PART II: Trace Element Ratios

Sample	K/Rb	K/Ba	Ba/Rb	Ba/Sr	Rb/Sr	Th/Kx10^4	U/Kx10^4	Th/U
6066	194	41.5	4.67	7.71	1.65	5.7	1.8	3.24
6067	197	44.3	4.44	10.7	2.42	5.5	1.7	3.25
6068	197	44.7	4.41	12.8	2.91	4.9	1.9	2.64
6069	180	37.1	4.85	4.27	0.88	10.1	3.1	3.23
6070	166	44.8	3.71	3.28	0.88	11.5	3.3	3.53
6071	194	40.9	4.74	4.93	1.04	7.9	2.4	3.28
6072	155	43.1	3.60	4.48	1.24	8.8	2.7	3.31
6073	169	39.5	4.27	4.39	1.03	9.7	2.7	3.58
6074	145	45.9	3.15	3.20	1.01	11.4	3.6	3.17
6075	185	34.7	5.34	6.75	1.26	8.7	2.0	4.46
6076	185	33.5	5.52	4.75	0.86	9.5	2.5	3.83
6077	136	46.1	2.95	9.19	3.11	8.1	2.1	3.81
6078	142	34.9	4.06	4.71	1.16	12.3	2.7	4.52
6079	147	39.4	3.72	4.40	1.18	11.8	2.9	4.07
6080	166	34.3	4.84	5.34	1.10	9.6	2.5	3.79
6081	200	42.4	4.71	5.91	1.26	6.2	1.3	4.63
6082	192	34.8	5.51	10.6	1.93	5.7	1.6	3.60
6083	180	35.5	5.07	9.25	1.83	6.5	1.9	3.40
6084	408	38.2	10.7	10.3	0.96	5.8	1.7	3.52
6085	207	37.6	5.50	13.2	2.41	4.8	1.4	3.53
6086	205	38.6	5.32	9.25	1.74	5.4	1.7	3.23
6087	219	38.0	5.75	10.8	1.88	4.7	1.4	3.49
6088	203	41.9	4.84	11.4	2.36	4.9	1.5	3.29
6089	208	39.5	5.28	12.0	2.28	5.0	1.4	3.54
6090	201	42.2	4.78	12.1	2.53	5.0	1.5	3.26
6091	194	39.2	4.95	11.6	2.34	5.6	1.9	3.00
6092	201	36.3	5.54	7.88	1.42	5.0	1.4	3.55
6093	209	41.0	5.10	11.3	2.22	5.2	1.3	3.97
6094	204	40.0	5.10	11.8	2.32	5.0	1.6	3.16
6095	204	32.2	6.36	7.53	1.19	5.8	1.7	3.39
6096	206	37.9	5.44	9.65	1.77	5.3	1.8	3.04
6097	209	41.2	5.07	8.47	1.67	5.1	1.5	3.34
6098	168	33.1	5.07	2.82	0.56	10.6	2.7	3.92
6099	194	39.6	4.89	8.75	1.79	5.6	2.0	2.87
6100	197	44.0	4.49	11.4	2.53	4.9	1.7	2.92
6101	185	43.6	4.23	10.7	2.53	4.7	1.6	2.94
6102	195	40.7	4.80	12.9	2.70	5.0	1.7	2.99
6103	210	43.3	4.84	8.28	1.71	5.0	1.6	3.13
6104	209	39.3	5.31	6.97	1.31	5.5	1.8	3.13
6105	226	32.2	7.02	5.09	0.72	5.8	1.9	3.00
6106	192	36.2	5.29	5.26	0.99	5.9	1.5	3.79
6107	210	35.5	5.92	5.15	0.87	5.7	0.66	8.61
6108	190	39.2	4.85	10.6	2.18	5.1	1.7	2.95
6109	198	43.2	4.58	9.50	2.08	5.4	1.7	3.20
6110	196	44.4	4.42	12.5	2.83	5.1	1.4	3.68
6111	184	45.2	4.07	10.2	2.51	5.1	1.4	3.59
6112	197	57.2	3.45	8.70	2.52	4.9	1.4	3.39
6113	214	56.9	3.77	8.52	2.26	5.0	1.6	3.17
6114	191	42.0	4.55	7.91	1.74	5.5	1.5	3.60
6115	212	45.8	4.64	11.2	2.42	4.8	1.6	3.00
6116	200	43.2	4.64	11.0	2.38	5.0	2.1	2.37
6117	197	38.0	5.20	7.14	1.37	6.4	1.5	4.39
6118	229	46.3	4.95	10.2	2.06	5.1	1.9	2.71
6119	176	34.7	5.06	9.30	1.84	8.1	1.5	5.31
6120	229	43.3	5.30	11.1	2.10	5.2	1.3	4.04
6121	216	49.5	4.37	11.0	2.53	5.3	1.1	4.67
6122	210	43.2	4.86	11.5	2.36	5.2	1.1	4.97
6123	202	43.0	4.70	10.8	2.30	5.4	1.4	3.89
6124	212	46.3	4.58	10.2	2.23	5.5	1.2	4.54
6125	183	41.6	4.41	11.0	2.48	6.7	1.7	3.99
6126	169	47.5	3.55	16.7	4.71	6.2	1.6	3.83
6128	194	40.5	4.78	16.9	3.55	5.0	0.96	5.21
6130	211	34.9	6.05	18.9	3.13	5.5	1.1	5.21
6132	207	40.0	5.16	21.2	4.11	4.2	0.68	6.24
6133	184	35.1	5.25	31.0	5.91	5.2	0.86	6.09
6134	153	39.4	3.89	8.08	2.08	6.5	0.64	10.1
6136	150	36.2	4.14	19.6	4.74	7.4	1.1	6.67
6135	159	44.2	3.59	16.5	4.59	10.5	1.8	5.94
6137	151	40.4	3.74	12.5	3.35	9.6	1.7	5.66

TABLE F-5

Khancoban Granodiorite, N.S.W.

PART I: Trace Elements (p.p.m.)[1]

Sample	Rb^{+}	Ba^{2+}	K^{+}(%)	Pb^{2+}	Sr^{2+}	eTh^{4+}	eU^{4+}	Y^{3+}	Zr^{4+}
6170	164	605	2.74	27	119	17.4	2.6	55.1	147
6171	160	476	2.49	28	139	18.2	1.9	56.1	160
6172	158	446	2.27	26	152	19.1	2.1	50.6	163
6173	157	770	3.01	31	173	11.6	2.0	42.3	142
6174	158	511	2.63	27	182	18.5	2.7	52.1	158
6175	159	573	2.64	27	177	16.8	2.4	46.3	148
6176	150	538	2.69	28	180	16.1	2.4	48.2	153
6177	161	540	2.54	26	173	17.8	2.5	37.9	157
6178	175	720	3.27	26	162	15.0	2.4	53.9	139
6179	161	553	2.64	29	170	15.9	1.9	41.0	157
6180	167	590	2.88	28	175	17.2	2.4	49.5	144
6181	170	584	2.92	30	174	16.5	2.6	63.2	150
6182	160	644	2.82	29	179	14.4	2.4	42.5	141
6183	156	577	2.79	28	165	16.3	3.5	43.5	149
6184	163	500	2.63	27	166	17.6	3.0	36.5	152
6185	158	575	2.79	29	173	16.4	2.8	41.8	135
6186	161	543	2.66	28	175	15.6	2.6	31.0	147
6187	162	595	2.92	30	155	15.2	3.0	46.1	127
6188	148	576	2.67	27	167	16.0	2.3	50.1	142
6189	162	552	2.87	25	150	15.6	2.3	47.8	143
6190	163	571	2.83	27	174	15.4	3.2	38.2	129
6191	153	576	2.78	27	163	15.8	4.3	42.4	151
6192	164	600	2.88	27	150	15.9	3.5	40.5	141
6193	159	574	2.75	28	155	15.4	3.9	45.6	144
6194	166	523	2.93	21	121	15.8	3.5	39.5	139
6195	158	566	2.61	27	157	15.8	3.4	43.8	149
6196	149	601	2.82	29	152	16.4	3.8	52.1	147
6197	170	536	2.96	21	152	16.4	3.1	46.1	156
6198	166	367	2.45	6.8	79.2	14.7	3.2	36.9	138
6199	179	511	2.95	22	135	16.4	4.4	34.3	150
6210	167	561	2.84	26	140	14.8	3.4	37.9	141
6211	186	660	3.00	25	147	14.5	5.9	34.9	146
6212	196	586	3.19	22	128	13.8	4.1	37.3	140
6213	135	405	2.32	9.4	109	15.3	4.4	38.6	142
6214	111	144	1.44	5.8	71.5	21.7	6.6	56.5	203
6215	150	166	1.66	5.0	45.4	17.3	5.3	53.3	153
6216	196	258	3.40	28	76.0	8.3	8.8	70.7	43
6217	226	167	3.92	54	61.3	8.8	8.1	72.7	43
6218	222	169	3.90	56	61.2	8.8	7.6	76.8	53
6220	160	446	2.53	30	176	17.0	4.7	49.4	145
6221	157	426	2.68	12	78.4	15.1	3.3	43.8	140
6222	151	557	2.59	29	174	15.3	3.1	43.4	143
6223	167	543	2.85	30	167	16.1	4.5	51.7	145
6224	154	526	2.61	25	154	15.2	5.2	43.3	151
6225	165	557	2.73	29	177	16.1	4.1	45.4	145
6226	153	555	2.64	29	93.4	16.3	5.2	41.6	153
6227	173	575	2.61	27	188	15.9	5.0	50.0	151
6228	156	460	2.41	26	119	15.2	4.6	51.4	146
6229	176	562	2.90	31	169	15.7	4.3	39.8	139
6230	174	522	2.65	27	163	12.2	4.6	43.4	144
6231	182	601	2.80	29	151	17.0	4.7	52.3	149
6232	178	538	2.83	29	148	15.1	4.4	33.9	134
6233	177	544	2.76	30	158	15.1	4.2	38.5	133
6234	110	281	1.85	5.7	110	23.1	6.3	59.7	211
6235	97.0	254	1.53	3.7	95.5	26.2	6.2	92.6	184
6236	151	416	2.11	22	168	14.6	2.8	32.4	131
6237	171	374	2.41	15	68.2	15.7	3.3	28.5	130
6238	159	515	2.44	25	142	9.0	3.4	35.8	124
6239	171	566	2.95	30	159	10.6	3.8	27.0	114
6240	163	500	2.72	26	177	10.3	3.8	36.7	122
6241	174	507	2.68	26	175	11.9	4.1	37.8	119
6242	167	579	2.70	30	175	15.8	4.0	42.2	140
6243	173	537	2.82	28	172	15.9	4.2	44.7	141

TABLE F-6

Khancoban Granodiorite, N.S.W.

PART II: Trace Element Ratios

Sample	K/Rb	K/Ba	Ba/Rb	Ba/Sr	Rb/Sr	Th/Kx10^4	U/Kx10^4	Th/U
6170	167	45.3	3.69	5.10	1.38	6.4	0.95	6.70
6171	156	52.2	2.98	3.43	1.15	7.3	0.78	9.46
6172	144	51.0	2.82	2.93	1.04	8.4	0.93	9.07
6173	192	39.1	4.92	4.44	0.90	3.9	0.65	5.96
6174	166	51.4	3.23	2.82	0.87	7.0	1.0	6.75
6175	166	46.0	3.60	3.25	0.90	6.4	0.92	6.93
6176	179	50.0	3.58	2.99	0.83	6.0	0.88	6.79
6177	157	47.0	3.35	3.13	0.93	7.0	0.99	7.06
6178	187	45.4	4.12	4.44	1.08	4.6	0.73	6.31
6179	164	47.7	3.43	3.26	0.95	6.0	0.72	8.40
6180	173	48.9	3.54	3.37	0.95	6.0	0.83	7.14
6181	172	50.1	3.43	3.36	0.98	5.7	0.87	6.47
6182	176	43.8	4.03	3.60	0.89	5.1	0.84	6.08
6183	179	48.3	3.71	3.51	0.95	5.9	1.3	4.63
6184	162	52.7	3.07	3.01	0.98	6.7	1.1	5.86
6185	177	48.6	3.64	3.33	0.92	5.9	1.0	5.86
6186	165	49.0	3.37	3.11	0.92	5.9	0.98	6.00
6187	180	49.0	3.67	3.85	1.05	5.2	1.0	5.05
6188	181	46.4	3.91	3.45	0.88	6.0	0.84	7.13
6189	178	52.1	3.42	3.68	1.08	5.4	0.79	6.85
6190	174	49.6	3.51	3.29	0.94	5.4	1.1	4.84
6191	182	48.2	3.78	3.53	0.94	5.7	1.6	3.64
6192	175	48.0	3.65	4.01	1.10	5.5	1.2	4.56
6193	173	47.9	3.62	3.72	1.03	5.6	1.4	3.97
6194	176	55.9	3.15	4.32	1.37	5.4	1.2	4.46
6195	165	46.0	3.57	3.60	1.01	6.1	1.3	4.61
6196	189	47.0	4.03	3.95	0.98	5.8	1.4	4.28
6197	175	55.2	3.16	3.52	1.11	5.5	1.0	5.36
6198	148	66.6	2.22	4.64	2.09	6.0	1.3	4.58
6199	165	57.8	2.86	3.79	1.33	5.5	1.5	3.76
6210	170	50.6	3.36	4.00	1.19	5.2	1.2	4.29
6211	161	45.4	3.55	4.48	1.26	4.8	2.0	2.44
6212	163	54.4	2.99	4.60	1.54	4.3	1.3	3.36
6213	172	57.2	3.00	3.71	1.24	6.6	1.9	3.44
6214	130	99.7	1.30	2.01	1.55	15.1	4.6	3.28
6215	111	99.9	1.11	3.65	3.29	10.4	3.2	3.23
6216	173	132	1.32	3.40	2.58	2.5	2.6	0.94
6217	173	235	0.74	2.72	3.69	2.2	2.1	1.09
6218	176	231	0.76	2.76	3.63	2.3	1.9	1.16
6220	158	56.7	2.79	2.53	0.91	6.7	1.9	3.61
6221	171	62.9	2.71	5.44	2.01	5.6	1.2	4.64
6222	172	46.5	3.69	3.21	0.87	5.9	1.2	4.96
6223	171	52.5	3.26	3.25	1.00	5.6	1.6	3.56
6224	169	49.6	3.41	3.41	1.00	5.8	2.0	2.95
6225	165	48.9	3.37	3.16	0.94	5.9	1.5	3.95
6226	173	47.5	3.64	5.94	1.64	6.2	2.0	3.13
6227	151	45.4	3.33	3.06	0.92	6.1	1.9	3.21
6228	155	52.4	2.95	3.88	1.31	6.3	1.9	3.32
6229	165	51.7	3.19	3.32	1.04	5.4	1.5	3.69
6230	153	50.8	3.01	3.21	1.07	4.6	1.7	2.65
6231	154	46.6	3.30	3.98	1.21	6.1	1.7	3.58
6232	160	52.7	3.03	3.64	1.20	5.3	1.6	3.43
6233	156	50.8	3.07	3.45	1.12	5.5	1.5	3.58
6234	168	65.9	2.55	2.55	1.00	12.5	3.4	3.66
6235	157	60.1	2.62	2.66	1.02	17.2	4.1	4.21
6236	140	50.8	2.76	2.47	0.89	6.9	1.3	5.25
6237	141	64.5	2.18	5.48	2.51	6.5	1.4	4.82
6238	154	47.4	3.25	3.62	1.11	3.7	1.4	2.69
6239	172	52.1	3.31	3.55	1.07	3.6	1.3	2.79
6240	167	54.3	3.07	2.82	0.92	3.8	1.4	2.68
6241	154	52.9	2.91	2.90	1.00	4.4	1.5	2.89
6242	162	46.6	3.47	3.31	0.95	5.9	1.5	3.92
6243	162	52.4	3.10	3.13	1.01	5.7	1.5	3.82

TABLE F-7

Mertondale DDH 1, W.A.

PART I: Trace Elements (p.p.m.)[1]

Sample	Rb$^+$	Ba^{2+}	K$^+$(%)	Pb^{2+}	Sr^{2+}	eTh^{4+}	eU^{4+}	Y^{3+}	Zr^{4+}
6280	12.6	47	0.28	n.d[2]	18.9	8.5	0.89	41.6	93
6281	15.1	70	0.34	0.85	5.3	11.9	1.0	57.5	126
6282	97.7	507	3.21	1.6	3.7	8.6	2.6	47.7	98
6283	122	514	3.94	3.5	3.7	7.4	2.0	53.1	106
6284	115	468	3.70	4.9	11.8	7.3	1.4	42.5	84
6285	110	405	3.39	4.6	12.6	5.8	1.5	45.0	86
6286	108	456	3.40	4.3	13.0	4.8	1.4	42.9	92
6287	100	321	3.01	11	6.3	7.2	3.3	59.8	101
6288	98.1	353	3.01	5.2	6.1	6.7	2.9	53.9	93
6289	118	435	3.48	6.6	9.3	6.2	3.0	56.5	112
6290	114	399	3.61	12	11.9	5.9	3.0	44.8	94
6291	106	360	3.32	17	13.2	6.3	2.1	185	95
6292	107	368	3.37	13	11.8	7.2	1.7	223	80
6356	10.2	258	0.21	n.d	26.9	9.6	1.2	42.6	116
6357	10.0	43	0.22	1.4	16.4	9.7	0.81	41.3	112
6358	10.9	57	0.21	1.6	14.9	9.7	1.0	45.6	106
6359	69.6	140	2.18	1.4	3.4	10.8	0.96	56.8	123
6360	103	335	3.30	2.1	3.4	10.8	1.3	64.2	151
6361	96.2	312	3.04	2.6	4.5	8.8	1.7	43.4	98
6362	122	418	3.70	3.2	3.6	9.5	1.2	49.2	111
6363	121	384	3.85	2.6	3.2	8.5	1.4	50.3	108
6364	167	16	3.62	5.7	3.8	14.7	2.0	59.9	182
6365	74.9	204	2.33	1.8	3.3	8.0	2.0	39.5	93
6366	97.6	432	3.16	1.9	3.2	9.1	2.2	39.8	108
6367	102	497	3.33	2.3	4.5	8.7	2.9	45.1	111
6368	110	604	3.55	1.7	17.6	5.2	1.3	40.7	99
6369	113	477	3.66	3.6	9.2	7.5	1.6	54.3	106
6370	119	468	3.88	1.6	3.9	8.6	1.5	44.2	109
6371	110	401	3.50	1.4	3.5	9.4	2.5	43.9	110
6372	98.8	356	3.15	3.9	3.3	8.9	2.6	43.2	102
6373	111	422	3.49	2.4	4.2	8.9	2.3	44.5	108
6374	108	434	3.50	3.7	13.4	7.2	1.5	43.3	102

TABLE F-8

Mertondale D.D.H. 1. W.A.

PART II: Trace Element Ratios

Sample	K/Rb	K/Ba	Ba/Rb	Ba/Sr	Rb/Sr	Th/Kx10^4	U/Kx10^4	Th/U
6280	218	58.3	3.74	2.50	0.67	30.9	3.2	9.56
6281	227	48.9	4.64	13.1	2.83	34.9	3.0	11.7
6282	329	63.4	5.19	136	26.1	2.7	0.8	3.36
6283	324	76.7	4.23	141	33.3	1.9	0.5	3.72
6284	323	79.1	4.08	39.8	9.76	2.0	0.4	5.22
6285	308	83.6	3.69	32.2	8.73	1.7	0.4	4.01
6286	315	74.6	4.23	35.1	8.29	1.4	0.4	3.45
6287	300	93.7	3.20	51.2	16.0	2.4	1.1	2.17
6288	307	85.4	3.60	57.8	16.1	2.2	1.0	2.34
6289	293	79.9	3.67	46.9	12.8	1.8	0.9	2.06
6290	318	90.4	3.52	33.4	9.51	1.6	0.8	2.00
6291	314	92.2	3.40	27.2	8.00	1.9	0.7	2.96
6292	315	91.5	3.44	31.3	9.10	2.1	0.5	4.20
6356	208	8.22	25.3	9.60	0.38	45.1	5.7	7.97
6357	214	49.5	4.33	2.65	0.61	44.9	3.8	11.9
6358	194	36.8	5.27	3.84	0.73	46.1	4.8	9.57
6359	313	156	2.01	41.5	20.7	5.0	0.4	11.2
6360	321	98.4	3.26	100	30.7	3.3	0.4	8.29
6361	316	97.4	3.24	69.3	21.4	2.9	0.6	5.11
6362	305	88.6	3.44	118	34.2	2.6	0.3	7.71
6363	318	100	3.18	121	38.0	2.2	0.4	6.01
6364	217	2222	0.10	4.34	44.5	4.1	0.6	7.42
6365	311	114	2.72	61.6	22.6	3.4	0.9	4.04
6366	324	73.1	4.43	134	30.2	2.9	0.7	4.15
6367	326	66.9	4.88	111	22.8	2.6	0.9	3.03
6368	322	58.7	5.49	34.3	6.25	1.5	0.4	3.96
6369	323	76.7	4.22	51.7	12.3	2.0	0.4	4.68
6370	327	83.0	3.94	120	30.4	2.2	0.4	5.81
6371	319	87.2	3.66	113	31.0	2.7	0.7	3.72
6372	319	88.5	3.60	108	29.8	2.8	0.8	3.42
6373	313	82.7	3.79	99.8	26.3	2.6	0.7	3.90
6374	323	80.6	4.00	32.4	8.09	2.1	0.4	4.73

Table F-9

Tuckanarra Quarry, W.A.

PART I: Trace elements (p.p.m.)[1]

Sample	Rb^{+}	Ba^{2+}	K^{+} (%)	Pb^{2+}	Sr^{2+}	eTh^{4+}	eU^{4+}	Y^{3+}	Zr^{4+}
6263	79.6	565	1.53	17	407	9.1	0.99	5.0	124
6264	86.9	659	1.62	18	410	9.7	1.6	4.4	124
6265	189	965	-	21	304	-	-	10.6	141
6266	93.5	814	1.98	23	389	9.3	14.7	5.7	111
6267	108	1068	2.36	22	371	10.1	8.1	4.9	110
6268	85.0	678	1.76	19	388	9.2	2.2	3.2	126
6269	138	1507	-	18	283	-	-	5.3	123
6270	140	955	2.14	22	374	7.8	1.8	3.0	112
6271	86.0	635	1.73	22	391	8.5	1.1	4.7	112
6272	72.1	332	1.14	18	410	7.9	1.7	4.9	127
6273	109	595	1.89	5.7	243	11.8	3.2	5.4	126
6274	85.0	641	-	21	380	-	-	4.1	113
6275	120	1247	-	23	363	-	-	3.8	92
6276	101	691	1.98	25	379	8.7	2.7	4.5	111
6277	92.9	793	2.03	22	367	9.8	1.0	6.0	105
6278	130	1030	2.73	16	292	8.7	1.7	4.5	95
6279	85.2	782	1.87	22	367	8.4	1.6	3.7	107

Table F-10

Tuckanarra Quarry, W.A.

Part 2: Trace element ratios

Sample	K/Rb	K/Ba	Ba/Rb	Ba/Sr	Rb/Sr	Th/K $\times 10^4$	U/K $\times 10^4$	Th/U
6263	193	27.1	7.10	1.39	0.20	5.9	0.7	9.18
6264	186	24.5	7.58	1.61	0.21	6.0	1.0	6.06
6265	-	-	5.11	3.17	0.62	-	-	-
6266	211	24.3	8.71	2.09	0.24	4.7	7.4	0.63
6267	218	22.1	9.87	2.88	0.29	4.3	3.5	1.24
6268	207	26.0	7.97	1.75	0.22	5.2	1.2	4.25
6269	-	-	10.9	5.32	0.49	-	-	-
6270	153	22.4	6.84	2.55	0.37	3.6	0.8	4.38
6271	201	27.2	7.39	1.62	0.22	4.9	0.6	7.89
6272	157	34.2	4.60	0.81	0.18	7.0	1.5	4.73
6273	173	31.8	5.44	2.45	0.45	6.2	1.7	3.67
6274	-	-	7.54	1.69	0.22	-	-	-
6275	-	-	10.4	3.43	0.33	-	-	-
6276	197	28.7	6.88	1.82	0.27	4.4	1.3	3.27
6277	219	25.6	8.54	2.16	0.25	4.8	0.5	9.36
6278	211	26.5	7.95	3.53	0.44	3.2	0.6	5.10
6279	220	23.9	9.18	2.13	0.23	4.5	0.8	5.38

Table F-11

Zamia Quarry W.A.

PART 1: Trace elements (p.p.m.)[1]

Sample	Rb^{+}	Ba^{2+}	K^{+} (%)	Pb^{2+}	Sr^{2+}	eTh^{4+}	eU^{4+}	Y^{3+}	Zr^{4+}
6251	210	839	3.58	45	118	37.6	12.5	23.3	144
6252	167	882	3.48	43	121	42.6	10.7	23.2	178
6253	218	915	3.46	45	120	38.7	11.8	28.3	173
6254	210	916	3.69	45	119	43.0	11.8	25.1	134
6255	210	795	3.25	44	116	46.4	7.4	27.7	138
6256	219	866	3.74	47	117	41.0	15.2	31.3	134
6257	227	811	3.76	44	114	43.3	9.8	30.7	138
6258	228	846	3.32	49	117	46.2	6.3	42.0	175
6259	230	826	3.72	41	114	35.5	7.7	28.8	134
6260	210	839	3.27	45	109	43.0	4.7	42.1	183
6261	216	872	3.37	46	107	45.8	6.0	32.2	192
6262	202	812	3.35	39	106	42.7	6.1	19.1	177

Table F-12

Zamia Quarry, W.A.

Part 2: Trace element ratios

Sample	K/Rb	K/Ba	Ba/Rb	Ba/Sr	Rb/Sr	Th/K $\times 10^4$	U/K $\times 10^4$	Th/U
6251	171	42.7	3.99	7.12	1.78	10.5	3.5	3.01
6252	208	39.5	5.28	7.29	1.38	12.2	3.1	3.98
6253	159	37.8	4.20	7.62	1.81	11.2	3.4	3.28
6254	176	40.3	4.36	7.68	1.76	11.7	3.2	3.64
6255	155	40.9	3.79	6.88	1.81	14.3	2.3	6.27
6256	171	43.2	3.96	7.43	1.88	11.0	4.1	2.70
6257	166	46.4	3.57	7.15	2.00	11.5	2.6	4.42
6258	146	39.2	3.71	7.21	1.94	13.9	1.9	7.33
6259	162	45.0	3.60	7.25	2.02	9.5	2.1	4.61
6260	156	39.0	4.00	7.69	1.92	13.1	1.4	9.15
6261	156	38.6	4.04	8.13	2.02	13.6	1.8	7.63
6262	166	41.3	4.01	7.70	1.92	12.7	1.8	7.00

Table F-13

Glen View Quarry, W.A.

PART 1: Trace elements (p.p.m.)[1]

Sample	Rb^+	Ba^{2+}	K^+ (%)	Pb^{2+}	Sr^{2+}	eTh^{4+}	eU^{4+}	Y^{3+}	Zr^{4+}
6293	9.4	13	0.09	73	58.2	1.1	2.1	11.6	128
6294	1.2	4.3	n.d.[2]	30	4.1	3.2	9.2	2.5	152
6295	1.2	7.4	0.01	12	2.9	8.1	10.7	3.3	206
6296	2.1	2.3	0.02	n.d.	6.7	5.7	12.3	1.6	194
6297	37.6	497	1.46	30	4.8	31.4	3.4	3.5	188
6298	64.3	487	1.46	n.d.	10.8	22.4	3.1	4.2	181
6299	70.1	440	1.30	n.d.	5.5	17.5	1.4	5.2	147
6300	n.d.	n.d.	-	n.d.	n.d.	-	-	1.5	117
6301A	13.0	127	-	n.d.	2.5	-	-	10.9	277
6301B	17.2	180	-	n.d.	3.1	-	-	5.8	164
6302	42.2	188	0.85	n.d.	9.3	25.0	5.4	6.0	162
6303	124	949	3.14	30	118	27.3	4.4	30.2	118
6304	132	938	3.10	37	121	28.8	4.9	20.2	125
6305	8.6	50	0.22	3.9	173	0.49	0.20	33.0	107
6306	120	861	3.09	29	124	23.2	6.6	14.5	133
6307	15.3	100	0.36	10	3.5	84.1	5.9	8.1	464
6308	45.2	284	1.06	11	6.2	98.3	6.9	8.1	350
6309	138	920	3.20	48	99.1	34.1	17.2	36.6	128
6310A	n.d.	96	-	22	1.8	-	-	5.1	301
6310B	n.d.	n.d.	-	n.d.	n.d.	-	-	1.8	109

Table F-14

Glen View Quarry, W.A.

Part 2: Trace element ratios

Sample	K/Rb	K/Ba	Ba/Rb	Ba/Sr	Rb/Sr	Th/K $\times 10^4$	U/K $\times 10^4$	Th/U
6293	95.4	68.2	1.40	0.23	0.16	12.6	23.7	0.53
6294	-	-	3.47	1.05	0.30	-	-	0.34
6295	66.1	10.8	6.12	2.59	0.42	1006	1339	0.75
6296	80.6	73.9	1.09	0.34	0.31	336	724	0.46
6297	387	29.3	13.2	103	7.82	21.6	2.3	9.34
6298	227	30.0	7.58	45.3	5.97	15.3	2.1	7.30
6299	186	29.5	6.28	80.1	12.8	13.5	1.1	12.2
6300	-	-	-	-	-	-	-	-
6301A	-	-	9.79	50.6	5.17	-	-	-
6301B	-	-	10.4	58.6	5.61	-	-	-
6302	201	45.2	4.45	20.3	4.55	29.4	6.4	4.63
6303	254	33.1	7.68	8.08	1.05	8.7	1.4	6.20
6304	234	30.3	7.09	7.74	1.09	9.3	1.6	5.91
6305	261	44.9	5.81	0.29	0.05	2.2	0.9	2.45
6306	257	35.9	7.16	6.94	0.97	7.5	2.1	3.52
6307	236	36.3	6.50	28.1	4.32	233	16.3	14.3
6308	234	37.2	6.28	45.7	7.27	93	6.5	14.3
6309	231	34.8	6.65	9.29	1.40	10.7	5.4	1.98
6310A	-	-	-	54.4	-	-	-	-
6310B	-	-	-	-	-	-	-	-

TABLE F-15

Koolanooka Hills, W.A.

Porphyry and Weathered Derivatives

PART I: Trace Elements (p.p.m.)[1]

Sample	Rb^+	Ba^{2+}	K^+(%)	Pb^{2+}	Sr^{2+}	eTh^{4+}	eU^{4+}	Y^{3+}	Zr^{4+}
6311	336	110	3.86	43	8.1	35.5	4.6	32.2	114
6312	333	87	3.81	43	7.9	36.6	4.5	32.9	115
6313	337	121	3.81	46	9.5	34.1	2.8	31.2	111
6314	340	98	3.81	44	8.2	33.3	3.1	30.5	108
6315	321	177	3.65	42	12.7	29.8	3.3	26.8	110
6316	334	1103	3.76	47	14.3	29.2	2.9	23.4	107
6317	323	364	3.13	62	15.6	34.1	3.3	24.3	90
6318	336	65	3.59	46	8.5	32.3	2.3	27.6	101
6319	333	108	3.75	44	9.4	31.6	2.7	27.1	98
6320	316	367	3.51	48	11.2	35.3	2.3	25.5	98
6321	339	244	3.47	77	12.3	50.8	3.4	25.5	102
6322	292	40	2.93	69	6.6	43.4	3.3	19.5	101
6323	331	413	3.37	88	21.8	50.4	4.7	24.1	99
6324	0.42	141	.002	1.6	1.7	8.1	2.4	6.4	388
6325	21.8	9.9	0.10	0.0	3.3	13.0	2.9	54.3	110
6326	13.3	0.6	0.12	n.d	4.0	14.8	2.2	22.4	160
6327	12.9	13	0.10	n.d	1.3	14.4	2.2	20.9	175
6328	6.8	9.9	0.09	n.d	0.99	15.6	2.6	23.4	212
6329	7.5	59	0.09	n.d	12.0	18.0	3.6	15.1	157
6330	17.5	74	0.12	n.d	12.1	21.7	5.4	24.1	119
6331	10.5	24	0.06	n.d	9.6	20.3	3.7	23.8	161
6332	2.9	35	0.02	n.d	8.3	12.2	2.6	12.4	96
6333	3.0	27	0.01	n.d	5.1	13.0	2.7	12.1	95
6334	3.6	12	0.04	n.d	2.8	11.6	1.9	11.6	103
6335	47.0	21	0.53	n.d	1.7	26.5	1.2	24.5	180
6336	5.0	29	0.03	3.7	1.1	12.9	4.4	39.7	266
6337	192	511	3.85	43	44.3	27.8	4.4	72.5	169
6338	185	562	3.81	42	47.3	26.5	5.2	55.5	175
6339	187	571	3.99	38	46.7	25.7	3.3	52.3	174
6340	187	574	3.90	39	46.1	25.9	3.6	52.4	172
6341	200	528	3.98	43	49.5	29.6	7.3	63.8	172
6343	207	498	3.96	43	43.4	30.2	4.7	79.5	176
6344	204	554	4.02	44	49.2	29.8	5.9	42.4	166
6345	189	587	3.93	45	60.9	27.4	4.6	35.8	172
6346	187	535	3.94	40	50.7	26.6	5.0	95.2	177
6347	183	571	3.90	41	50.8	26.8	6.1	59.7	170
6348	245	328	3.95	50	28.7	36.0	7.1	92.2	149
6349	241	331	3.90	49	28.7	35.5	8.3	99.4	152
6350	232	366	3.88	49	31.6	34.3	6.4	80.1	160
6351	236	296	3.95	52	27.1	38.1	8.2	95.2	148
6352	261	334	3.95	39	27.2	37.3	4.6	59.8	146
6353	248	333	3.93	54	27.8	37.7	6.9	49.5	157
6354	231	352	3.83	49	30.6	35.0	8.2	93.7	154
6355	244	331	3.91	51	30.4	35.6	6.8	65.8	148
6201	192	551	-	44	47.0	-	-	64.6	180
6202	193	558	-	44	47.7	-	-	55.7	180
6203	192	514	-	41	46.6	-	-	41.0	175
6204	214	512	-	47	44.7	-	-	72.5	192
6205	336	84	-	43	9.2	-	-	31.6	124
6206A	383	57	-	50	8.6	-	-	24.4	116
6206B	383	61	-	49	8.3	-	-	25.3	113
6207	3.6	n.d	-	3.0	2.0	-	-	31.8	139
6208	66.3	147	-	11	25.6	-	-	27.9	83
6209A	5.6	483	-	2.6	9.4	-	-	21.0	158
6209B	5.7	189	-	3.1	4.4	-	-	22.1	127
5646A	141	769	-	197	120	-	-	56.4	262
KP1	187	545	-	47	49.3	-	-	48.3	158
83-870	251	255	-	54	26.9	-	-	102	128

TABLE F-16

Koolanooka Hills, W.A.

Porphyry and Weathered Derivatives

PART II: Trace Element Ratios

Sample	K/Rb	K/Ba	Ba/Rb	Ba/Sr	Rb/Sr	Th/Kx10^4	U/Kx10^4	Th/U
6311	115	351	0.33	13.6	41.5	9.2	1.2	7.74
6312	114	439	0.26	11.0	42.2	9.6	1.2	8.05
6313	113	315	0.36	12.7	35.3	9.0	0.7	12.1
6314	112	388	0.29	11.9	41.3	8.7	0.8	10.8
6315	114	206	0.55	14.0	25.3	8.2	0.9	8.90
6316	113	34.1	3.31	77.1	23.3	7.8	0.8	10.2
6317	97.1	86.0	1.13	23.4	20.7	10.9	1.1	10.4
6318	107	556	0.19	7.62	39.7	9.0	0.6	14.0
6319	113	347	0.32	11.5	35.4	8.4	0.7	11.9
6320	111	95.7	1.16	32.8	28.2	10.1	0.7	15.2
6321	102	142	0.72	19.9	27.6	14.6	1.0	14.9
6322	101	737	0.14	6.01	44.1	14.8	1.1	13.1
6323	102	81.7	1.25	18.9	15.2	15.0	1.4	10.8
6324	47.6	0.14	336	83.9	0.25	4070	1180	3.45
6325	47.7	105	0.45	3.01	6.63	125	28.1	4.45
6326	93.3	2067	0.05	0.15	3.29	119	17.5	6.81
6327	75.0	73.5	1.02	10.4	10.2	149	23.0	6.47
6328	124	85.9	1.45	10.0	6.90	184	30.2	6.07
6329	118	15.0	7.86	4.87	0.62	204	41.3	4.95
6330	69.6	16.5	4.21	6.08	1.45	178	44.4	4.01
6331	56.0	24.3	2.31	2.54	1.10	3447	62.5	5.51
6332	71.9	5.93	12.1	4.28	0.35	580	122	4.74
6333	46.8	5.13	9.13	5.35	0.59	925	196	4.73
6334	96.2	28.2	3.41	4.44	1.30	333	54.6	6.09
6335	112	252	0.44	12.2	27.6	50.5	2.3	21.5
6336	64.7	11.0	5.86	26.9	4.58	404	138	2.92
6337	201	75.3	2.67	11.5	4.32	7.2	1.2	6.32
6338	206	67.8	3.03	11.9	3.92	6.9	1.4	5.07
6339	214	69.9	3.06	12.2	4.00	6.4	0.8	7.73
6340	209	67.9	3.08	12.5	4.05	6.6	0.9	7.11
6341	199	75.4	2.63	10.7	4.05	7.4	1.8	4.04
6343	192	79.6	2.41	11.5	4.76	7.6	1.2	6.39
6344	197	72.6	2.71	11.3	4.15	7.4	1.5	5.04
6345	208	66.9	3.10	9.65	3.11	7.0	1.2	6.00
6346	210	73.7	2.85	10.6	3.69	6.8	1.3	5.37
6347	213	68.2	3.12	11.3	3.61	6.9	1.6	4.40
6348	161	120	1.34	11.4	8.54	9.1	1.8	5.06
6349	162	118	1.37	11.5	8.41	9.1	2.1	4.27
6350	167	106	1.57	11.6	7.37	8.9	1.6	5.39
6351	168	134	1.26	10.9	8.71	9.6	2.1	4.63
6352	151	118	1.28	12.3	9.62	9.5	1.2	8.14
6353	158	118	1.34	12.0	8.93	9.6	1.8	5.46
6354	166	109	1.52	11.5	7.54	9.1	2.1	4.29
6355	160	118	1.36	10.9	8.03	9.1	1.7	5.27
6201	-	-	2.87	11.7	4.08	-	-	-
6202	-	-	2.89	11.7	4.06	-	-	-
6203	-	-	2.68	11.0	4.11	-	-	-
6204	-	-	2.39	11.5	4.79	-	-	-
6205	-	-	0.25	9.16	36.6	-	-	-
6206A	-	-	0.15	6.61	44.5	-	-	-
6206B	-	-	0.16	7.31	45.9	-	-	-
6207	-	-	-	-	1.79	-	-	-
6208	-	-	2.22	5.73	2.58	-	-	-
6209A	-	-	86.6	51.3	0.59	-	-	-
6209B	-	-	32.9	43.4	1.32	-	-	-
5646A	-	-	5.47	6.39	1.17	-	-	-
KP1	-	-	2.92	11.1	3.79	-	-	-
83-870	-	-	1.02	9.49	9.35	-	-	-

APPENDIX G

A.N.U., G.A. and S.M.A. sample numbers

APPENDIX

A.N.U., G.A. and S.M.A. Sample Numbers

Rock Type	A.N.U.	G.A.	S.M.A.
Chocolate to grey brown soil	6009	-	Geehi Damsite, DH 2401, 0"-6"
Grey brown, clayey sub soil	6010	-	" " DH 2401, 5'
Grey brown friable weathered diorite	6011	-	" " " ", 10'
" "	6012	-	" " " ", 15'
" "	6013	-	" " " ", 20'
" "	6014	-	" " " ", 25'
As above, fine grained	6015	-	" " " ", 30'
" "	6016	-	" " " ", 35'
" "	6017	-	" " " ", 40'
" "	6018	-	" " " ", 44'
Grey-brown. Medium grained, friable diorite	6019	-	" " " ", 50'
" "	6020	-	" " " ", 55'
Brownish-grey, medium grained, mostly massive, moderately to highly altered, slightly friable Windy Creek diorite	6021	-	" " " ", 60'
" "	6022	-	" " " ", 65'
" "	6023	-	" " " ", 70'
" "	6024	-	" " " ", 75'
" "	6025	-	" " " ", 80'
" "	6026	-	" " " ", 85'
Brownish-grey, coarse medium grained	6027	-	" " " ", 90'
Brownish-grey, medium grained, moderately to highly altered, slightly friable	6028	-	" " " ", 95'
" "	6029	-	" " " ", 100'
Brownish grey, medium-fine grained	6030	-	" " " ", 105'
" "	6031	-	" " " ", 110'
Grey, fine and coarse grained. Slightly altered.	6032	-	" " " ", 115'
Grey, mostly fine grained, massive	6033	-	" " " ", 120'
" "	6034	-	" " " ", 125'
" "	6035	-	" " " ", 130'
Dark grey. Mostly medium-coarse grained, massive diorite	6036	-	" " " ", 135'
" "	6037	-	" " " ", 140'
" "	6038	-	" " " ", 145'
" "	6039	-	" " " ", 150'
" "	6040	-	" " " ", 155'
" "	6041	-	" " " ", 160'
" "	6042	-	" " " ", 165'
" "	6043	-	" " " ", 170'
" "	6044	-	" " " ", 175'
" "	6045	-	" " " ", 180'
" "	6046	-	" " " ", 185'
" "	6047	-	" " " ", 190'
" "	6048	-	" " " ", 195'
" "	6049	-	" " " ", 200'
Dark grey, mostly medium-fine grained. Massive Windy Creek diorite	6050	-	" " " ", 205'
" "	6051	-	" " " ", 210'
" "	6052	-	" " " ", 215'
" "	6053	-	" " " ", 220'
" "	6054	-	" " " ", 225'
" "	6055	-	" " " ", 230'
" "	6056	-	" " " ", 235'
Dark grey, mostly medium-fine grained. Massive diorite	6057	-	" " " ", 240'
" "	6058	-	" " " ", 245'
" "	6059	-	" " " ", 250'
" "	6060	-	" " " ", 255'
" "	6061	-	" " " ", 260'
" "	6062	-	" " " ", 265'
" "	6063	-	" " " ", 270'
" "	6064	-	" " " ", 275'
" "	6065	-	" " " ", 278'
Medium coarse-grained, mainly yellow-pink with green feldspars granite	6066	-	Bogong Creek Intake DH 2511, 418'
" "	6067	-	" " " ", 415'
" "	6068	-	" " " ", 410'
Dominant green feldspar granite	6069	-	" " " ", 405'
" "	6070	-	" " " ", 400'
" "	6071	-	" " " ", 395'
50/50% yellow-pink and green feldspars. Practically all biotite has been hydrothermally altered	6072	-	" " " ", 390'
" "	6073	-	" " " ", 385'
" "	6074	-	" " " ", 380'
" "	6075	-	" " " ", 375'
" "	6076	-	" " " ", 370'
" "	6077	-	" " " ", 365'
" "	6078	-	" " " ", 360'
" "	6079	-	" " " ", 355'
" "	6080	-	" " " ", 350'
Medium-coarse grained granite. Variable colour of feldspars, from yellow-pink, green and grey-white	6081	-	" " " ",, 345'
" "	6082	-	" " " ", 340'
" "	6083	-	" " " ", 335'
" "	6084	-	" " " ", 330'
" "	6085	-	" " " ", 325'
" "	6086	-	" " " ", 320'
" "	6087	-	" " " ", 315'
" "	6088	-	" " " ", 310'
" "	6089	-	" " " ", 305'
" "	6090	-	" " " ", 300'
Mainly fine-medium grained. Feldspar variable as before, but less green feldspar	6091	-	" " " ", 295'
" "	6092	-	" " " ", 290'
" "	6093	-	" " " ", 285'
" "	6094	-	" " " ", 280'
" "	6095	-	" " " ", 275'
" "	6096	-	" " " ", 270'
" "	6097	-	" " " ", 265'
" "	6098	-	" " " ", 260'
" "	6099	-	" " " ", 255'
" "	6100	-	" " " ", 250'
" "	6101	-	" " " ", 245'

Rock Type	A.N.U.	G.A.	S.M.A.
Mainly fine-medium grained. Feldspar variable as before, but less green feldspar			Bogong Creek Intake DH 2511,
" "	6102	-	" " " ", 240'
" "	6103	-	" " " ", 235'
" "	6104	-	" " " ", 230'
Mainly fine-medium grained. Feldspar variable in colour as before	6105	-	" " " ", 225'
" "	6106	-	" " " ", 220'
" "	6107	-	" " " ", 215'
" "	6108	-	" " " ", 210'
" "	6109	-	" " " ", 205'
" "	6110	-	" " " ", 200'
" "	6111	-	" " " ", 195'
" "	6112	-	" " " ", 190'
As above, except phenocrystic tendency in feldspars	6113	-	" " " ", 185'
" "	6114	-	" " " ", 180'
" "	6115	-	" " " ", 175'
" "	6116	-	" " " ", 170'
Fine-medium grained, yellow-pink and green felspars. All biotite hydrothermally altered	6117	-	" " " ", 165'
Medium-coarse grained. 50/50% grey-white and yellow-pink feldspars	6118	-	" " " ", 160'
" "	6119	-	" " " ", 155'
" "	6120	-	" " " ", 150'
" "	6121	-	" " " ", 145'
" "	6122	-	" " " ", 140'
Feldspars predominantly yellow-pink, but some green. No biotite	6123	-	" " " ", 135'
" "	6124	-	" " " ", 130'
Fine-medium grained. Yellow-pink and green feldspars. Biotite present	6125	-	" " " ", 125'
" "	6126	-	" " " ", 120'
Soil on diorite (grey brown)	6127	-	Geehi Damsite DH 2401, 2'6"
Medium grained, leucocratic granite	6128	-	Bogong Creek Intake DH 2511, 110'
Medium-coarse grained, leucocratic granite, highly weathered	6130	-	" " " ", 100'
" "	6132	-	" " " ", 90'
Weathered granite	6133	-	" " " ", 85'
"	6134	-	" " " ", 80'
Granitic soil on leucogranite	6135	-	" " " ", 67'
" "	6136	-	" " " ", 70'
" "	6137	-	" " " ", 65'
Windy Creek diorite (dark grey, mostly medium-fine grained, massive)	6151	-	Geehi Damsite, DH 2401, 212'
" "	6152	-	" " " ", 214'
" "	6153	-	" " " ", 216'
" "	6154	-	" " " ", 218'
" "	6155	-	" " " ", 222'
" "	6156	-	" " " ", 224'
" "	6157	-	" " " ", 226'
" "	6158	-	" " " ", 228'
" "	6159	-	" " " ", 232'
" "	6160	-	" " " ", 234'
" "	6161	-	" " " ", 236'
" "	6162	-	" " " ", 238'
" "	6163	-	" " " ", 242'
" "	6164	-	" " " ", 244'
" "	6165	-	" " " ", 246'
" "	6166	-	" " " ", 248'
" "	6167	-	" " " ", 262'6"
" "	6168	-	" " " ", 267'6"
" "	6169	-	" " " ", 272'6"
"Granite soil" on Khancoban granite	6170	-	Clew's Ridge, Khancoban DH 2660, 0"-5"
" "	6171	-	" " " ", 2'9"-3'0"
Completely weathered, buff-grey, clayey and friable granite	6172	-	" " " ", 5'
" "	6173	-	" " " ", 10'0"-10'9"
Highly weathered, pale grey-buff, medium-coarse grained granite	6174	-	Clew's Ridge, Khancoban DH 2660, 20'0"-20'11'
" "	6175	-	" " " ", 25'
" "	6176	-	" " " ", 30'
" "	6177	-	" " " ", 35'
" "	6178	-	" " " ", 38'
" "	6179	-	" " " ", 42'
" "	6180	-	" " " ", 45'
" "	6181	-	" " " ", 50'
" "	6182	-	" " " ", 60'
Moderately weathered, pale grey-buff medium-coarse grained granite	6183	-	" " " ", 65'
" "	6184	-	" " " ", 70'
" "	6185	-	" " " ", 75'
" "	6186	-	" " " ", 80'
" "	6187	-	" " " ", 85'
" "	6188	-	" " " ", 90'
Slightly weathered, as above	6189	-	" " " ", 95'
" "	6190	-	" " " ", 100'
" "	6191	-	" " " ", 105'
Stained to slightly weathered pale grey-buff granite	6192	-	" " " ", 110'
Fresh stained granite, pale grey-buff with few pink feldspars	6193	-	" " " ", 115'
" "	6194	-	" " " ", 120'
" "	6195	-	" " " ", 125'6"
" "	6196	-	" " " ", 130'
" "	6197	-	" " " ", 135'
" "	6198	-	" " " ", 140'
" "	6199	-	" " " ", 145'
Quartz feldspar porphyry	6201	-	Koolanooka Hills, W.A.
" "	6202	-	" " " "
" "	6203	-	" " " "
Iron stained porphyry	6204	-	" " " "
" "	6205	-	" " " "
Weathered porphyry	6206	-	" " " "
Clay residual, weathered porphyry	6207	-	" " " "
" "	6208	-	" " " "
Silicified remanent of clay weathered porphyry	6209	-	" " " "

Rock Type	A.N.U.	G.A.	S.M.A.	
Fresh stained granite, pale grey-buff	6210	-	Clew's Ridge, DH 2660, Khancoban	150'
" "	6211	-	" " " ",	155'
" "	6212	-	" " " ",	160'
" "	6213	-	" " " ",	165'
Greyish, vesicular granite (altered), white feldspars in fine-medium grained dark groundmass	6214	-	" " " ",	170'
" "	6215	-	" " " ",	175'
Pale grey, fine-medium grained aplite phase	6216	-	" " " ",	176'
Pale grey fine-medium grained aplite	6217	-	" " " ",	180'
" "	6218	-	" " " ",	185'
Pale grey, medium-coarse grained granite	,6219	-	" " " ",	188'
" "	6220	-	" " " ",	190'
" "	6221	-	" " " ",	195'
" "	6222	-	" " " ",	200'
" "	6223	-	" " " ",	210'
" "	6224	-	" " " ",	220'
" "	6225	-	" " " ",	230'
As above, except pink alteration. (Hydrothermal alteration	6226	-	" " " ",	240'
Pale grey medium-coarse grained granite	6227	-	" " " ",	250'
" "	6228	-	" " " ",	260'
" "	6229	-	" " " ",	270'
As above, but many pink feldspars	6230	-	" " " ",	280'
" "	6231	-	" " " ",	290'
" "	6232	-	" " " ",	299'-300'
" "	6233	-	" " " ",	310'
Pale grey, medium-coarse grained aplite	6234	-	" " " ",	320'
" "	6235	-	" " " ",	330'
Pale grey, medium-coarse grained granite with pink feldspars	6236	-	" " " ",	337'
" "	6237	-	" " " ",	342'
" "	6238	-	" " " ",	350'
Pale grey, medium-coarse grained granite	6239	-	" " " ",	360'
" "	6240	-	" " " ",	370'
" "	6241	-	" " " ",	380'
" "	6242	-	" " " ",	390'
" "	6243	-	" " " ",	400'
Grey coarse granite	6251	4446	Zamia Quarry, W.A.	Z1Q
"	6252	4447	" " "	Z2Q
"	6253	4448	" " "	Z3Q
"	6254	4449A	" " "	Z4Q
Stained granite	6255	4449B	" " "	Z4QB
Granite	6256	4450	" " "	Z5Q
"	6257	4451	" " "	Z6Q
"	6258	4452	" " "	Z7Q
"	6259	4453	" " "	Z8Q
"	6260	4454	" " "	Z9Q
"	6261	4455	" " "	Z10Q
"	6262	4456	" " "	Z11Q
"	6263	3263	Tuckanarra Quarry, W.A.	60
Granite with iron-stained quartz	6264	3264	" " "	61
Biotite rich clot in granite	6265	3265	" " "	62
Iron-stained weathering crust on granite	6266	3266	" " "	63
" "	6267	3267	" " "	64
Feldspars milky-weathered granite	6268	3268	" " "	65
Hydrothermally altered granite	6269	3269	" " "	66
Yellow altered granite	6270	3270	" " "	67
Pale disaggregating granular granite	6271	3271	" " "	68
Yellow disaggregating granite	6272	3272	" " "	69
Yellow hydrothermally altered granite	6273	3273	" " "	70
Pale disaggregating granite	6274	3274	" " "	71
Deep yellow altered granite	6275	3275	" " "	72
Dark yellow altered granite	6276	3276	" " "	73
Rotten yellowcrumbling granite	6277	3277	" " "	74
Rotten redcrumbling granite	6278	3278	" " "	75
Sample intermediate between 6277 and 6278	6279	3279	" " "	76
White kaolin residual on granite	6280	3280	Mertondale D.D.H. 1, W.A.	4' ex W.M.C.
" "	6281	3281	" " "	20'
White, bleached weathered granite	6282	3282	" " "	40'
Weathered granite	6283	3283	" " "	60'
Mildly altered granite. Friable and limonite stained joints	6284	3284	" " "	78'4½"-80'8½"
" "	6285	3285	" " "	80'8½"-82'0"
Dull red and white granite	6286	3286	" " "	82'0" -83'8"
Dull red with many white hard veins	6287	3287	" " "	109'2½"-110'4½"
Dull red with pale orange alteration	6288	3288	" " "	110'4½"-111'11½"
Dull light pink with few fine veins	6289	3289	" " "	111'11½"-113'4"
Dull red with limonitic staining	6290	3290	" " "	113'4" -114'8"
Dull red with fine white alteration on joints	6291	3291	" " "	114'8" -116'1½"
Red fresh granite	6292	3292	" " "	116'1½"-117'
Dark brown kernel of residual boulder of dolerite	6293	3293	Glenview Quarry, Ridge Road, W.A.	Bench 2
Outer core - light brown	6294	3294	" " " " "	"
Reddish outer rim, surrounding outer core	6295	3295	" " " " "	"
Bleached white outer rim of residual	6296	3296	" " " " "	"
Weathered, Mottled granite with many quartz shear veins, or pegmatite	6297	3297	" " " " "	"
Pallid weathered dolerite dyke	6298	3298	" " " " "	
Pallid " granite, surrounding dyke	6299	3299	" " " " "	
Pale-yellow-white weathered dolerite near contact	6300	3300	" " " " "	
Weathered dolerite-bleached in contact with mottled weathered dolerite (B)	6301A	3301A	" " " " "	
	6301B	3301B	" " " " "	
Very clayey and moist weathered granite	6302	3302	" " " " "	
Pinkish-red exfoliation crust on granite	6303	3303	" " " " "	
Yellowish exfoliation crust on granite	6304	3304	" " " " "	

Rock Type	A.N.U.	G.A.	Locality	
Fresh dark grey dolerite	6305	3305	Glenview Quarry, Ridge Road, W.A. Bench	
Fresh grey granite	6306	3306	" " " " "	
Laterite (concretionary)	6307	3307	" " " " "	
Soft brownish-grey sub-lateritic sand	6308	3308	" " " " "	
Weathered friable granite	6309	3309	North side of Ridge Road-$^1/_4$ mile East	
Contact sample of dolerite and granite. A = granite, B = dolerite. Both are bleached and weathered	6310A	3310A	Glenview Quarry, Ridge Road, W.A. Bench 3	
	6310B	3310B	" " " " " "	
Purplish grey porphyry	6311	3311	Koolanooka Hills, W.A.	
Porphyry with weathered surface	6312	3312	" " "	
Yellow-orange stained weathered porphyry	6313	3313	" " "	
Iron stained and silicified variant of porphyry	6314	3314	" " "	
Dull grey weathered porphyry	6315	3315	" " "	
Iron stained, feldspars weathered, porphyry	6316	3316	" " "	
Heavily iron stained, "rotten" porphyry	6317	3317	" " "	
Iron stained, fractured and partially disaggregating porphyry	6318	3318	" " "	
As above, but less iron staining	6319	3319	" " "	
"Rotten" porphyry, feldspars weathered	6320	3320	" " "	
Highly weathered porphyry	6321	3321	" " "	
Clay weathered variant of 6321	6322	3322	" " "	
Iron stained, clay variant of 6321	6323	3323	" " "	
Red-Yellow mottled, disaggregated residual	6324	3324	" " "	
Clay-white residual with residual phenocrystic quartz	6325	3325	" " "	
Slightly Fe stained variant of 6325	6326	3326	" " "	
Mottled version of 6325, less clay	6327	3327	" " "	
More highly weathered residual of 6325	6328	3328	" " "	
" "	6329	3329	" " "	
Pure quartz-clay residual (bleached)	6330	3330	Koolanooka Hills, W.A.	
Clay rich residual, white	6331	3421	" " "	
Clay residual, with secondary silicification	6332	3422	" " "	
More silicified variant of 6332	6333	3423	" " "	
Clay version of 6333, less silica	6334	3424	" " "	
Residual, large quartz grains set in hard clay matrix	6335	3425	" " "	
Part silicified, friable surface weathered porphyry	6336	3426	" " "	
Fresh greasy-green brown porphyry	6337	3427	" " "	North end of Mass
Weathered exfoliation crust on 6337	6338	3428	" " "	" " " "
As for 6338, but more highly weathered	6339	3429	" " "	" " " "
Weathered crust, intermediate between 6338 and 6339	6340	3430	" " "	" " " "
Slightly weathered porphyry	6341	3431	" " "	" " " "
Weathered crust on porphyry	6343	3433	" " "	" " " "
Surface weathered greasy porphyry	6344	3434	" " "	" " " "
Surface weathered greasy porphyry	6345	3435	" " "	" " " "
More highly weathered surface crust	6346	3436	" " "	" " " "
Less weathered than 6346	6347	3437	" " "	" " " "
Fresh grey porphyry	6348	3438	" " "	East end of Mass
"	6349	3439	" " "	" " " "
Iron stained and partly weathered porphyry	6350	3440	" " "	" " " "
More intensely altered porphyry from core of "rotten" boulder	6351	3441	" " "	" " " "
Part of "rotten" boulder as above	6352	3442	" " "	" " " "
"Rotten" outer rim of 'rotten' boulder	6353	3443	" " "	" " " "
Fresh porphyry	6354	3444	" " "	" " " "
Exfoliation surface - weathering porphyry	6355	3445	" " "	" " " "
Residual, silicified remanent on granite	6356	-	Mertondale DDH, W.A.	
Brown, with some veins (weathered granite)	6357	-	" "	
Weathered granite	6358	-	" "	
" (bleached white)	6359	-	" "	
" (pale red, clay seams)	6360	-	" "	
" (pale red)	6361	-	" "	
" (deeper red)	6362	-	" "	
" (palest pink-white clay)	6363	-	" "	
" aplite with veins (white)	6364	-	" "	
Weathered granite (white)	6365	-	" "	
" (white)	6366	-	" "	
Weathered granite, with veins	6367	-	" "	
Weathered, friable, reddish granite	6368	-	" "	
Weathered, white-buff granite with green altered zones	6369	-	" "	
Weathered pink granite	6370	-	" "	
Weathered granite with white veins	6371	-	" "	
Weathered, pale pink granite with green zones	6372	-	" "	
Weathered granite	6373	-	" "	
Weathered granite (red)	6374	-	" "	

APPENDIX H

H.1 PREVIOUS STUDIES OF WEATHERING

One of the earliest studies of weathering employing geochemical techniques was by Goldich (1938). He demonstrated removal of alkali and alkaline elements and traced the relative destruction of mineral phases. From these studies he was able to propose a stability series, the reverse of the Bowen reaction series, which indicated the order of selective weathering. Subsequently Brock (1943) published the results of weathering studies on a range of rock types from Hong Kong. He found similar changes to those outlined by Goldich for a compositional range of lamprophyre to granite. An apparently uniform suite of weathering products formed from all rock types.

Carroll and Jones (1947) analysed lateritic weathering over three granitic rocks from Western Australia and demonstrated that kaolinite was the dominant clay mineral. More recently Walhstrom (1948), Reiche (1950), Gordon and Murata (1952), Butler (1953, 1954), Fields and Swindale (1954), McLaughlin (1955, 1959), Keller (1955) and Yamasaki, Iida and Yokoi (1955) have examined different aspects of weathering processes. The lattermost authors were amongst the first to investigate the behaviour of trace elements during weathering. Their data indicated significantly different behaviour for Sr, Ba, V and Zr from that indicated by Butler (op. cit.). Later workers Horstman (1957), Anderson and Hawkes (1958), Santos-Ynigo and Esguerra (1961), Short (1961), Kelly and Zumberge (1961), Dennen and Anderson (1962), Pliler and Adams (1962), Richardson and Adams (1963), Brewer (1964), Wolfenden (1965), Harriss and Adams (1966), Ruxton (1968) and Hart (1969) have continued to use trace and major elements to characterize weathering processes.

Published isotopic studies relevant to weathering have been discussed in the introductions to Chapters 10 and 11.